FINAL ENGINEERING/PROJECT REPORT

FOR

SURFACE COMPOSITION MAPPING RADIOMETER INSTRUMENT

Contract No. NAS 5-21112

Prepared by

ITT Aerospace/Optical Division
Fort Wayne, Indiana 46803

Prepared for

NATIONAL AERONAUTICS AND SPACE ADMINISTRATION
GODDARD SPACE FLIGHT CENTER
Greenbelt, Maryland 20771

FINAL ENGINEERING/PROJECT REPORT

FOR

SURFACE COMPOSITION MAPPING RADIOMETER INSTRUMENT

Contract No. NAS 5-21112

Prepared by

ITT Aerospace/Optical Division
Fort Wayne, Indiana 46803

Prepared for

NATIONAL AERONAUTICS AND SPACE ADMINISTRATION
GODDARD SPACE FLIGHT CENTER
Greenbelt, Maryland 20771

Contributors

R. Annable	H. Kalina
N. Franklin	D. Juarez
R. Harber	J. Stark

Approved

D. Juarez, Program Manager

TABLE OF CONTENTS

TABLE OF CONTENTS (Cont.)

LIST OF ILLUSTRATIONS

LIST OF TABLES

1.0 INTRODUCTION

ITT Aerospace/Optical Division has completed NASA Contract NAS 5-21112 which was to provide a design study, to design, to develop, to fabricate and to test a three-channel scanning radiometer. The instrument was flown on the GSFC Nimbus 5 Satellite and measured infrared energy in the 8.3-9.3 micron, 10.2-11.2 micron and 0.8-1.1 micron spectral regions. Instrument parameters are shown in Fig. 1.0-1.

The scope of work includes:

a. The design study, design, fabrication and assembly of an Engineering Model, a Prototype Model, and a Flight Model instrument.

b. The generation of acceptance test procedures, ground support and test equipment.

c. The qualification testing of the instrument.

d. The field engineering as required for experiment-spacecraft integration, testing and launch support.

This report provides a description of the SCMR Flight Model instrument and contains theoretical discussions of the instrument subassemblies. Operational details of the mechanical and electrical portions of the instrument are included.

TABLE 1.0-1

NIMBUS "E"
SURFACE COMPOSITION MAPPING RADIOMETER
PARAMETERS

PRIMARY MODE - MEASUREMENT OF "RESTSTRAHLEN" EFFECT TO IDENTIFY SURFACE MINERAL COVER.

SECONDARY MODE - I.R. MAPPING OF EARTH SURFACE

SIZE	22.25" L x 9" W x 17.68" H
WEIGHT	51 POUNDS
POWER	16.4 WATTS
LINE RATE	10 LINES/SEC.
VIDEO PASSBAND	50 KHz
INFRARED BANDWIDTH	
CHANNEL 1	8.3 - 9.3 MICRONS
CHANNEL 2	10.2 - 11.2 MICRONS
VISIBLE BANDWIDTH	0.8 - 1.1 MICRONS
INSTANTANEOUS FIELD OF VIEW	0.6 MILLIRAD
GROUND RESOLUTION AT SUBSATELLITE POINT	0.41 MILES
NOISE EQUIVALENT TEMP DIFFERENCE (NE T) (280^{o}K)	0.3^{o}K (GOAL) 1.0^{o}K (REQUIRED)
PEAK SIGNAL/RMS NOISE RATIO	52 DB
OPTICS SIZE	8 INCH
OPTICS SPEED	f/.82
DETECTOR TEMPERATURE	115^{o}K
NUMBER OF COMMANDS	16
NUMBER OF TM POINTS	22

2.0 INSTRUMENT DESCRIPTION

The Nimbus E High Resolution Surface Composition Mapping Radiometer (SCMR) is a three channel radiometrically calibrated scanning radiometer. Two narrow IR spectral bands, 8.3 μm to 9.3 μm and 10.2 μm to 11.2 μm, are utilized to measure the thermal emission of igneous rocks which exhibit the reststrahlen effect. The third channel, 0.8 μm to 1.1 μm, is a near IR channel used for cloud mapping and albedo measurements. The SCMR also produces strip maps of the Earth and seas in all three channels simultaneously by rotation of the field of view in a plane normal to the spacecraft velocity vector. The multispectral data which is separated by dichroic beam splitters, is registered channel to channel within a single instantaneous field of view (0.6 milliradians).

Figure 2.0-1 indicates the absorbtion of ozone as measured by Chaney, et al[1] against a 290°K blackbody, together with the calculated spectrum for solid samples of granite and dunite both at 290°K, with emissivities determined from the results of Hovis and Callahan[2]. The relative spectral position of the two SCMR IR channels used to measure the reststrahlen are also indicated. The difference between the simultaneous radiance measurements made in the two narrow band IR channels is used to determine the relationship of acidic and ultra-basic compositions of the Earth's surface.

Physically, the SCMR is 22.25 inches long, 9.00 inches wide, and 17.68 inches high. The instrument weighs slightly more than 50 pounds and uses 15 watts of power in the normal operation mode. The SCMR consists of five basic modules. These are the Baseplate Unit, the Scanner Module, Optics Module, Radiant Cooler Module, and the Electronics Module (see Figure 2.0-2).

The Baseplate Unit is the basic structure to which the other modules are mechanically referenced and coupled. The momentum compensator and scan motor electronic drive circuits are contained within this structure. A reference blackbody which completely fills the optical field of view is mounted on the top side of the baseplate unit directly under the scan mirror. The blackbody is thermally coupled to the baseplate unit and its temperature, while monitored and telemetered, is not controlled.

---

1. L.W. Chaney, S.R. Drayson and C. Young, Appl. Opt. 6,347 1967.

2. W.A. Hovis, Jr.; L.R. Blaine and Wm. R. Callahan Appl. Opt. Vol. 7 1137 1968.

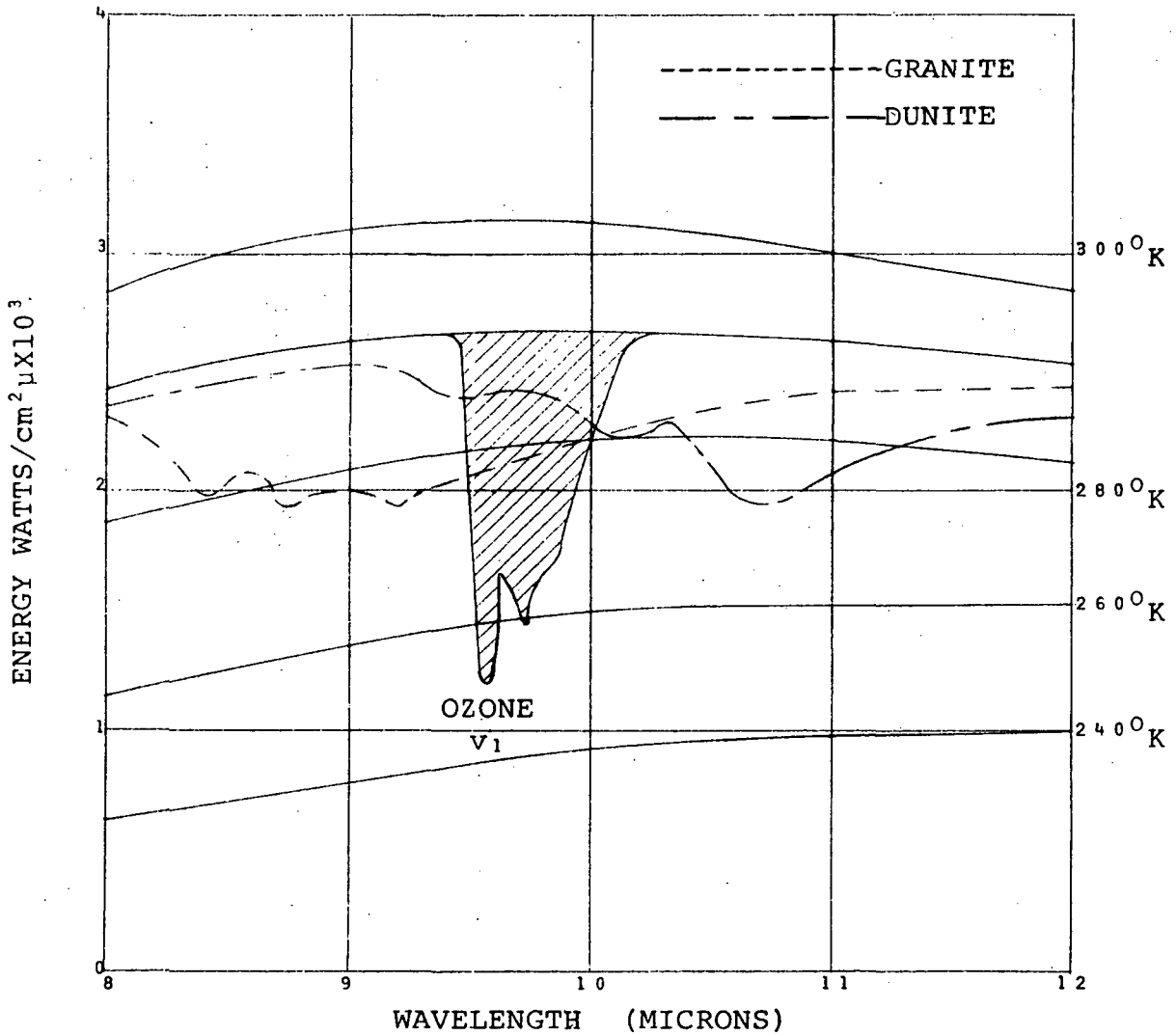

Figure 2.0-1

OZONE ABSORPTION AND CALCULATED RESTSTRAHLEN EFFECT

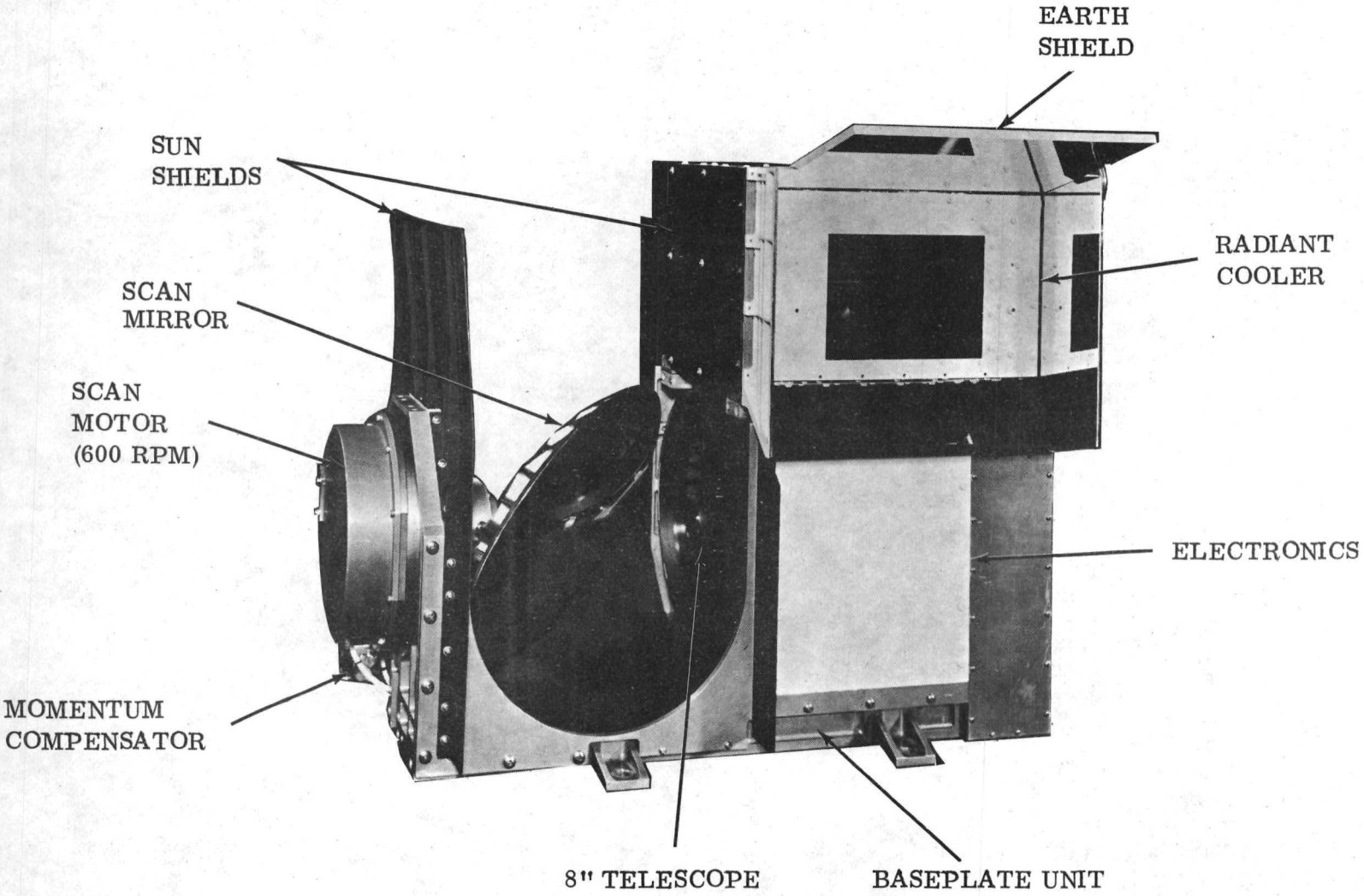

SATELLITE: NIMBUS 5
INFRARED CHANNELS: 8.3 - 9.3 MICRONS
10.2 - 11.2 MICRONS
RESOLUTION: 0.6 MILLIRADIANS

FIGURE 2.0-2 SCMR INSTRUMENT

The Scanner Module is comprised of the scanner mechanical housing, the eliptically shaped beryllium scan mirror, the hysteresis synchronous scan and momentum compensator motors, and a scan cavity sun shield.

The Optics Module consists of a modified 8 inch Dall-Kirkham operating afocally at a speed of f/.92. The beam diameter is reduced from 8 inches to 1 inch. Spectral separation is accomplished by two beam splitters. The near IR detector and associated preamplifier is contained within the optics module as are the beam splitter and focusing lens assembly.

The Radiant Cooler Assembly is comprised of a thermally isolated housing, a truncated pyramid cooling "cone" around which is an apron for radiation of heat to space. The cone walls are optically polished, hard coated, and finished with evaporated gold. The cone is thermally isolated from the housing and optical ports sealed off with irtran windows close off the cone from all but the optical radiative inputs. Located in the truncation plane and centered within the cooling "cone" is a radiative patch. Two mercury cadmium telluride (HgCdTe) detector packages are mounted on the patch which is thermally decoupled from the cooling cone. The radiant cooler is designed to cool the patch under normal operating conditions to $\approx$ 105K. The actual operating temperature is regulated at 115K $\pm$ 0.1K giving a reserve capacity of about 10^{o}K. Incorporated into the radiant cooler system are a number of features dedicated to the prevention of condensation of contaminants on the cooled areas. The features include a deployable Earth shield, cold traps, cone wall and patch heaters, and a dry Gas Patch Purge System. Operational use of the cooler requires the cooler be heated to $\approx$ 300K in vacuum for a period of time sufficiently long enough to outgas water vapor and other contaminants which may be trapped within the instrument. The HgCdTe detector preamplifiers are also located on the radiant cooler housing.

The Electronics Module contains the signal processing circuits, electronic calibration and sync circuits, digital to analog telemetry conversion, and buffer interface circuitry. Normal operation requires approximately 16 watts of power. The electronic circuit boards are heat sinked to the electronics module frame which is thermally isolated from the baseplate unit. The power dissipated by the electronics is radiated to space by an attached radiating panel that extends in front of the optical module and has a view of space.

Electrical Interface

The electrical interface requirements, in addition to commands which are described in Section 7 of this report, are shown in Table 2.0-1 ELECTRICAL INTERFACE.

A power profile for operational modes and power required for decontamination modes are shown in Table 2.0-2. In the minimum operational mode all telemetry circuits are functional as well as the patch temperature control circuitry.

TABLE 2.0-1

ELECTRICAL INTERFACE

POWER REQUIREMENT

-24.5VDC (SEE FIG. 1.0-2.1 POWER PROFILE)

CLOCK REQUIREMENT

50 KHZ 5V.P.P. SQUAREWAVE
10 KHZ 5V.P.P. SQUAREWAVE
400 HZ 20V.P.P. TWO PHASE SQUAREWAVE

INTERFACE CONNECTORS

CONNECTOR NO.	FUNCTION	CONNECTOR TYPE
J1	VIDEO OUTPUT	DAM-15S
*J2	TEST	DCM-37S
J3	CLOCK	DBM-25P
J4	COMMAND	DDJ-50P
J5	ANALOG TELEMETRY	DBJ-25P
J6	POWER	DEJ-9P
J7	DIGITAL TELEMETRY	DAJ-15P

*TEST ONLY - NO INTERFACE REQUIRED

TABLE 2.0-2

POWER PROFILE

OPERATIONAL MODES

MINIMUM - MOTOR ON/MOTOR LOW POWER	=	6.25 WATTS
NOMINAL - MOTOR ON/MOTOR LOW POWER/ELECTRONICS ON	=	16.25 WATTS
MAXIMUM - MOTOR ON/MOTOR HIGH POWER/ELECTRONICS ON	=	20.33 WATTS

DECONTAMINATION MODES

PATCH HEAT FULL TIME	=	0.245 WATTS
PURGE VALVE OPEN	=	0.80 WATTS
CONE HEAT ON	=	3.0 WATTS
CONE COVER STORE/DEPLOY	=	14.7 WATTS (10-SECOND DURATION)

Mechanical Interface

An outline drawing (ITT Dwg. #8113887) showing mechanical interface of the SCMR instrument is included in this report as Figure 2.0-3. The instrument is shown with outside dimensions of 25.28 long x 11.5 wide x 17.68 high with the cover door closed. The instrument weighs 51 lbs. The c.g. is located on the drawing. Uncompensated angular momentum will not exceed .01 ft. 16 sec. based upon tolerances of the rotating masses. A momentum compensator is included in the instrument to reduce the uncompensated portion to .01 or less.

The view angle for the scanner is shown in this figure. When the instrument is mounted on the spacecraft, 145° of scanner angle as shown must be unobstructed. In addition, the following areas listed below must be left open.

1. Area surrounding daylight calibration assembly

2. Area in front of radiant cooler including viewing angle and path of cooler door deployment.

3. Radiating Panel for cooling electronics.

4. Radiating Panel for cooling radiant cooler housing

5. Access area for filling patch purge system

Means is provided for attachment of a thermal blanket to the exterior of the instrument after installation of the spacecraft. This blanket was supplied by the spacecraft contractor and not by ITT.

Built into the instrument is a purge system for flushing the volume around the radiant cover patch with ultra-dry nitrogen while in orbit. This system may be exercised during pre-launch test but should be recharged prior to launch. A transducer is installed in the system for measuring gas supply pressure.

The instrument is designed with 4 mounting feet. Mounting bolts are 3/8-16. The four mounting feet are to be in thermal contact with the spacecraft. A compensation heater of 8 watts capacity is attached to the base plate and motor housing.

The motor and momentum compensator operated continuously--even during launch. For further details on the thermal interface, refer to SCMR Thermal Design Status and Effects on S/C Interface by F. Florio of GE (PIR # 1R44-NE-554).

FOLDOUT FRAME

FOLDOUT FRAME

		6.85 WAS 6.83. 7.00 WAS 6.96. ADDED 17.68 DIM. CHANGED 10.75 DIM TO 10.50 AS INDICATED WHEN ADDED FILL VALVE LOCATION. ADDED TO 32 POS. 10-32 THREADS WAS 1/4-40 6 PLACES ADDED DETAIL B PCN 61240-102	11/4/71	
	B	ADDED FLAG NOTE 6 PCN 61240-134	5/16/74	
D1 D2	C	ADDED NOTES 7 & 8, REVISED DETAIL B TO AGREE WITH ACT, REVISED END VIEW TO AGREE WITH ACT, ADDED DIMENSIONS TO COOLER PCN 61240-140	NOV 2, 1971	
D1 D2	D	ADDED CAP ASSY ADDED NAME TAG PCN 61240-138	JUNE 22	
	E	REVISED NOTE 6 PCN 61240-139	9/7/72	
	F	NOTE 5 REPAINT WAS SE-121, DELETED THIS NOTE, INSTALLATION NOTE ON BOTTOM VIEW, ADDED SHADED AREA ON TOP VIEW FOOTE PCN 61240-136	5/14/74	

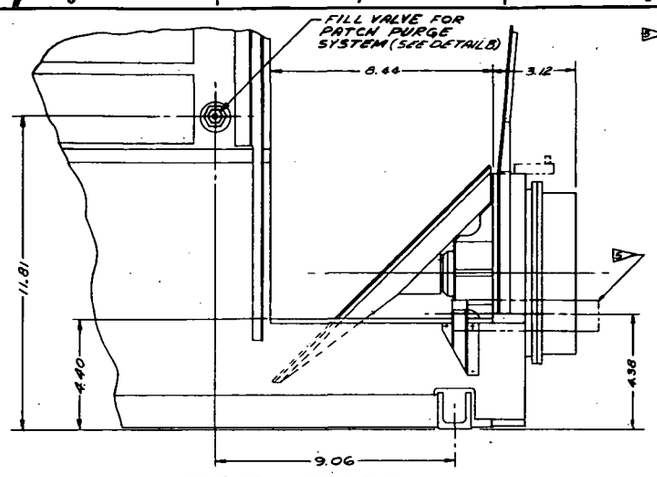

PARTIAL VIEW A-A

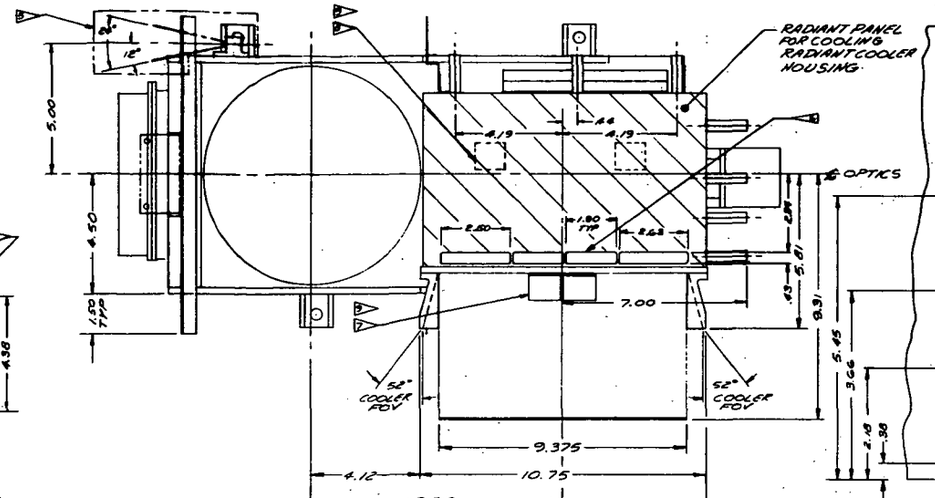

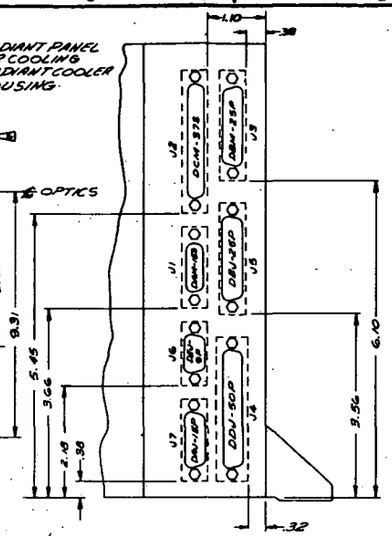

CONNECTOR LAYOUT SCALE 1/1

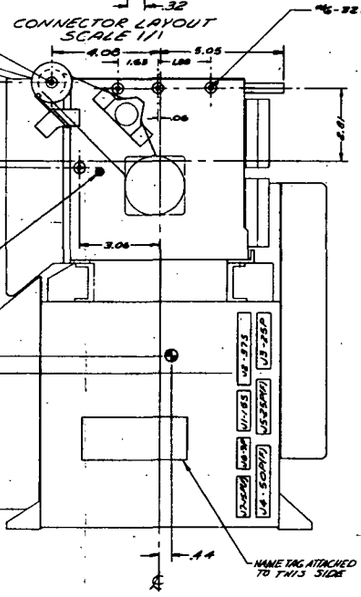

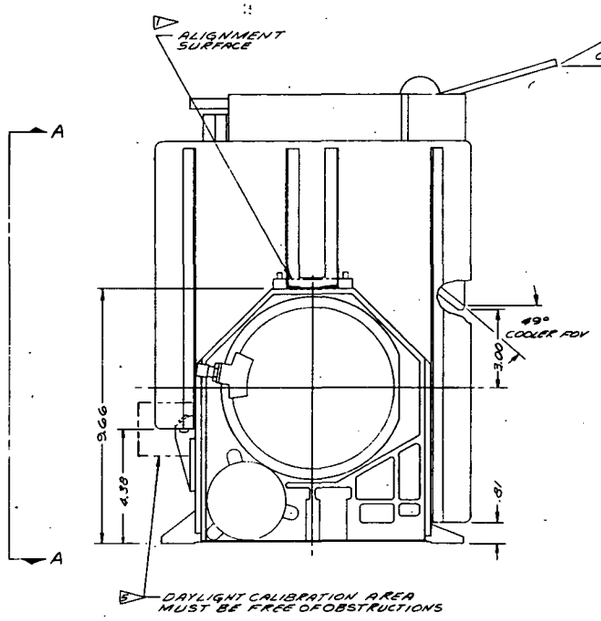

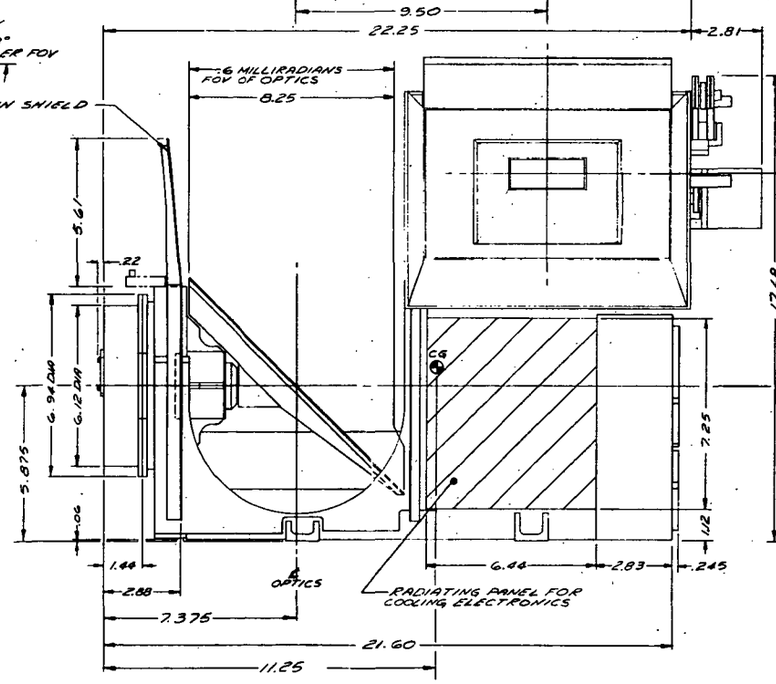

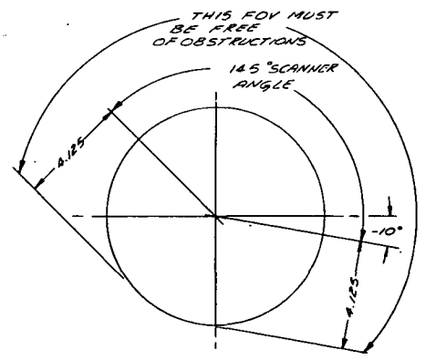

SCAN MIRROR-VIEWED FROM MOTOR END

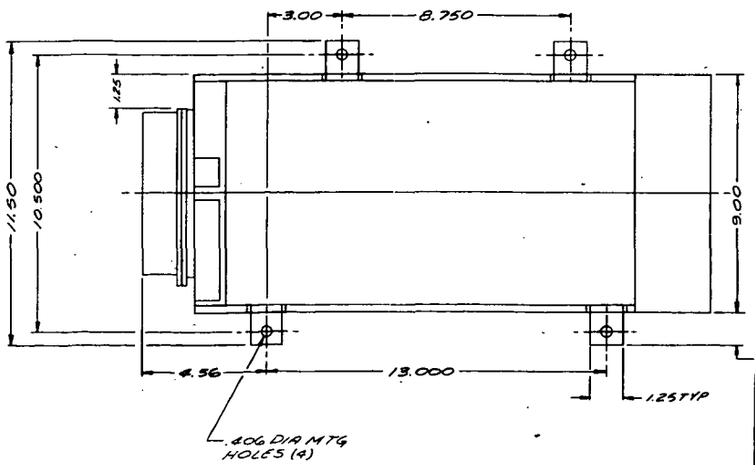

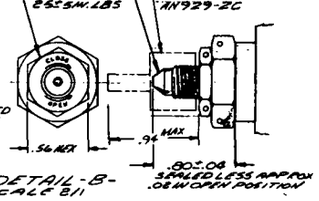

DETAIL-B-
SCALE 2/1

NOTES:

1. ALIGNMENT PAD 8116034 TO BE INSTALLED ON INSTRUMENT FOR ALIGNMENT WITH SPACECRAFT, IT SHOULD BE REMOVED PRIOR TO LAUNCH.
2. APPROXIMATE TOTAL WEIGHT = 51.0 POUNDS.
3. UNCOMPENSATED ANGULAR MOMENTUM WILL NOT EXCEED 0.01 FT. LB. SEC.
4. INDIVIDUAL MOUNTING FOOT AREA 1.56 IN², ALL 4 MOUNTING FEET TO BE IN THERMAL CONTACT WITH THE SPACECRAFT.
5. THE AREA SURROUNDING THE DAYLIGHT CALIBRATION ASSY MUST BE FREE OF ANY OBSTRUCTIONS WHICH WOULD IMPAIR ITS OPERATION.
6. PLANNED OUT GASSING PORTS
7. PRIOR TO LAUNCH CUT 4 RED LEADS OFF FLUSH WITH HEATERS ON COOLER DOOR.
8. PRIOR TO LAUNCH CUT 4 RED LEADS OFF FLUSH AT [illegible] ON END PLATE FOR HEATERS IN COOLER ASSY.
9. THESE HEATERS ARE FOR SOLAR INPUT SIMULATION IN CHAMBER TEST ONLY.

QUANTITY PER GROUP	ITEM NO.	PART OR IDENTIFYING NO.	NOMENCLATURE OR DESCRIPTION

LIST OF MATERIALS OR PARTS LIST

MATERIAL	
FINISH	
NEXT ASSEMBLY	61240
APPLICATION	USED ON

UNLESS OTHERWISE SPECIFIED DIMENSIONS ARE IN INCHES AND TOLERANCES APPLY AFTER SPECIAL FINISHES

TOLERANCES

BASIC DIMENSIONS	DECIMALS 2 PLACE	DECIMALS 3 PLACE	ANGLES
UNDER 6	±.03	±.010	±1°
6 to 24 INCL.	±.06	±.020	
OVER 24	±.09	±.030	

DO NOT SCALE PRINT

CONSULT TOOL TO STOCK SIZES

SHOP PRACTICE, SS-101 APPLIES

CONTRACT NO. NAS5-21112

APPROVALS

DRAWN [illegible] 5-6-70

PURCHASING [illegible] 5-11-70

DESIGN [illegible]

ITT AEROSPACE/OPTICAL DIVISION
FORT WAYNE, INDIANA, U.S.A.
INTERNATIONAL TELEPHONE AND TELEGRAPH CORPORATION

OUTLINE SURFACE COMPOSITION MAPPING RADIOMETER

SIZE	CODE IDENT NO.	8113887
E	31550	

SCALE 1/2 SHEET

2-9

3.0 INSTRUMENT FUNCTIONAL DESCRIPTION

3.1 Optics

Radiation from the Earth or the internal calibration blackbody is reflected from the continuously rotating scan mirror into the 8 inch diameter collecting telescope as shown in Figure 3.0-1. The modified Dall-Kirkham telescope is operated afocally at a speed of f/.92. The secondary mirror of the telescope collimates the optical beam into a smaller diameter which is 1 inch. The first dichroic beam splitter is thinly gold coated glass which transmits the near-infrared radiation but reflects the 8 to 12 micron radiation. The near infrared (0.8 to 1.1 m) beam passes through the dichroic beam splitter and then through a long wavelength pass (interference) filter and is then focused by use of a parabolic mirror onto a hybrid silicon detector/preamplifier assembly. The parabolic mirror position is adjustable for purposes of channel registration. The short wavelength beam splitter is set at a 45^{o} angle to the collimated 1 inch beam and folds the beam at 90^{o} to the telescope so that the long wavelength radiation emerges through the side of the telescope between the primary and secondary mirrors. The second IR beam splitter is a multiple coated germanium substrate dichroic again set at 45^{o} to the 1 inch collimated beam. This beam splitter transmits >80% of the radiation between 8.3 and 9.3µm and reflects 98% or more of the radiation between 10.2 and 11.2µm. The spectrally separated 1 inch diameter beams are focused on their respective detectors by a large (1 inch) germanium focusing lens and a germanium aplanat lens in each leg. The two long wavelength IR beams also pass through an Irtran optical port window that separates the interior of the radiant cooling cone from the cooler housing and then through the narrow spectral band pass filters which are located on the radiant patch with the detectors. The final aplanats speed the total system operating speed to f/0.82 enabling the 0.6 milliradian field of view to be focused on the 0.10 mm by 0.10 mm detectors.

IR Detectors

The IR detectors are located on a patch assembly shown in Figure 3.0-2 as Item #1. The temperature of the patch assembly is controlled by the electronics utilizing a sensing and heating element located on the patch to minimize the detector responsivity changes with temperature variations that would occur due to heat load variations over an orbital period. The temperature of the patch and the heat load variations are also monitored and telemetered. Table 3.0-1 and 3.0-2 describes the flight model IR detectors.

Bias for the detectors is provided by a regulated voltage source generated by the detector pre-amplifiers. Figure 3.0-3 and Figure 3.0-4 are graphs of D* vs bias current and responsivity as a function of wavelength for the flight model detectors.

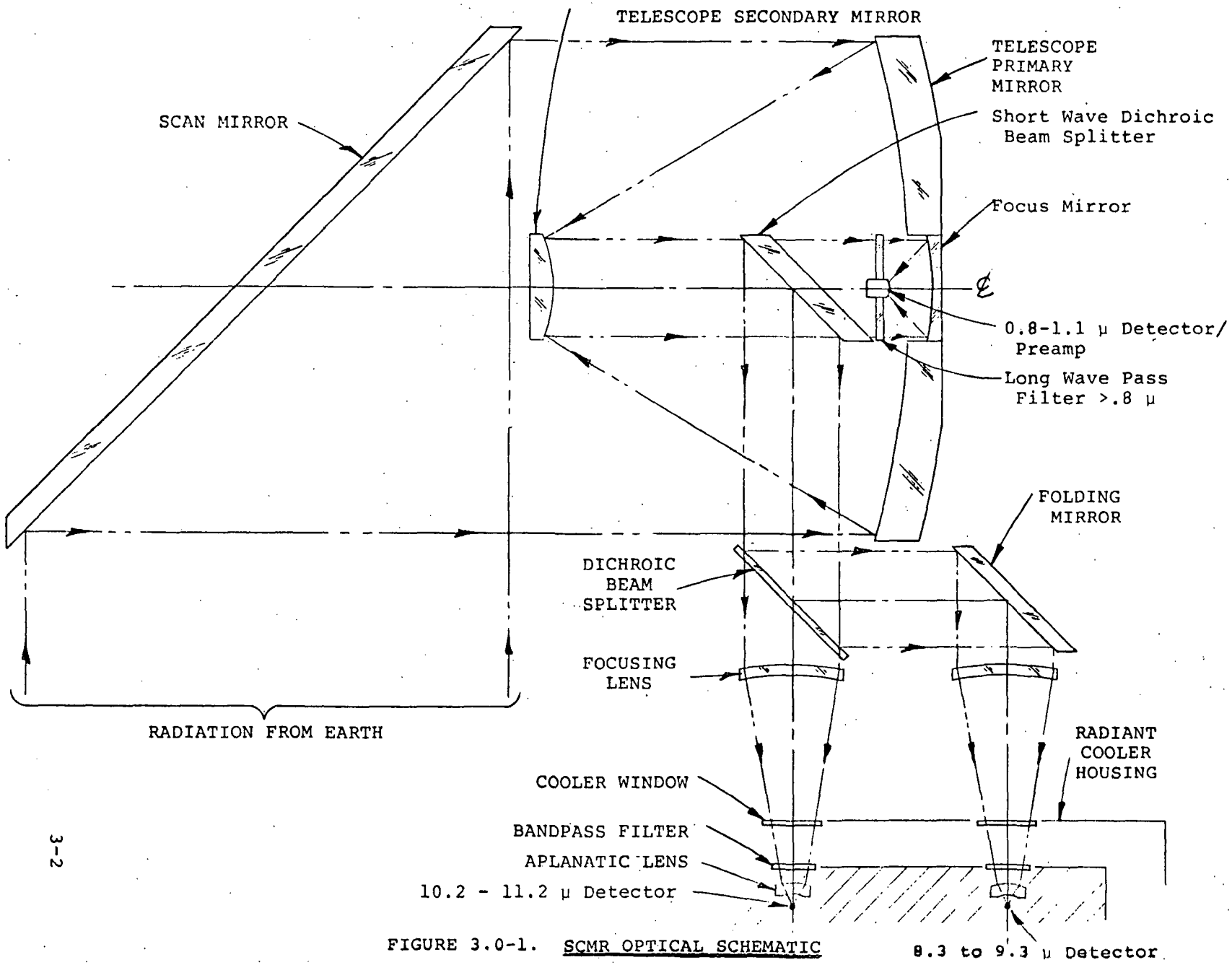

FIGURE 3.0-1. SCMR OPTICAL SCHEMATIC

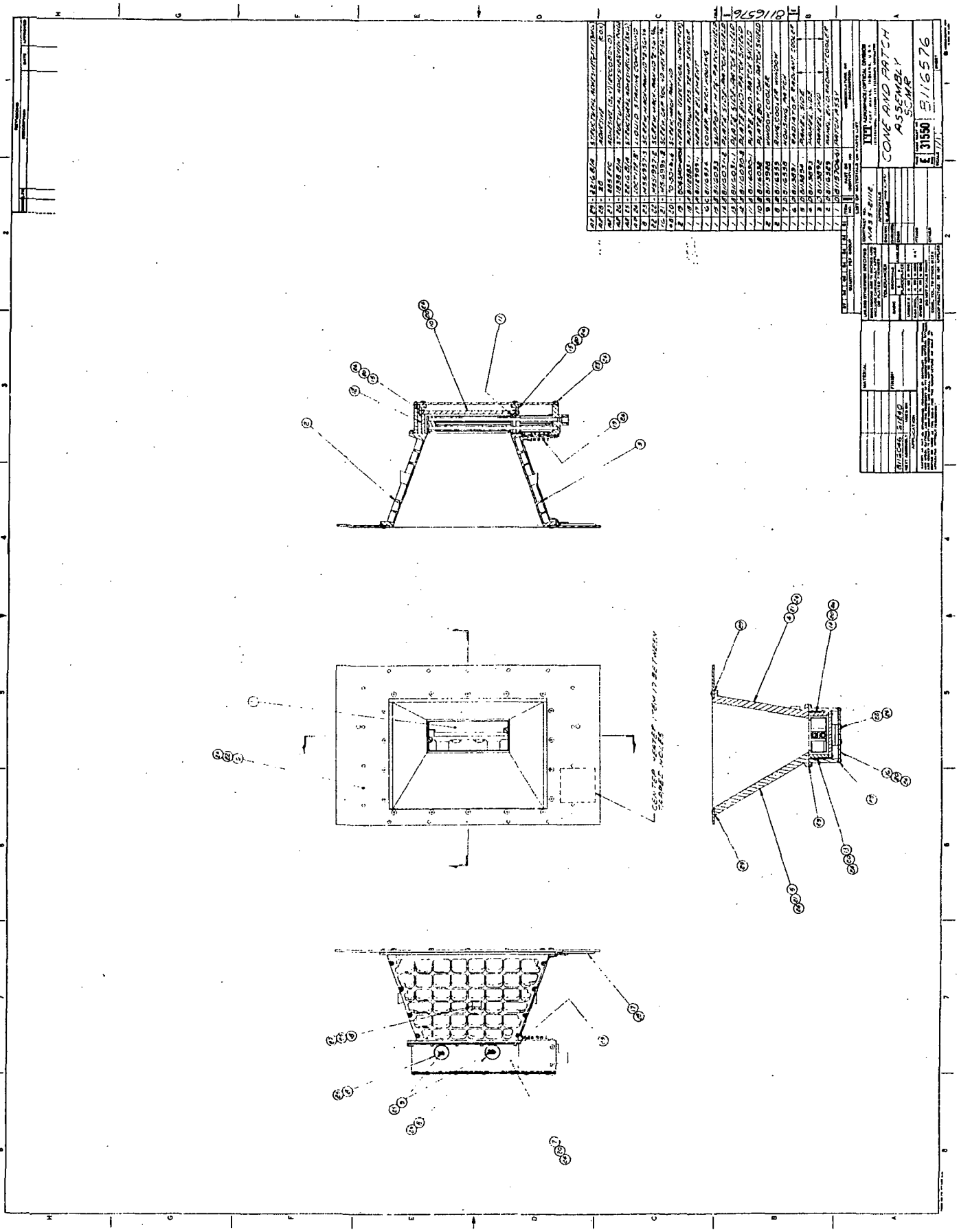

FIGURE 3.0-2

TABLE 3.0-1

FLIGHT MODEL SWL CHANNEL DETECTOR

Description of Detector

Type	Mercury Cadmium Telluride (Hg Cd Te)
Identification Number	DLK21E1 S/N Z1
Detector Type	Photoconductive
Date of Manufacture	October 1970
Window	Irtran II, AR Coated
Element Size	Length .097 mm
	Width .097 mm
Element Area	.0094 mm^2
Maximum Bias Not to be Exceeded	20.0 milliamps
Field of View	80°
Element-Backside of Housing	.100 inches

Test Results at $100^{\circ}K$

Resistance at $100^{\circ}K$	17.5 ohms
Power at Optimum Bias	.280 m watts
Optimum Bias	4.0 milliamps
Peak Spectral Response	9.5 microns
D^*_{bb} (500, 10KHz, 1)	3.38×10^{10} cm-$Hz^{\frac{1}{2}}w^{-1}$
D^*_{λ} (9.5μ, 10KHz, 1)	8.3×10^{10} cm-$Hz^{\frac{1}{2}}w^{-1}$
Responsivity (R_{λ})	22,100 volts/watt

TABLE 3.0-2

FLIGHT MODEL LWL CHANNEL DETECTOR

Description of Detector

Type	Mercury Cadmium Telluride (Hg Cd Te)
Identification Number	DLK 21 F1 Z2
Detector Type	Photoconductive
Date of Manufacture	October 1970
Window	Irtran II, AR Coated
Element Size	Length .093 mm Width .099 mm^2
Element Area	.0092 mm^2
Maximum Bias Not to be Exceeded	20.0 milliamps
Field of View	80°
Element-Backside of Housing	.100 inches

Test Results at $100^{\circ}K$

Resistance at $100^{\circ}K$	30 ohms
Power at Optimum Bias	.760 m watts
Optimum Bias	5 milliamps
Peak Spectral Response	11 microns
D^*_{bb} (500, 10KHz, 1)	2.67×10^{10} cm-$Hz^{\frac{1}{2}}w^{-1}$
D^*_{λ} (11μ, 10KHz, 1)	6.4×10^{10} cm-$Hz^{\frac{1}{2}}w^{-1}$
Responsivity (R_{λ})	65,170 volts/watt

2.6 D* vs Bias at 100°K

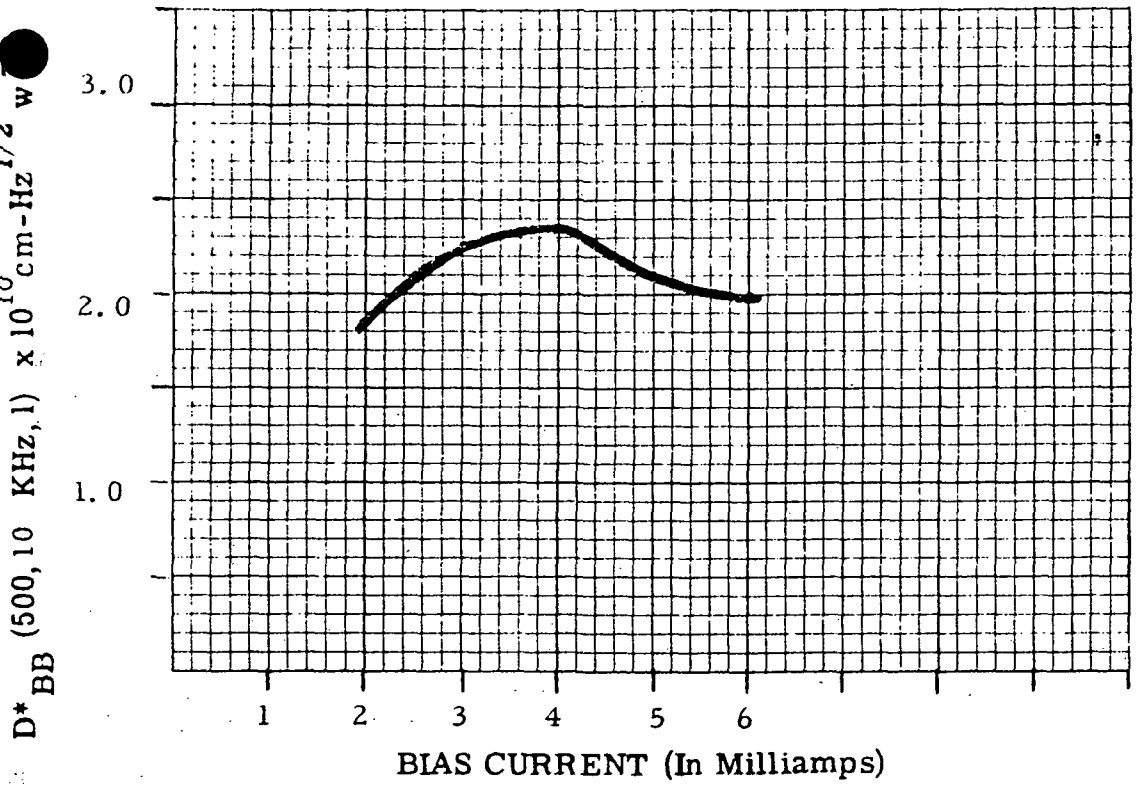

2.5 Relative Spectral Response at 100°K

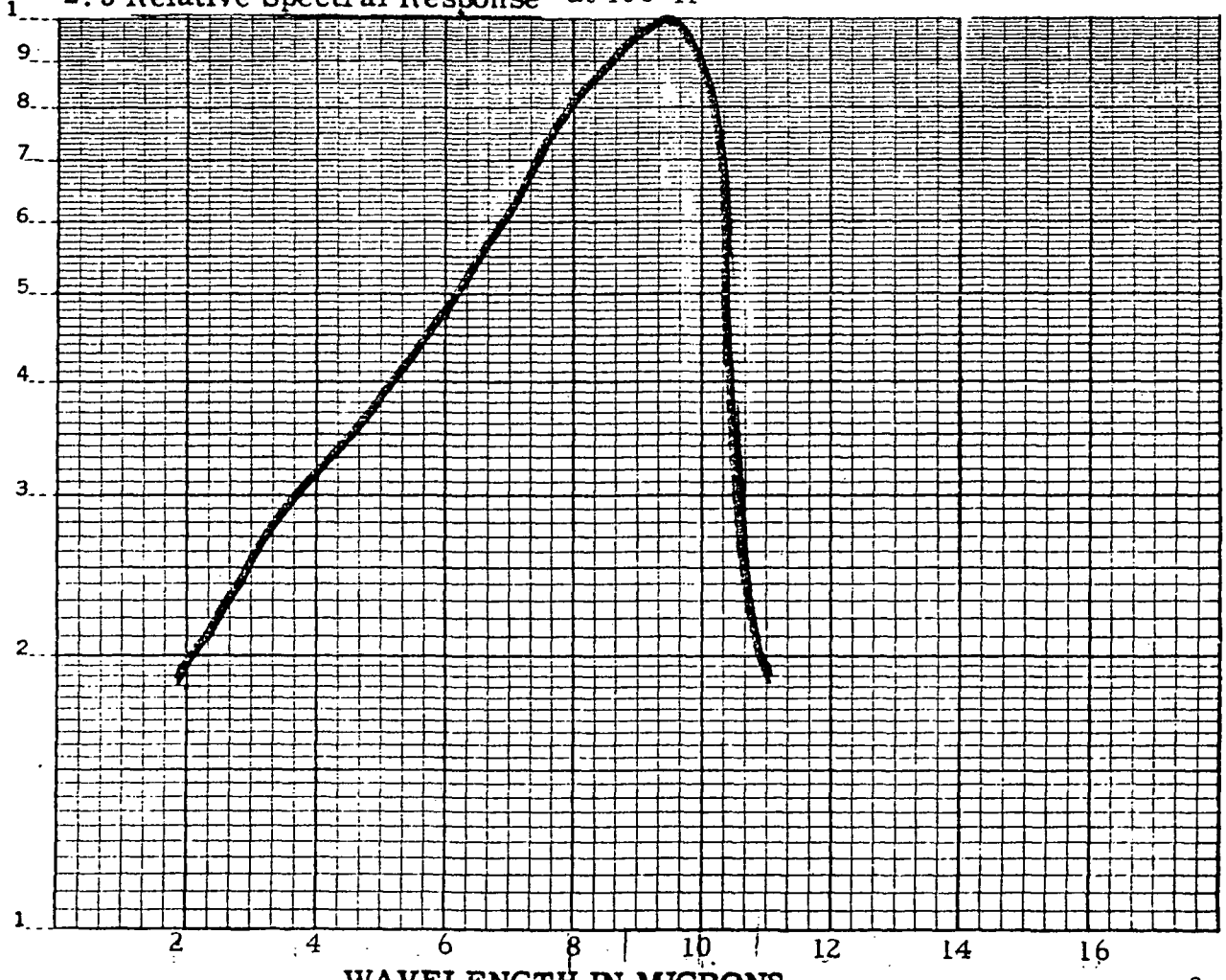

FIGURE 3.0-3 SWL DETECTOR D*, SPECTRAL RESPONSE

2.6 D* vs Bias at 100°K

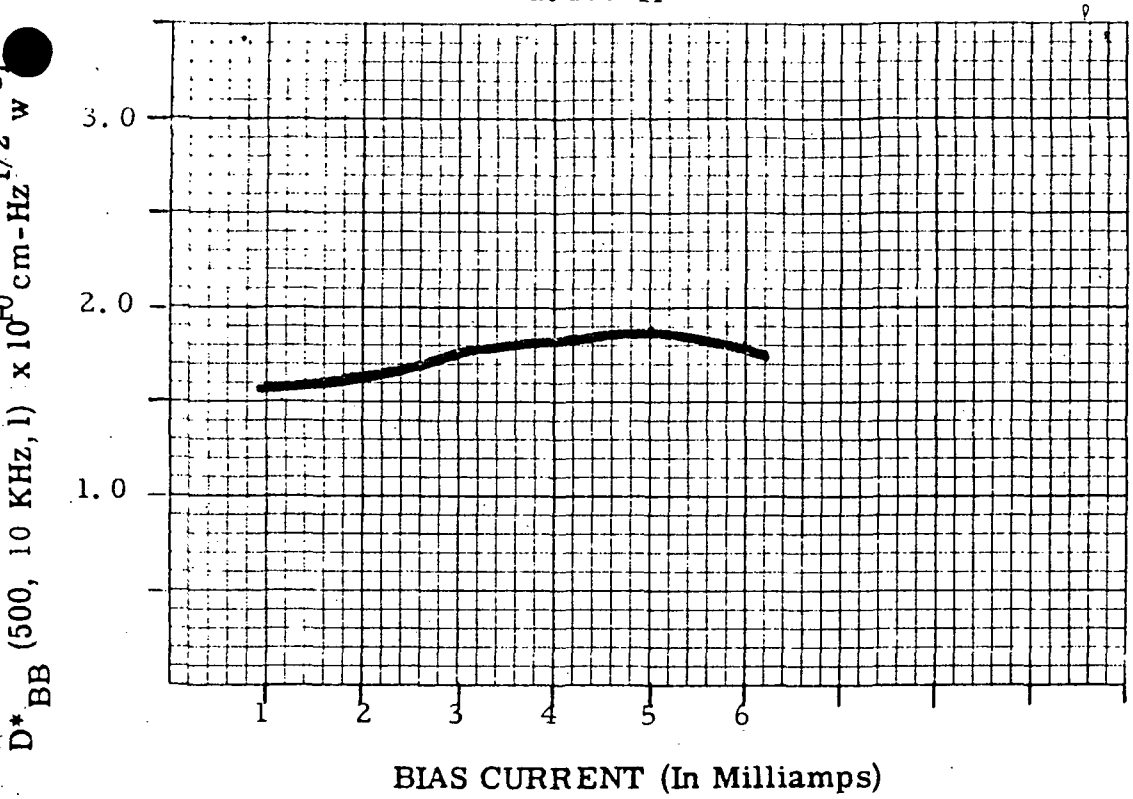

2.5 Relative Spectral Response at 100°K

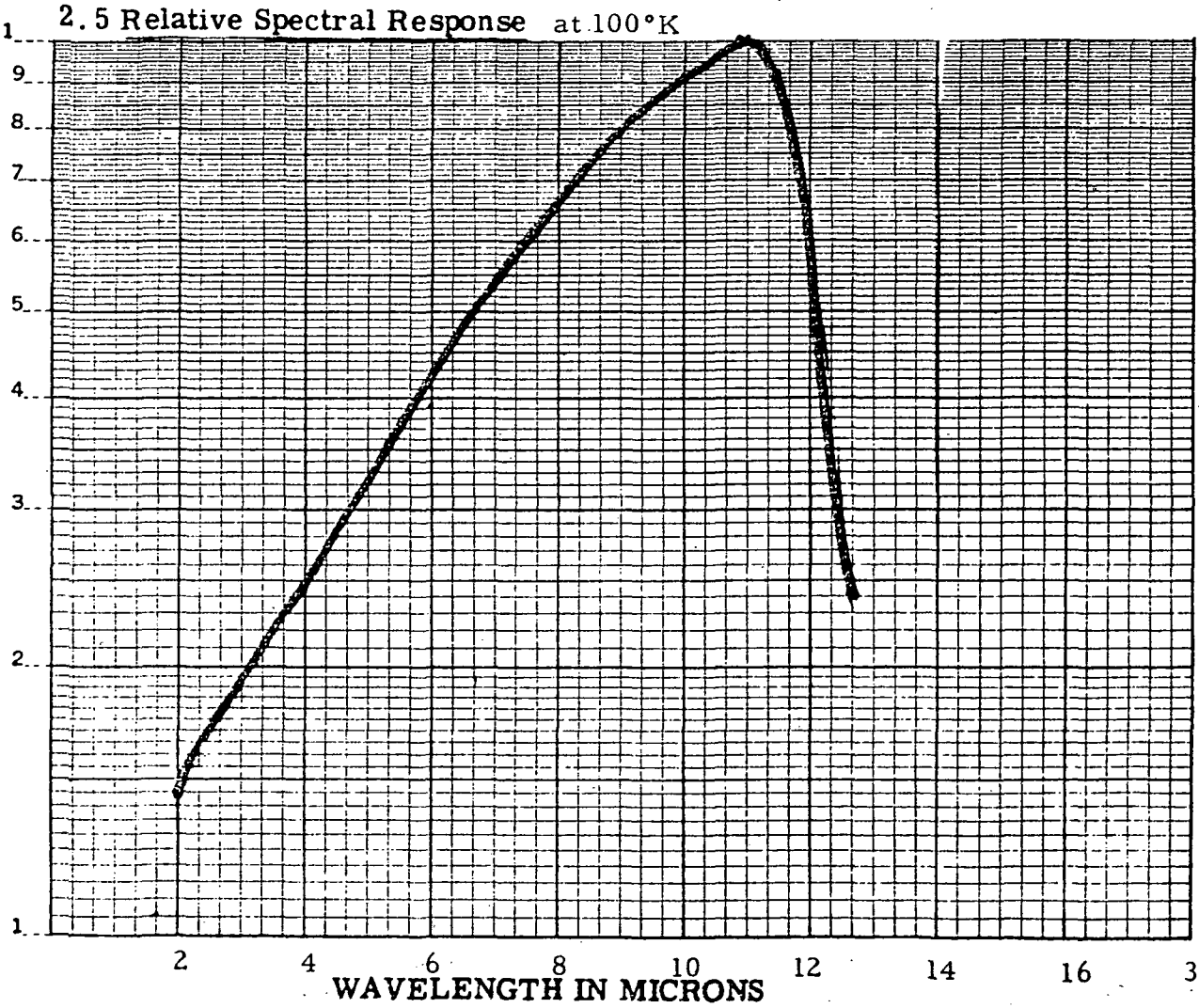

FIGURE 3.0-4 LWL Detector D*, SPECTRAL RESPONSE

Visible Detector

The near IR Channel Detector (0.80 to 1.10 microns) is a silicon photodiode. The photodiode is packaged along with a preamplifier in a TO-5 package with a window. Guard ring construction is used to reduce leakage current and the unit is similar to the EG&G Type HAD-130.

The effective focal length of the near infrared channel is 11.17 inches so that a detector with a sensitive area of 0.0067" by 0.0067" is required to produce the IFOV of 0.6 m.r. by 0.6 m.r. This corresponds to an f-number of 1.39 for this channel. The parabolic focusing mirror which focuses the energy onto the silicon photodiode has a focal length of 1.39 inches and has an evaporated aluminum reflective coating with silicon monoxide protective overcoat. The near infrared filter transmission characteristics are given in Figure 5.6-9, p. 5-36; the coatings are proprietary to O.C.L.I. The beam-splitter which reflects the two far infrared channels but transmits the near infrared is a flat glass substrate with a thin layer of gold evaporated on one side; characteristics are given in Section 5.6.2, p. 5-26.

Measured data for Spectral Response, Noise, NEP and off-set voltage for the SCMR Flight Model Detector is shown in Tables 3.0-5 and 3.0-6.

Signal Processing

Instrument signal processing of the IR data begins in the pre-amplifier assembly which provides voltage gain, injects the space clamp reference and injects a voltage calibration signal to provide a means to monitor the stability of the voltage gain of the amplifier stages. Restoration of the space clamp is accomplished once every rotation of the scanner and is held for the duration of the scan.

Signal processing is completed in the post amplifier assembly which provides additional gain, synchronization pulses, output calibration for monitoring the stability of the spacecraft data link and a low output impedance unity gain buffer to provide an analog signal at the video interface connector with a line structure as shown in Figure 7.1-2 of the Electrical system description.

Visible Data Channel

Signal processing of the visible data begins in the visible pre-amplifier which is an integral part of the visible detector assembly. The detector assembly is illustrated in Figure 3.0-5. Signal processing is completed in the visible post-amplifier assembly in much the same manner as the IR data, the exception being that in place of Blackbody Temperature telemetry, an internal visible calibration target is inserted into the data line structure.

Visible analog data can be substituted for CH 1 SWL data of the video interface connector upon execution of ground command.

EG&G

ITT II

TEST REPORT SHEET 8.1.3.

SPECTRAL RESPONSE

			ATP. REF.
ID	PART NUMBER:		
	DEVICE SERIAL NUMBER: 11A (D100E; 02111-1-517)		8.1.3.5.
	EG&G JOB NUMBER: 2-H78-01		
CAL	BARNES CHOPPER	Cal #: N/R Cal Due Date: On request	8.1.3.4.
	PRECISION POWER SUPPLY	Cal #: N/A Cal Due Date: N/A	
	~~TAU PHASE LOCK~~ AMPLIFIER QUAN TECH	Cal #: 1954 Cal Due Date: 2-26-72	
	POWER SUPPLIES	Cal #: N/R Cal Due Date: N/R	

DATA

λ (μ)	V_{pSTD} (mV)	V_{psref} (↑)	V_{pDUT} (mV)	V_{pDref} (↑)	K	S @ λ (a/w)	
0.4	0.051		0.019			0.002	
0.45	0.078		0.32			0.063	
0.5	0.29		2.10			0.153	
0.55	0.24		1.75			0.197	
0.6	0.40		3.20			0.245	8.1.3.13
0.65	0.54		4.60			0.288	8.1.3.14
0.7	0.67	N/A	5.50	N/A	3.44×10^3	0.319	8.1.3.19
0.75	0.75		6.20			0.349	8.1.3.20
0.8	0.91		7.60			0.386	8.1.3.24
0.85	1.30		9.45			0.360	
0.9	1.11		7.40			→ 0.356 ←	
0.95	1.23		6.55			0.298	
1.0	1.59		5.90			0.188	
1.06	0.59		1.81			0.064	
1.1	0.255	↓	0.73	↓		0.018	

SIG.	Test Executor: Ken Pearson	Test Engineer: 10/19/71	8.1.3.5.
	Date: 19 October 1971	Temp: 23 °C	8.1.3.3.

TABLE 3.0-3 VISIBLE DETECTOR SPECTRAL RESPONSE

EG&G

ITT II

TEST REPORT SHEET 7.1.3., 9.1.3.

NOISE, NEP, OFFSET VOLTAGE

				ATP. REF.
ID	PART NUMBER:			7.1.3.4. 9.1.3.4.
	DEVICE SERIAL NUMBER: 11A (DIODE: 02111-1-517)			
	EG&G JOB NUMBER: - 2-H78-01			
CAL	TEST FIXTURE	Cal # N/R	Due Date N/R	7.1.3.4. 9.1.3.4.
	5459/454 SCOPE	Cal # 948	Due Date 12-1-71	
	HARRISON POWER SUPPLY	Cal # N/A	Due Date N/A	
	HP POWER SUPPLY	Cal # N/A	Due Date N/A	
	WAVE ANALYZER	Cal # 7159	Due Date 2-17-72	
	KEITHLEY AMPLIFIER	Cal # 2351	Due Date 2-25-72	

DATA

NOISE

f(Hz)	Δf(Hz)	V_N(μv)	Rf(MΩ)	In	
1 K	10	0.58	2.0	0.29 pa	9.1.3.11
2 K	10	0.62	2.0	0.31 pa	
4 K	10	0.58	2.0	0.29 pa	
7 K	10	0.64	2.0	0.32 pa	
10 K	10	0.62	2.0	0.31 pa	
20 K	10	0.62	2.0	0.31 pa	
50 K	10	0.75	2.0	0.38 pa	
100 K	10	0.76	2.0	0.38 pa	
4 K	1 K	5.4	2.0	2.7 pa *	

NEP: $NEP = \frac{I_n^*}{S.9.\mu} \times 7.0$ NEP = 5.31 X10^{-11} watts — 9.1.3.15

OFFSET: E_{OS} = − 0.002 volts (indicate polarity) — 7.1.3.8.

SIG DT

DATE: 19 OCT 1971 TEMP: 23°C — 7.1.3.3. 9.1.3.3.

TEST EXECUTOR: K. Pearson TEST ENGINEER 10/19/71 — 7.1.3.4. 9.1.3.4.

TABLE 3.0-4 VISIBLE DETECTOR NOISE, NEP, OFFSET VOLTAGE

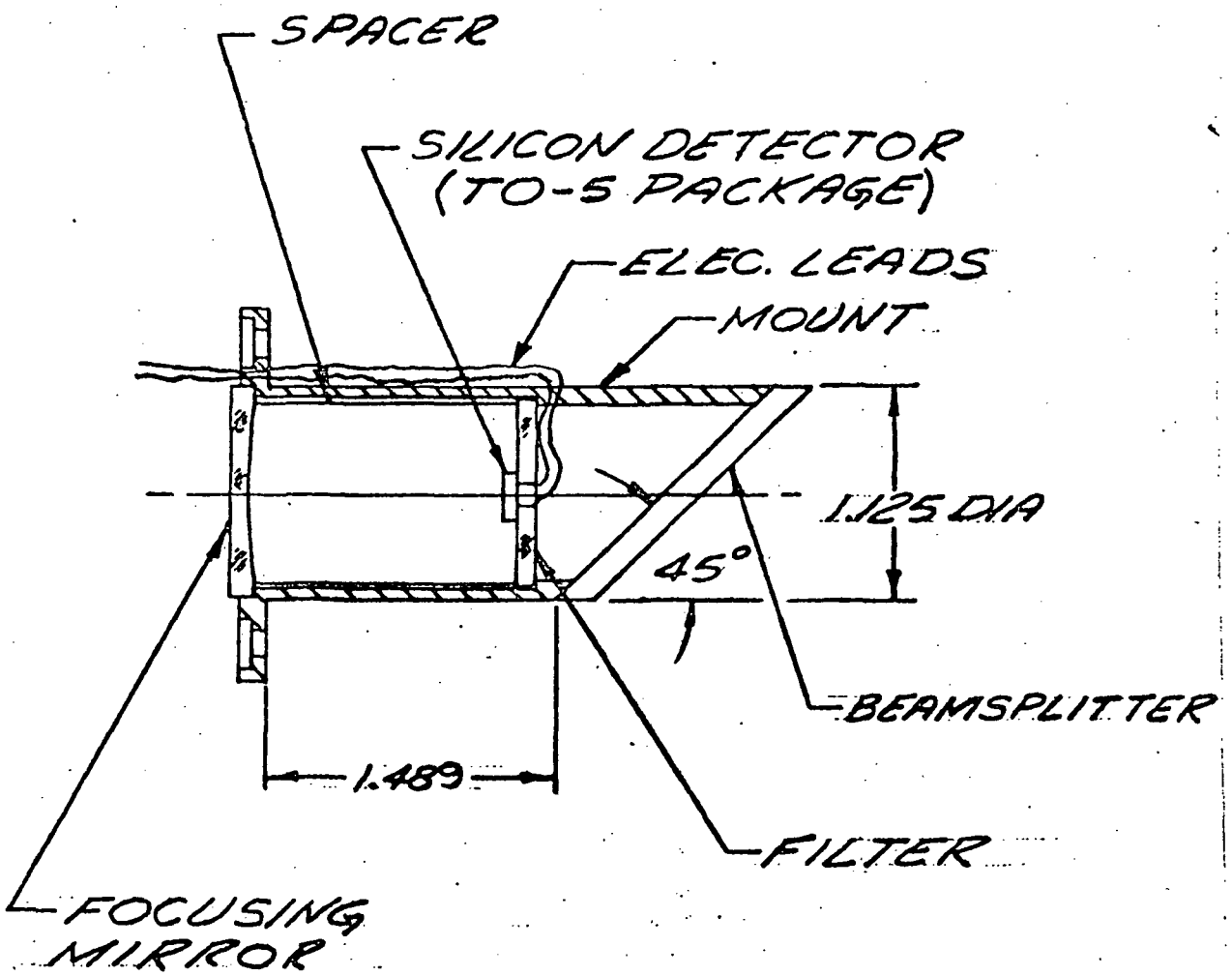
SPACER
SILICON DETECTOR
(TO-5 PACKAGE)
ELEC. LEADS
MOUNT
1.125 DIA
45°
BEAMSPLITTER
1.489
FILTER
FOCUSING
MIRROR

FIGURE 3.0.5

4.0 SCANNER DESCRIPTION

The SCMR Scanner is shown schematically in Figure 4.0-1. The scanner consists of a scan motor, shaft, bearings, mirror, balance weights, oil reservoir and housing.

The scan motor is an 80-pole hysteresis, synchronous motor which rotates at 10 Hz. The motor drives the scan mirror directly with no gear passes. It is a dual power level motor and develops 4.25 in. oz. torque at 24 Volts and 1.0 in. oz. torque at 15 Volts. Torque curves for the serial number 003 motor used in the SCMR Flight Model is shown in Figures 4.0-2 and 4.0-3.

Two different bearings are used in the scanner. A preloaded duplex set is used on the mirror end of the shaft for stability. On the motor end of the shaft, a single bearing is used. The single bearing is allowed to float on the shaft in order to compensate for differences in thermal expansion.

The SCMR Flight Motor Bearings are:

Duplex	8113937-2 Rev. B	Serial No. 006
Single	8113936-1 Rev. B	Serial No. 001A

Drawings of these bearings are shown in Figures 4.0-4 and 4.0-5, respectively. Both bearings were cleaned in hot chloroform and lubricated at GSFC in January of 1972. Data received from GSFC indicates that the S/N 006 bearing retained 0.0354 gms and .0343 gms of F-50 Versilube for the front and rear, respectively. The S/N 001A bearing retained .0193 gms of F-50.

Jitter tests were run at ITT using the two bearings in March 1972. Copies of the test printout are included in this report as Table 4.0-1.

The momentum compensator used on the SCMR Flight Model was S/N 002. This unit had been modified with the necessary design changes required to withstand vibration tests (see SCMR Quarterly Report 10 for the period 1 May 1972 to 1 August 1972).

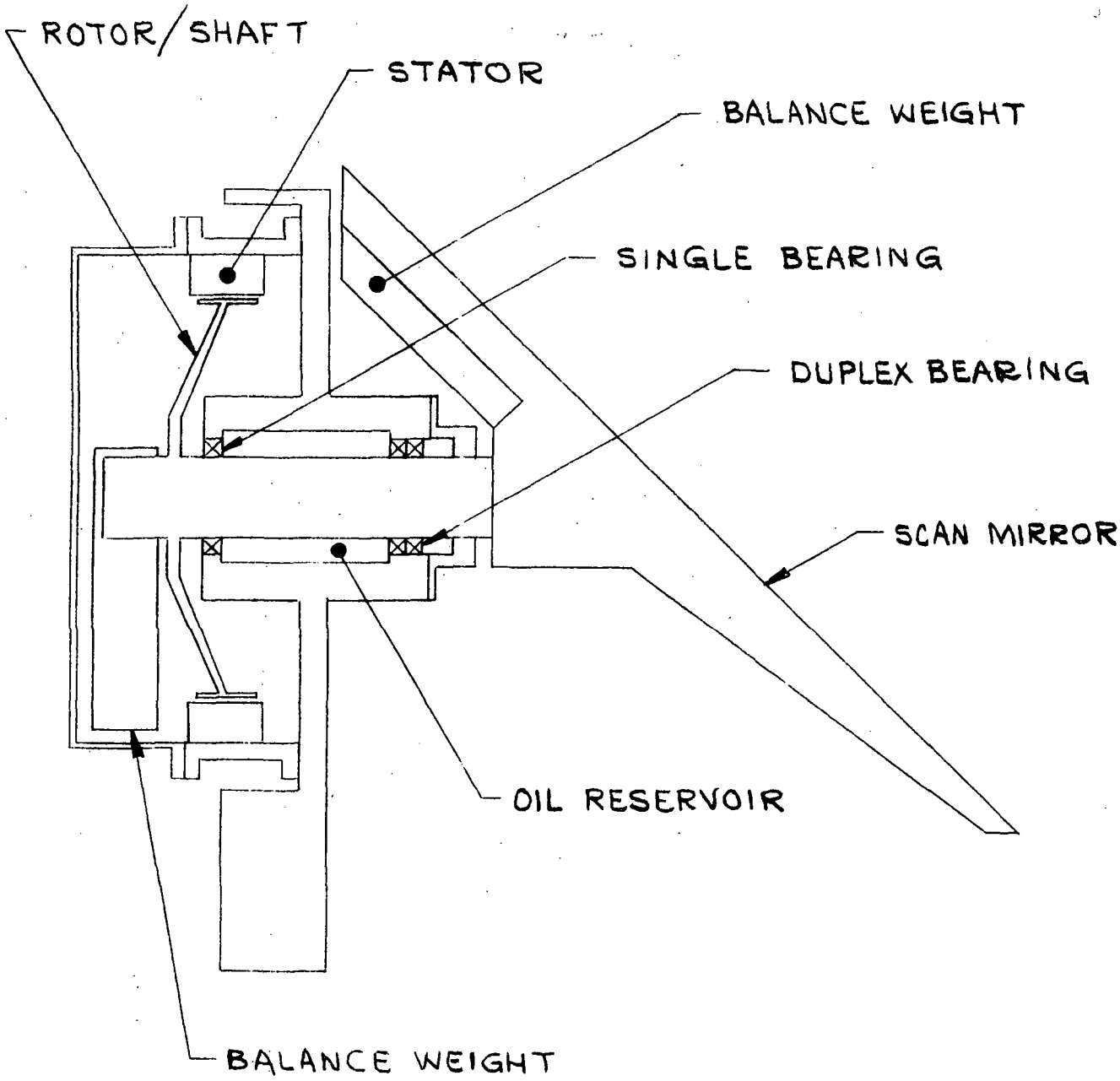

SCMR SCAN MOTOR

Figure 4.0-1

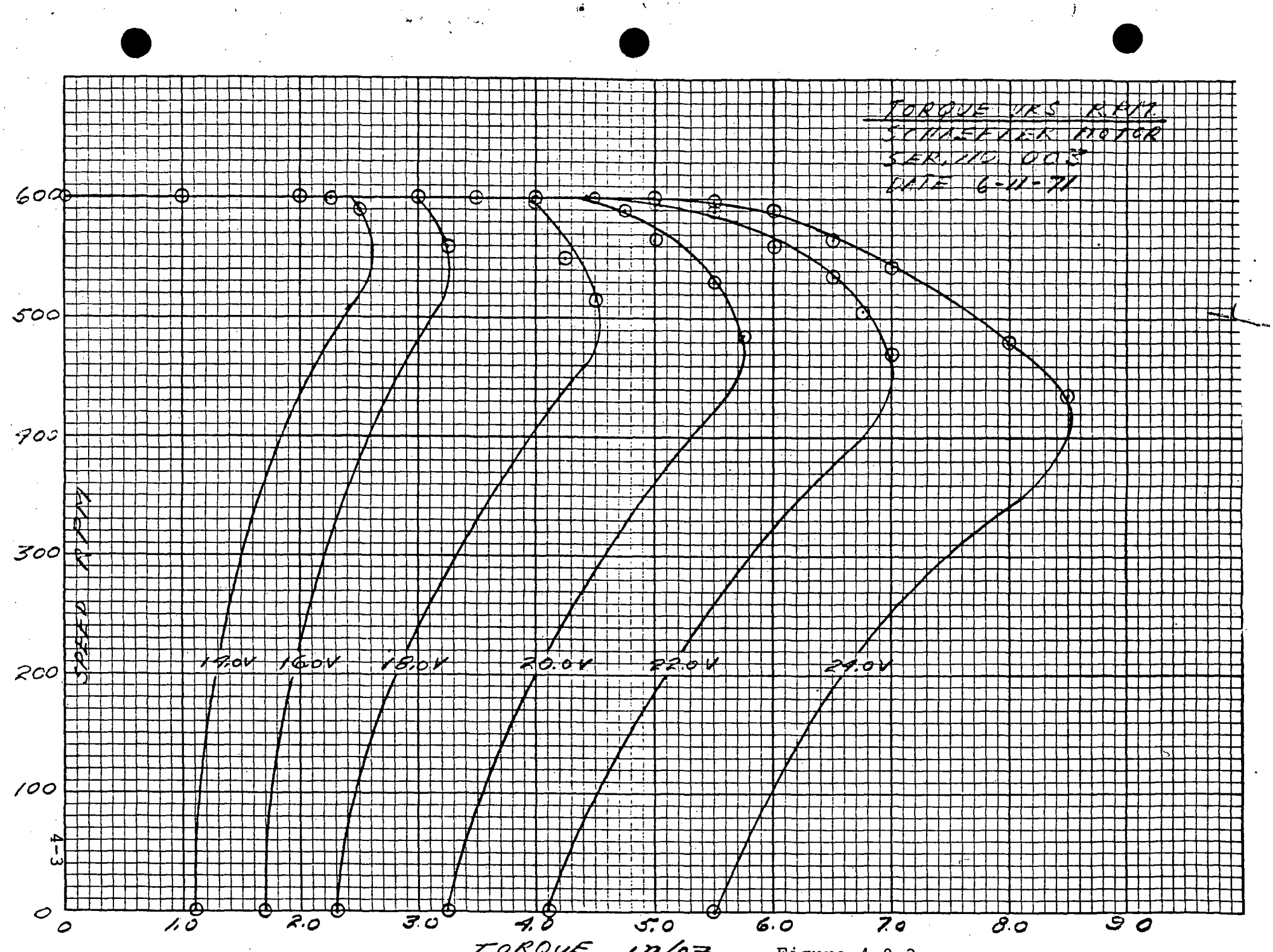
TORQUE VRS R.P.M.
STRATEGIC MOTOR
SER. NO. 0033
DATE 6-11-71
600
500
400
300
200
100
0
SPEED R.P.M.
12.0V
16.0V
18.0V
20.0V
22.0V
24.0V
0
1.0
2.0
3.0
4.0
5.0
6.0
7.0
8.0
9.0
TORQUE IN/OZ.

Figure 4.0-2

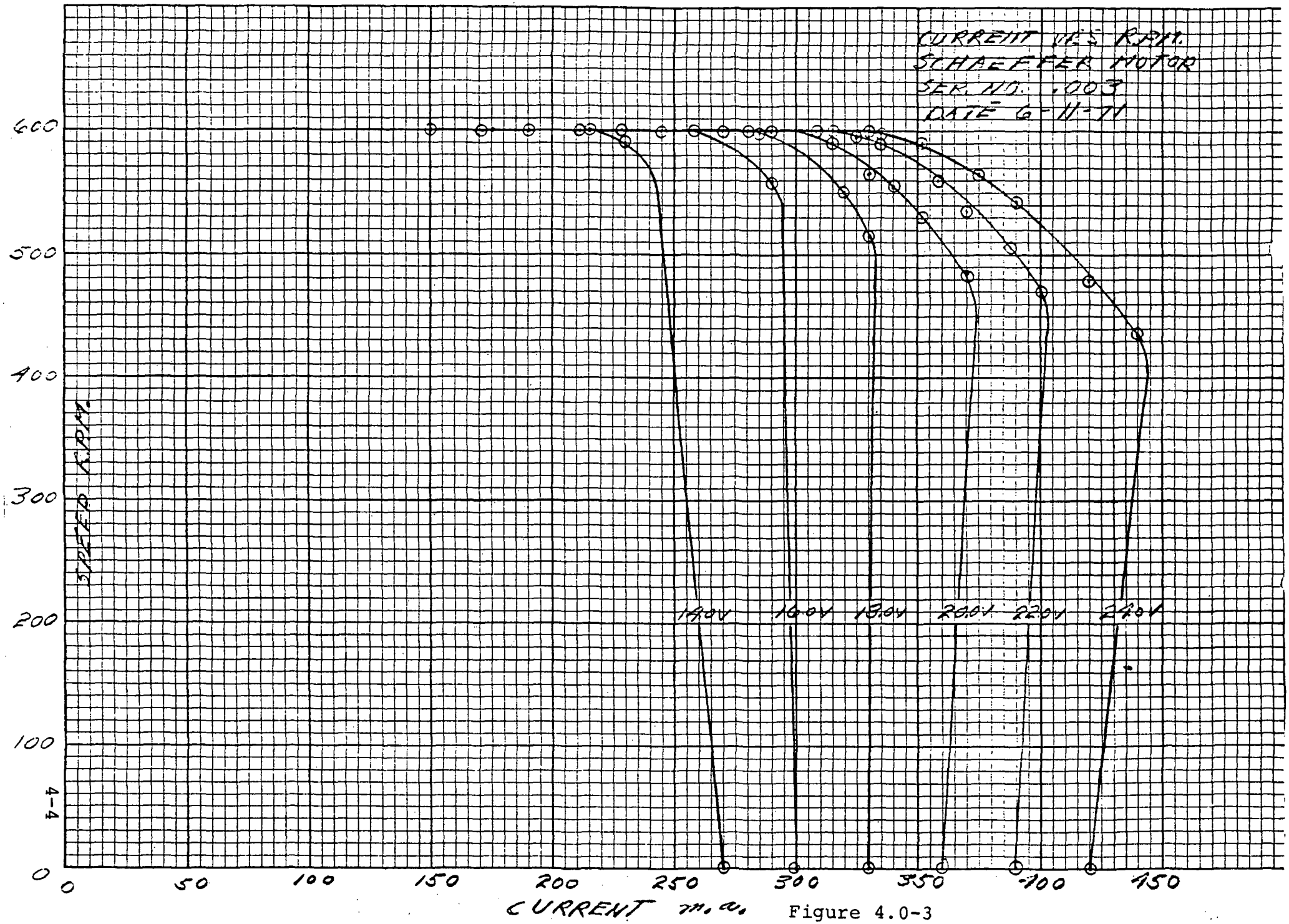
CURRENT VS R.P.M.
SCHAEFFER MOTOR
SER. NO. .003
DATE 6-11-11
14.0V
16.0V
18.0V
20.0V
22.0V
24.0V
SPEED R.P.M.
CURRENT m.a.
0
100
200
300
400
500
600
50
150
250
350
450

Figure 4.0-3

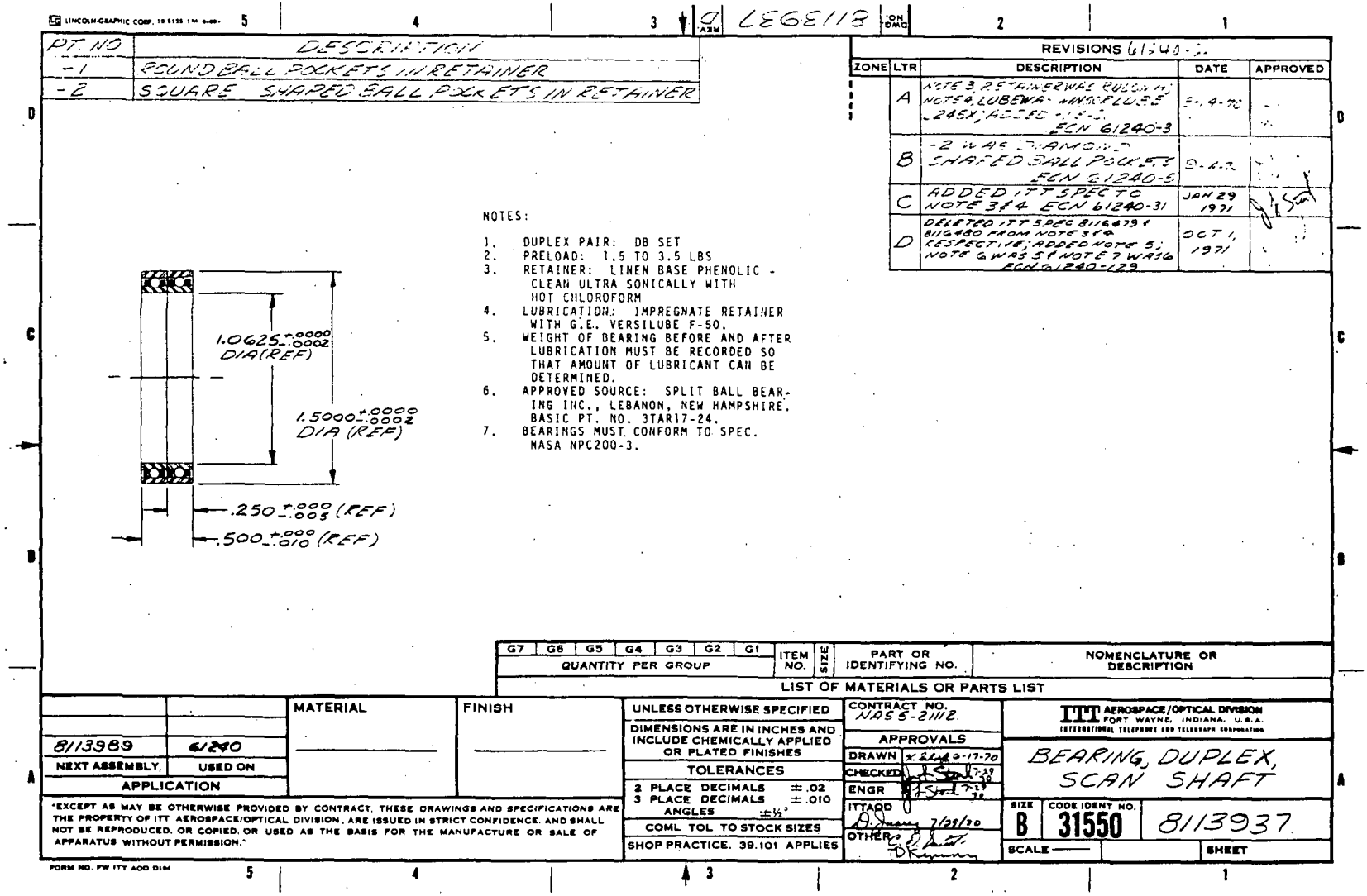
LEGEND
PT. NO | DESCRIPTION
-1 | ROUND BALL POCKETS IN RETAINER
-2 | SQUARE SHAPED BALL POCKETS IN RETAINER
REVISIONS
ZONE | LTR | DESCRIPTION | DATE | APPROVED
A | NOTE 3, RETAINER WAS ROLLON #1 NOTE 4, LUBEWA - MANSFIELD L-245X, ADDED ECN 61240-3 | 5-4-70
B | -2 WAS DIAMOND SHAPED BALL POCKETS ECN 61240-5 | 9-4-70
C | ADDED ITT SPEC TO NOTE 3 & 4 ECN 61240-31 | JAN 29 1971
D | DELETED ITT SPEC 81164379 & 81164380 FROM NOTE 3 & 4 RESPECTIVELY, ADDED NOTE 5; NOTE 6 WAS 5 & NOTE 7 WAS 6 ECN 61240-129 | OCT 1, 1971
NOTES:
1. DUPLEX PAIR: DB SET
2. PRELOAD: 1.5 TO 3.5 LBS
3. RETAINER: LINEN BASE PHENOLIC - CLEAN ULTRA SONICALLY WITH HOT CHLOROFORM
4. LUBRICATION: IMPREGNATE RETAINER WITH G.E. VERSILUBE F-50.
5. WEIGHT OF BEARING BEFORE AND AFTER LUBRICATION MUST BE RECORDED SO THAT AMOUNT OF LUBRICANT CAN BE DETERMINED.
6. APPROVED SOURCE: SPLIT BALL BEARING INC., LEBANON, NEW HAMPSHIRE, BASIC PT. NO. 3TAR17-24.
7. BEARINGS MUST CONFORM TO SPEC. NASA NPC200-3.
1.0625 +.0000 -.0002 DIA (REF)
1.5000 +.0000 -.0002 DIA (REF)
.250 +.000 -.005 (REF)
.500 +.000 -.010 (REF)
LIST OF MATERIALS OR PARTS LIST
G7 G6 G5 G4 G3 G2 G1 QUANTITY PER GROUP | ITEM NO. | SIZE | PART OR IDENTIFYING NO. | NOMENCLATURE OR DESCRIPTION
8113989 | 61240
NEXT ASSEMBLY | USED ON
APPLICATION
MATERIAL
FINISH
UNLESS OTHERWISE SPECIFIED
DIMENSIONS ARE IN INCHES AND INCLUDE CHEMICALLY APPLIED OR PLATED FINISHES
TOLERANCES
2 PLACE DECIMALS ±.02
3 PLACE DECIMALS ±.010
ANGLES ±½°
COML TOL TO STOCK SIZES
SHOP PRACTICE. 39.101 APPLIES
CONTRACT NO. NAS 5-21112
APPROVALS
DRAWN 6-17-70
CHECKED 7-29-70
ENGR 7-29-70
ITTADD 7/29/70
OTHER
ITT AEROSPACE/OPTICAL DIVISION FORT WAYNE, INDIANA, U.S.A.
BEARING, DUPLEX, SCAN SHAFT
SIZE B | CODE IDENT NO. 31550 | 8113937
SCALE | SHEET
"EXCEPT AS MAY BE OTHERWISE PROVIDED BY CONTRACT, THESE DRAWINGS AND SPECIFICATIONS ARE THE PROPERTY OF ITT AEROSPACE/OPTICAL DIVISION, ARE ISSUED IN STRICT CONFIDENCE, AND SHALL NOT BE REPRODUCED, OR COPIED, OR USED AS THE BASIS FOR THE MANUFACTURE OR SALE OF APPARATUS WITHOUT PERMISSION."
FORM NO. FW ITT ADD DIM

Figure 4.0-4

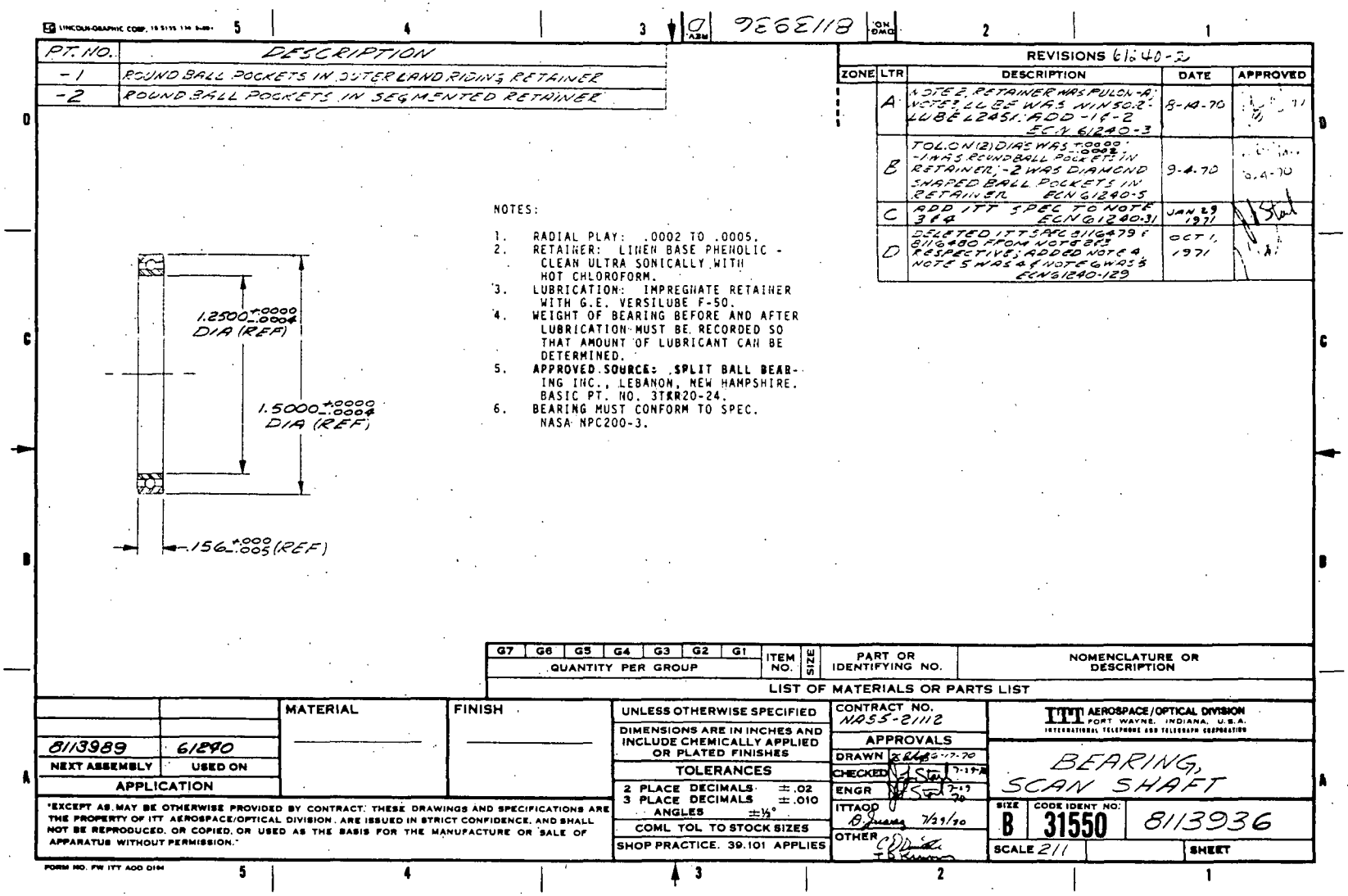
PT. NO.
DESCRIPTION
-1
ROUND BALL POCKETS IN OUTER LAND RIDING RETAINER
-2
ROUND BALL POCKETS IN SEGMENTED RETAINER
REVISIONS 61240-3
ZONE
LTR
DESCRIPTION
DATE
APPROVED
A
NOTE 2 RETAINER WAS PULON-A; NOTE 3 LUBE WAS MIN 50:2-LUBE L2451. ADD -1 & -2 ECN 61240-3
8-14-70
B
TOL ON (2) DIAS WAS ±.0005 -1 WAS ROUND BALL POCKETS IN RETAINER, -2 WAS DIAMOND SHAPED BALL POCKETS IN RETAINER ECN 61240-5
9-4-70
C
ADD ITT SPEC TO NOTE 3 & 4 ECN 61240-31
JAN 29 1971
D
DELETED ITT SPEC 81164791 81164801 FROM NOTES 3 & 4 RESPECTIVELY; ADDED NOTE 4. NOTE 5 WAS 4 & NOTE 6 WAS 5 ECN 61240-129
OCT 1, 1971
1.2500 +.0000 -.0004 DIA (REF)
1.5000 +.0000 -.0004 DIA (REF)
.156 +.000 -.005 (REF)
NOTES:
1. RADIAL PLAY: .0002 TO .0005.
2. RETAINER: LINEN BASE PHENOLIC - CLEAN ULTRA SONICALLY WITH HOT CHLOROFORM.
3. LUBRICATION: IMPREGNATE RETAINER WITH G.E. VERSILUBE F-50.
4. WEIGHT OF BEARING BEFORE AND AFTER LUBRICATION MUST BE RECORDED SO THAT AMOUNT OF LUBRICANT CAN BE DETERMINED.
5. APPROVED SOURCE: SPLIT BALL BEARING INC., LEBANON, NEW HAMPSHIRE. BASIC PT. NO. 3TRR20-24.
6. BEARING MUST CONFORM TO SPEC. NASA NPC200-3.
G7 G6 G5 G4 G3 G2 G1
QUANTITY PER GROUP
ITEM NO.
SIZE
PART OR IDENTIFYING NO.
NOMENCLATURE OR DESCRIPTION
LIST OF MATERIALS OR PARTS LIST
8113989
NEXT ASSEMBLY
61240
USED ON
APPLICATION
MATERIAL
FINISH
UNLESS OTHERWISE SPECIFIED
DIMENSIONS ARE IN INCHES AND INCLUDE CHEMICALLY APPLIED OR PLATED FINISHES
TOLERANCES
2 PLACE DECIMALS ±.02
3 PLACE DECIMALS ±.010
ANGLES ±½°
COML TOL TO STOCK SIZES
SHOP PRACTICE 39.101 APPLIES
CONTRACT NO. NAS5-21112
APPROVALS
DRAWN
CHECKED
ENGR
ITTAOD
OTHER
ITT AEROSPACE/OPTICAL DIVISION
FORT WAYNE, INDIANA, U.S.A.
INTERNATIONAL TELEPHONE AND TELEGRAPH CORPORATION
BEARING, SCAN SHAFT
SIZE B
CODE IDENT NO. 31550
8113936
SCALE 2/1
SHEET
"EXCEPT AS MAY BE OTHERWISE PROVIDED BY CONTRACT: THESE DRAWINGS AND SPECIFICATIONS ARE THE PROPERTY OF ITT AEROSPACE/OPTICAL DIVISION, ARE ISSUED IN STRICT CONFIDENCE, AND SHALL NOT BE REPRODUCED, OR COPIED, OR USED AS THE BASIS FOR THE MANUFACTURE OR SALE OF APPARATUS WITHOUT PERMISSION."
FORM NO. FW ITT AOD 0164

Figure 4.0-5

TABLE 4.0-1 BEARING JITTER

TEST DATE 3-28-72

BEARING SER # 006
001A

NUMBER OF SAMPLES = 100

PEAK/PEAK JITTER = 8μsec.

LINE/LINE JITTERμsec	# OF OCCURENCES
0 μsec	34
1 μsec	48
2 μsec	8
	100

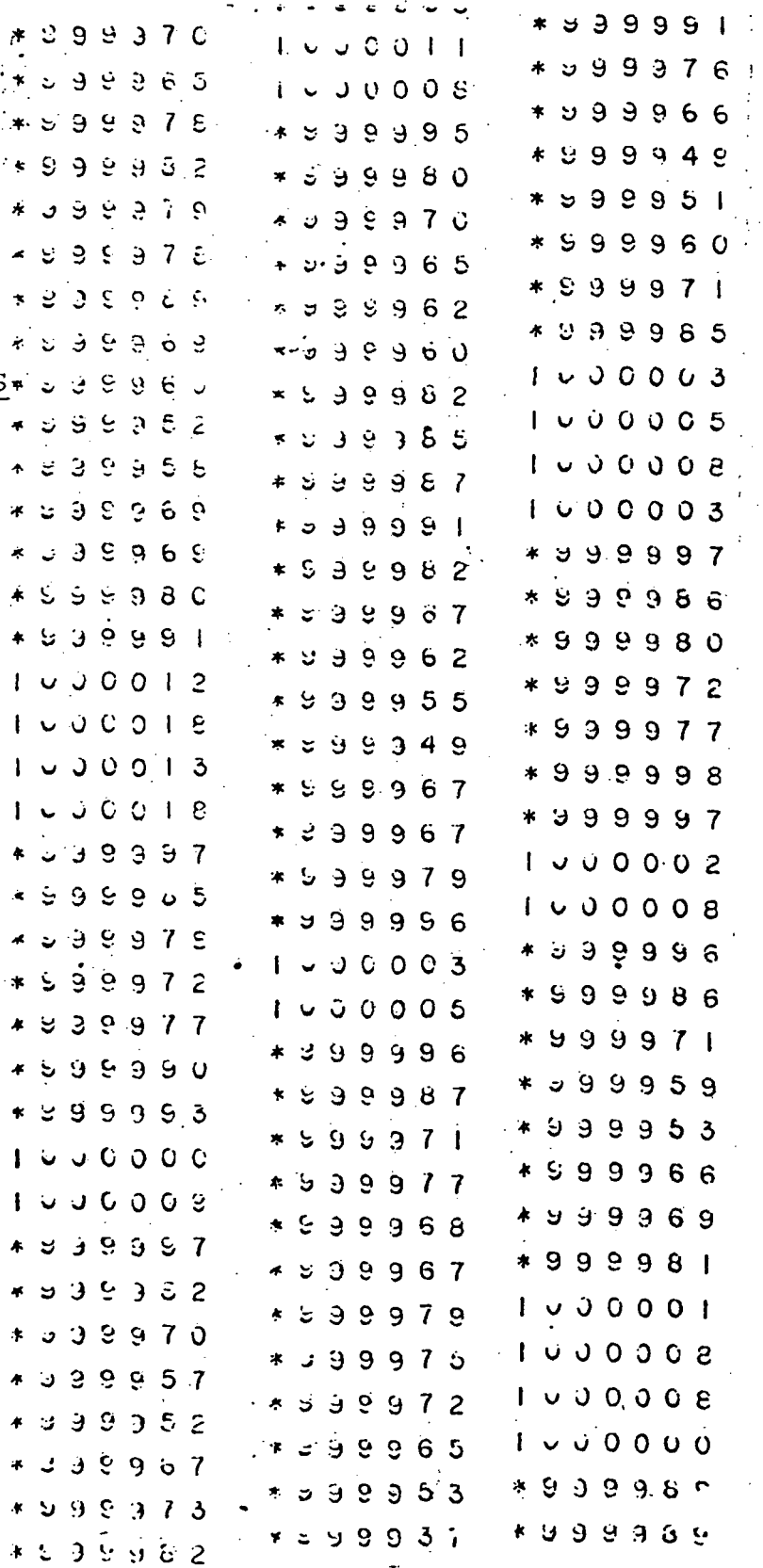

5.0 OPTICS DESCRIPTION

The SCMR optical subsystem is best described in the Final Design Review report written by Ferson Optics and dated June 15, 1972. This report is included in this report on the following pages (Section 5.6).

A schematic illustration of the optical layout is given in Figure 3.0-1 and a general description of the methods used to focus the optical beam and divide it into the three channels is given in Section 3.0. The three spectral bands are 0.8 to 1.0 μm, 8.3 to 9.3 μm and 10.2 to 11.2 μm.

5.1 Technical Description

The optical system for the SCMR is catadioptric, collecting with an afocal reflecting telescope and focusing with refractive elements at the detectors. To project the required 0.6 by 0.6 milliradian field of view on the 0.10 mm by 0.10 mm square detector, a focal length of 167 mm, or 6.562 inches, is required, indicating a total system operating at an effective f-number of f/0.82.

The collecting telescope is a modified Dall-Kirkham configuration operating afocally at a speed of f/0.92. It reduces the beam diameter from 8 inches to 1 inch and folds the far infrared beam to the side with the flat, transparent gold beam splitter. The Dall-Kirkham type was chosen because of theoretical performance over the limited field, ease of manufacture and testing, and cost.

After separation spectrally by the infrared dichroic beamsplitter outside the telescope, the 1 inch diameter beams are focused on their respective detectors. Focusing was achieved by moving the larger germanium focusing lens in each leg. The focusing lenses operate at about f/3.2. After passing through a window and filter the beam is focused on the detector by a germanium aplanat operating through a thin window.

Reflecting optics were manufactured of CERVIT for thermal insensitivity. Cooler windows were made of Irtran II and lenses and infrared dichroic of optical grade germanium, accurate to 1/10 wave at the wavelengths used.

Housing of the primary telescope is critical because of the f/numbers involved. An invar tube was used to separate the primary and secondary mirrors. More conventional materials were used to house the focusing optics because of relative insensitivity to temperature defocusing.

The beam transmitted through the transparent gold beam-splitter (between the primary and secondary telescope mirrors) then passed through an optical filter which transmitted energy only for wavelengths longer than 0.8 μm. A parabolic mirror then focused the energy onto the silicon detector which was insensitive to energy with wavelengths greater than about 1.0 μm.

5.2 Flight Model Changes

Several changes were made to the flight model optical sub-assembly in an attempt to increase the percentage of energy collected within one geometric IFOV (instantaneous field of view). These included:

1. Rework of the telescope mounting interface with the instrument structure to eliminate distortions caused by the original mounting arrangement,

2. Removal of the germanium wedges used in the 8.3 to 9.3 μm channel, and

3. Repolish of the scan mirror to achieve a flatter reflecting surface.

The telescope mount was changed to a three-point type arrangement so that no stresses would be introduced into the telescope mirrors or associated structure. This proved to be very worthwhile and much smaller blur spot images were observed when the telescope was firmly bolted into the instrument structure.

The germanium wedges used to register or align the two far infrared channels were removed because it was possible to direct the beam into the focusing germanium lenses at an angle considerably off of the optical axes of these lenses using the wedges. Instead, channel registration was accomplished by adjusting the position of the focus lens in an X-Y plane normal to the lens optical axis. Some vignetting could occur with this technique but at least the optical beam would be parallel to the optical axis as designed.

The scan mirrors were procured from Speedring Systems Div. of Schiller Industries. They reported that the scan mirrors could be polished flat within specification but that after setting for a day or two the flatness had changed so that it was not within specification. After several repolishes to restore the flatness, and subsequent changes to out-of-spec flatness, they reported that the stresses introduced by the balance weights attached to the mirror were slowly relieving and causing the mirror to distort. The flight model scan mirror was taken to Surfaces Finishes Inc., Addison, Ill. for repolish since they had been doing some nice polishing on metal parts for our radiant coolers. Surfaces Finishes was able to polish a flatter reflecting surface on the mirror than Speedring and it did not appear to change significantly with time.

In spite of the above changes, the performance of the SCMR instrument (i.e. percentage signal from one geometric IFOV) was approximately the same as that of the prototype model. The conclusion was that the optical performance was limited by the basic optical design. A review of the design was made by Ferson Optics and is given in Section 5.6. A calculation of expected energy collection is given in Section 5.5.

5.3 Final Optical Design Review

As part of the rework of the flight model optics, Ferson Optics performed a reanalysis of the design. A copy of their report is given on the following pages (Section 5.6).

5.4 Acceptance Test Procedure

A summary of the SCMR flight model optics tests is shown in Table 5.4-1.

The Optical Subassembly test procedures and measured results are given on the following pages.

5.5 Field of View

The instrument specification states that 85% of the energy within one geometric IFOV shall fall on the detector sensitive surface. For measurement purposes this was taken to mean that the signal from the preamplifier (i.e. before electronic filtering) when scanning a hot aperture equal to one IFOV located in the focal plane of a 9.0 inch clear aperture diameter collimator should be 85% as large as the signal from an aperture at least five times larger (linear dimension) than one IFOV. This is a very rigid test since such effects as detector time constant must be insignificant.

It can be shown that on the basis of diffraction effects only the signal from a one IFOV target will be approximately 87% (see ITT Technical Proposal for SCMR). This leaves practically no manufacturing errors for optical element fabrication or mounting errors. For a point source at infinity the energy in the central diffraction disc (Airy circle) drops from 85% for a perfect optical system to 68% for an optical system having a total "optical path difference" of $\frac{1}{4}\ \lambda$, the latter representing a well corrected and manufactured system (see Modern Optical Engineering by Warren J. Smith, McGraw-Hill Book Co., p. 298, 1966). Ferson Optical Div. of Bausch and Lamb also estimated the expected energy in one IFOV and state that 65% is a reasonable expectation (see next section for their calculations). Thus, the measured value of about 65% seems to be the best that could have been expected.

TABLE 5.4-1

SUMMARY OF SCMR FLIGHT MODEL OPTICS TESTS

SERIAL NUMBER(1)	2A
ACCEPTANCE TEST PROCEDURE(2)	#909390
DATE TESTED	6-22-72
SIZE OF TEST SOURCE	0.0014" DIA.
DIA. OF SOURCE WHEN IMAGED AT FOCUS OF TEST LENS (WITHOUT ABERRATIONS)	0.00021"
PRIMARY MIRROR ALIGNMENT	<1 min. arc
DIA. OF OBSERVED BLUR SPOT	0.0018"
ALLOWABLE MAX. DIA. OF BLUR SPOT	0.0045"
PENTHOUSE BORESIGHT (MAX. ALLOWABLE 15 min.)	2 min. arc
RADII OF GERMANIUM LENSES:	
PART NO. $909305R_1$	2.919"
PART NO. $909305R_2$	4.524"
PART NO. $909308R_1$	0.183"
PART NO. $909308R_2$	0.150"
SYSTEM FOCAL LENGTH	6.535"
MECHANICAL DIMENSIONS	PER DWG. #8113881
WEIGHT	6.5 LBS.

(1) THE TELESCOPE HAD THE IMPROVED THREE POINT MOUNTING ARRANGEMENT.

(2) A TEST COLLIMATOR WITH A 12" DIAMETER PRIMARY MIRROR AND 192" FOCAL LENGTH WAS USED IN PLACE OF THE 8" DIA., 84" F.L. MIRROR IN ORDER TO PROVIDE A SMALLER TEST SPOT OF LIGHT.

5.5.1 FOV Calculations by Ferson Optics

A series of diffraction response calculations were run and results at various wavelengths from 8.0 to 11.0 microns were plotted. From these point source results calculations were made to predict field of view response.

The system, with a clear aperture of 202.6 mm, has a focal length of 166.7 mm. The nominal 0.6 milliradian field of view subtends 0.100 mm, or 100 microns.

The optical subsystem consists of an afocal reflecting telescope, whose performance can be measured visually, and refracting optics opaque to visible radiation, which remain unknown until IR performance is measured.

The entire optical system theoretically is about ¼ λ at 10μ, and predicted performance shows several clear diffraction rings. Field images are essentially the same as axial over the small field. The general image has all of its energy in 40μ diameter and 70% within 18μ diameter at 10μ wavelength. The polychromatic nature of the radiation tends to smooth the diffraction rings into a triangular form of energy distribution.

Assume for estimation purposes that the theoretical image has an even distribution and a 40μ diameter. This will give the one-dimensional field of view a trapezoidal shape 0.140 mm wide at the base and 0.060 mm wide at the top. This would throw about 10% of the energy out of the 0.100 mm field. When projected on a square format, the percent response reduces to 80.5% due to losses in the other direction as well.

The introduction of errors in the reflecting telescope adds to the system final blur circle. Assume here a circular blur of 0.003 inch diameter as seen in the 3¼ inch test lens through the 8.0 power telescope. The angular blur is then

$$\frac{0.003 \text{ inch}}{3\frac{1}{4} \text{ inches}} \times 8 = 0.000115$$

This is equivalent to a 19μ blur in the final image plane. Assuming a 59μ blur at system focus this gives 72.7% response.

Adding degradation from the additional dichroics, folding mirrors, and germanium optics, a reasonable field of view response would seem to be in the order of 65%.

5.6 Final Design Review

FINAL DESIGN REVIEW
SCMR OPTICAL SUBSYSTEM
FOR

ITT/NASA

PREPARED BY

FERSON OPTICS DIVISION OF BAUSCH AND LOMB

Job Number 9539
June 15, 1972

1.0 SCMR OPTICAL SUBSYSTEM DESIGN PERFORMANCE PREDICTIONS

The optical design consists of an afocal reflecting Dall-Kirkham telescope of eight inch aperture operating at eight power feeding a visible channel and two infra-red channels. The IR channels are folded out by dichoric beamsplitters and focus on small detectors through germanium lenses.

To keep the detectors as small as possible the system operates at an effective focal length of 6.5 inches, about f/0.82. This is accomplished by aplanatic elements close to focus.

The afocal telescope design prediction is about .02 milliradians equivalent blur in object space. It is aligned at assembly to as close to parallel as the components permit, generally .002" blur at an equivalent 25" focal length, or .08 milliradians.

The germanium optics are designed with a slight residual spherical aberration, keeping curves and mounting sensitivities of the first germanium lens low. The aplanat adds very little aberration. Total system aberration prediction is about .0006" diameter blur from geometric aberrations, comparing with a diffraction size of .00062" at 8μ and .00078" diameter at 10μ. The system, then, if properly aligned, should give performance close to the diffraction limit. Chromatic aberration is negligible.

Assuming the system has a total blur diameter of .0006", optimistic because of diffraction effects, 90.9% of the energy from within the field of view falls on the detector. Using the more

reasonable diameter of .0008", equivalent to 10μ radiation, this decreases to about 88.7%. Obviously performance close to the diffraction limit is required. A geometric blur of .0008" diameter in the final image plane is well within manufacturing tolerances.

2.0 COOLER THERMAL EFFECTS

The optical elements in the detector vicinity are cooled to about 110°K during operation. Thermal runs were made to evaluate predicted performance, considering the changes in material index, mechanical spacing, thickness, and radii of curvature. Index shifts and linear coefficients of expansion were taken from "Properties of Infra-red Sensor Materials" by Caren, et al, MATERIAL RESEARCH AND STANDARDS, June 1971.

The chief effect of the thermal simulation was defocussing caused by curve and index shifts in the germanium aplanat. Left unfocussed, these generated a smooth defocus giving a .0030" diameter blur. To correct this the airspace between the focusing lens and aplanat was changed, .011" longer. With the refocus no detectable difference in performance between this condition and nominal design was noted. The effective focal length shifted .066 longer, or by about 1.0%. Chromatic, spherical and field aberrations were identical.

If the system were focussed with the aplanat at room temperature and used with it cooled, there would be a definite focus problem. The blur circle changes about .0001" diameter for every 10°K change in detector/aplanat temperature. If the bench cooler,

test chamber cooler, and actual projected temperature are within 30°K the blur will be less than half the diffraction limit. At present the cooled detector is used, indicating no real problem on SCMR.

A general result of this study indicates that precise measurement of IR focal positions using uncooled detectors in the optical laboratory is subject to error due to thermal defocussing when a cooled aplanat is used. The difference from nominal could be computed and used to refocus, or some focus adjustment should be retained on future similar systems.

3.0 TEST EQUIPMENT PERFORMANCE EFFECTS

If the system, with its focal length of 5.5 inches, is checked by a long focal length collimator, perhaps 190" EFL, the defects of the collimator are demagnified by the ratio of the focal lengths. If the 190" collimator has a .005" diameter blur, the equivalent blur in the IR focal plane is

$$.005" \times \frac{5.5}{190} = .00014"$$

This is about a quarter of the Airy disc diameter, making the test beam diffraction limited in the infra-red.

If the test collimator is misaligned and used off-axis, or the entrance beam is not parallel to the system axis, rather gross errors can occur. In this case, both channels should read equally bad, neglecting diffraction.

4.0 CHANGES IN FUTURE SYSTEMS

In order to improve system resolution in the future with a greater confidence factor in achieving design predictions, the following general recommendations are made:

4.1 Increase the envelope length available for the reflecting telescope. System difficulty, including correction of optical elements and sensitivity to mechanical errors, increases roughly as the inverse cube of the primary mirror f/number. In wide field systems like HIRS, theoretical performance at the field stop edge suffers badly as speed increases, by about the N.A. squared.

4.2 Increase the weight allowance of the optical subsystem and reduce informal pressures for ultra light weight. The rigidity of optical elements, especially mirrors and beamsplitters is a question of degree, with thicker elements being easier to figure to a good accuracy and being more likely to hold that accuracy in mounting. Cells, spacers, and retainers also resist torques and bending if heavier.

4.3 Design the system interface to a pseudo-kinematic configuration, adequately constraining the optical subsystem while not applying forces tending to misalign and skew. Provide complete enough interface drawings to avoid interference. Use a dummy interface during testing to simulate the actual integration.

4.4 Design adjustments in the optical system to have small enough travel not to degrade the final image. Provide reference surfaces on the optical subsystem to align to external sources and to check alignment during assembly. IR components opaque in the visible should be removable as a subassembly and the flange squareness checkable by autocollimation. If space permits, levelling screws or shims can realign skewed components, in translation as well as tilt.

4.5 At the primary assembly facility for the optical subsystem, usually the optical vendor, facilities should be made available for checking and aligning the system to the final IR focus. This can be done with room temperature detectors and black body sources collimated by reflecting optics. Tests for squareness, alignment and system blur can be made with graduated apertures.

NOMINAL SYSTEM

AXIAL FAN

8.8 μ

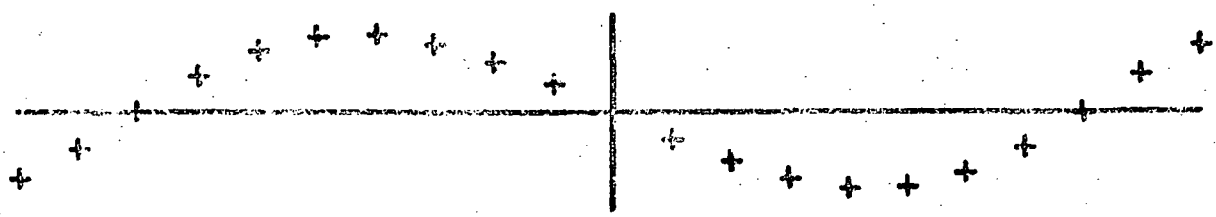

S FAN

FRAC OBJECT HEIGHT 0.0000

CHIEF RAY HEIGHT 0.0000

1 INCH = 0.001000

NOMINAL SYSTEM

SPOT DIAGRAM ON AXIS

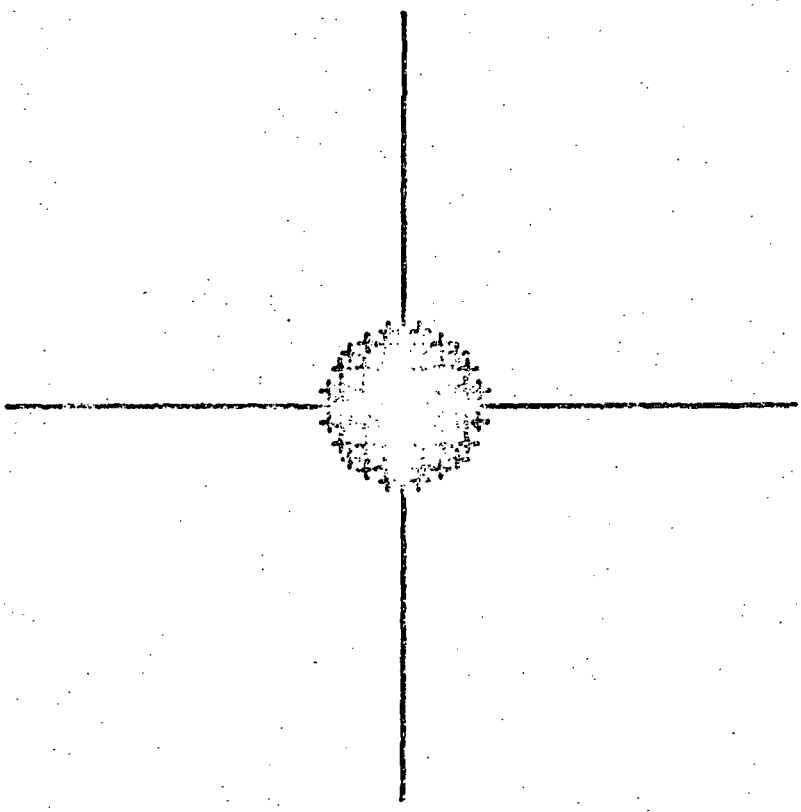

CHIEF RAY HEIGHT	0.0000
FOCUS SHIFT	0.000000

1 INCH = 0.001000

5-13

NOMINAL SYSTEM
FREQUENCY RESPONSE
ON AXIS

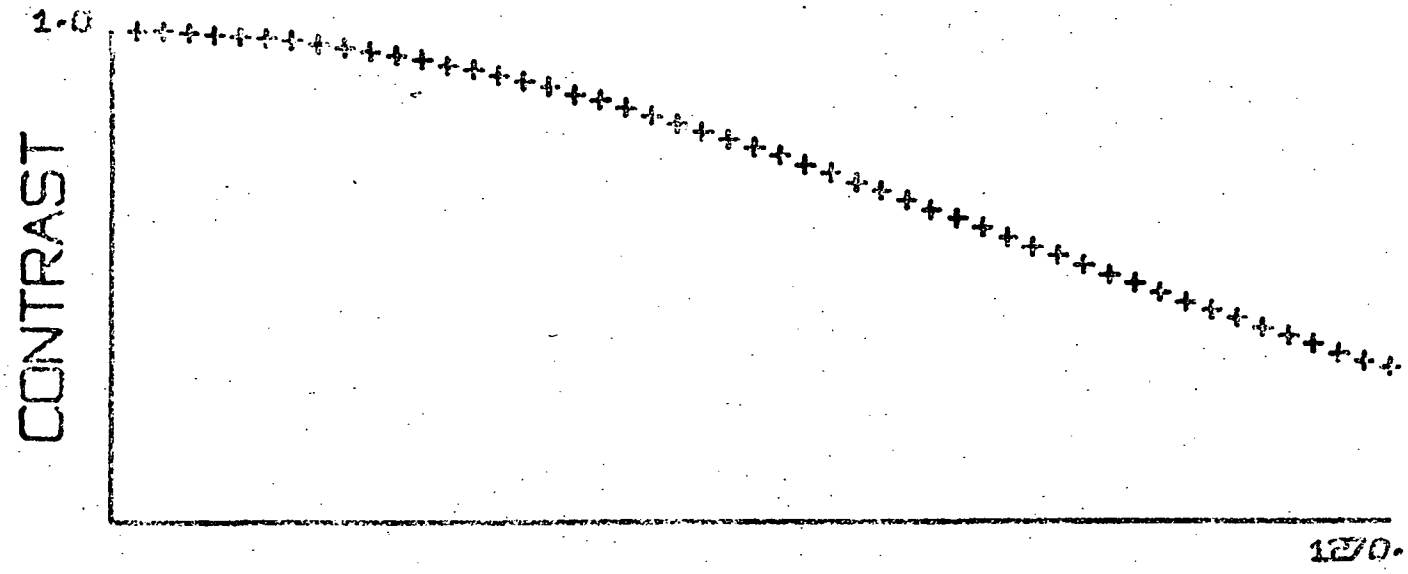

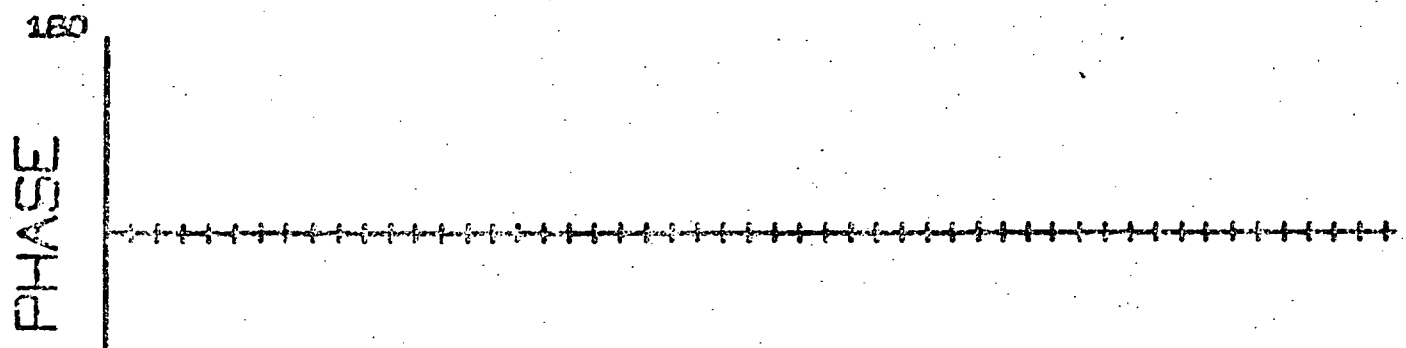

TARGET ORIENTATION	0.0
FOCUS SHIFT	0.000000
FRAC OBJECT HEIGHT	0.0000 1.0

NOMINAL SYSTEM

AXIAL FAN

8.3 μ

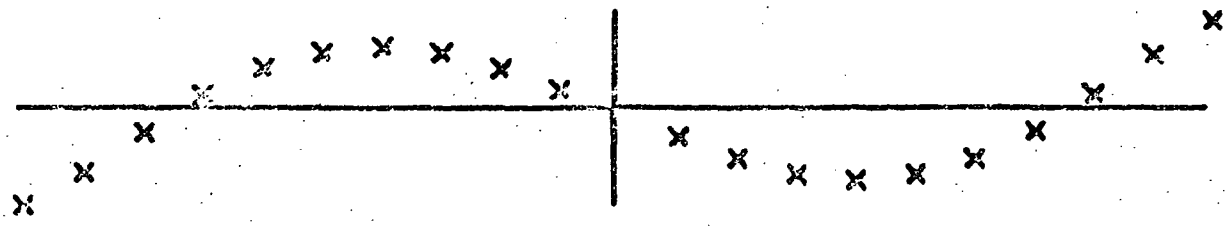

S FAN

FRAC OBJECT HEIGHT 0.0000

CHIEF RAY HEIGHT 0.0000

1 INCH = 0.001000

NOMINAL SYSTEM

AXIAL FAN

11 μ

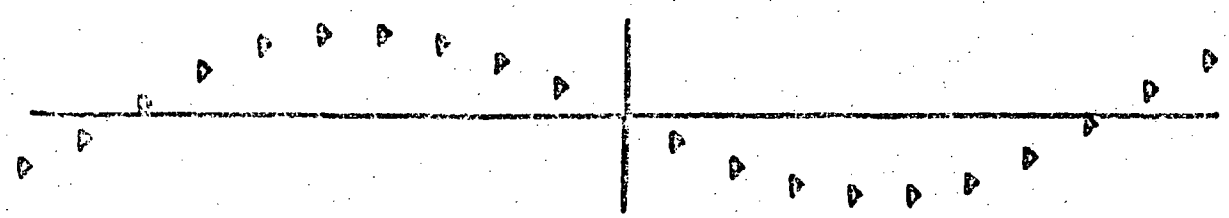

S FAN

FRAC OBJECT HEIGHT	0.0000
CHIEF RAY HEIGHT	0.0000

1 INCH = 0.001000

NOM SYSTEM WITH APLANAT ASSY AT 110°K
REFOCUSED .011 WITH FOCUSING LENS
AXIAL FAN

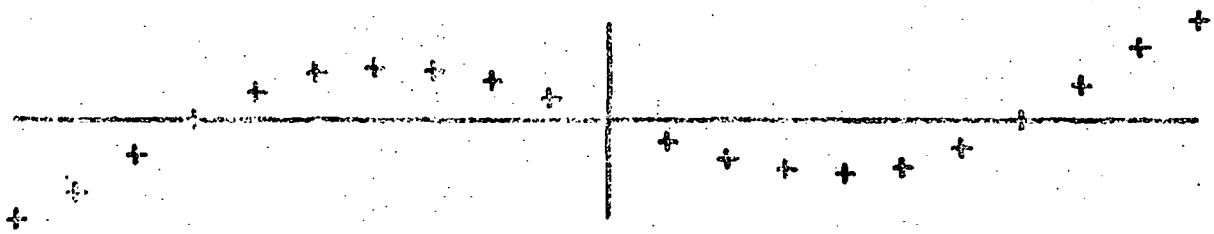

S FAN

FRAC OBJECT HEIGHT 0.0000

CHIEF RAY HEIGHT 0.0000

1 INCH = 0.001000

5-17

```
CALL PRT     0.0000000E 00  0.0000000E 00  0.00000E 00  0.0000000E 00
ITT SCMR 9093    System_Description
STOP IS SURF  1
IMAGE IS 16
PXRAY        0.4000000E 01 -0.3000000E 06  0.3000000E-03  0.0000000E 00
WVLNS.  0.8800000E 01  0.8300000E 01  0.1100000E 02

  1  0 CURVATURE DATA          0.0000000E 00  0.0000000E 00  0.0000000E 00
  2  0 AXIAL SEPARATION        0.1000000E 10
  3  0 AIRSPACE

  1  1 CURVATURE DATA          0.0000000E 00  0.0000000E 00  0.0000000E 00
  2  1 AXIAL SEPARATION        0.5963756E 00
  3  1 AIRSPACE

  1  2 CURVATURE DATA         -0.7409000E-01 -0.1349709E 02 -0.8800000E 00
  2  2 AXIAL SEPARATION       -0.5875000E 01
  3  2 REFLECTING SURF.       -0.1000000E 01 -0.1000000E 01 -0.1000000E 01

  1  3 CURVATURE DATA         -0.5720000E 00 -0.1748251E 01  0.0000000E 00
  2  3 AXIAL SEPARATION        0.8470000E 01
  3  3 REFLECTING SURF.        0.1000000E 01  0.1000000E 01  0.1000000E 01

  1  4 CURVATURE DATA          0.0000000E 00  0.0000000E 00  0.0000000E 00
  2  4 AXIAL SEPARATION       -0.1750000E 01
  3  4 REFLECTING SURF.       -0.1000000E 01 -0.1000000E 01 -0.1000000E 01
  6  4 CURV OF REVOLUTION-TORIC  0.0000000E 00

  1  5 CURVATURE DATA          0.0000000E 00  0.0000000E 00  0.0000000E 00
  2  5 AXIAL SEPARATION        0.2000000E 01
  3  5 REFLECTING SURF.        0.1000000E 01  0.1000000E 01  0.1000000E 01

  1  6 RADIUS DATA             0.3425836E 00  0.2919000E 01  0.0000000E 00
  2  6 AXIAL SEPARATION        0.1750000E 00
  3  6 INDICES                 0.4004100E 01  0.4004800E 01  0.4002600E 01

  1  7 RADIUS DATA             0.2210433E 00  0.4524000E 01  0.0000000E 00
  2  7 AXIAL SEPARATION        0.8525729E 00
  3  7 AIRSPACE

  1  8 CURVATURE DATA          0.0000000E 00  0.0000000E 00  0.0000000E 00
  2  8 AXIAL SEPARATION        0.1000000E 00
  3  8 INDICES                 0.2155000E 01  0.2180000E 01  0.2130000E 01

  1  9 CURVATURE DATA          0.0000000E 00  0.0000000E 00  0.0000000E 00
  2  9 AXIAL SEPARATION        0.9420000E 00
  3  9 AIRSPACE

  1 10 CURVATURE DATA          0.0000000E 00  0.0000000E 00  0.0000000E 00
  2 10 AXIAL SEPARATION        0.4000000E-01
  3 10 PICKUP  8               0.2155000E 01  0.2180000E 01  0.2130000E 01

  1 11 CURVATURE DATA          0.0000000E 00  0.0000000E 00  0.0000000E 00
  2 11 AXIAL SEPARATION        0.1000000E-01
  3 11 AIRSPACE

  1 12 RADIUS DATA             0.5464480E 01  0.1830000E 00  0.0000000E 00
  2 12 AXIAL SEPARATION        0.8000000E-01
  3 12 PICKUP  6               0.4004100E 01  0.4004800E 01  0.4002600E 01
```

```
 1 13 RADIUS DATA                0.6666666E 01  0.1500000E 00  0.0000000E 00
 2 13 AXIAL SEPARATION           0.7250000E-01
 3 13 AIRSPACE

 1 14 CURVATURE DATA             0.0000000E 00  0.0000000E 00  0.0000000E 00
 2 14 AXIAL SEPARATION           0.4000000E-01
 3 14 PICKUP  8                  0.2155000E 01  0.2180000E 01  0.2130000E 01

 1 15 CURVATURE DATA             0.0000000E 00  0.0000000E 00  0.0000000E 00
 2 15 AXIAL SEPARATION           0.2600000E-01
 3 15 AIRSPACE

 1 16 CURVATURE DATA             0.0000000E 00  0.0000000E 00  0.0000000E 00
```

THIRD ORDER ABERRATIONS

```
PRX RAYS   -0.3000000E 06  0.4000000E-08  0.3000000E-03  0.4000000E 01  0.0000000E 00

FCLN,GSHT,SKFC,OVLN  0.6551656E 01  0.1861433E-02  0.2600000E-01  0.5779448E 01
REN,TEN,TEX          0.4000000E 01  0.0000000E 00  0.6642051E-01
SPHR,COMA,DIST       0.2867018E-02  0.9147276E-03  0.1089169E-02
TANG,SAGT,PETZ       0.7493329E-04  0.2483227E-04 -0.2182393E-06
PA,PL,SA,SL          0.1932357E-03  0.1246791E-04  0.1277932E-03  0.8438980E-05
```

FIFTH ORDER ABERRATIONS

```
PRX RAYS   -0.3000000E 06  0.4000000E-08  0.3000000E-03  0.4000000E 01  0.0000000E 00
FCLN,GSHT,SKFC,OVLN  0.6551656E 01  0.1861433E-02  0.2600000E-01  0.5779448E 01
REN,TEN,TEX          0.4000000E 01  0.0000000E 00  0.6642051E-01
  0.2867018E-02  0.9147276E-03  0.7493329E-04  0.2483227E-04 -0.2182393E-06  0.1089169E-02
 -0.6450222E-03  0.3199396E-03  0.2314743E-06  0.4963586E-07  0.4176253E-08  0.2472667E-05
 -0.2605435E-03  0.5096809E-05  0.5931693E-04  0.1109805E-04
PA,PL,SA,SL          0.1932357E-03  0.1246791E-04  0.1277932E-03  0.8438980E-05
```

SAGITTAL FAN, ON AXIS 8.8μm

REF HEIGHT =0.0000000E 00 2000.0000000E 00 0.0000000E 00 0.0000000E 00

1P	0.0000000E 00	0.0000000E 00	0.0000000E 00	-0.4000000E 01	0.0000000E 00	-0.4000000E-08	0.0000000E 00
1 16	-0.3377165 -03	0.0000000 00	0.0000000 00	0.2693051 -01	0.0000000 00	0.6746136 00	0.0000000 00
2P	0.0000000E 00	0.0000000E 00	0.0000000E 00	-0.3600000E 01	0.0000000E 00	-0.3600000E-08	0.0000000E 00
2 16	-0.1877524 -03	0.0000000 00	0.0000000 00	0.2408657 -01	0.0000000 00	0.6005445 00	0.0000000 00
3P	0.0000000E 00	0.0000000E 00	0.0000000E 00	-0.3200000E 01	0.0000000E 00	-0.3200000E-08	0.0000000E 00
3 16	0.2178225 -05	0.0000000 00	0.0000000 00	0.2128885 -01	0.0000000 00	0.5266305 00	0.0000000 00
4P	0.0000000E 00	0.0000000E 00	0.0000000E 00	-0.2800000E 01	0.0000000E 00	-0.2800000E-08	0.0000000E 00
4 16	0.1770121 -03	0.0000000 00	0.0000000 00	0.1853421 -01	0.0000000 00	0.4541555 00	0.0000000 00
5P	0.0000000E 00	0.0000000E 00	0.0000000E 00	-0.2400000E 01	0.0000000E 00	-0.2400000E-08	0.0000000E 00
5 16	0.3064015 -03	0.0000000 00	0.0000000 00	0.1581772 -01	0.0000000 00	0.3837487 00	0.0000000 00
6P	0.0000000E 00	0.0000000E 00	0.0000000E 00	-0.2000000E 01	0.0000000E 00	-0.2000000E-08	0.0000000E 00
6 16	0.3771641 -03	0.0000000 00	0.0000000 00	0.1313369 -01	0.0000000 00	0.3155954 00	0.0000000 00
7P	0.0000000E 00	0.0000000E 00	0.0000000E 00	-0.1600000E 01	0.0000000E 00	-0.1600000E-08	0.0000000E 00
7 16	0.3875672 -03	0.0000000 00	0.0000000 00	0.1047623 -01	0.0000000 00	0.2495925 00	0.0000000 00
8P	0.0000000E 00	0.0000000E 00	0.0000000E 00	-0.1200000E 01	0.0000000E 00	-0.1200000E-08	0.0000000E 00
8 16	0.3432880 -03	0.0000000 00	0.0000000 00	0.7839541 -02	0.0000000 00	0.1854566 00	0.0000000 00
9P	0.0000000E 00	0.0000000E 00	0.0000000E 00	-0.8000000E 00	0.0000000E 00	-0.8000000E-09	0.0000000E 00
9 16	0.2547441 -03	0.0000000 00	0.0000000 00	0.5218081 -02	0.0000000 00	0.1227925 00	0.0000000 00
10P	0.0000000E 00	0.0000000E 00	0.0000000E 00	-0.4000000E 00	0.0000000E 00	-0.4000000E-09	0.0000000E 00
10 16	0.1352941 -03	0.0000000 00	0.0000000 00	0.2606581 -02	0.0000000 00	0.6113943 -01	0.0000000 00
11P	0.0000000E 00	0.0000000E 00	0.0000000E 00	0.3999999E 00	0.0000000E 00	0.3999999E-09	0.0000000E 00
11 16	-0.1352941 -03	0.0000000 00	0.0000000 00	-0.2606581 -02	0.0000000 00	-0.6113943 -01	0.0000000 00
12P	0.0000000E 00	0.0000000E 00	0.0000000E 00	0.7999999E 00	0.0000000E 00	0.7999999E-09	0.0000000E 00
12 16	-0.2547433 -03	0.0000000 00	0.0000000 00	-0.5218081 -02	0.0000000 00	-0.1227925 00	0.0000000 00
13P	0.0000000E 00	0.0000000E 00	0.0000000E 00	0.1199999E 01	0.0000000E 00	0.1199999E-08	0.0000000E 00
13 16	-0.3432865 -03	0.0000000 00	0.0000000 00	-0.7839541 -02	0.0000000 00	-0.1854566 00	0.0000000 00
14P	0.0000000E 00	0.0000000E 00	0.0000000E 00	0.1599999E 01	0.0000000E 00	0.1599999E-08	0.0000000E 00
14 16	-0.3875669 -03	0.0000000 00	0.0000000 00	-0.1047623 -01	0.0000000 00	-0.2495927 00	0.0000000 00
15P	0.0000000E 00	0.0000000E 00	0.0000000E 00	0.1999999E 01	0.0000000E 00	0.1999999E-08	0.0000000E 00
15 16	-0.3771650 -03	0.0000000 00	0.0000000 00	-0.1313369 -01	0.0000000 00	-0.3155954 00	0.0000000 00
16P	0.0000000E 00	0.0000000E 00	0.0000000E 00	0.2399999E 01	0.0000000E 00	0.2399999E-08	0.0000000E 00
16 16	-0.3064029 -03	0.0000000 00	0.0000000 00	-0.1581772 -01	0.0000000 00	-0.3837489 00	0.0000000 00
17P	0.0000000E 00	0.0000000E 00	0.0000000E 00	0.2799999E 01	0.0000000E 00	0.2799999E-08	0.0000000E 00
17 16	-0.1770110 -03	0.0000000 00	0.0000000 00	-0.1853421 -01	0.0000000 00	-0.4541555 00	0.0000000 00
18P	0.0000000E 00	0.0000000E 00	0.0000000E 00	0.3199999E 01	0.0000000E 00	0.3199999E-08	0.0000000E 00
18 16	-0.2183063 -05	0.0000000 00	0.0000000 00	-0.2128885 -01	0.0000000 00	-0.5266303 00	0.0000000 00
19P	0.0000000E 00	0.0000000E 00	0.0000000E 00	0.3599999E 01	0.0000000E 00	0.3599999E-08	0.0000000E 00
19 16	0.1877557 -03	0.0000000 00	0.0000000 00	-0.2408656 -01	0.0000000 00	-0.6005446 00	0.0000000 00
20P	0.0000000E 00	0.0000000E 00	0.0000000E 00	0.3999999E 01	0.0000000E 00	0.3999999E-08	0.0000000E 00
20 16	0.3377212 -03	0.0000000 00	0.0000000 00	-0.2693051 -01	0.0000000 00	-0.6746137 00	0.0000000 00

CALL FRQ 0.2540000E 02 0.0000000E 00 0.0000000E 00 0.0000000E 00

NO.	OBJ HT	CHF RAY	FOCUS SHFT	ORIENTATION	CUT-OFF
1	0.0000000E 00	0.0000000E 00	0.0000000E 00	0.0000000E 00	0.1270000E 04

	FREQUENCY		CONTRAST		PHASE ANGLE	
1.	0.2540000	02	0.9995710	00	-0.1247706	-07
2.	0.5080000	02	0.9982852	00	-0.2500801	-07
3.	0.7620000	02	0.9961452	00	-0.3786071	-07
4.	0.1016000	03	0.9931556	00	-0.5027436	-07
5.	0.1270000	03	0.9893227	00	-0.6279453	-07
6.	0.1524000	03	0.9846646	00	-0.7568775	-07
7.	0.1778000	03	0.9791612	00	-0.3829071	-07
8.	0.2032000	03	0.9728541	00	-0.1007186	-06
9.	0.2286000	03	0.9657467	00	-0.1140502	-06
10.	0.2540000	03	0.9578539	00	-0.1267410	-06
11.	0.2794000	03	0.9491924	00	-0.1399754	-06
12.	0.3048000	03	0.9397503	00	-0.1535762	-06
13.	0.3302000	03	0.9296375	00	-0.1672848	-06
14.	0.3556000	03	0.9187851	00	-0.1811522	-06
15.	0.3810000	03	0.9072458	00	-0.1944844	-06
16.	0.4064000	03	0.8950436	00	-0.2093234	-06
17.	0.4317999	03	0.8822039	00	-0.2251285	-06
18.	0.4572000	03	0.8687533	00	-0.2406107	-06
19.	0.4826000	03	0.8547196	00	-0.2564297	-06
20.	0.5080000	03	0.8401315	00	-0.2734530	-06
21.	0.5334000	03	0.8250191	00	-0.2915998	-06
22.	0.5588000	03	0.8094131	00	-0.3102698	-06
23.	0.5842000	03	0.7933452	00	-0.3300410	-06
24.	0.6096000	03	0.7768479	00	-0.3502867	-06
25.	0.6350000	03	0.7599545	00	-0.3719703	-06
26.	0.6604000	03	0.7426988	00	-0.3946452	-06
27.	0.6858000	03	0.7251151	00	-0.4195463	-06
28.	0.7112000	03	0.7072382	00	-0.4461155	-06
29.	0.7366000	03	0.6891033	00	-0.4745931	-06
30.	0.7620000	03	0.6707458	00	-0.5047775	-06
31.	0.7874000	03	0.6522014	00	-0.5355360	-06
32.	0.8128000	03	0.6335057	00	-0.5704241	-06
33.	0.8382000	03	0.6146944	00	-0.6073222	-06
34.	0.8635999	03	0.5958031	00	-0.6466367	-06
35.	0.8890000	03	0.5768673	00	-0.6885791	-06
36.	0.9144000	03	0.5579221	00	-0.7318863	-06
37.	0.9397999	03	0.5390025	00	-0.7818106	-06
38.	0.9652000	03	0.5201427	00	-0.8325995	-06
39.	0.9905999	03	0.5013767	00	-0.8870442	-06
40.	0.1016000	04	0.4827377	00	-0.9489284	-06
41.	0.1041400	04	0.4642583	00	-0.1013039	-05
42.	0.1066800	04	0.4459705	00	-0.1085740	-05
43.	0.1092200	04	0.4279051	00	-0.1163403	-05
44.	0.1117600	04	0.4100924	00	-0.1247143	-05
45.	0.1143000	04	0.3925616	00	-0.1338236	-05
46.	0.1168400	04	0.3753407	00	-0.1436658	-05
47.	0.1193800	04	0.3584568	00	-0.1544644	-05
48.	0.1219200	04	0.3419357	00	-0.1661541	-05
49.	0.1244600	04	0.3258022	00	-0.1789030	-05
50.	0.1270000	04	0.3100797	00	-0.1925453	-05

CHIEF RAY, EVERY SURFACE

```
CALL RAYP  0.1000000E 01  0.0000000E 00  0.0000000E 00  0.0000000E 00

 1P     0.0000000E 00 -0.3000000E 06  0.0000000E 00  0.0000000E 00  0.0000000E 00  0.0000000E 00  0.3000000E-03
 1  1    0.0000000  00  0.0000000  00  0.0000000  00  0.0000000  00  0.3000000 -03
 1  2    0.0000000  00  0.1739126 -03 -0.1185301 -03  0.0000000  00 -0.2734687 -03
 1  3    0.0000000  00  0.1785659 -02 -0.9119337 -05  0.0000000  00  0.2316287 -02
 1  4    0.0000000  00  0.2140461 -01  0.0000000  00  0.0000000  00 -0.2316287 -02
 1  5    0.0000000  00  0.2545811 -01  0.0000000  00  0.0000000  00  0.2316287 -02
 1  6    0.0000000  00  0.3009105 -01  0.1551036 -03  0.0000000  00 -0.7156012 -02
 1  7    0.0000000  00  0.2883920 -01  0.9192174 -04  0.0000000  00 -0.9502786 -02
 1  8    0.0000000  00  0.2073825 -01  0.0000000  00  0.0000000  00 -0.4409489 -02
 1  9    0.0000000  00  0.2029730 -01  0.0000000  00  0.0000000  00 -0.9502786 -02
 1 10    0.0000000  00  0.1134568 -01  0.0000000  00  0.0000000  00 -0.4409489 -02
 1 11    0.0000000  00  0.1116930 -01  0.0000000  00  0.0000000  00 -0.9502786 -02
 1 12    0.0000000  00  0.1107109 -01  0.3351950 -03  0.0000000  00 -0.4783134 -01
 1 13    0.0000000  00  0.7252224 -02  0.1754184 -03  0.0000000  00 -0.4610889 -01
 1 14    0.0000000  00  0.3917418 -02  0.0000000  00  0.0000000  00 -0.2137841 -01
 1 15    0.0000000  00  0.3062281 -02  0.0000000  00  0.0000000  00 -0.4610889 -01
 1 16    0.0000000  00  0.1863450 -02  0.0000000  00  0.0000000  00 -0.2953456 -06  0.0000000  00 -0.4610889 -01
```

MARGINAL AXIAL RAY EVERY SURFACE
CALL RAYP 0.0000000E 00 0.1000000E 01 0.0000000E 00 0.0000000E 00

IP		0.0000000E	00	0.0000000E	00	0.0000000E	00	0.4000000E	01	0.0000000E	00	0.4000000E-08	0.0000000E	00	
1	1	0.4000000	01	0.0000000	00	0.0000000	00	0.4000000	-08	0.0000000	00				
1	2	0.4000000	01	0.0000000	00	-0.5942900	00	0.6539128	00	0.0000000	00				
1	3	0.4992669	00	0.0000000	00	-0.7230651	-01	0.1035728	-03	0.0000000	00				
1	4	0.5001517	00	0.0000000	00	0.0000000	00	-0.1035728	-03	0.0000000	00				
1	5	0.6003329	00	0.0000000	00	0.0000000	00	0.1035728	-03	0.0000000	00				
1	6	0.6005445	00	0.0000000	00	0.4323642	-01	-0.1301937	00	0.0000000	00				
1	7	0.4800642	00	0.0000000	00	0.2554311	-01	-0.2015113	00	0.0000000	00				
1	8	0.3131602	00	0.0000000	00	0.0000000	00	-0.9218650	-01	0.0000000	00				
1	9	0.3039415	00	0.0000000	00	0.0000000	00	-0.2018113	00	0.0000000	00				
1	10	0.1138352	00	0.0000000	00	0.0000000	00	-0.9218650	-01	0.0000000	00				
1	11	0.1101478	00	0.0000000	00	0.0000000	00	-0.2018113	00	0.0000000	00				
1	12	0.1018775	00	0.0000000	00	0.3098035	-01	-0.5393829	00	0.0000000	00				
1	13	0.6691059	-01	0.0000000	00	0.1575033	-01	-0.6746136	00	0.0000000	00				
1	14	0.2762649	-01	0.0000000	00	0.0000000	00	-0.2687206	00	0.0000000	00				
1	15	0.1787767	-01	0.0000000	00	0.0000000	00	-0.6746136	00	0.0000000	00				
1	16	0.3377166	-03	0.0000000	00	0.0000000	00	-0.2693051	-01	0.0000000	00	-0.6746136	00	0.0000000	00

SAGITTAL FAN ON AXIS 8.3μ
REF. HEIGHT = 0.0000000E 00

1S	0.0000000E 00	0.0000000E 00	0.0000000E 00	-0.4000000E 01	0.0000000E 00	-0.4000000E-08	0.0000000E 00
1 16	-0.4671816 -03	0.0000000 00	0.0000000 00	0.2682203 -01	0.0000000 00	0.6751328 00	0.0000000 00
2S	0.0000000E 00	0.0000000E 00	0.0000000E 00	-0.3600000E 01	0.0000000E 00	-0.3600000E-08	0.0000000E 00
2 16	-0.3044488 -03	0.0000000 00	0.0000000 00	0.2398774 -01	0.0000000 00	0.6009867 00	0.0000000 00
3S	0.0000000E 00	0.0000000E 00	0.0000000E 00	-0.3200000E 01	0.0000000E 00	-0.3200000E-08	0.0000000E 00
3 16	-0.1013252 -03	0.0000000 00	0.0000000 00	0.2120038 -01	0.0000000 00	0.5270024 00	0.0000000 00
4S	0.0000000E 00	0.0000000E 00	0.0000000E 00	-0.2800000E 01	0.0000000E 00	-0.2800000E-08	0.0000000E 00
4 16	0.8685502 -04	0.0000000 00	0.0000000 00	0.1845654 -01	0.0000000 00	0.4544644 00	0.0000000 00
5S	0.0000000E 00	0.0000000E 00	0.0000000E 00	-0.2400000E 01	0.0000000E 00	-0.2400000E-08	0.0000000E 00
5 16	0.2296718 -03	0.0000000 00	0.0000000 00	0.1575110 -01	0.0000000 00	0.3840014 00	0.0000000 00
6S	0.0000000E 00	0.0000000E 00	0.0000000E 00	-0.2000000E 01	0.0000000E 00	-0.2000000E-08	0.0000000E 00
6 16	0.3135350 -03	0.0000000 00	0.0000000 00	0.1307823 -01	0.0000000 00	0.3157976 00	0.0000000 00
7S	0.0000000E 00	0.0000000E 00	0.0000000E 00	-0.1600000E 01	0.0000000E 00	-0.1600000E-08	0.0000000E 00
7 16	0.3369673 -03	0.0000000 00	0.0000000 00	0.1043195 -01	0.0000000 00	0.2497489 00	0.0000000 00
8S	0.0000000E 00	0.0000000E 00	0.0000000E 00	-0.1200000E 01	0.0000000E 00	-0.1200000E-08	0.0000000E 00
8 16	0.3055314 -03	0.0000000 00	0.0000000 00	0.7806400 -02	0.0000000 00	0.1855708 00	0.0000000 00
9S	0.0000000E 00	0.0000000E 00	0.0000000E 00	-0.8000000E 00	0.0000000E 00	-0.8000000E-09	0.0000000E 00
9 16	0.2296718 -03	0.0000000 00	0.0000000 00	0.5196028 -02	0.0000000 00	0.1228672 00	0.0000000 00
10S	0.0000000E 00	0.0000000E 00	0.0000000E 00	-0.4000000E 00	0.0000000E 00	-0.4000000E-09	0.0000000E 00
10 16	0.1227886 -03	0.0000000 00	0.0000000 00	0.2595568 -02	0.0000000 00	0.6117636 -01	0.0000000 00
11S	0.0000000E 00	0.0000000E 00	0.0000000E 00	0.3999999E 00	0.0000000E 00	0.3999999E-09	0.0000000E 00
11 16	-0.1227886 -03	0.0000000 00	0.0000000 00	-0.2595568 -02	0.0000000 00	-0.6117635 -01	0.0000000 00
12S	0.0000000E 00	0.0000000E 00	0.0000000E 00	0.7999999E 00	0.0000000E 00	0.7999999E-09	0.0000000E 00
12 16	-0.2296710 -03	0.0000000 00	0.0000000 00	-0.5196027 -02	0.0000000 00	-0.1228672 00	0.0000000 00
13S	0.0000000E 00	0.0000000E 00	0.0000000E 00	0.1199999E 01	0.0000000E 00	0.1199999E-08	0.0000000E 00
13 16	-0.3055300 -03	0.0000000 00	0.0000000 00	-0.7806399 -02	0.0000000 00	-0.1855708 00	0.0000000 00
14S	0.0000000E 00	0.0000000E 00	0.0000000E 00	0.1599999E 01	0.0000000E 00	0.1599999E-08	0.0000000E 00
14 16	-0.3369625 -03	0.0000000 00	0.0000000 00	-0.1043195 -01	0.0000000 00	-0.2497491 00	0.0000000 00
15S	0.0000000E 00	0.0000000E 00	0.0000000E 00	0.1999999E 01	0.0000000E 00	0.1999999E-08	0.0000000E 00
15 16	-0.3135381 -03	0.0000000 00	0.0000000 00	-0.1307823 -01	0.0000000 00	-0.3157975 00	0.0000000 00
16S	0.0000000E 00	0.0000000E 00	0.0000000E 00	0.2399999E 01	0.0000000E 00	0.2399999E-08	0.0000000E 00
16 16	-0.2296746 -03	0.0000000 00	0.0000000 00	-0.1575111 -01	0.0000000 00	-0.3840014 00	0.0000000 00
17S	0.0000000E 00	0.0000000E 00	0.0000000E 00	0.2799999E 01	0.0000000E 00	0.2799999E-08	0.0000000E 00
17 16	-0.8685860 -04	0.0000000 00	0.0000000 00	-0.1845654 -01	0.0000000 00	-0.4544644 00	0.0000000 00
18S	0.0000000E 00	0.0000000E 00	0.0000000E 00	0.3199999E 01	0.0000000E 00	0.3199999E-08	0.0000000E 00
18 16	0.1013214 -03	0.0000000 00	0.0000000 00	-0.2120038 -01	0.0000000 00	-0.5270023 00	0.0000000 00
19S	0.0000000E 00	0.0000000E 00	0.0000000E 00	0.3599999E 01	0.0000000E 00	0.3599999E-08	0.0000000E 00
19 16	0.3044501 -03	0.0000000 00	0.0000000 00	-0.2398774 -01	0.0000000 00	-0.6009867 00	0.0000000 00
20S	0.0000000E 00	0.0000000E 00	0.0000000E 00	0.3999999E 01	0.0000000E 00	0.3999999E-08	0.0000000E 00
20 16	0.4671862 -03	0.0000000 00	0.0000000 00	-0.2682203 -01	0.0000000 00	-0.6751329 00	0.0000000 00

SAGITTAL FAN ON AXIS 11.0 m

CALL SENT 0.10000000E 02 0.00000000E 00 0.00000000E 00 0.00000000E 00

REF. HEIGHT = 0.00000000E 00

1T	0.00000000E 00	0.00000000E 00	0.00000000E 00	-0.40000000E 01	0.00000000E 00	-0.40000000E-08	0.00000000E 00
1 16	-0.2795421 -03	0.0000000 00	0.0000000 00	0.2697540 -01	0.0000000 00	0.6742849 00	0.0000000 00
2T	0.00000000E 00	0.00000000E 00	0.00000000E 00	-0.36000000E 01	0.00000000E 00	-0.36000000E-08	0.00000000E 00
2 16	-0.1332133 -03	0.0000000 00	0.0000000 00	0.2412932 -01	0.0000000 00	0.6002530 00	0.0000000 00
3T	0.00000000E 00	0.00000000E 00	0.00000000E 00	-0.32000000E 01	0.00000000E 00	-0.32000000E-08	0.00000000E 00
3 16	0.5217432 -04	0.0000000 00	0.0000000 00	0.2132856 -01	0.0000000 00	0.5263759 00	0.0000000 00
4T	0.00000000E 00	0.00000000E 00	0.00000000E 00	-0.28000000E 01	0.00000000E 00	-0.28000000E-08	0.00000000E 00
4 16	0.2217606 -03	0.0000000 00	0.0000000 00	0.1857013 -01	0.0000000 00	0.4539370 00	0.0000000 00
5T	0.00000000E 00	0.00000000E 00	0.00000000E 00	-0.24000000E 01	0.00000000E 00	-0.24000000E-08	0.00000000E 00
5 16	0.3453547 -03	0.0000000 00	0.0000000 00	0.1584928 -01	0.0000000 00	0.3835650 00	0.0000000 00
6T	0.00000000E 00	0.00000000E 00	0.00000000E 00	-0.20000000E 01	0.00000000E 00	-0.20000000E-08	0.00000000E 00
6 16	0.4100122 -03	0.0000000 00	0.0000000 00	0.1316046 -01	0.0000000 00	0.3154451 00	0.0000000 00
7T	0.00000000E 00	0.00000000E 00	0.00000000E 00	-0.16000000E 01	0.00000000E 00	-0.16000000E-08	0.00000000E 00
7 16	0.4140404 -03	0.0000000 00	0.0000000 00	0.1049792 -01	0.0000000 00	0.2494742 00	0.0000000 00
8T	0.00000000E 00	0.00000000E 00	0.00000000E 00	-0.12000000E 01	0.00000000E 00	-0.12000000E-08	0.00000000E 00
8 16	0.3832422 -03	0.0000000 00	0.0000000 00	0.7855953 -02	0.0000000 00	0.1853690 00	0.0000000 00
9T	0.00000000E 00	0.00000000E 00	0.00000000E 00	-0.80000000E 00	0.00000000E 00	-0.80000000E-09	0.00000000E 00
9 16	0.2680844 -03	0.0000000 00	0.0000000 00	0.5229083 -02	0.0000000 00	0.1227346 00	0.0000000 00
10T	0.00000000E 00	0.00000000E 00	0.00000000E 00	-0.40000000E 00	0.00000000E 00	-0.40000000E-09	0.00000000E 00
10 16	0.1419747 -03	0.0000000 00	0.0000000 00	0.2612100 -02	0.0000000 00	0.6111068 -01	0.0000000 00
11T	0.00000000E 00	0.00000000E 00	0.00000000E 00	0.39999999E 00	0.00000000E 00	0.39999999E-09	0.00000000E 00
11 16	-0.1419746 -03	0.0000000 00	0.0000000 00	-0.2612100 -02	0.0000000 00	-0.6111068 -01	0.0000000 00
12T	0.00000000E 00	0.00000000E 00	0.00000000E 00	0.79999999E 00	0.00000000E 00	0.79999999E-09	0.00000000E 00
12 16	-0.2680835 -03	0.0000000 00	0.0000000 00	-0.5229082 -02	0.0000000 00	-0.1227346 00	0.0000000 00
13T	0.00000000E 00	0.00000000E 00	0.00000000E 00	0.11999999E 01	0.00000000E 00	0.11999999E-08	0.00000000E 00
13 16	-0.3832397 -03	0.0000000 00	0.0000000 00	-0.7855952 -02	0.0000000 00	-0.1853690 00	0.0000000 00
14T	0.00000000E 00	0.00000000E 00	0.00000000E 00	0.15999999E 01	0.00000000E 00	0.15999999E-08	0.00000000E 00
14 16	-0.4140384 -03	0.0000000 00	0.0000000 00	-0.1049792 -01	0.0000000 00	-0.2494743 00	0.0000000 00
15T	0.00000000E 00	0.00000000E 00	0.00000000E 00	0.19999999E 01	0.00000000E 00	0.19999999E-08	0.00000000E 00
15 16	-0.4100146 -03	0.0000000 00	0.0000000 00	-0.1316046 -01	0.0000000 00	-0.3154450 00	0.0000000 00
16T	0.00000000E 00	0.00000000E 00	0.00000000E 00	0.23999999E 01	0.00000000E 00	0.23999999E-08	0.00000000E 00
16 16	-0.3453846 -03	0.0000000 00	0.0000000 00	-0.1584928 -01	0.0000000 00	-0.3835650 00	0.0000000 00
17T	0.00000000E 00	0.00000000E 00	0.00000000E 00	0.27999999E 01	0.00000000E 00	0.27999999E-08	0.00000000E 00
17 16	-0.2217654 -03	0.0000000 00	0.0000000 00	-0.1857013 -01	0.0000000 00	-0.4539370 00	0.0000000 00
18T	0.00000000E 00	0.00000000E 00	0.00000000E 00	0.31999999E 01	0.00000000E 00	0.31999999E-08	0.00000000E 00
18 16	-0.5218257 -04	0.0000000 00	0.0000000 00	-0.2132856 -01	0.0000000 00	-0.5263758 00	0.0000000 00
19T	0.00000000E 00	0.00000000E 00	0.00000000E 00	0.35999999E 01	0.00000000E 00	0.35999999E-08	0.00000000E 00
19 16	0.1332200 -03	0.0000000 00	0.0000000 00	-0.2412932 -01	0.0000000 00	-0.6002531 00	0.0000000 00
20T	0.00000000E 00	0.00000000E 00	0.00000000E 00	0.39999999E 01	0.00000000E 00	0.39999999E-08	0.00000000E 00
20 16	0.2795464 -03	0.0000000 00	0.0000000 00	-0.2697540 -01	0.0000000 00	-0.6742850 00	0.0000000 00

5.6.1 Scan Mirror

As noted in Section 5.2 the scan mirror supplied by Speedring was repolished by Surface Finishes Inc. The flatness of the mirror is illustrated by the fringe pattern which occurs when the scan mirror reflecting surface is placed in contact with a precision optical flat and suitably illuminated; the fringe pattern is shown in Figure 5.6-1. The mirror was then aluminized by D.L. Clausing Co., Skokie, Ill.

5.6.2 Near Infrared Channel Beamsplitter

The transmission and reflectance characteristics of the beamsplitter used to reflect the two long wavelength infrared channels and transmit the near infrared channel are given in Figure 5.6-2 and Figure 5.6-3.

5.6.3 Infrared Dichroic

This dichroic reflected energy in the 8.3 to 9.3 μm band and transmitted in the 10.2 to 11.2 μm band. Figures 5.6-4 and 5.6-5 show that the reflectance is very high, averaging about 98%, with the transmittance averaging about 82% in the band. The dichroic was of the "balanced stress" design which means that the substrate material (germanium) was coated on both sides to equal the multilayer coating stresses and keep the part optically flat after coating. Tests on the "penthouse" assembly attached to the side of the telescope and containing the dichroic showed that the dichroic remained optically flat (within requirements). The parallelism of the two sides of the dichroic were within 0.7 milliradian compared to the beam spread of 4.8 milliradians so that even a reflection from the second surface should not have caused significant optical degradation.

5.6.4 Bandpass Filters (LW Infrared Channels)

Transmission curves for the two longwavelength channels are given in Figures 5.6-6 and 5.6-7. These curves were measured by the manufacturer, OCLI, with the filters cooled to 100 Kelvin. The shift with wavelength is linear with temperature. At 25°C, the short wavelength cutoff of the 10.2 to 11.2 μm filter was at 10.33 μm (50% point) which gives a shift of (10.33 - 10.11 μm)÷ 200 K or 0.0011 μm/K shift. At 115 Kelvin the 50% T point would therefore be at 10.11 + 0.0011 (15) = 10.126 μm. The shift of the 8.3 to 9.3 μm filter is 0.0008 μm per Kelvin.

5.6.5 Cooler Windows

The transmission of the Irtran II windows used in the radiant cooler is given in Figure 5.6-8. The windows were antireflection coated so that they would transmit either of the long wave infrared bands.

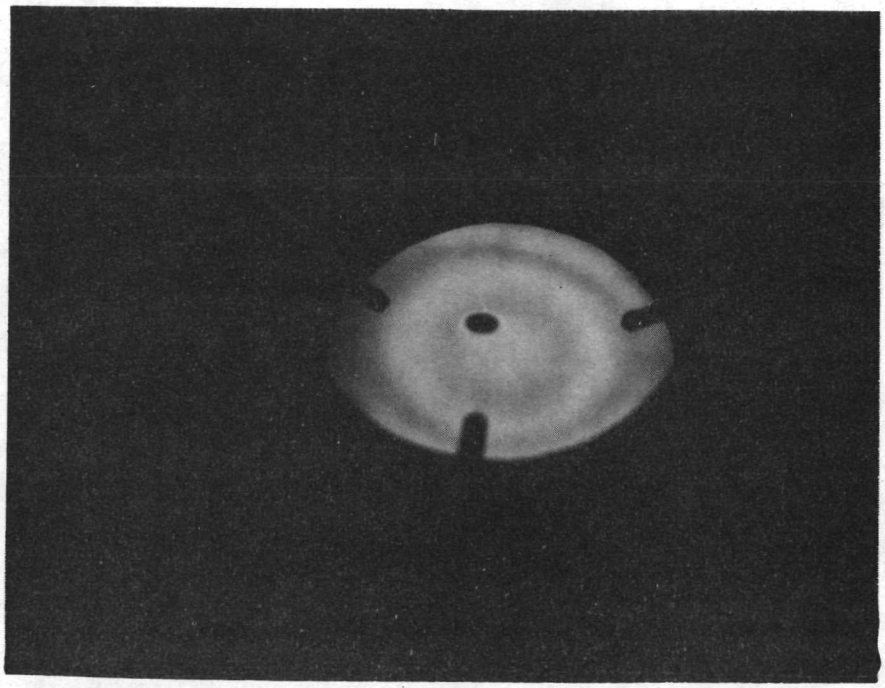

FIGURE 5.6-1 FLIGHT MODEL SCAN MIRROR

SCMR Dichroic (Near Infrared)

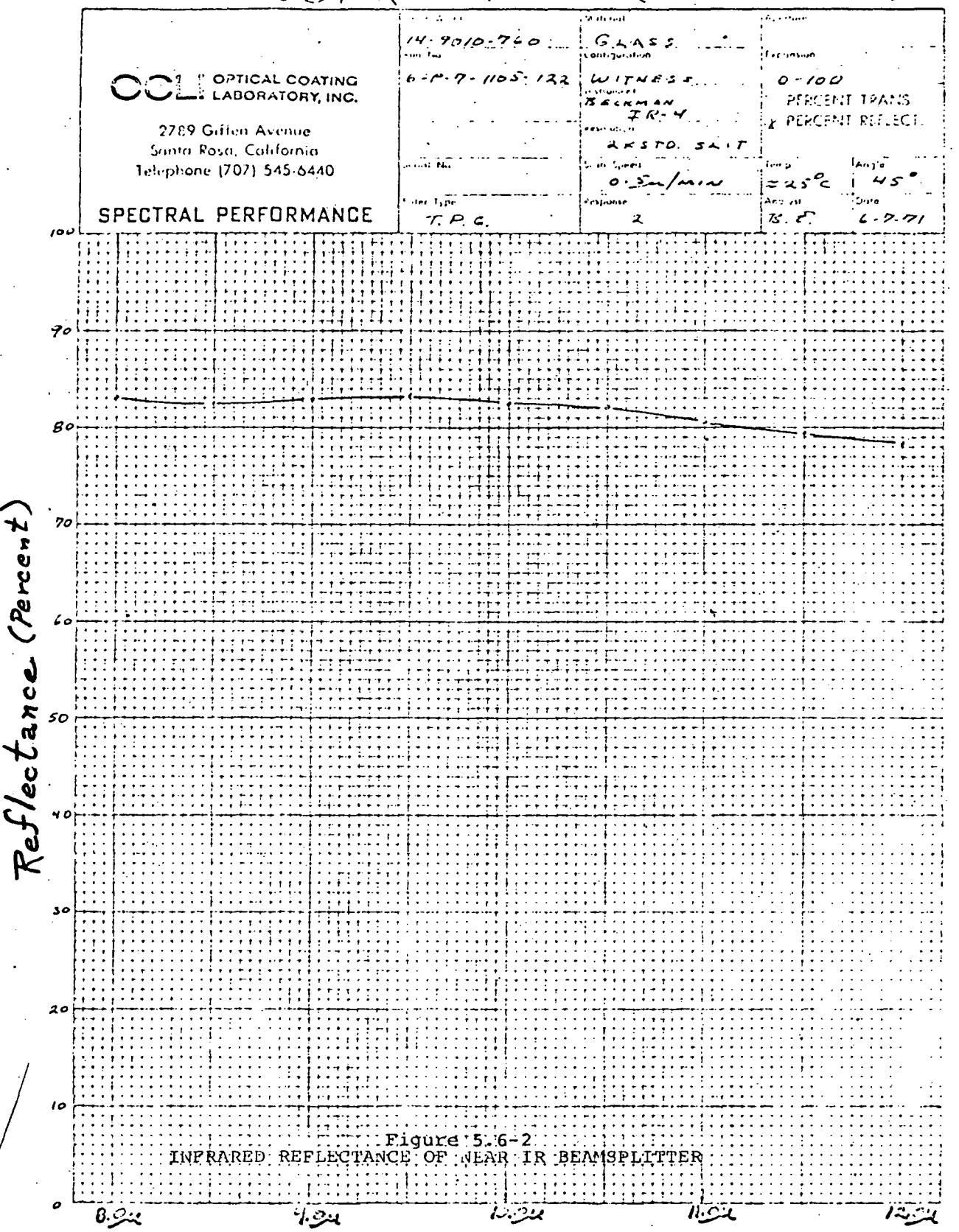

Figure 5.6-2
INFRARED REFLECTANCE OF NEAR IR BEAMSPLITTER

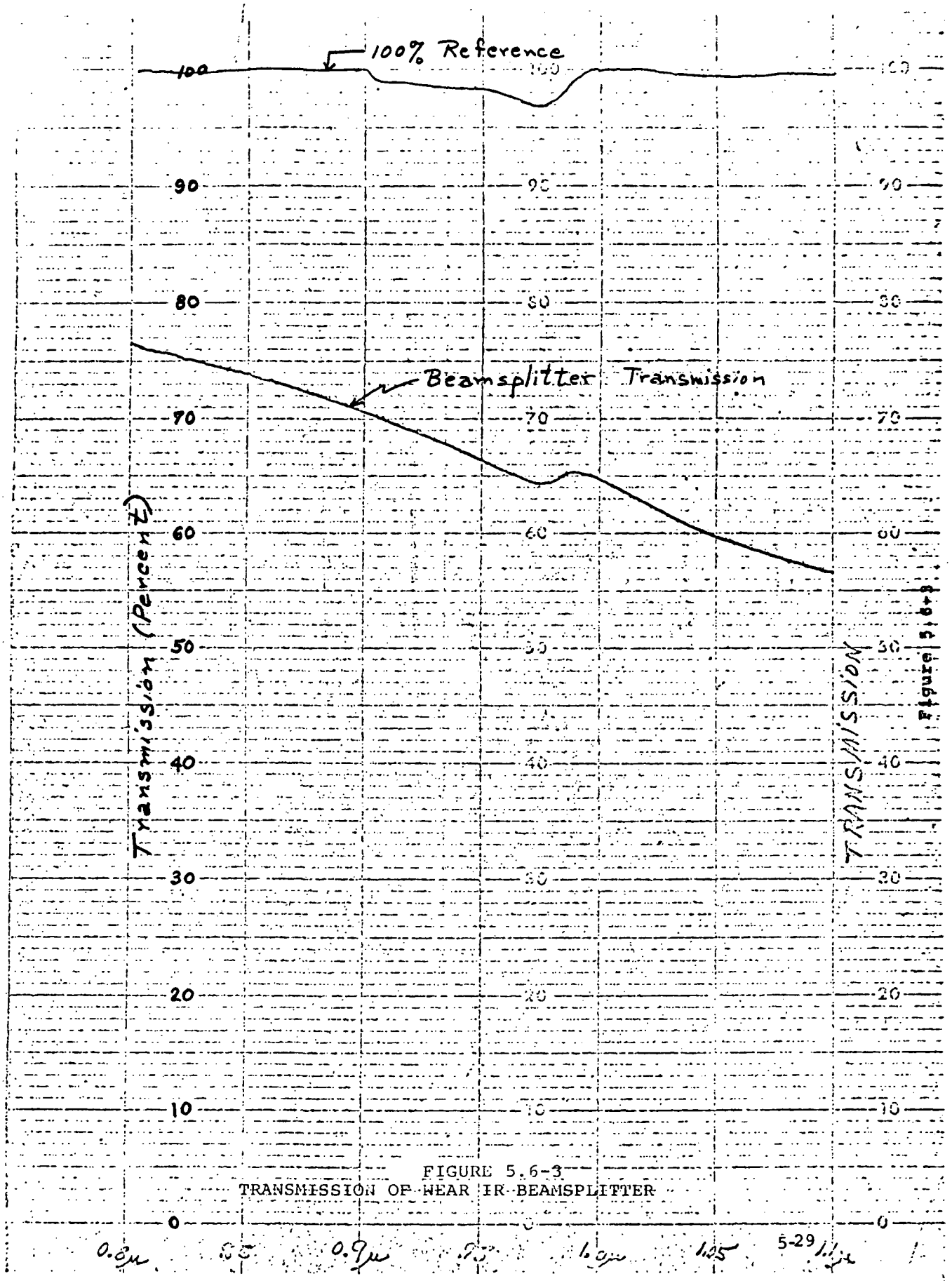

FIGURE 5.6-3
TRANSMISSION OF NEAR IR BEAMSPLITTER

OCLI W/O 14-9057-760 GERMANIUM 45° ANGLE BLOCK & POLARIZER

OPTICAL COATING LABORATORY, INC.

Telephone (707) 545-6440

GP-B-543-108 1.0" ϕ WITNESS 0-100%

P/N 90934 IR-12 X

2.0 x STD. SLIT

S.N. → 1, 2, #3 20 cm⁻¹/MIN. ≈25°C 45°R

SPECTRAL PERFORMANCE B/S 2.0 F.J. 6/18/71

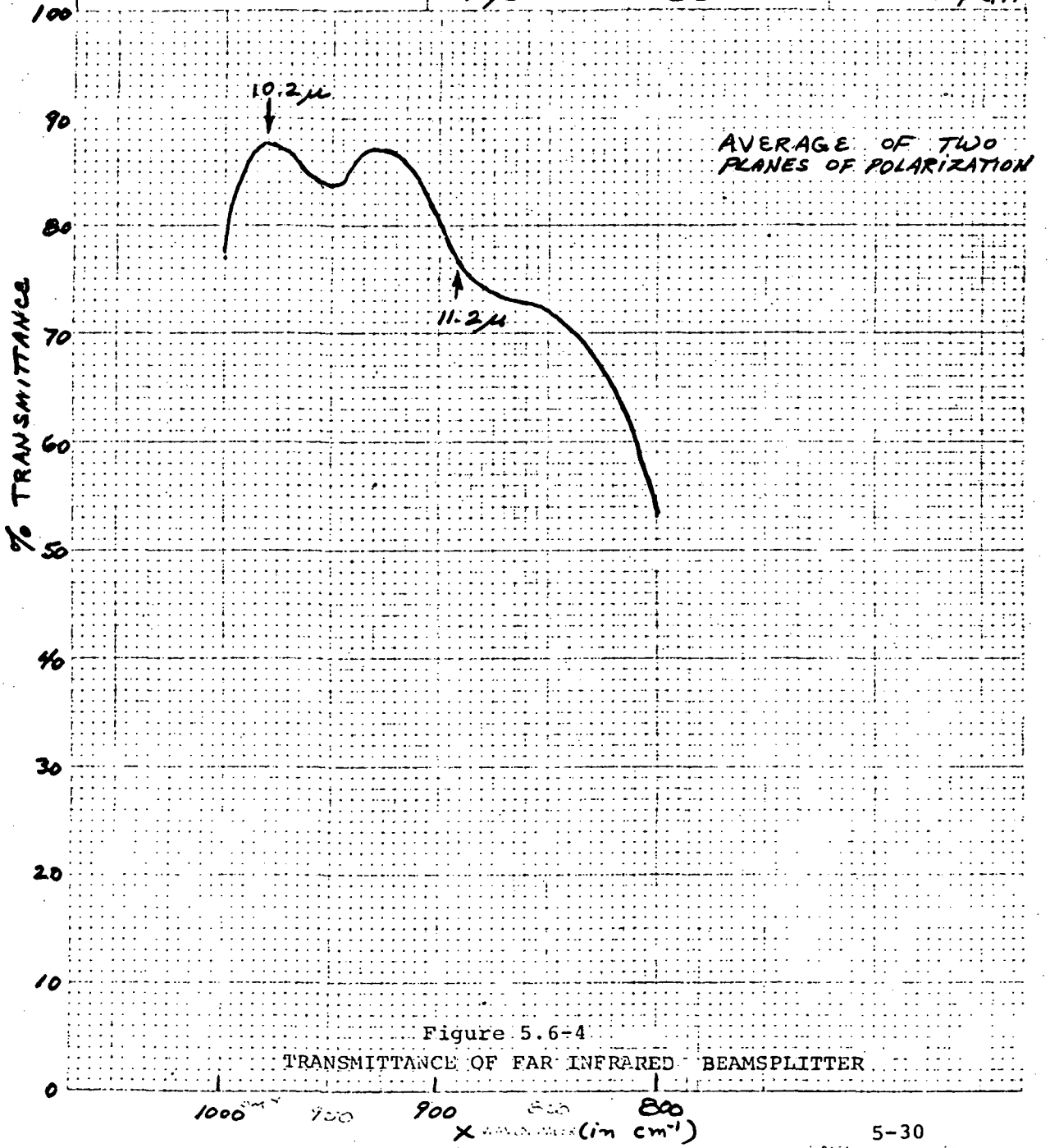

Figure 5.6-4
TRANSMITTANCE OF FAR INFRARED BEAMSPLITTER

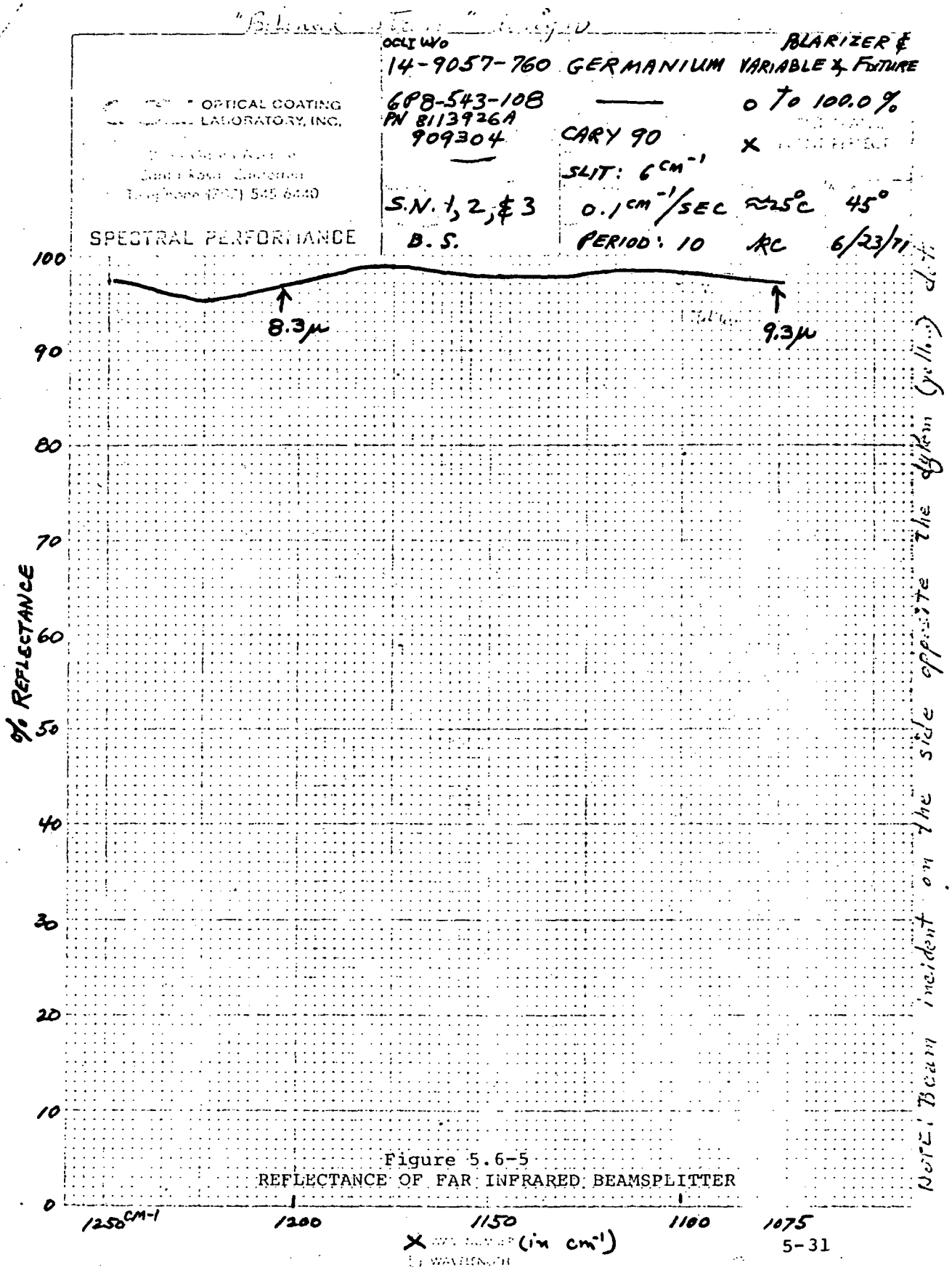

Figure 5.6-5
REFLECTANCE OF FAR INFRARED BEAMSPLITTER

FIGURE 5.6-6
TRANSMISSION OF 8.3-9.3μm BANDPASS FILTER

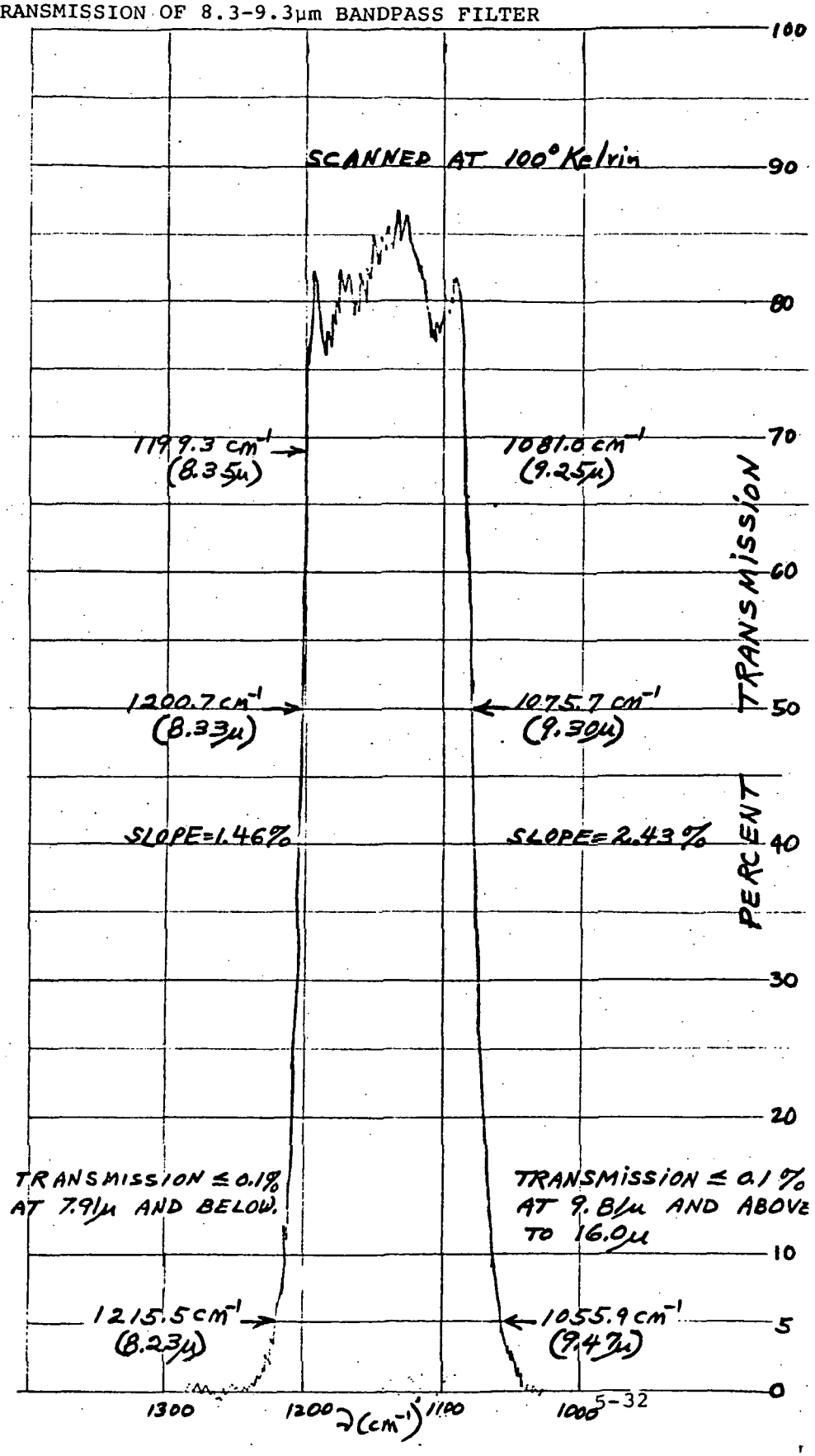

DATA IDENTIFICATION

S/N 14-7200-760
11-N-5-562-266
I.T.T. P/O # 3-933043
TYPE #1

SAMPLE IDENTIFICATION

B.P.
GERMANIUM

1.0" X 0.040" WITNESS

TEST OPERATING PARAMETERS

CARY 90 ☐ IR-12
CARY 14 ☐ IR-4

5.0 cm-1 SLIT
0.3 cm-1/sec.
3
0.5"
0-10%

Percent Transmission
Percent Reflection

TEST CONDITIONS

Reflected Angle 5°

Date 11-6-

FIGURE 5.6-6
TRANSMISSION OF 8.3-9.3μm BANDPASS FILTER

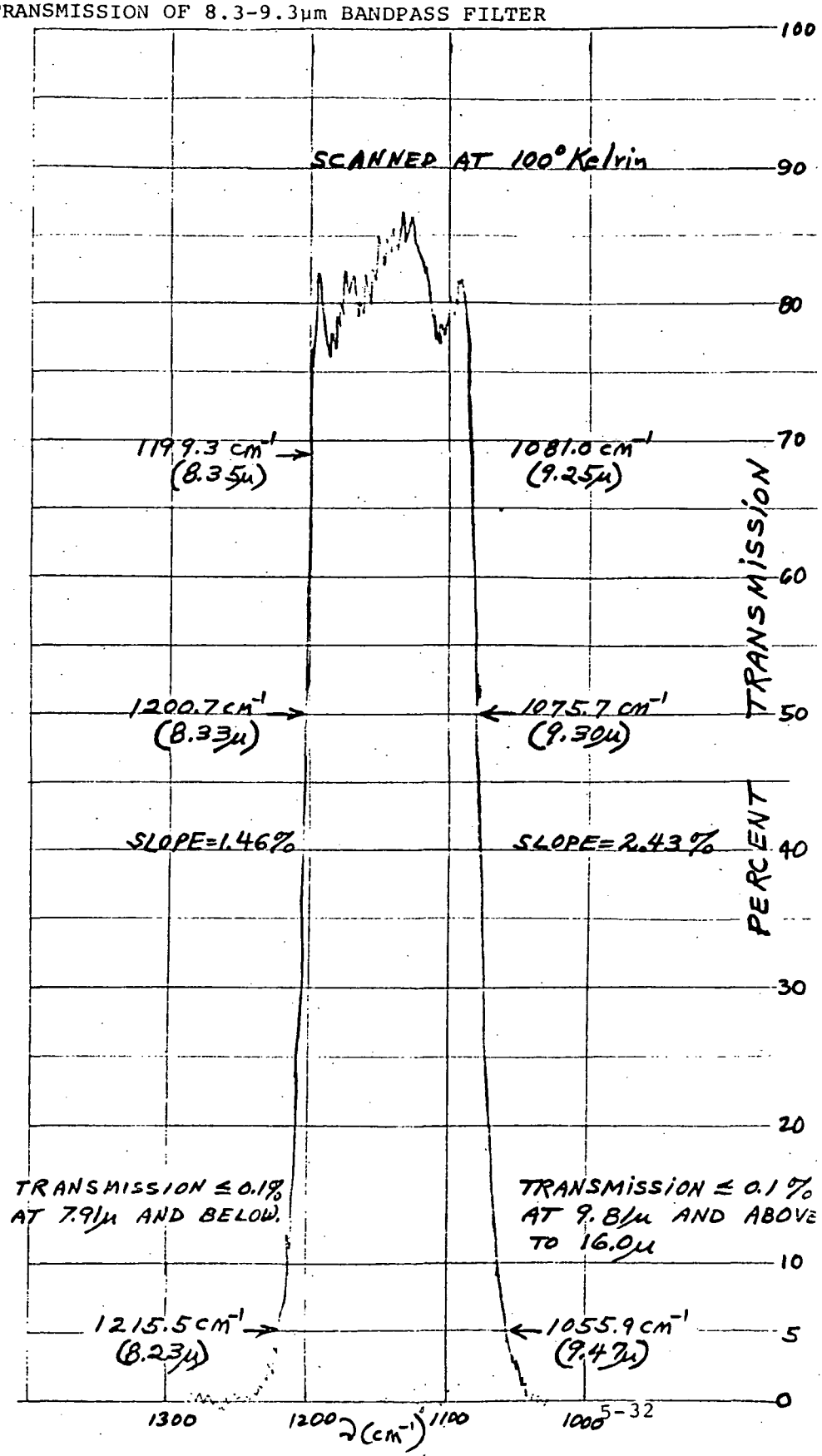

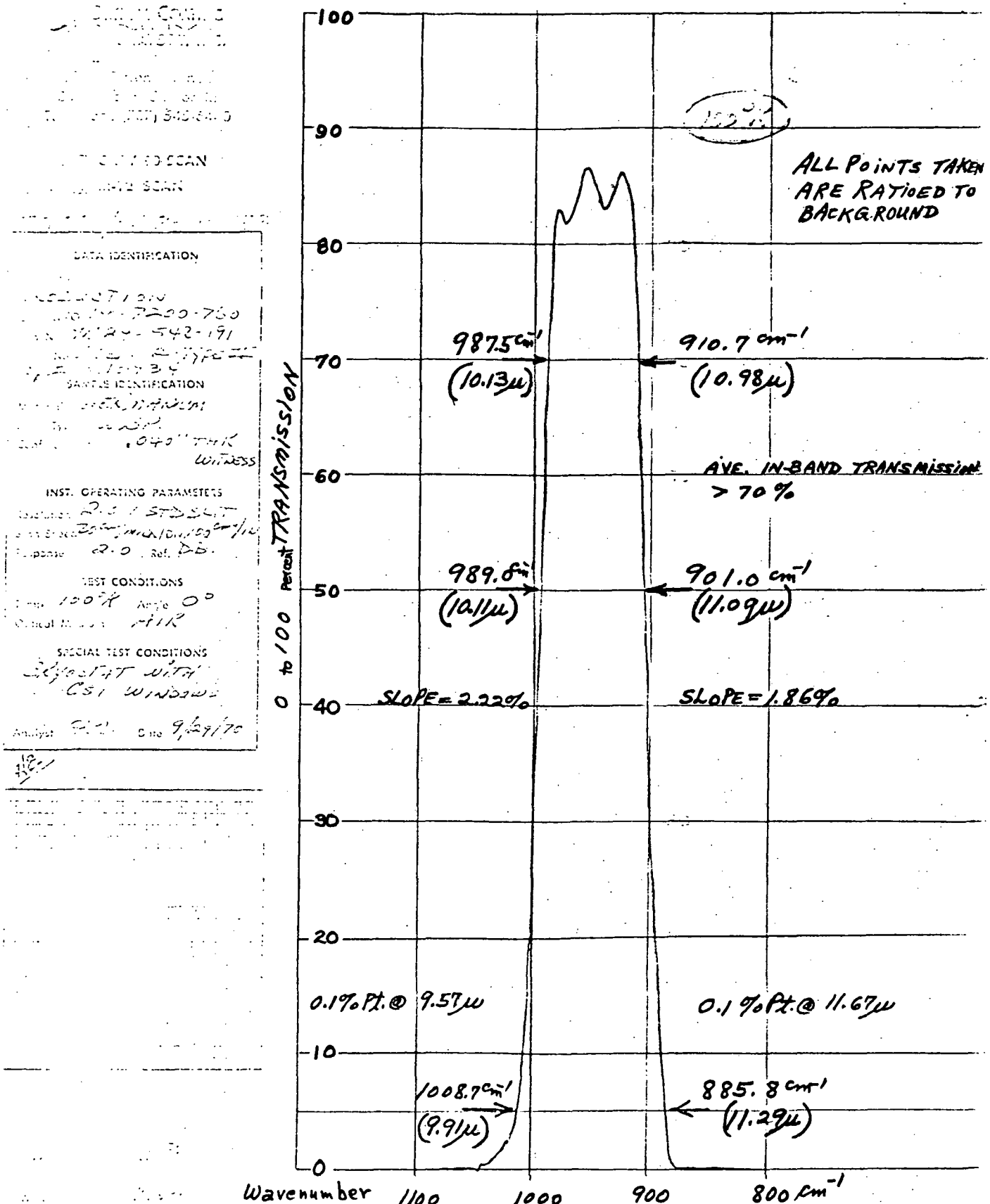

FIGURE 5.6-7

TRANSMISSION OF 10.2 - 11.2μm BANDPASS FILTER

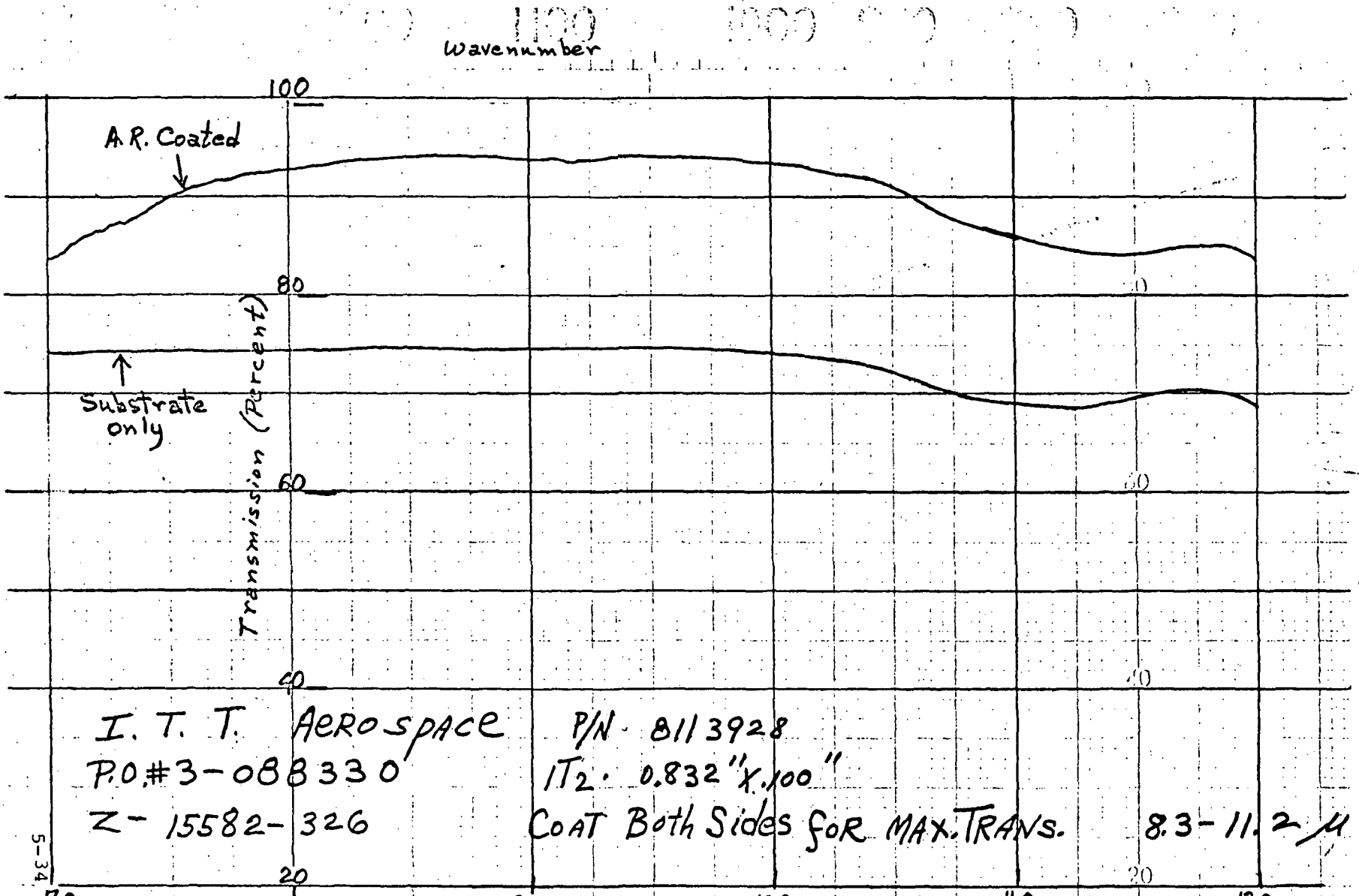

Transmission of Antireflection Coated Irtran II Cooler Windows

Figure 5.6-8

5.6.6 Near Infrared Filter

The transmission of the near infrared filter, which is a long wave pass (LWP) filter, is given in Figure 5.6-9.

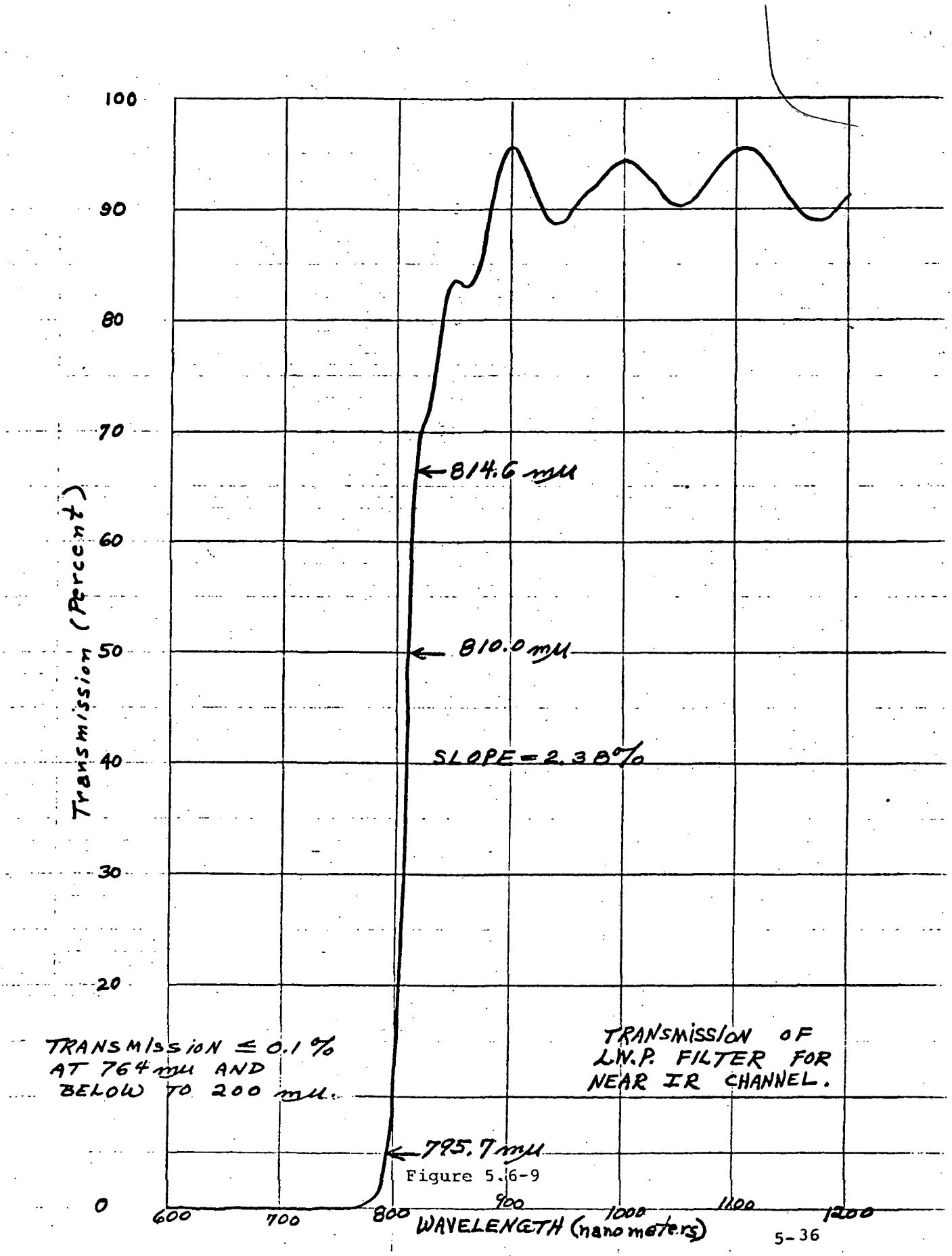
100
90
80
70
60
50
40
30
20
0
Transmission (Percent)
814.6 mμ
810.0 mμ
SLOPE = 2.38%
TRANSMISSION ≤ 0.1 % AT 764 mμ AND BELOW TO 200 mμ.
TRANSMISSION OF L.W.P. FILTER FOR NEAR IR CHANNEL.
795.7 mμ
600
700
800
900
1000
1100
1200
WAVELENGTH (nanometers)

Figure 5.6-9

6.0 RADIANT COOLER DESIGN

The infrared detectors are cooled to the vicinity of 100K by means of a radiant cooler. The conditions imposed by the spacecraft and its orbit in combination with additional mechanical and thermal constraints were used to establish a range of radiant cooler designs (Section 6.1). Three examples from this range, including two modifications to one design (Section 6.2) were then analyzed in detail (Section 6.3).

The design of the radiant cooler used in the instrument is close to that of modification 2 to design IIIB. The earth shield is modified to permit its use as a deployable cone mouth cover. The cover is used during launch to prevent the deposition of frost on the cone structure by delaying operation of the cooler until the bulk of spacecraft and instrument outgassing has taken place. It is also used to aid in the removal of frost accumulated after operation in orbit.

The patch has a view to cold space in the vertical plane of 28^{o} toward the earth (measure from the horizontal). This permits operation at a minimum altitude of 925 km with a spacecraft wobble of 1^{o}. The view angle away from earth in the vertical plane is 48.8^{o} and in the horizontal plane, $\pm 52.0^{o}$.

6.1 Range of Designs

It is assumed that the radiant cooler has a rectangular geometry in which the patch normal (cone axis) is parallel to the orbit normal and the plane of the cone mouth is parallel to that of the patch. To start with, a range of rectangular radiant cooler designs was subjected to a set of conditions or constraints. The basic conditions are those inposed by the spacecraft and its orbit:

a. Minimum spacecraft altitude of 925 km.
b. Maximum orbit plane to earth-sun line angle of 12^{o}.
c. Instrument temperature range of $25^{o}C \pm 25^{o}C$.

The specific requirements to be met by the radiant cooler design are:

1. Maximum view angle to cold space in the vertical plane through the centers of the patch and earth of 28^{o} toward the earth (includes 1^{o} for spacecraft wobble).
2. No direct sunlight in the cone mouth for sun angles from 0^{o} to 12^{o}.
3. Maximum view angle to cold space in the vertical plane of 50^{o} away from the earth.
4. No more than one cone wall reflection to cold space for rays leaving the patch in the horizontal plane and away from earth in the vertical plane.

5. Minimum area at the patch opening (cone cross-section at the plane of the patch top) of 3.2 in^2.
6. Maximum cooler length of 10.6 inches.

The cooler is designed to operate at a minimum spacecraft altitude of 925 km; however, the thermal analysis was carried out at the nominal altitude of 1100 km.

Several initial designs of varying patch opening area and aspect ratio were studied; they are listed in Table 6.1-1.

Table 6.1-1

Range of Radiant Cooler Designs

Patch Opening

Design	Width	Length		
		A	B	C
I	0.80	4.00	4.375	
II	1.00	3.20	3.50	
III	1.20	2.66	2.92	3.17
IV	1.40	2.28	2.50	
V	1.60	2.00	2.19	
Area of Opening (in^2)		3.2	3.5	3.8

All designs except IA, IB, and IIB met or very nearly met all the requirements. Designs IV and V were rejected because of their relatively large over-all vertical dimension and their reduced ratio of cone end area to cone mouth area. Designs IIA, IIIB, and IIIC were selected for detailed thermal analysis.

The exact geometry of radiant cooler design IIIB is shown in Figures 6.1-1, 6.1-2, and 6.1-3. The patch dimensions are those of the cone opening at the top of the patch and therefore include the cone-patch clearances. Similarly, the dimensions of the cone top (cone end and cone mouth) include the end-shield clearances.

To meet conditions (1) and (4), the upper vertical plane cone wall angle with respect to the patch normal (Figure 6.1-1) must be 31° or greater. The angle was set at the 31° minimum and various lower wall angles tried. At each lower wall angle, the cone length was adjusted to meet condition (1) and the design checked to see if it met condition (3). It was found that 10° is a good choice for the lower vertical cone wall angle. The

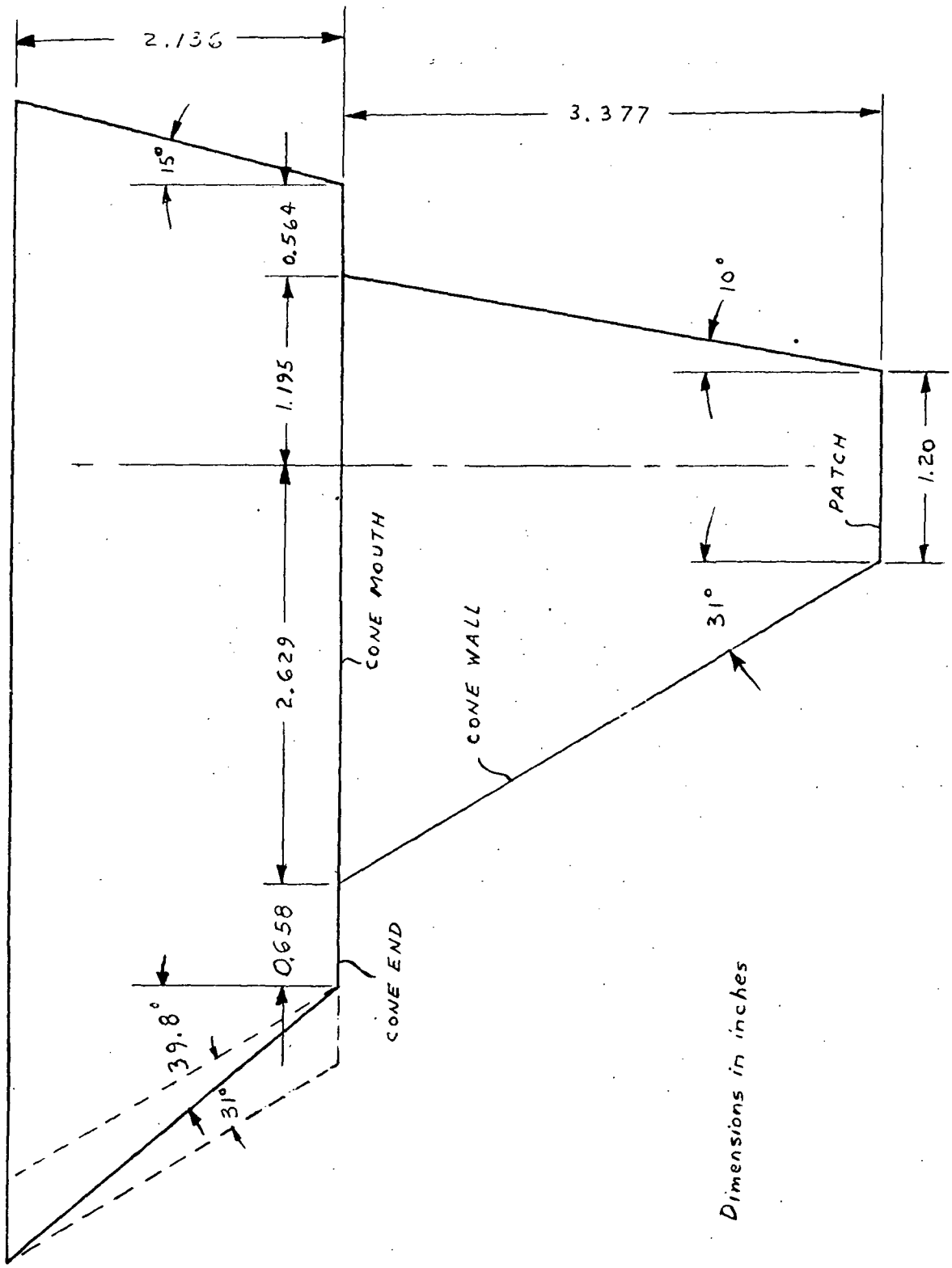

Figure 6.1-1 Vertical Plane of Design III B

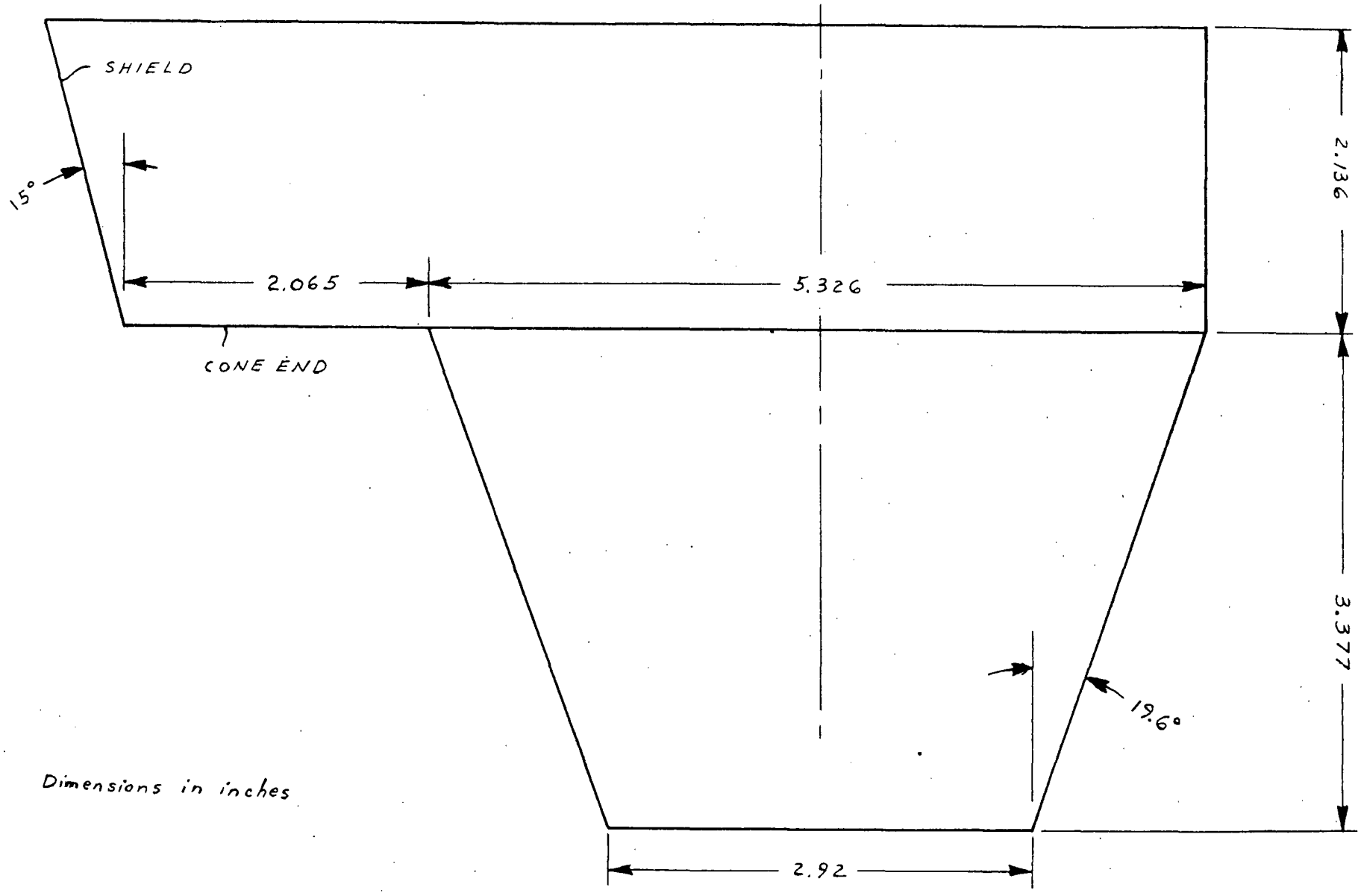

Figure 6.1-2 Horizontal Plane of Design III B

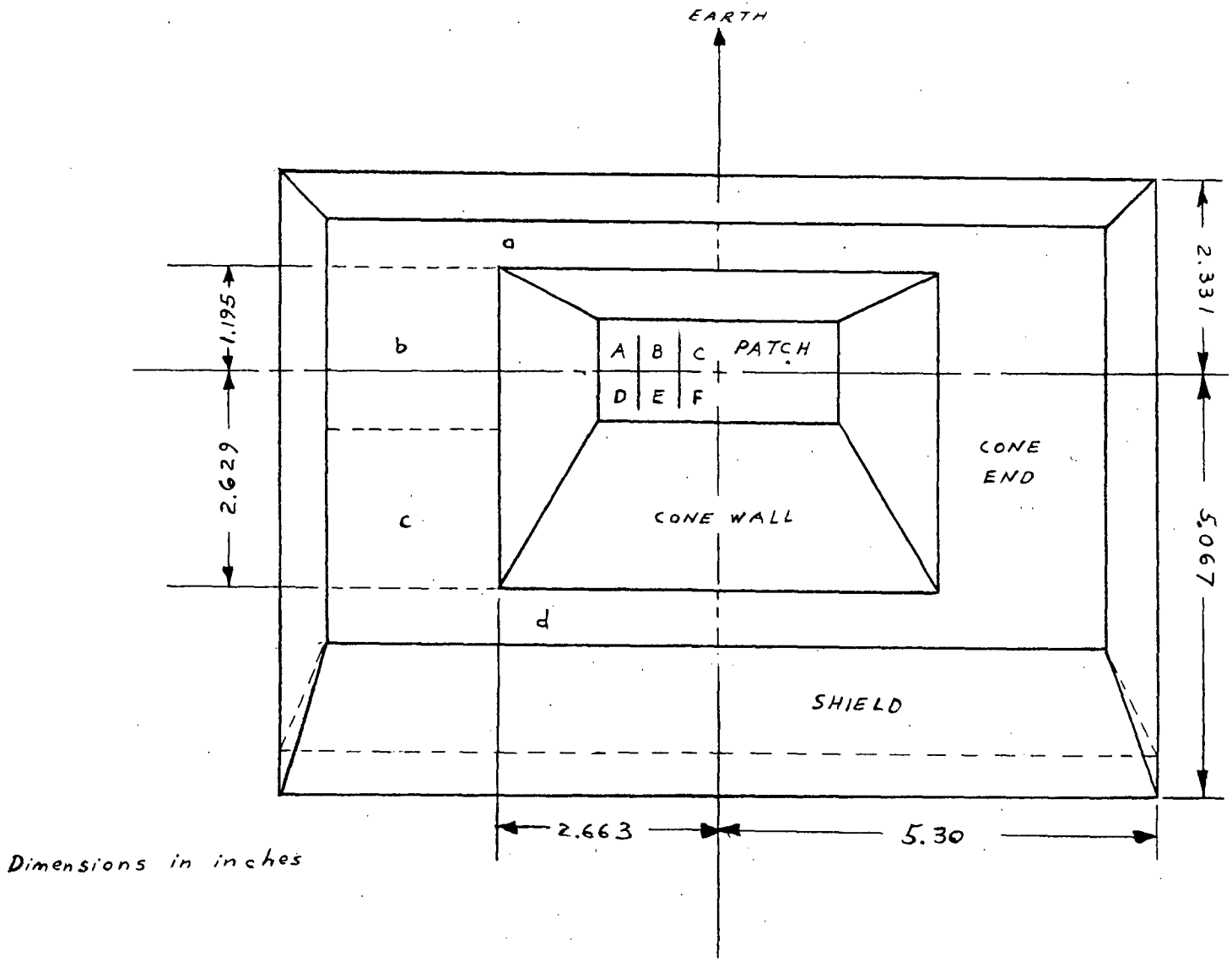

Figure 6.1-3 Top View of Design III B

maximum view angle to cold space away from earth in the vertical plane is then 48.8°. Because the constraints in the vertical plane are all angular in nature, all cone designs are the same in this plane except for a scale factor set by the selected patch width.

The wall angle in the horizontal plane was then determined by condition (4) that no more than one reflection be required for a horizontal patch ray to reach cold space

$$\tan \theta_H = \frac{-1 + \sqrt{3_a^2 + 1}}{3a},$$

where a is the ratio of cone length to patch length. The maximum cooler length (condition 6) and the requirement that the patch not see the shield then determine the height of the shield. The patch length and cone wall angle also determine the cone mouth dimension in the horizontal plane.

The position of the shield edges in the vertical plane are also set by the requirement that the patch not see the shield. The shield angle was set at 15° in the horizontal plane and in the lower direction of the vertical plane. This reduces the influence of sunlight scattering off the shields at solar elevation angles (above the orbital plane) of 15° and less. The shield angle in the upper vertical direction must be 31° or greater to prevent the cone top from seeing the earth by reflection in the shield. The angle was set at 39.8° in design IIIB. The values are 39.2° and 40.3° in designs IIA and IIIC, respectively. The larger than minimum shield wall angle reduces the radiative coupling between the shield and cone end and between the earth and cone end (assuming the cone end fills the space available for it). These reductions, however, are offset by a reduction in the size of the cone end area used to cool the cone. The prime reason for use of the larger angle is to provide clearance for the circuit boards mounted above the cooler.

6.2 Modifications to Design IIIB

Two modifications to the cone end and shield of design IIIB were studied, with the objective of improving thermal performance. In modification 1 (Figure 6.2-1), part of the cone end was tilted into the shield to reduce the radiative coupling to the earth. This change also eliminated solar exposure of the cone end at the 12° elevation angle. The improvements, however, were offset by the increased radiative coupling to the shield and by the reduced cone end area (Section 6.3).

a & d, Flat elements of cone end

b & c, Tilted (15°) elements of cone end

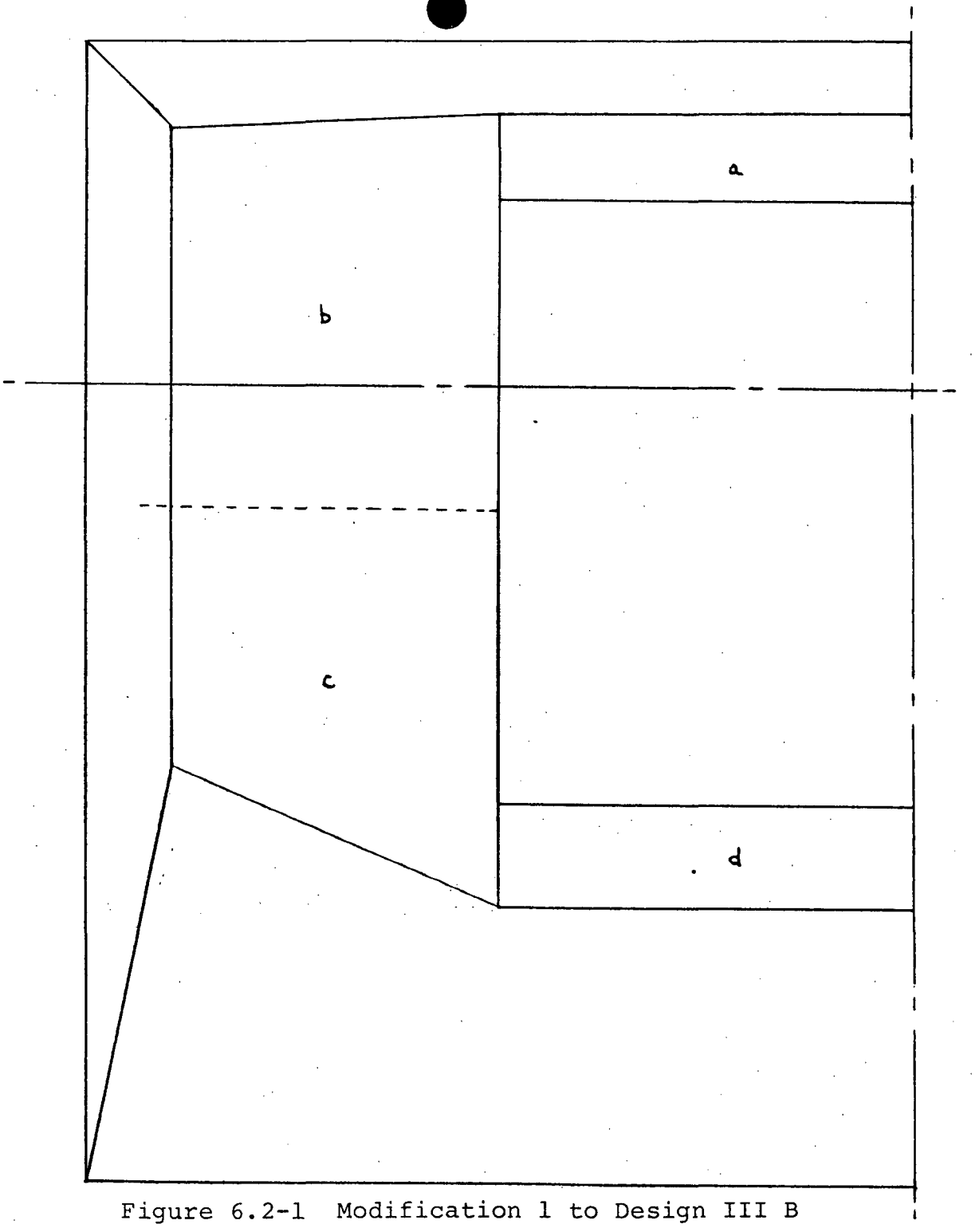

Figure 6.2-1 Modification 1 to Design III B

As a result, modification 2 (Figure 6.2-2) was made. In this design, the shield on the earth side was extended to reduce the input from the earth, but the shield angle left unchanged to allow an increase in cone end area. The cooler length was maintained at 10.6 inches. This modification resulted in a significant improvement in thermal performance (Section 6.3) and will be incorporated into the final cooler design.

6.3 Thermal Analysis

The radiative transfer parameters calculated in Section 6.4 are applied below to the calculation of the cone and patch temperatures in the range of cooler designs described in Sections 6.1 and 6.2. The analysis is carried out for the anticipated ranges of housing temperature and sun angle. In addition, temperatures are determined for degraded values of thermal properties and for increased thermal loads on the patch.

For modification 2 of design IIIB, the cone temperature for no direct sunlight varies from 154.2K at a housing temperature of 0^{o}C to 172.5K at 50^{o}C. The corresponding patch temperatures (T_p) are 94.1K and 100.0K. Direct sunlight at the maximum expected elevation angle (above the orbital plane) of 12^{o} increase the cone temperature by only 0.5K (ΔT_p = 0.17K). A degradation in the cone multilayer insulation by a factor of 0.8 increases the cone temperature by 3.9K. Combined with the same degradation in the patch insulation, the resultant increase in patch temperature is 1.7K. Doubling the solar absorptivity of the low α/ε cone end (to 0.30) increases the cone temperature by 1.1K (ΔT_p = 0.35K). Increasing the infrared emissivity of the shield and cone wall from 0.05 to 0.07 increases the cone temperature by 3.9K and the patch temperature by 4.2K. The patch is heated not only by the warmer cone but also by the increased emission of the cone walls. If the input to the patch through the optical opening or by bias heating is increased by 1×10^{-3} W, the patch temperature increases by 2.1K.

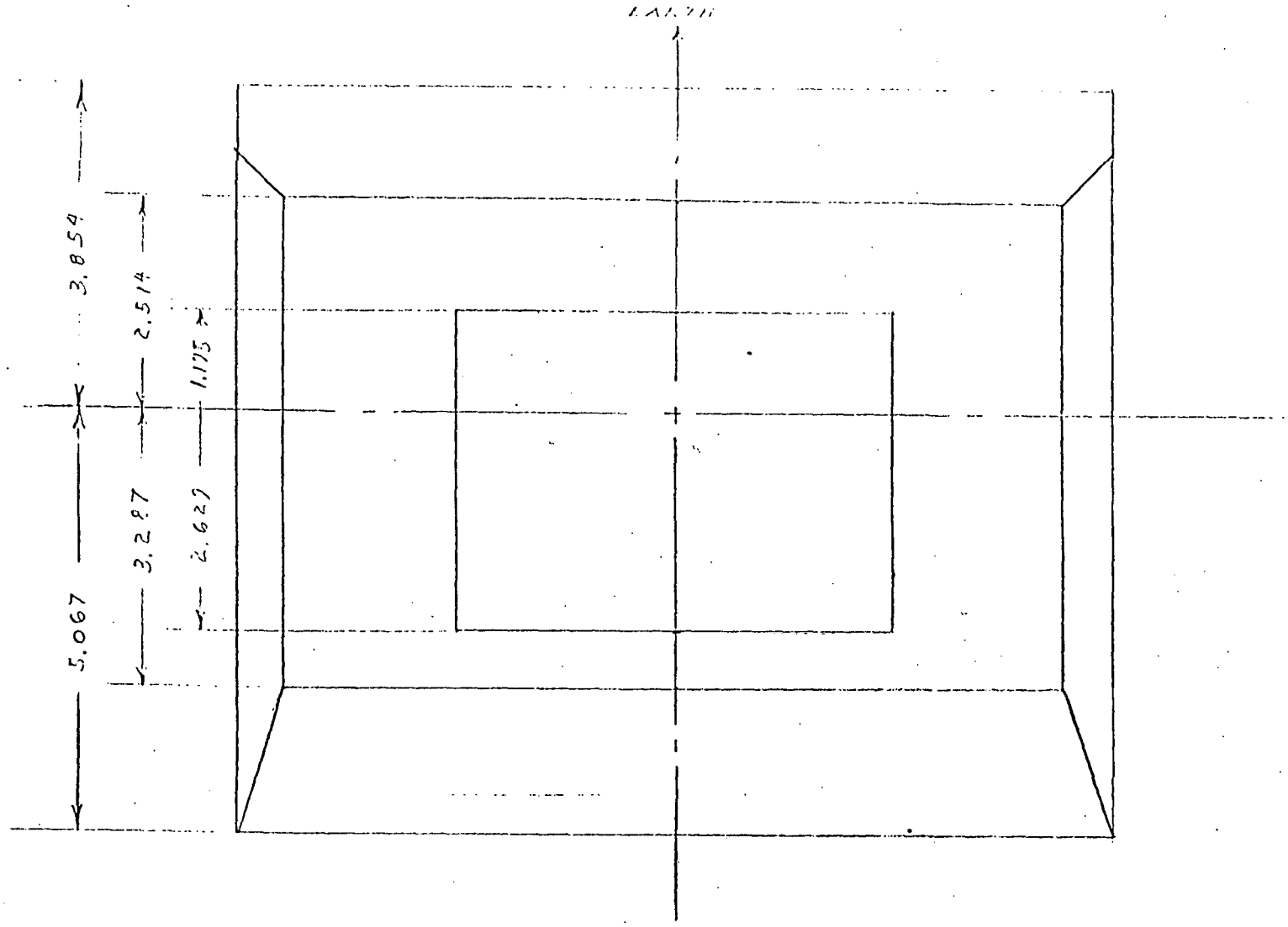

Figure 6.2-2 Modification 2 to Design III B

6.3.1 Cone Temperature Range

The steady-state (equilibrium) thermal balance equation of the cone is:

$$\varepsilon_d \quad \sigma T_c^4 = \frac{1}{A_d} \quad (\Phi_e + \Phi_h + \Phi_s + \Phi_k + \Phi_i),$$

where

ε_d = emissivity of cone end

A_d = area of cone end

Φ_e = input from earth

Φ_h = input from shield

Φ_s = input from direct sunlight

Φ_k = input through supports and leads

Φ_i = input through multilayer insulation

The radiative input from the earth is given by

$$H_e = \frac{\Phi e}{A_d} = (\alpha_{me} W_r + \varepsilon_{me} W_e) \frac{Am}{A_d} + (\alpha_d W_r + \varepsilon_d W_e) Fde,$$

where

α_{me} = cone mouth absorptivity for earth reflected sunlight

ε_{me} = cone mouth absorptivity for earth infrared

W_r = average reflected sunlight exitance of earth

W_e = average infrared exitance of earth

A_m/A_d = ratio of cone mouth area to cone end area

αd = solar absorptivity of cone end

Fde = view factor from cone end to earth

The radiative input from the shield is given by

$$H_h = \frac{\Phi h}{A_d} = \varepsilon_d \; a_{dh} \; \sigma T_h^4$$

wnere a_{dh} is the effective emissivity of the shield as seen from the cone end and T_h the temperature of the shield (instrument housing). The radiative input from direct sunlight is given by

$$Hs = \frac{\Phi_s}{A_d} = \alpha_d \; g_d \quad S_o \sin \beta_s,$$

where

g_d = average fraction of cone end area exposed to direct sunlight

S_o = solar constant = 0.14 W cm^{-2}

β_s = elevation angle of sun above orbital plane

From Appendix I to the Final Report on Contract No. NAS5-10113 (Dec. 1967) we have

$$W_e = 2.1 \times 10^{-2} \quad W \; cm^{-2}$$

$$W_r = \frac{1}{2\pi} \quad S_o \cos \beta_s A \quad \frac{\cos^2 \beta_e}{1 - \sin \beta_e} \; ,$$

Where A is the average solar reflection factor for the earth (0.4) and β_e is the angle from the nadir to earth tangent line. At an altitude of 1100 km, β_e is 58.5^o, and

$$W_r = 1.65 \times 10^{-2} \quad \cos \beta_s \quad W \; cm^{-2}.$$

The coupling factors needed to complete the calculation of radiative inputs to the cone are given in Section 6.4.

The input from the instrument housing to the cone through mechanical supports and electrical leads is given by

$$K = K_c \; (T_h - T_c),$$

where K_c is the thermal conductance between the housing and cone. K_c is given by

$$K_c = \sum \frac{k_i A_i}{l_i}$$

where k_i = thermal conductivity of connection i

A_i = cross-sectional area of connection i

l_i = length of connection i.

The supports and leads are listed in Table 6.3.1-1. The resultant thermal conductance is

$$K_c = 4.93 \times 10^{-4} \text{ W/K.}$$

Table 6.3.1-1

Cone Supports and Electrical Leads

Length (inches)	Quantity to dia. (inch)	Material	k*
3.50	2 supports ¼ X 3/16	Synthane	3.3×10^{-3}
1.50	2 " "	"	"
2.75	2 " "	"	"
2.75	4 Detectors 2 X 10^{-3}	Ni	0.78
2.75	2 C. Thermistor 3.3 X 10^{-3}	Chromel	0.13
2.75	2 P. " "	"	"
3.50	2 C. Heater "	"	"
3.50	2 P. " 5.2 X 10^{-3}	"	"

* Thermal conductivity in W/cm. K

The input through the multilayer insulation may be considered entirely radiative (it is, in fact, a complex combination of radiative and conductive). The interchange between the housing and outer cone surface (wall and end) is reduced by the shielding factor s_i of the insulation,

$$H_i = \frac{\Phi_i}{A_d} = \frac{\sigma A_i}{s_i A_d} (T_h^4 - T_c^4)$$

where A_i is the area of the outer cone surface (Table 6.3.1-2).

Table 6.3.1-2

Cone Surface Areas

Design	A_i	A_d
IIA	100	25.40
IIIB	113	27.34
IIIC	111	26.03
Mod. 1 IIIB	110	24.41
Mod. 2 IIIB	120	34.48

All in square inches

The cone temperatures of the various designs were first calculated for the following set of nominal radiative properties

ε_h = infrared emissivity of shield = 0.05

ε_c = infrared absorptivity of cone wall = 0.05

α_c = solar absorptivity of cone wall = 0.13 (Aluminum)

ε_d = infrared emissivity of cone end = 0.85

α_d = solar absorptivity of cone end = 0.15

s_i = shielding factor of cone insulation = 100*

The resultant cone temperatures are listed in Table 6.3.1-3 for no direct solar inputs and three values of housing temperature. The influence of direct sunlight at 12° is shown in Table 6.3.1-4 for designs IIA, IIIB, and IIIC.

---

*In practice, a shielding factor of about 70 was realized. To obtain performance equivalent to a factor of 100, the cooler housing was thermally isolated from the main instrument structure and operated in the vicinity of 0°C.

Table 6.3.1-3

Cone Temperatures for Nominal Radiative Properties

	T_c for T_h equal to		
Design	0^oC	25^oC	50^oC
IIA	166.7	174.3	182.6
IIIB	168.4	176.0	184.3
IIIC	169.6	177.2	185.5
Mod. 1 IIIB	170.0	178.2	187.4
Mod. 2 IIIB	154.2	163.1	172.5

Temperatures in kelvins; $\beta_s = 0^o$

Table 6.3.1-4

Cone Temperature for 12^o Sun Angle

Design	T_c	ΔT_c
IIA	176.1	1.8
IIIB	176.5	0.5
IIIC	178.9	1.7

Temperatures in kelvins; $T_h = 25^oC$

The cone temperatures for degraded values of radiative properties are listed in Table 6.3.1-5 for design IIIB and its second modification. The increases listed are above the nominal values given in Table 6.3.1-3 at a housing temperature T_h of 25^oC.

Table 6.3.1-5

Cone Temperature For
Degraded Thermal Properties

Design	Insulation		Degraded Property Solar Absorptivity		Infrared Absorptivity	
	$s_i = 80$		$\alpha_d = 0.30$		$\varepsilon_h = \varepsilon_c = 0.07$	
	T_c	ΔT_c	T_c	ΔT_c	T_c	ΔT_c
IIIB	179.4	3.4	177.6	1.6	178.7	2.7
Mod. 2 IIB	167.0	3.9	164.2	1.1	167.0	3.9

Temperatures in kelvins; $T_h = 25^{\circ}C$ and $\beta_s = 0^{\circ}$.

6.3.2 Patch Temperature Range

The steady-state (equilibrium) thermal balance equation of the patch is

$$\Phi_p = \alpha A_p T_p^4 = \Phi_k + \Phi_r + \Phi_o + \Phi_j + \Phi_i,$$

where

A_p = black radiating area of patch

Φ_k = input through supports, leads, and anti-frost enclosure

Φ_r = input from cone walls

Φ_o = input through optical opening

Φ_j = detector joule heating

Φ_i = input through multilayer insulation.

The mechanical supports and electrical leads are listed in Table 6.3.2-1. They contribute an equivalent thermal conductance of

$$K_p = 4.62 \times 10^{-5} \text{ W/K}$$

when the effect of the support shields is included (HIRS for Nimbus F, Quarterly Report for July-Sept., 1972, NAS5-21651, Section 2.1.3.3).

Table 6.3.2-1

Conductive Couplings to the Patch

Quantity	to	dia (inch)	Material
2	supports	1/8 X 3/32	Synthane
4	detectors	2×10^{-3}	Ni
2	p. thermistor	3.3×10^{-3}	Chromel
2	p. heater	3.3×10^{-3}	Chromel

Supports and leads are all 4 inches long.

The radiative input from the low-emissivity cone walls above the black patch area is given by

$$\Phi_r = A_p \quad \varepsilon_{pc} \, \sigma T_c^4$$

where ε_{pc} is the effective patch-to-cone emissivity. The values of ε_{pc} for the three cone designs and for two values of effective specular cone wall emissivity are given in Section 6.4.

The detector thermal input through the optical connection to the patch and the joule heating of the detectors is approximately

$$\Phi_o + \Phi_j = 2.8 \times 10^{-3} \text{ W}$$

The radiative input through the optical opening (Φ_o) is about 1.8×10^{-3} W (Section 6.5). We have therefore allowed joule heating of 0.5×10^{-3} W for each of the two detectors.

The multilayer insulation between the patch (back and side areas) has a nominal shielding factor of 200*. The areas covered are listed in Table 6.3.2-2 together with the black patch area A_p.

* Such a high value can be obtained only over very large areas. In fact the multilayer between the cone and patch was replaced by a gold-to-gold radiative decoupling to eliminate an outgassing source and to allow for the addition of N_2 gas purge. See Section 6.7.

Table 6.3.2-2

Patch Surface Areas

	Design	A_p	A_{ip}
	IIA	2.790	7.790
	IIIB	3.102	6.752
	IIIC	3.377	8.5895
Mod. 1	IIIB	3.102	6.752
Mod. 2	IIIB	3.102	6.752

All in square inches; the patches are 0.625 inch thick.

The patch temperatures of the various designs were first calculated for a nominal cone wall emissivity ε_c of 0.05 and the above shielding factor for patch insulation. The results are listed in Table 6.3.2-3 for no direct sunlight on the cone and three values of housing temperature. The corresponding cone temperatures are given in Table 6.3.1-3.

Table 6.3.2-3

Patch Temperatures for Nominal Radiative Properties

		T_p for T_h equal to		
	Design	0^o	25^oC	50^oC
	IIA	99.9	102.5	105.4
	IIIB	98.6	101.2	104.0
	IIIC	98.25	100.9	103.8
Mod. 1	IIIB	99.2	101.9	105.1
Mod. 2	IIIB	94.1	96.9	100.0

Temperature in kelvins; $\beta_s = 0^o$

The influence of direct sunlight at 12^o is shown in Table 6.3.2-4 for designs IIA, IIIB, and IIIC. The corresponding cone temperatures are listed in Table 6.3.1-4.

Table 6.3.2-4

Patch Temperatures for 12^{o} Sun Angle

Design	T_p	ΔT_p
IIA	103.1	0.6
IIIB	101.3	0.17
IIIC	101.5	0.6

Temperatures in kelvins; $T_h = 25^{o}C$.

The patch temperatures for degraded values of radiative properties are listed in Table 6.3.2-5 for design IIIB and its second modification. The corresponding cone temperatures are listed in Table 6.3.1-5.

Table 6.3.2-5

Patch Temperatures for Degraded Thermal Properties

Design	Insulation		Degraded Property Solar Absorptivity		Infrared Emissivity	
	S_i (Patch) = 160		$\alpha_d = 0.30$		$\varepsilon_h = \varepsilon_c = 0.07$	
	S_i (Cone) = 80					
	T_p	ΔT_p	T_p	ΔT_p	T_p	ΔT_p
IIIB	102.9	1.7	101.7	0.5	105.5	4.3
Mod. 2 IIIB	98.6	1.7	97.25	0.35	101.1	4.2

Temperatures in kelvins; $T_h = 25^{o}C$ and $\beta_s = 0^{o}$

The patch temperatures for an increased bias heating (or increased rediative input through the optical opening) are given in Table 6.3.2-6. The increase of 1×10^{-3} W would enable each detector to operate at a bias level of 1×10^{-3} W.

Table 6.3.2-6

Patch Temperature for Increased Bias

Design	T_p	ΔT_p
IIIB	103.05	1.85
Mod. 2 IIIB	99.00	2.1

$\Phi_o + \Phi_j = 3.8 \times 10^{-3}$ W; temperatures in kelvins.

In addition to thermal inputs considered above, the patch has a very small view of a solar panel. A representative situation is analyzed in Section 3.3 of Part I to the Final Report on Contract NAS5-11683 (8 April-31 Oct. 1969). The thermal input is shown to be approximately 0.3×10^{-3} W and the increase in patch temperature, 0.6K.

6.4 Radiative Coupling Factors

The radiative coupling factors within the cooler and between the cooler and external sources were evaluated by means of the specular image array and contour integral techniques described in the Final Report on Contract No. NAS5-11603 (Part II 8 April-15 December 1969) and in Applied Optics for January, 1970 (p. 185). First it is necessary to calculate several view factors (The fraction of power diffusely emitted from one area that directly strikes a second area is the view factor from the first area to the second). The view factors required for thermal analysis of the radiant cooler are:

a. $F_{p-m}(n)$ = view factor from the patch to the cone mouth images seen by n specular reflections in the cone walls.
b. $F_{d-h}(n)$ = view factor from the cone end to the shield mouth images seen by n specular reflections in the shield wall.
c. F_{d-e} = view factor from the cone end to the visible region of the earth.
d. $F_{m-e}(n)$ = view factor from the cone mouth to the visible region of the earth whose radiation is reflected n times in the cone walls.

The view factors (a) are used to determine the patch-cone radiative coupling factor or effective patch-to-cone emissivity. (Final Report on Contract NAS5-10113, December 1967, Section 1.3).

$$\varepsilon_{pc} = 1 - \Sigma_n F_{p-m(n)} (1 - \varepsilon_c)^n,$$

where ε_c is the emissivity of the cone walls and the patch is black (emissivity of one).

The view factors (b) are used to determine the effective emissivity of the shield as seen from the cone end (equal to the effective absorptivity of the shield for cone end radiation),

$$a_{dh} = \Sigma_n \quad a_n F_{d-h(n)},$$

where a_n is the emissivity (absorptivity) produced by n shield wall reflections. For infrared radiation, $a_n = 1 - (1 - \varepsilon_h)^n$, where ε_h is the infrared absorptivity (emissivity) of the shield walls. Using the conservation condition

$$\Sigma F_{d-h(n)} = 1,$$

the above may also be written as

$$a_{dh} = 1 - \Sigma F_{d-h(n)} \ (1 - \varepsilon_h)^n.$$

The cone end-shield radiative coupling factor or effective emissivity is obtained by multiplying a_{dh} by the emissivity ε_d of the cone end. This is the case because radiation leaving the cone end by emission or reflection never returns when the shield walls are specularly reflecting and outward sloping (a condition which also holds between the patch and cone walls).

The view factors (c) and (d) are used to determine the absorptivity of the cone end and cone mouth, respectively, for radiation from the earth. In the case of the cone mouth, multiple reflections at the cone walls must be taken into account. The effective absorptivity for earth radiation is then

$$a_{me} = \Sigma a_n F_{m-e}(n),$$

wher a_n is the absorptivity produced by n cone wall reflections. For infrared from the earth, $a_n = 1 - (1 - \varepsilon_c)^n$ and for reflected sunlight, $a_n = 1 - (1 - \alpha_c)^n$, where ε_c and α_c are the infrared absorptivity (emissivity) and solar absorptivity, respectively.

The radiative view factors and radiative coupling factors are listed in Tables 6.4-1 through 6.4-3 for cooler designs IIA, IIIB, and IIIC, including the modifications to IIIB. For purposes of calculating the view factors, the patch was divided into 12 equal elements, and the cone end (bib) into 8 unequal elements. By symmetry, there are 6 different view factors from the patch elements and 4 different view factors from the cone end elements (See Figure 6.1-3). Values of ε_{pc} are shown for two values of effective specular cone wall emissivity ε_c, 0.07 and 0.05. Values of a_{dh} and ε_{me} (infrared value of a_{me}) are shown for a cone wall

and shield wall infrared absorptivity of 0.05. Values of α_{me} (reflected sunlight value of a_{me}) are shown for cone wall solar absorptivities of 0.22 (gold) and 0.13 (aluminum). Coupling factors to the earth are from the nominal altitude of 1100 km.

Table 6.4-1

Cone-Patch Coupling Factors*

Design	F_{p-m} (o)	$F_{p-m(1)}$	$F_{p-m(2)}$	ε_{pc} (ε_c) (0.07)	(ε_c) (0.05)
IIA	0.3196	0.5083	0.1721	0.0588	0.0422
IIIB	0.3231	0.5078	0.1691	0.0584	0.0419
IIIC	0.3271	0.5050	0.1679	0.0580	0.0416

* Results neglect very small $F_{p-m(3)}$

Table 6.4-2

Cone-End (Bib) Coupling Factors

Design	F_{de}	a_{dh} (0.05)	A_d/A_m*
IIA	0.0779	0.0161	1.61
IIIB	0.0787	0.0167	1.34
IIIC	0.0809	0.0162	1.24
Mod. 1 IIIB	0.0587	0.0219	1.20
Mod. 2 IIIB	0.0403	0.0189	1.69

* Ratio of cone end to cone mouth area

Table 6.4-3

Cone Mouth Coupling Factors

Design	$\varepsilon_{me}(0.05)$	$\alpha_{me}(0.22)$	$\alpha_{me}(0.13)$	F_{me}*
IIA	8.40×10^{-3}	3.38×10^{-2}	2.09×10^{-2}	0.0935
IIIB	9.28×10^{-3}	3.71×10^{-2}	2.31×10^{-2}	0.1014
IIIC	9.19×10^{-3}	3.71×10^{-2}	2.30×10^{-2}	0.1063
Mod. 1 IIIB	9.28×10^{-3}	3.71×10^{-2}	2.31×10^{-2}	0.1014
Mod. 2 IIIB	4.43×10^{-3}	1.725×10^{-2}	1.09×10^{-2}	0.0403

*From cone mouth center

An example of the specular image array technique used to determine view factors is shown in Figure 6.4-1. The boundaries of the shield and cone mouth images (formed by reflection in the cone walls) are projected onto the equivalent earth disk (H.C. Hottel and A.F. Sarofim, Radiative Transfer, McGraw-Hill, 1967, p. 65). The view is from the center of the cone mouth in Design IIIB. The projections divide the earth into regions whose radiation requires from 1 to 3 cone wall reflections to leave the cone or whose radiation is blocked by the shield.

The radiant cooler will also be exposed to direct sunlight during part of the year. The shield is designed to shade the cone mouth up to the maximum expected solar elevation angle of 12° above the orbital plane. As a result, we need to consider only the direct solar irradiance of the low α/ε cone end. Because of the large thermal time constant of the cone structure, the influence of direct sunlight is averaged over an orbital period. The average fraction of cone end area exposed over an orbit (the solar exposure factor) is given by

$$g_d = \frac{1}{\pi} \int_0^{\pi} g_d(\varphi_s)\, d\varphi_s,$$

where $g_d(\varphi_s)$ is the fraction of exposed area at a solar aximuth angle φ_s.

The variations of $g_d(\varphi_s)$ with φ_s are given in Figures 6.4-2 through 6.4-4, for designs IIA, IIIB, and IIIC, respectively. The $\varphi_s = 0^{\circ}$ point is when the spacecraft, earth, and sun are in line in that order. The earth shades the spacecraft from direct sunlight from 0° to 58.5°. It is seen that the maximum exposure at the 12° solar elevation angle is less than 9% of the end area for design IIIB.

(N) = number of cone wall reflections

Images and shield edge projected onto plane of earth disk

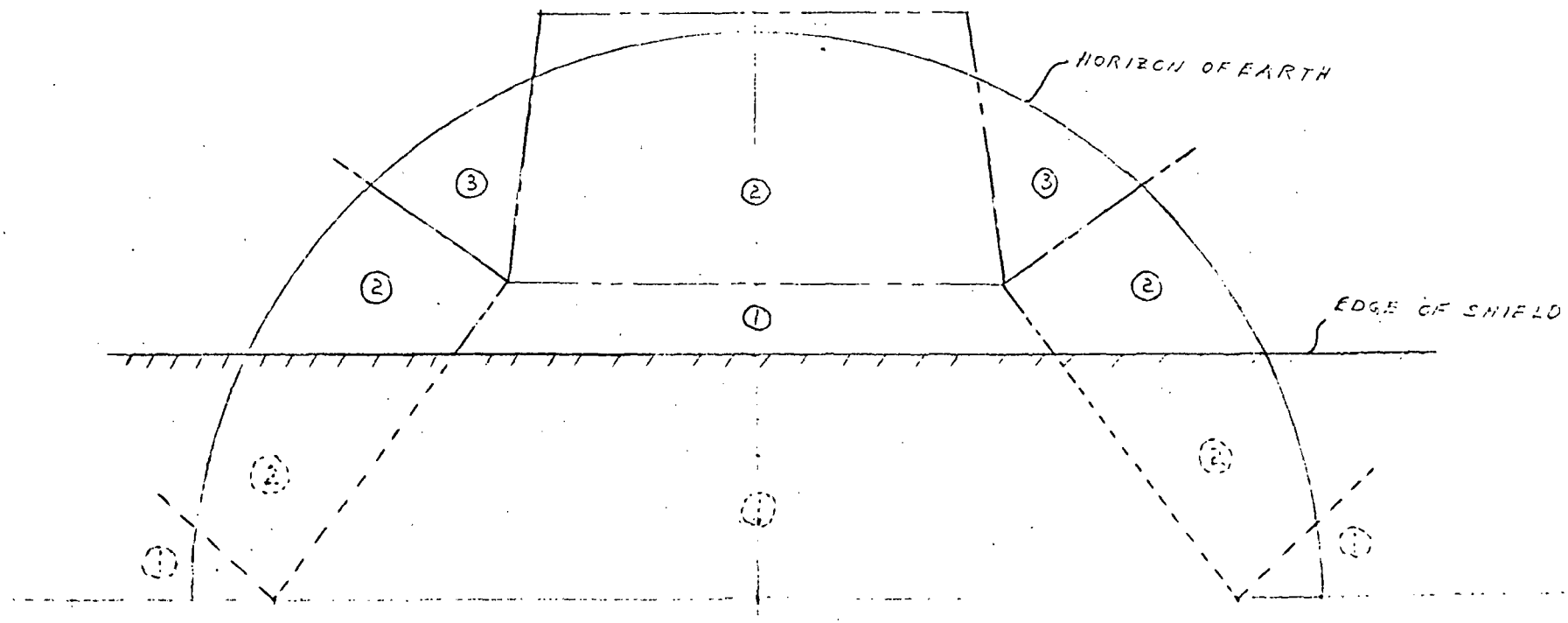

Figure 6.4-1 Equivalent Earth for Cone Wall Absorption as seen from Cone Mouth Center (Design III B)

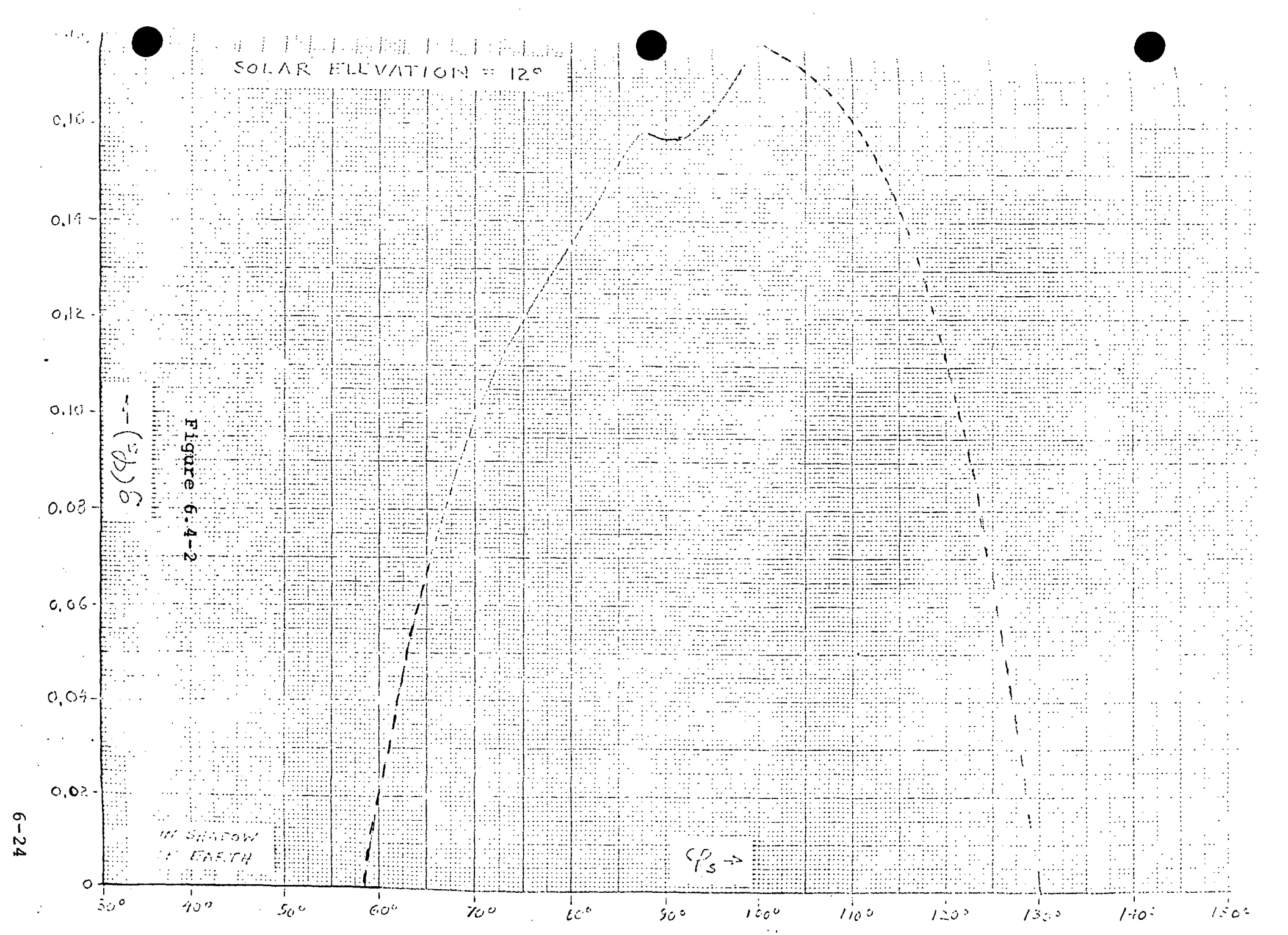
SOLAR ELEVATION = 12°
0.16
0.14
0.12
0.10
0.08
0.06
0.04
0.02
0
$\sigma(\phi_s)$ --
IN SHADOW
OF EARTH
$\phi_s \rightarrow$
50°
40°
30°
60°
70°
80°
90°
100°
110°
120°
130°
140°
150°

Figure 6.4-2

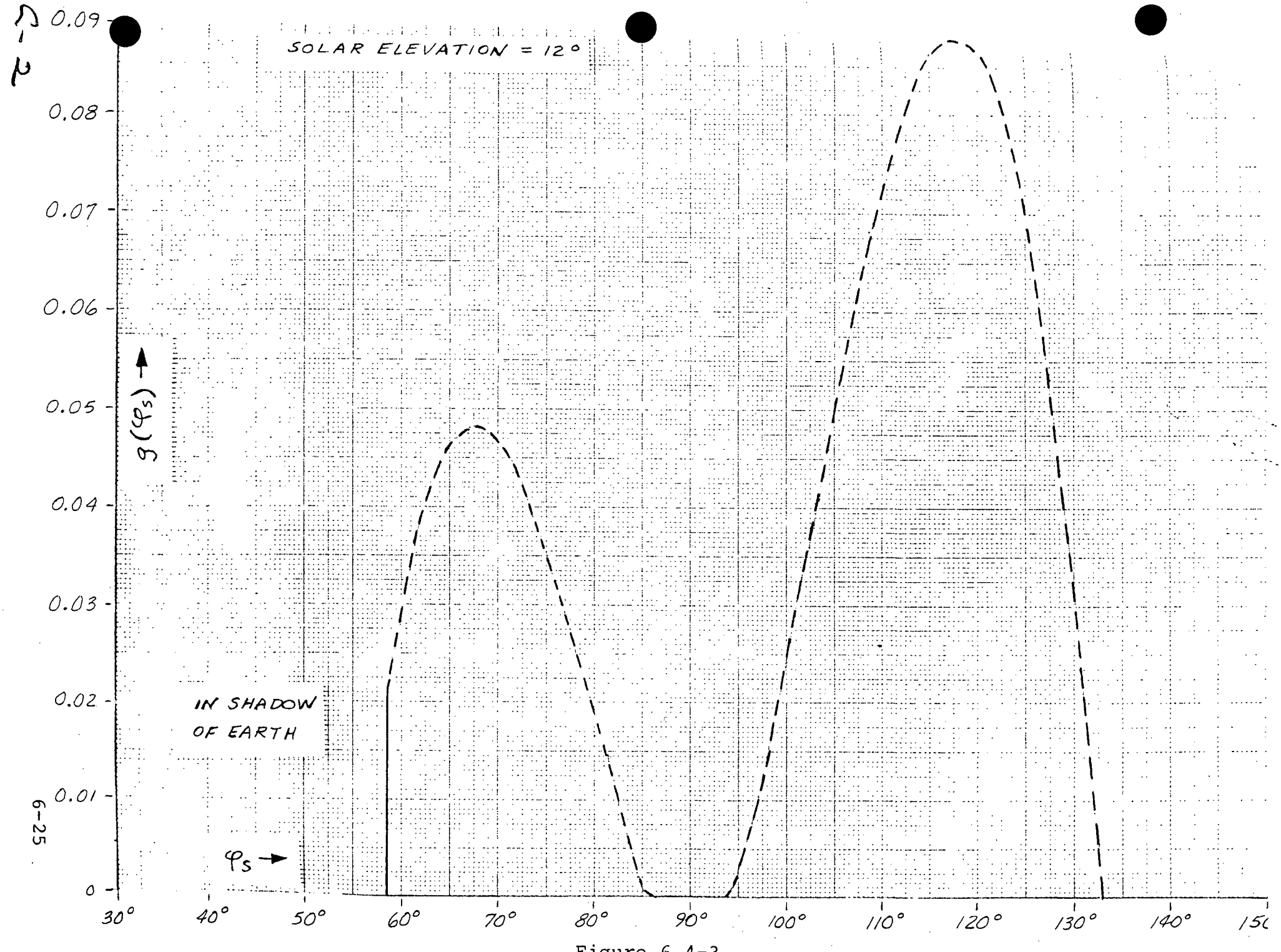
SOLAR ELEVATION = 12°
0.09
0.08
0.07
0.06
0.05
0.04
0.03
0.02
0.01
0
g(φs)
IN SHADOW
OF EARTH
φs
30°
40°
50°
60°
70°
80°
90°
100°
110°
120°
130°
140°

Figure 6.4-3

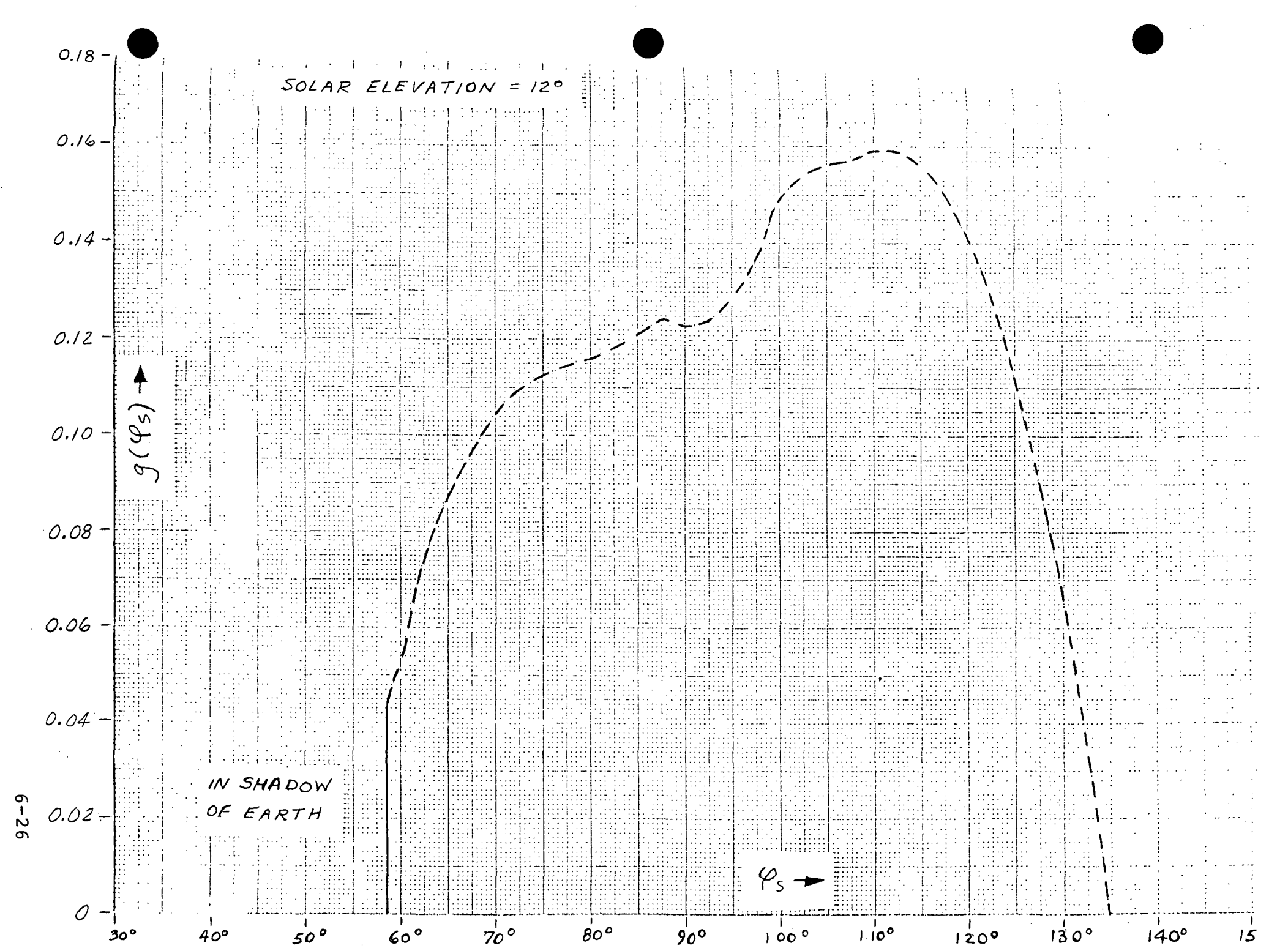
SOLAR ELEVATION = 12°
0.18
0.16
0.14
0.12
0.10
0.08
0.06
0.04
0.02
0
g(φs)
IN SHADOW
OF EARTH
φs
30°
40°
50°
60°
70°
80°
90°
100°
110°
120°
130°
140°
15

Figure 6.4-4

Integration of the curves yields the solar exposure factors listed in Table 6.4-4.

Table 6.4-4

Solar Exposure Factor at 12^{o} Sun Angle
(Cone End)

Design	g_d
IIA	4.89×10^{-2}
IIIB	1.66×10^{-2}
IIIC	4.98×10^{-2}

6.5 Radiative Input through Optical Openings to Patch

The magnitude of the radiative input (Φo) to the patch through the optical openings depends on the optical and mechanical design of the instrument. To maintain accurate positioning of the detector with respect to the optics, the last lens is mounted in the patch with the detector element. Use of an aplantic lens in this position allows an increase in the speed of the optical beam by a factor equal to the refractive index of the lens material (4 in the case of germanium). The speed of the beam striking the aplanatic element is then relatively low and allows the placement of the spectral filter on the patch in front of the element without significantly changing the filter's characteristics (as a result of variations in incidence angle). In this position, the interference filter reduces Φ_o by reflecting part of the incident radiation.

In addition, the optical opening is designed so that it does not pass through the cone wall area seen by the black top of the patch. The first structure seen from the patch is then the space between the patch and cone rather than that between the cone and housing. As a result, the source closest to the optical opening on the patch is at a lower temperature.

Finally, the Irtran 2 window on the cone wall serves to block radiation from components beyond it in the direction of the instrument housing. Irtran 2 absorbs or reflects wavelengths of 15 μm and greater (D.E. McCarthy, Appl. Opt. 2, 591, 1963). In combination with the reflective properties of the spectral filter at wavelengths below 15 μm, the window essentially eliminates radiative coupling between the patch and objects beyond the window. The window also serves two other purposes. It provides a cone enclosure seal to permit evacuation during bench cooling of the detector and to prevent outgassing of the instrument through the cooler.

The value of Φ_o may be estimated by assuming that an area A_o of each of two spectral filters at the edge of the patch views a black window at the cone temperature and a black space between the patch and cone. We then have

$$\Phi_o = 2\,\sigma A_o\,(E_A F_{PA} T_A^4 + E_c\,F_{pc}\,T_c^4)$$

where E_j = fraction of blackbody radiation at a temperature T_j that is transmitted by the filter (the remainder being relected)

F_{pj} = view factor from A_o to area j

A = multilayer between patch and cone

C = window on cone structure

The insulation is assumed to be at a temperature given by

$$T_A^4 = \tfrac{1}{2}\,(T_C^4 + T_p^4) \cong \tfrac{1}{2}\,T_c^4.$$

The cone window is about 0.9 inch from the patch edge and has a diameter of approximately 0.55 inch. The opening (A_o) at the edge of the patch is a circle whose diameter is about 0.30 inch. The two openings are therefore circles with a common central normal. The view factors between them may therefore be calculated from the formula given by M. Jakob (Heat Transfer, Vol. II, John Wiley and Sons, 1957, p. 14). If F_{pc} is the view factor from A_o to the window, the other view factor is given by

$$F_{pA} = 1 - F_{pc}$$

For the geometry described above, the results are

$$F_{pc} = 0.084$$

$$F_pA = 0.916$$

We will neglect the small fraction of radiation passed by the narrow spectral band to which a channel is sensitive. Instead, we will assume that all wavelengths greater than 18 μm (where the detector is insensitive) are transmitted by the filter. For T_c = 170 K and T_A = 140 K, we then have the approximate values

$$E_A = 0.8$$

$$E_c = 0.7$$

Finally, the radiative input through two optical channels is approximately

$$\Phi_o = 1.8 \times 10^{-3} \text{ W.}$$

6.6 Final Radiant Cooler Design for SCMR

The final radiant cooler design for the SCMR is close to that of Modification 2 to design IIIB described in Section 6.2. The only difference is in the shield design, as shown in Figures 6.6-1 and 6.6-2. The shield wall on the earth side of the cooler is longer but not as wide to permit its use as a deployable cone mouth cover. The cone temperature of the final design was calculated for the nominal set of conditions and radiative properties. It was found to be identical to that of Modification 2 to design IIIB (Table 6.3.1-3). Addition of a solar input to the cone end at a solar elevation of 12^o increases the cone temperature by about 0.9K.

The cone end and cone mouth view factors for the final design are (See Section 6.4).

$$F_{de} = 4.085 \times 10^{-2}$$

	$F_{m-e(n)}$	$F_{d-h(n)}$
0	-	0.6515
1	0	0.3147
2	0.0289	0.0338
3	0.0072	-

And the radiative coupling factors for the nominal property values are

$$\varepsilon_{me}(0.05) = 3.84 \times 10^{-3}$$

$$\alpha_{me}(0.22) = 1.39 \times 10^{-2}$$

$$a_{dh}(0.05) = 1.90 \times 10^{-3}.$$

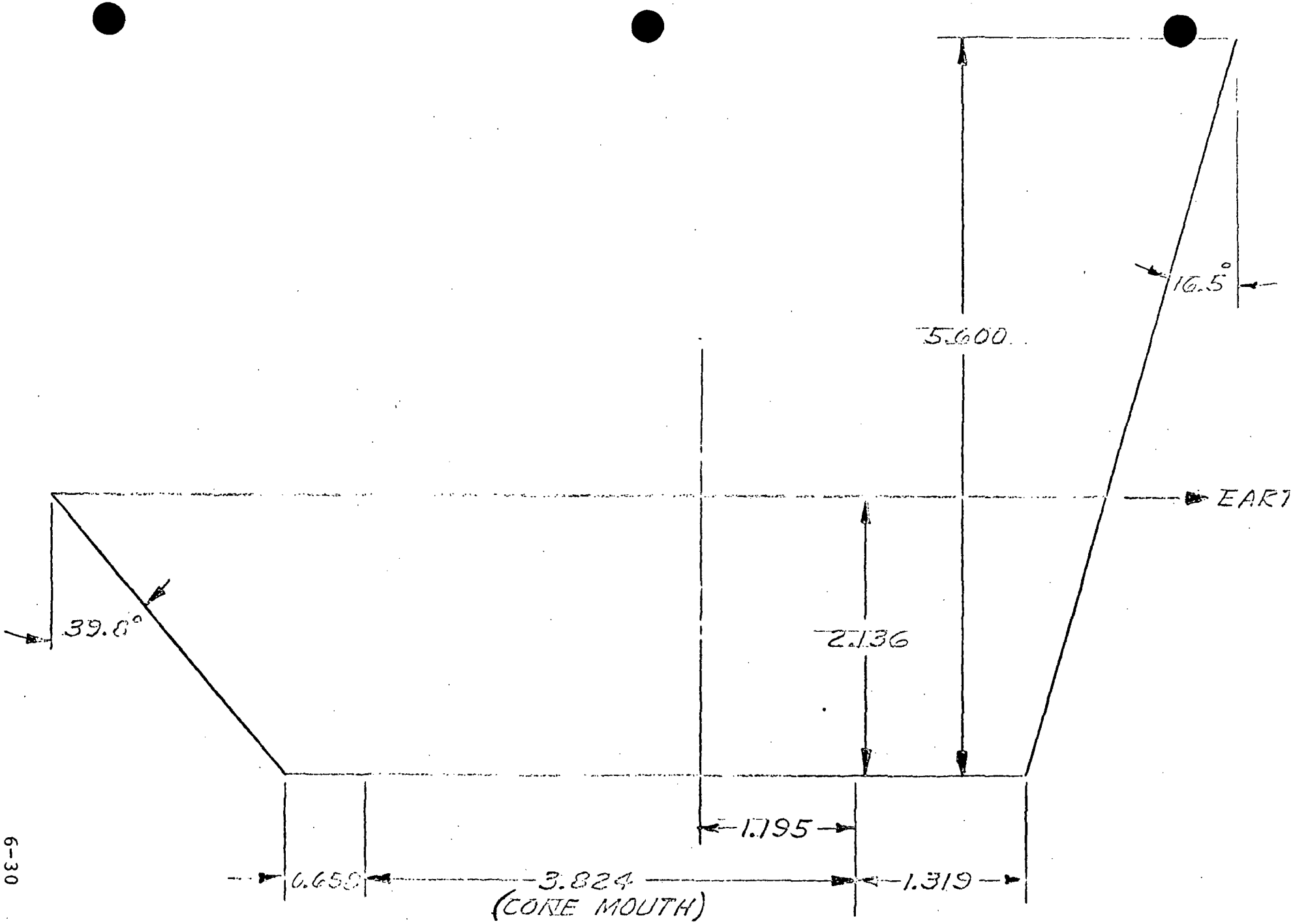

Figure 6.6-1 Shield Vertical Plane, Final SCMR Cooler Design

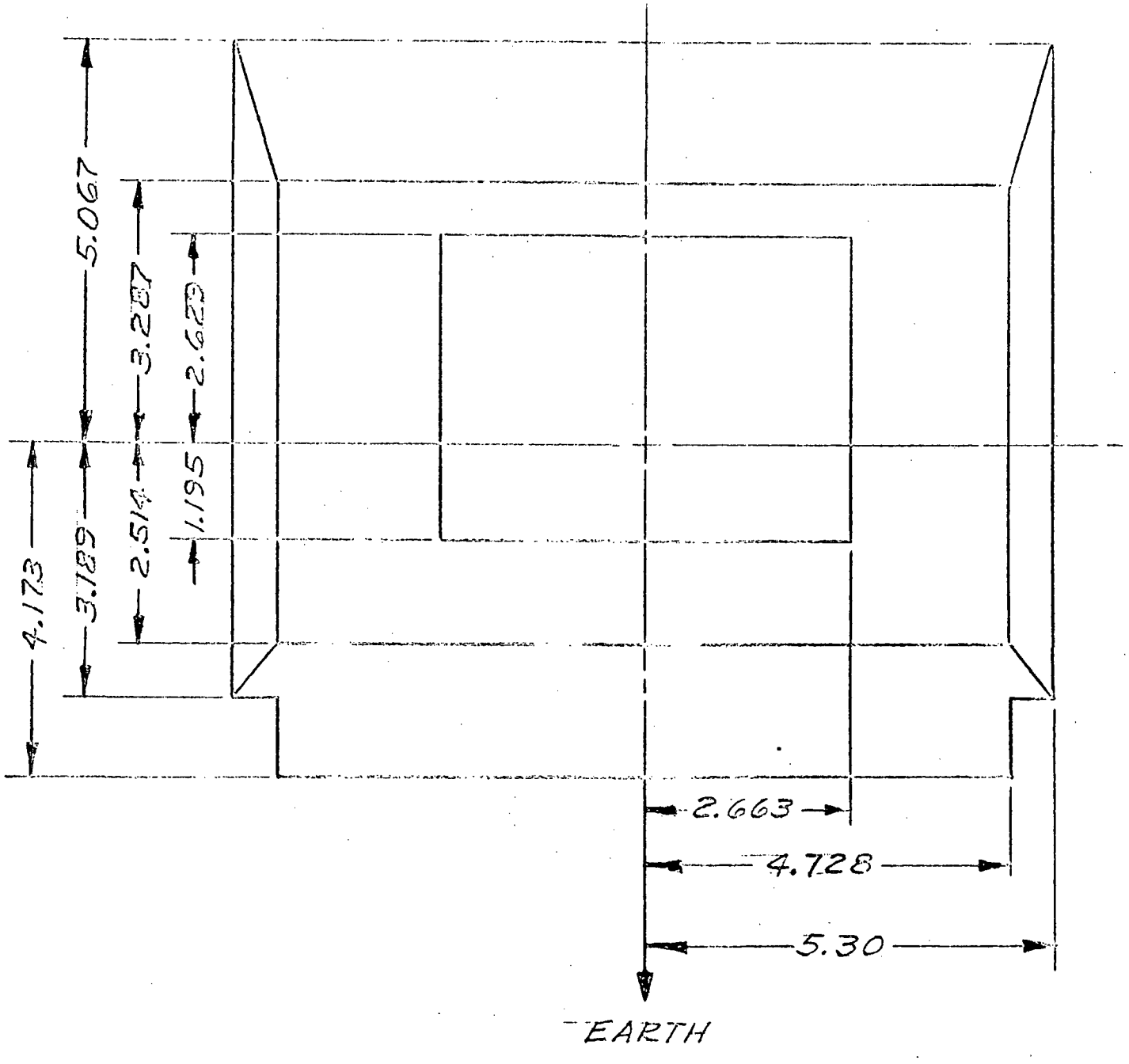

Figure 6.6-2 Top View of Shield & Cone End, Final SCMR Design

The fraction g_d (φ_S) of cone end area in the final design exposed to sunlight is shown in Figure 6.6-3 as a function of solar azimuth φ_s at a solar elevation of 12^o. The average value over an orbit is

$$g_d = 2.06 \times 10^{-2}.$$

At a housing temperature T_h of 25^oC and a solar elevation of 0^o, the thermal balance equation of the cone in the final design yields

$$5.015 \times 10^{-12} T_c^4 + 2.2 \times 10^{-6} T_c = 3.910 \times 10^{-3} \text{ W cm}^{-2}$$

for the nominal radiative properties. The solution is

$$T_c = 163.1 \text{ K}.$$

This is identical to the cone temperature of modification 2 to design IIIB under the same conditions. At a solar elevation of 12^o, the right side of the above equation is increased to 3.995×10^{-3} W cm^{-2} and the equilibrium cone temperature to 164.0 K.

The distribution of thermal inputs to the cone at a temperature of 163.1 K is

Source	Watts	Percentage
Earth	0.216	28.5%
Shield	0.161	21.2
Supports and Leads	0.067	8.8
Multilayer Insulation	0.315	41.5

Of the earth load, 0.185 W or about 85% is absorbed in the white cone end and the remainder in the cone walls.

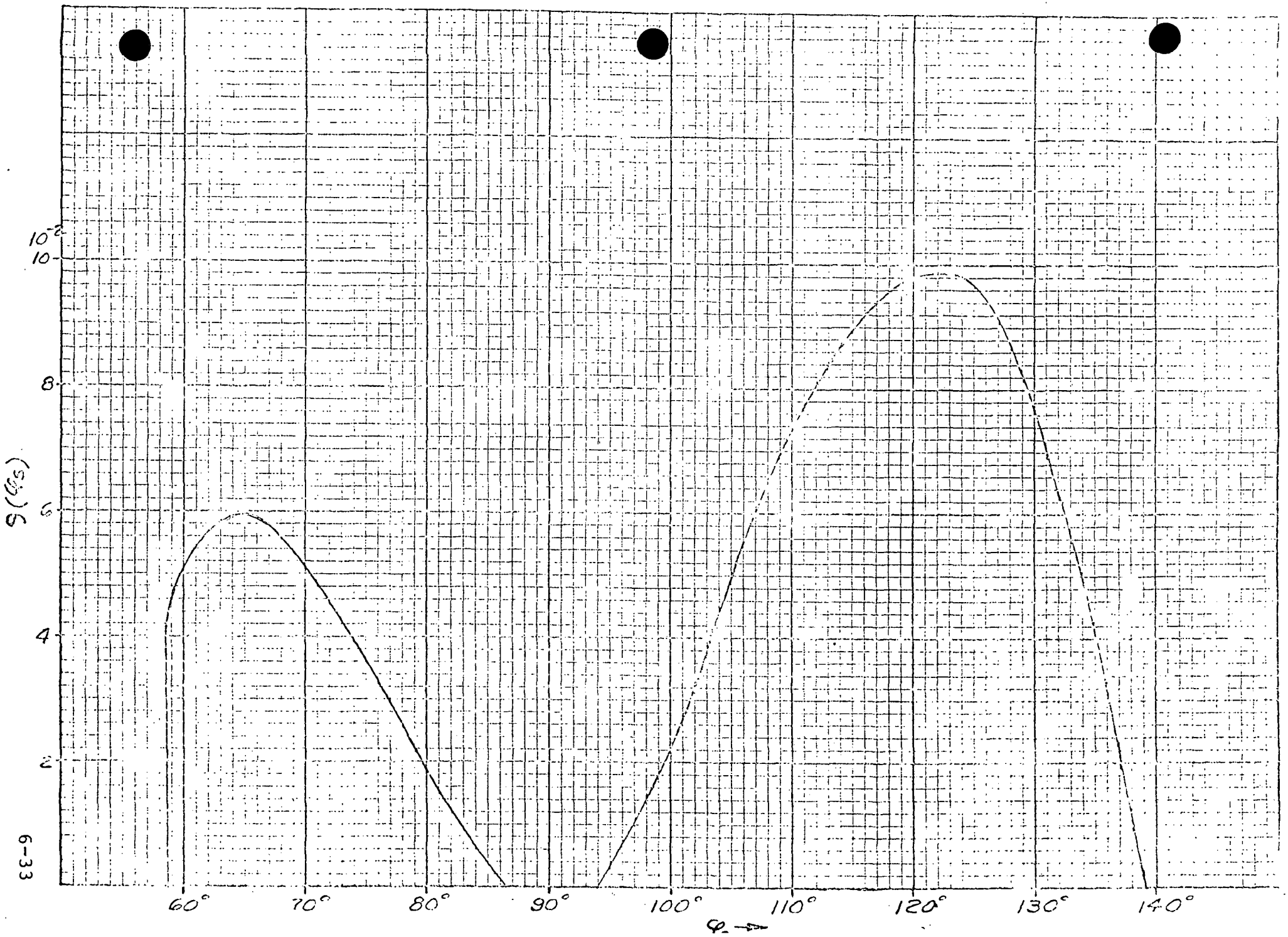

Figure 6.6-3 Cone End Exposure Factor at $\beta_s=12^{\circ}$; Final SCMR Design

6.7 Analysis of Tests on the Prototype Radiant Cooler

The measurements on the SCMR prototype cooler at the ends of the 48 hour hot and cold cycles in the thermal-vacuum test are listed in Table 6.7-1.

Table 6.7-1

Results of SCMR Prototype Tests

	Hot	Cold
Nominal baseplate	40°C	-5°C
Cooler housing	270.7K	259.4K
Cone	162K	157K
Patch	115.6K	115.6K
Patch control heat	2.50×10^{-3}W	4.90×10^{-3}W
Detector joule heat	1.2×10^{-3}W	1.2×10^{-3}W

The analysis shows that the thermal performance of the cone was very good. For an assumed white paint emissivity ε_d of 0.85, the insulation factor of the multilayer blanket between the cone and cooler housing was 72 at the end of the hot cycle and 83.5 at the end of the cold. If ε_d is 0.87 instead, the respective insulation factors are 69 and 78.5. On the other hand, the analysis shows that the thermal performance of the patch is severely limited by the poor insulation factor between the sides and rear of the patch and the gold box. This insulation factor was only about 18, which corresponds to an average surface emissivity of 0.10.

However, an analysis of the orbital performance shows that the heat input to the patch was reduced by 3.95 milliwatts. This is attributed to the absence of reflecitons from cold space. In the chamber, a very small fraction of the radiant emission from the cone is reflected from the space target to the patch (see Construction and Test of a Dual Patch Multielement Radiant Cooler, NAS5-21132, June 1971, Section 2.3.3). The actual insulation factor was therefore about 32 rather than 18.

The patch operated in orbit with nearly the same temperature and control heat (i.e., cooling margin) realized during chamber testing on the ground. The absence of space reflections was compensated in orbit by a higher cone temperature (171 K). Based on the model described below, the SCMR cooler had an in-orbit cone to housing insulation factor of about 46. The reduction from the chamber value of about 71 is apparently the result of little or no outgassing of the insulation blanket in the vicinity of the cooler housing. This housing quickly reached 0°C and remained there; no provision was made for in-orbit heating of the housing.

Cone

The thermal balance equation of the cone is:

$$\Phi_d = \varepsilon_d A_d \sigma T_c^4 = \Phi_e + \Phi_s + \Phi_h + \Phi_k + \Phi_i$$

where d = cone end, e = earth, s = direct sunlight

h = shield, k = conduction, i = insulation

ε = emissivity

A = area

T = Temperature

$\Phi_h = A_d \varepsilon_d a_{dh} \sigma T_h^4$

a_{dh} = effective shield emissivity

$\Phi_k = K_c (T_h - T_c)$, K_c = thermal conductance

$$\Phi_i = \frac{A_i \sigma}{S_i} (T_h^4 - T_c^4), \quad S_i = \text{insulation factor}$$

For a cone end emissivity of 0.85 and solar absorptivity of 0.20, the calculated value of $\Phi_e + \Phi_s$ at a 12^o sun angle is 0.248W. The tests were run with a $\Phi_e + \Phi_s$ value (heater) of 0.296W including an estimated 0.016W from lead wire dissipation. Based on published data, experiments conducted on the dual patch cooler (Contract NAS5-21132), and calculations in Section 6.3, we assumed the following values:

$\varepsilon_d = 0.85$

$\varepsilon_h = 0.04$, so that $a_{dh} = 0.01524$

$A_d = 33.0 \text{ in}^2$

$A_i = 120 \text{ in}^2$

$K_c = 4.93 \times 10^{-4} \text{W/K}$

The insulation factor S_i is then determined by the thermal balance equation. For the hot cycle, the result is:

$S_i = 71.6$

If we assume ε_d is 0.87 instead of 0.85, S_i is reduced to 69.2. In either case, the insulation factor is comparable to the values obtained in the dual patch cooler and in separate insulation tests (See Construction and Test of a Dual Patch, Multi-Element Radiant Cooler, NAS5-21132, June 1971, Sections 2.2.1 and 2.2.4).

The thermal inputs to the cone during the cold cycle are listed in Table 6.7-2. We see that the cone temperature is largely determined by the fixed inputs from the earth and sun and by the input from the cooler housing through the insulation blanket.

Table 6.7-2

Cone Thermal Inputs During Cold Cycle (ε_d = 0.85)

Source	Watts	%
Earth and Sun	0.296	48
Shield	0.0708	11
Conduction	0.0505	8
Insulation	0.2061	33

Using the temperatures recorded at the end of the cold cycle (Table 6.7-1), we find that S_i has increased to 83.5 (78.5) for ε_d equal to 0.85 (0.87). In general, the effectiveness of the insulation blanket increases with a reduction in the temperature of the warm boundary (Thermal Insulation Systems, NASA SP-5027, 1967).

Patch

The thermal balance equation of the patch is:

$$\Phi_p = \varepsilon_p \sigma A_p T_p^4 = \Phi_r + \Phi_o + \Phi_j + \Phi_k + \Phi_i$$

where p = patch, r = cone walls

o = optical ports, j = joule heat

$\Phi_r = \varepsilon_p \varepsilon_{pe} \sigma A_p T_c^4$, ε_{pc} = effective emissivity of cone walls as seen from patch

$\Phi_o = 2\sigma(\varepsilon_o A_o + \pi d_o \delta)\ (T_c^4 - T_p^4)$

ε_o = absorptance of patch optical port

d_o = diameter of optical port

δ = thickness of black ring around port

The joule heat is the sum of the detector dissipation (1.2×10^{-3}W) and the control heat. The following values were used:

$\varepsilon_p = 0.93$

$A_p = 3.50 \text{ in}^2$

$\varepsilon_{pc} = 0.03357$ ($\varepsilon_c = 0.04$, See SCMR Design Study Report)

$\varepsilon_g = 0.6$ (germanium substrate)

$d_o = 0.40$ inch

$\delta = 0.015$ inch

$K_p = 4.62 \times 10^{-5}$ W/K

$A_i = 8.89 \text{ in}^2$

For the hot cycle (Table 6.7-1), we then obtain

$$S_i = 18.1.$$

The average surface emissivity ε_i of the insulated patch area A_i and the facing gold box area A_o can be calculated from:

$$S_i = \frac{1}{\varepsilon_i} + \left(\frac{1}{\varepsilon_i} - 1 \right) \frac{A_i}{A_o} .$$

The value of A_o is 10.105 in^2, so that

$$\varepsilon_i = 0.10.$$

The emissivity of the gold surfaces has obviously been severely degraded by areas of high emissivity, such as the support openings and vibration bumpers. For the cold cycle, the calculated insulation values are:

$$S_i = 17.7$$

$$\varepsilon_i = 0.10 .$$

This shows that the thermal model of the cooler yields consistent results.

The distribution of heat inputs to the patch is shown in Table 6.7-3 for the hot cycle. Again, the poor quality of the insulation is brought out.

Table 6.7-3

Patch Thermal Inputs During Hot Cycle

Source	Milliwatts	%
Cone Walls	2.76	13
Optic Ports	3.52	16
Detector Bias	1.20	6
Control Heat	2.50	12
Conduction	2.14	10
Insulation	9.17	43

6.8 Radiant Cooler Configuration SCMR Flight Model

The radiant cooler configuration can best be seen by examination of the Radiant Cooler Assembly drawing, ITT Drawing No. 8116040. This drawing is not included in this report but is available in the drawing sets supplied to GSFC by ITT.

Figure 6.8-1 shows schematically the mechanical configuration of the cooler from the patch to the optical focus lens.

6.9 SCMR Flight Model Radiant Cooler Performance

Data was taken with stable baseplate during thermal vacuum test conducted on Flight Model instrument Oct. 15 through Oct. 27, 1972. The following tabulation shows Flight Model performance.

Baseplate Temperature	$+40^{\circ}C$	$0^{\circ}C$
Cone Wall Temperature	$160^{\circ}K$	$157.0^{\circ}K$
Patch Temperature	$114.9^{\circ}K$	$114.9^{\circ}K$
Cone Housing Temperature	$-8.5^{\circ}C$	$-16.5^{\circ}C$
Patch Control Heat	1.8 mw	5 mw
Patch Heat Margin		$1.8^{\circ}K/mw$

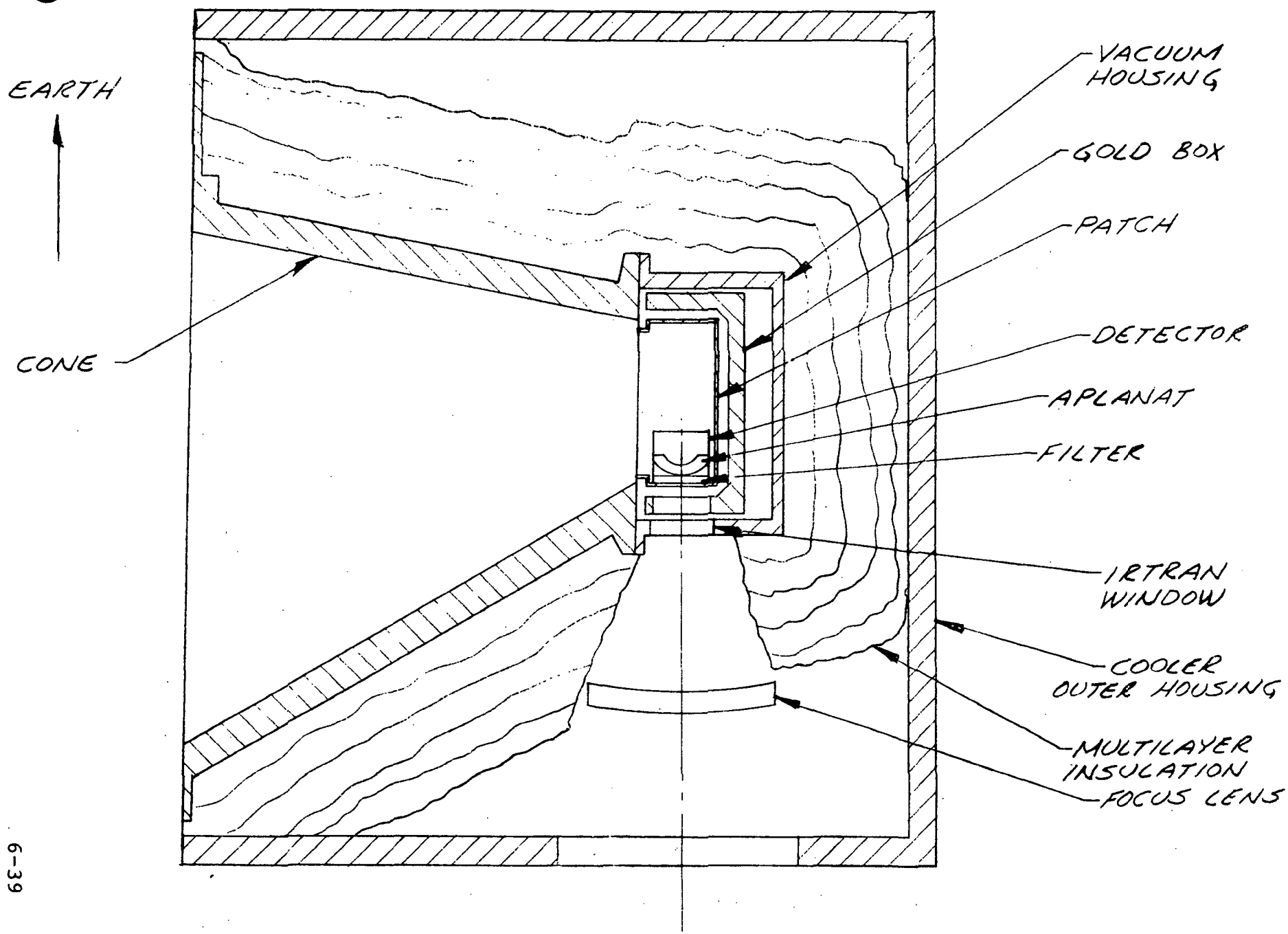
EARTH
CONE
VACUUM HOUSING
GOLD BOX
PATCH
DETECTOR
APLANAT
FILTER
IRTRAN WINDOW
COOLER OUTER HOUSING
MULTILAYER INSULATION
FOCUS LENS
SCHEMATIC OF COOLER CONFIGURATION

Figure 6.8-1

7.0 SCMR ELECTRICAL SYSTEM

A simplified Block Diagram of the SCMR Electronics is shown in Figure 7.0-1. The SCMR Electronics has the basic function to transmit to the spacecraft two channels of video data synchronized with the spacecraft clock and the rotation of the SCMR scan Mirror. The input signals to the SCMR are the spacecraft -24.5 VDC bus, clock signals of 50 KHz, 10 KHz and 400 Hz 2-phase, and spacecraft commands to the SCMR to implement the available modes of operation. The SCMR electronics provides the power conversion, timing and control, signal generation, digital and analog telemetry for verification of operation, and signal amplification for required operation.

The basic blocks of the SCMR are:

1. IR Data Amplifiers
2. Visible Data Amplifiers
3. Power Converter
4. Voltage Regulators
5. Timing and Control Circuits
6. Calibration signal generation circuits
7. Analog TM circuits
8. Command and Digital TM circuits

These functions are individually described in the following sections. Schematics referenced in the following text are located in tne Appendix of this report.

7.1 Video Output

A representation of the video output for one scan line is shown in Figure 7.1-1. An angular representation of one scan is shown in Figure 7.1-2. Both diagrams are referenced to the occurrence of the sync pulse which occurs at the start of the interval when the scan mirror views space just prior to the view of the earth.

7.2 Commands and Digital TM

Commands are received by the SCMR from the spacecraft as pulses of 40 millisecond duration on two isolated lines for each command. The command is stored by means of latching relays and digital command verification telemetry is outputted.

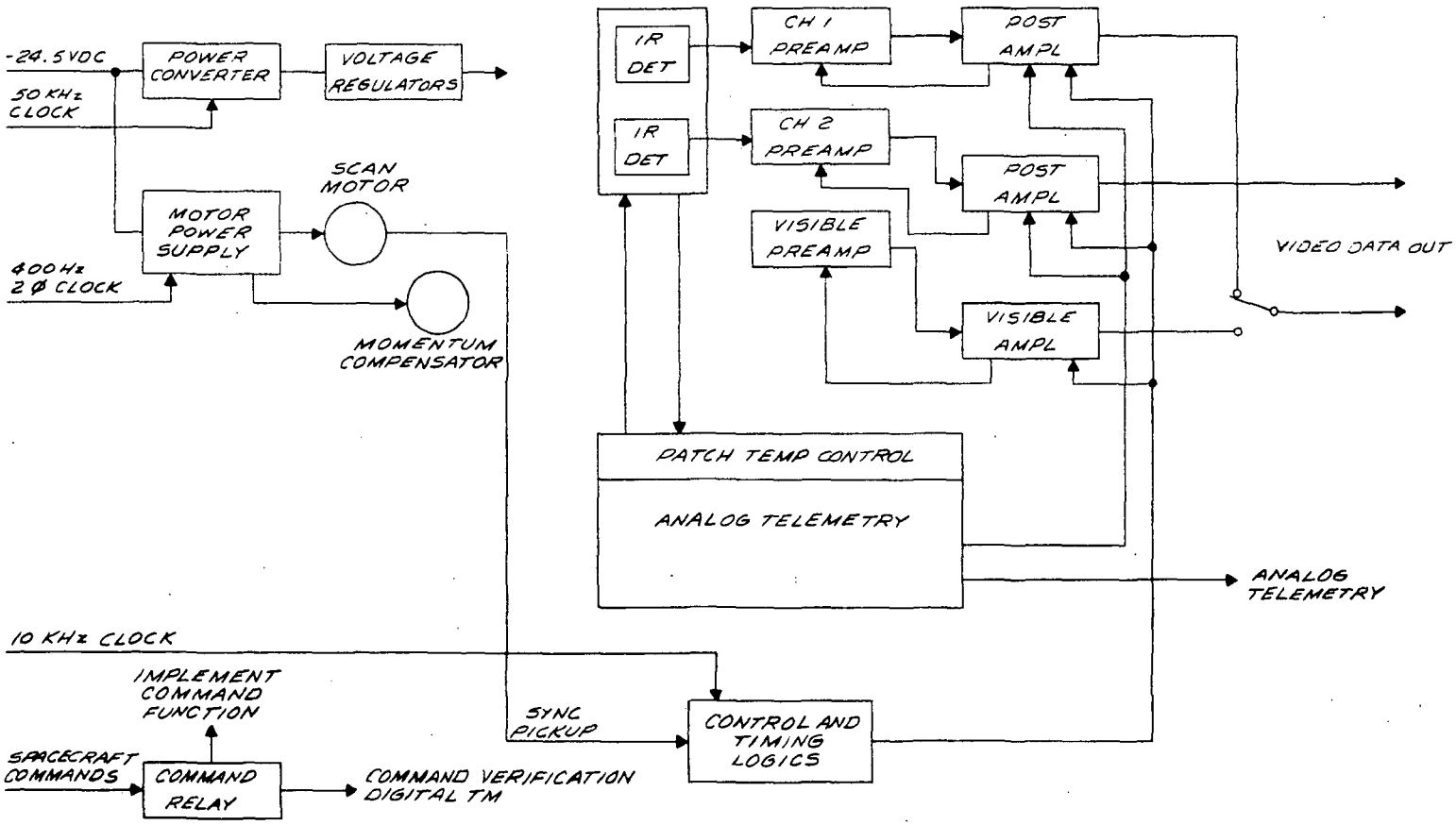

SCMR ELECTRONICS
SIMPLIFIED BLOCK DIAGRAM

Figure 7.0-1

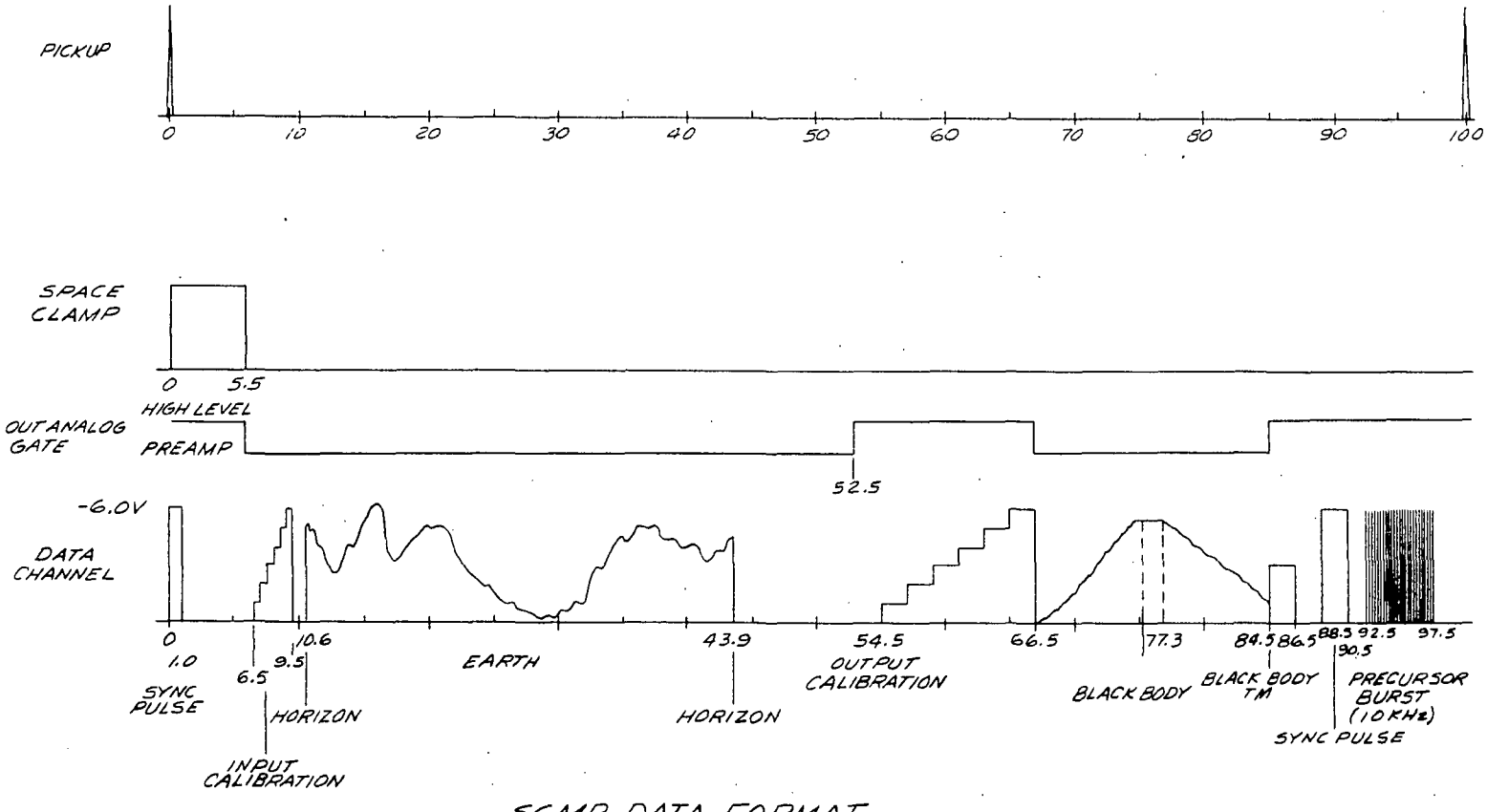

SCMR DATA FORMAT

Figure 7.1-1

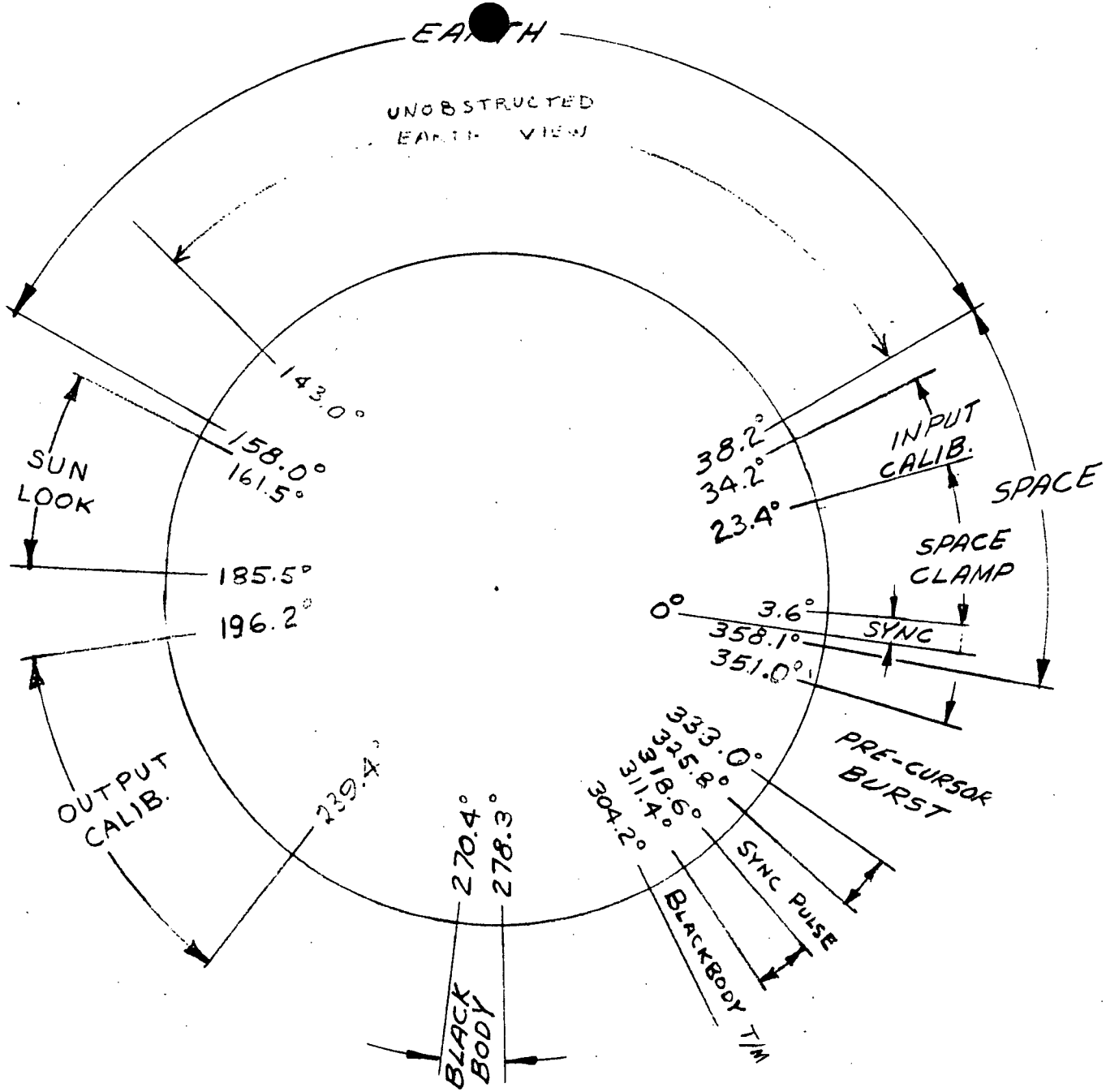

Figure 7.1-2 SCMR ANGULAR DATA FORMAT

The schematics of the command system of the SCMR are shown on drawings 8116466 and 8116462.

The commands, their functions, and the telemetry response are as follow:

Motor ON/OFF - Applies DC power to the scan motor and momentum compensator. Turns on analog telemetry through the power converter. Motor ON is Logic 1.

Motor High/Low Power Mode - High power mode applies -24.5 VDC to Scan Motor P.S. Low Power Mode applies -15 VDC to Scan Motor P.S. through a switching regulator. Motor Low Power Mode is Logic 1.

Electronics ON/OFF - Applies power to theSCMR Electronics through the power converter. Also turns on the analog telemetry through the Power Converter. Electronics ON is Logic 1.

Purge ON/OFF - Applies -24.5 VDC to the SCMR purge system to release a flow of dry nitrogen gas around the patch. Purge ON is Logic 1.

Cone Heater ON/OFF - Applies -24.5 VDC to the heater on the cooler cone walls. Cone Heater ON is Logic 1.

Patch Heater ON/OFF - Applies -24.5 VDC to the patch heater. Patch Heat ON is Logic 1.

Visible Video/IR Video - Connects to output of the designated amplifier to the video interface connector. Visible Video is Logic 1.

Cone Cover Deploy/Store 1 & 2 - Duplicate Pair of commands. Both must be in the same state to cause operation. Applies -24.5 VDC to cone cover circuits to operate cooler door in commanded direction. Circuit removes -24.5 VDC load at completion of operation. Cone Cover Deploy is Logic 1.

7.3 Power Conversion Circuits

DC power for the SCMR Electronics is obtained by the Power Converter shown in Schematic 8115674. The clock signal for the converter is derived by AMP 1 operating as an oscillator. The 100 KHz oscillator is normally synchronized to the spacecraft 50 KHz clock. Two separate converter circuits are separately powered. One is used for the electronic circuits, the other is used for the Analog Telemetry circuits.

Linear regulator circuits for the DC power are shown in schematic 8116516. Plus 15 volts, minus 15 volts, and plus 5 volts are provided for the Electronics. Plus and minus 15 volts are provided for telemetry circuits.

7.4 SCMR Clock Signals

The SCMR normally operates with a 50 KHz and 10 KHz spacecraft clock signals. The 50 KHz clock is used to synchronize a 100 KHz oscillator in the power converter for power conversion. The 10 KHz clock is used for the logic timing function.

In the event of the loss of the 10 KHz clock from the spacecraft, a clock detector circuit on the logic No. 2 board switches in a 10 KHz clock which is counted down from the 100 KHz power converter clock. This provides a 10 KHz clock timing signal which is synchronous to the spacecraft 10 KHz clock but not necessarily coherent to it.

In the event of the loss of the 50 KHz clock line, the power converter oscillator will continue to operate at a frequency near 100 KHz. The logic timer clock will continue to operate from the spacecraft 10 KHz clock line as long as it is present.

With the loss of both clock lines the SCMR will continue to operate but internal timing will be a function of the internal oscillator. The scan period, however, will be maintained as long as the 400 Hz clock to the scan motor is maintained.

7.5 Logic Clock

The timing anc control functions of the SCMR are shown on Schematics for Logics No. 1, drawing 8116450, and Logic No. 2, drawing 8116502.

The 10 KHz spacecraft clock enters at pins 40 and 41 of the Logic No. 2 board. AMP 1 functions as a receiver and a shaping circuit. Positive feedback supplied by R2 and R3 provide controlled hysteresis of this circuit to provide immunity from the noise occurring during the transition causing multiple triggering. Transistor Q1 and associated components provide an AC coupled detection circuit. A positive voltage across R26 provides a logic 1 input at pin 5 of 12 which gates in the clock output of AMP 1. The absence of this signal gates in the output of the divide by 10 counters comprised of U7 through U10. The selected clock appears at the output of the OR gate at U12, pin 3. The gating of the U1 and the status of FFU2 determine the phase of the clock which appears at pin 37 for use by the scan counter.

The negative going transition of the clock at pin 37 triggers the monostable U4. The transition of the pick-up signal to initiate scan timing triggers monostable U5. If these transitions occur within 10 microseconds of each other, the combined signal will reverse the state of Flip-Flop U2, causing the opposite phase of the 10 KHz clock to be present at pin 32. This is done to prevent the clock edge which advances the scan counter to occur near the sync pulse so that scan motor jitter will not come a continuous 100 microsecond jitter in the timed calibration signals.

7.6 Logic Timing & Control

The logics for controlling the gating signals for the SCMR scan timing are shown on 8116450 - Schematic Logics No. 1.

The time base for the scan count is the 10 KHz clock from the Logic No. 2 board which is under normal operation the spacecraft 10 KHz clock signal. Flip-Flop 1, 2 and 3 are a divide by five counter to give a 2 KHz time base (500 μsecond interval) for decoding. Flip-Flops 4 through 11 are connected as a conventional binary ripple counter. The counter is preset to a 11.5 millisecond count to allow proper sequence of counter operation for the staircase input and output calibration signals at the required times. Weighted input calibration signals are obtained from Flip-Flops 4 through 7 while output calibration is derived from Flip Flops 6 through 8.

The counter string is held in a reset condition by the toggle composed of NAND 1 and NAND 2. The reset is removed by a negative going pick-up pulse signal at NAND 16 thtough NAND 47. The count continues for 97.5 milliseconds when the reset is again applied.

The gating outputs from the logics are the five signals:

1. Space Clamp
2. Data Amp Logic
3. Black Body Logic
4. Analog Gate
5. Visible Bias Gate

Space Clamp causes a sample of the Video Amplifier output to be taken for zero reference correction. Data Amp logic causes the output of the Video Amplifier for each stage to be connected to the output driver. Blackbody logic gates the Blackbody TM signals to output driver in the IR Channels. The Analog Gate signal gates the D to A output to the output Driver. The Visible Bias Gate gates in a 3 volt offset during input calibration time on the Visible channel since the output calibration signals are set up to normally operate in the IR channels which are offset by 3 volts. A zero logic level on these outputs is the level which causes the stated operation.

Four logic Levels which are the inputs to the D to A converter are also generated. Table 7.6-1 shows the signal source and time intervals for these signals.

The timing for the gating and calibration signals are shown in Figures 7.6-1 and 7.6-2.

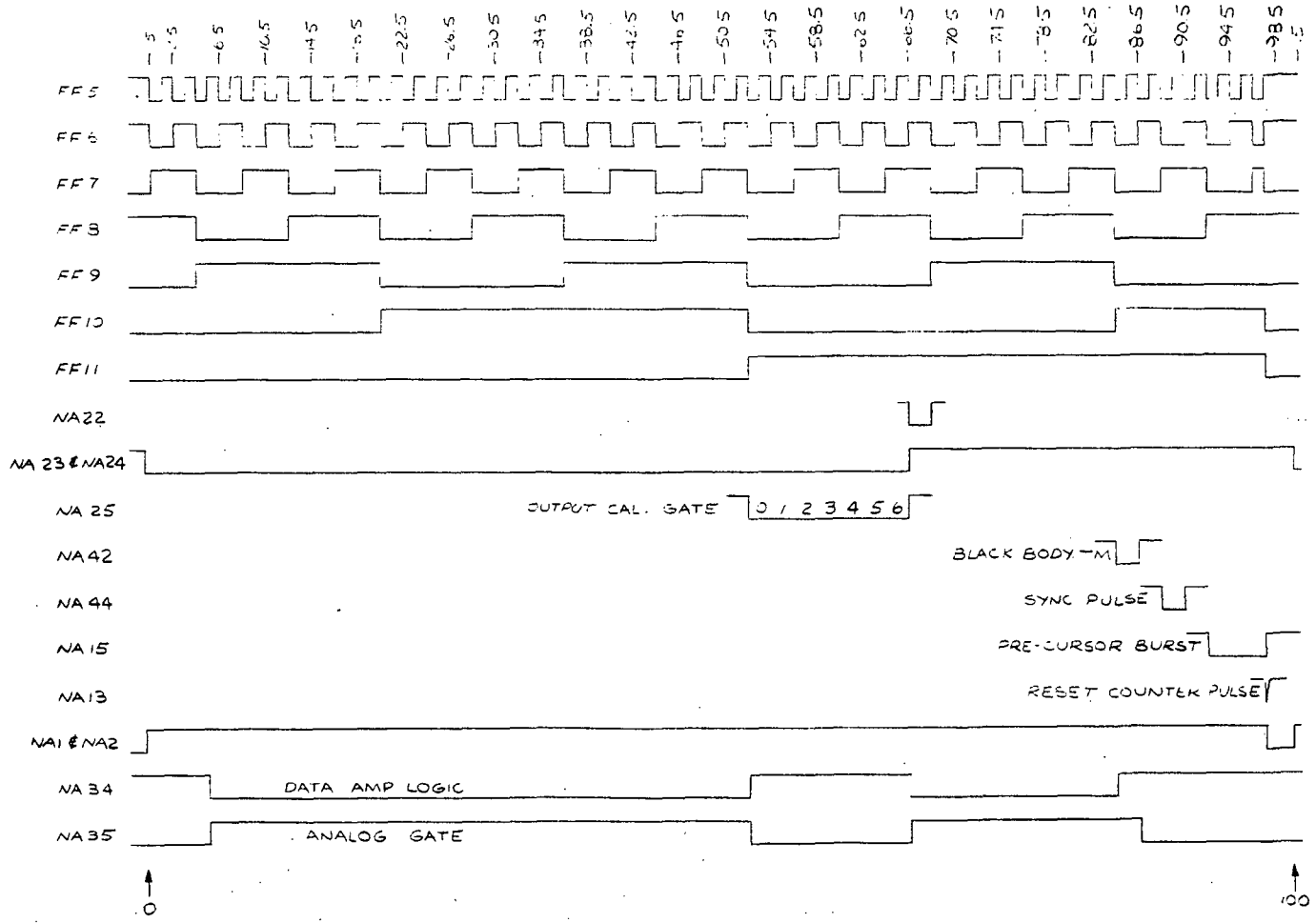

SCMR LOGIC TIMING

Figure 7.6-1

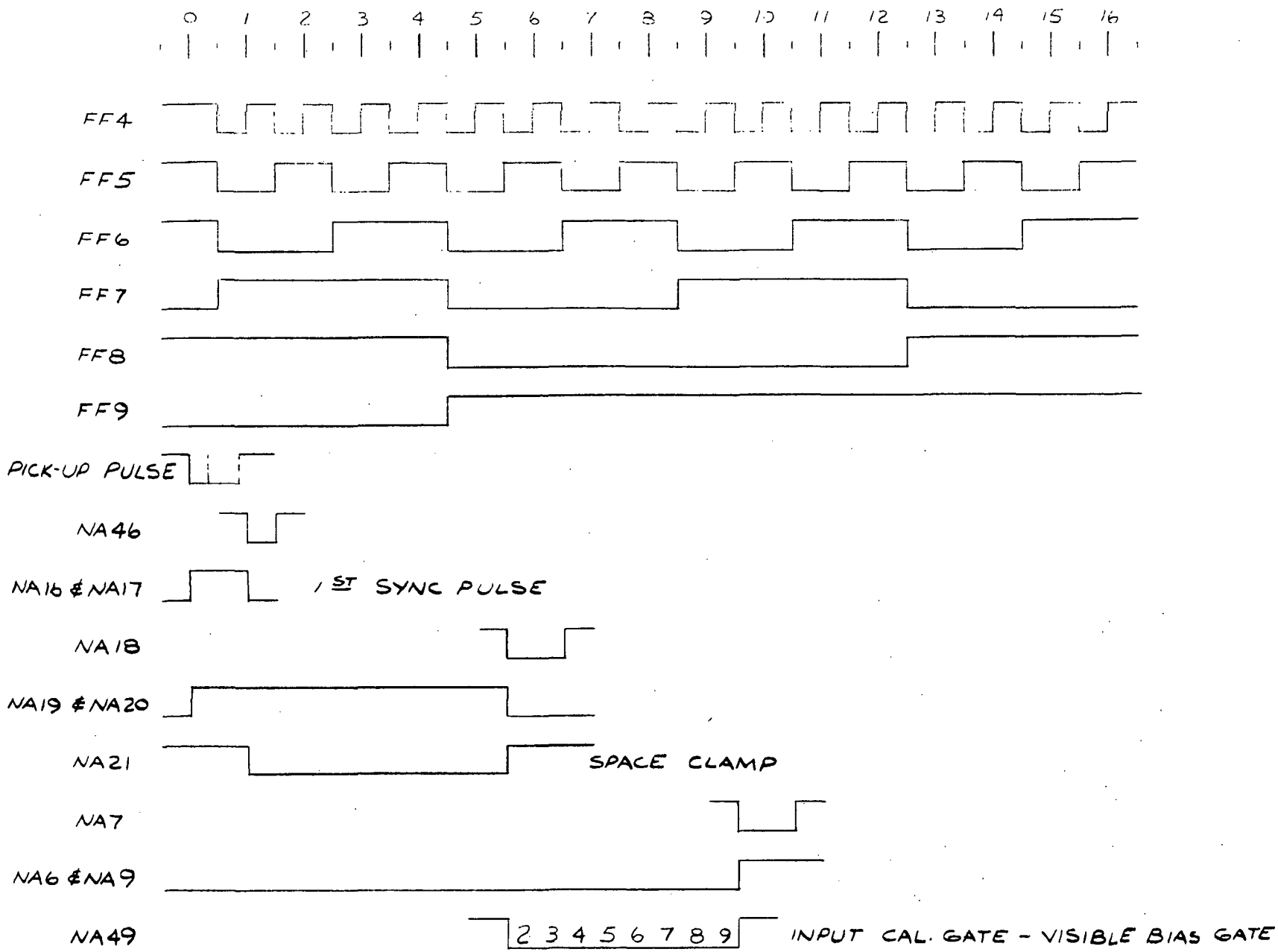

SCMR LOGIC TIMING

Figure 7.6-2

Table 7.6-1

D to A Logic Control Signals

Name	Time	Signal	Signal Path	Binary Weight
Sync	0 - 1 msec	6 V	FF(NA16 & NA17)-NA45-NA28-NA36	2^1_2
			FF(NA16 & NA17)-NA45-NA29-NA38	2
Input Cal.	5.5 to 9.5 msec	2V to 9V	FF4 - NA - NA37	2^0
			FF5 - NA9 - NA36	2^1
			FF6 - NA11 - NA38	2^2
			FF7 - NA48 - NA12 - NA39	2^3
Output Cal.	52.5 to 66.5 msec	0 V to 6 V	FF6 - NA30 - NA37	2^0
			FF7 - NA48 - NA32 - NA36	2^1
			FF8 - NA33 - NA38	2^2
Sync.	88.5 to 90.5 millsec	6 V	NA44 - NA45 - NA28 - NA36	2^1_2
			NA44 - NA45 - NA24 - NA38	2
Pre-cursor	92.5 to 97.5 msec	6 V modulated by 10 Kh	NA4 - NA27 - NA45 - NA28 - NA36	2^1_2
			NA4 - NA27 - NA45 - NA29 - NA38	2

7.7 IR Data Amplifiers

The IR data amplifiers are physically divided into two sections; the IR preamplifiers which are individually packaged, and mounted to the cooler housing, and the Post Amplifiers, two of which are on the same printed circuit card in the Electronics Box. The data amplifiers for each channel are identical except for tailoring to its own detector.

7.7.1 IR Preamplifier

The schematic for the IR Preamplifier is shown on drawing 8116495. Each preamplifier has its own plus and minus 12 volt regulators to provide isolation from the SCMR plus and minus 15 volt Electronics supplies. In addition, the -12 volt supply is compensated to maintain a constant voltage over the ambient temperature range. The temperature varying voltage drop of diode CR6 is divided down by R33 and R34. The voltage drop across R34 modifies the voltage at pin 1 of the LM104 regulator to compensate for its voltage variation with temperature. The circuit is tailored and tested to maintain a voltage which will vary less than $\pm$ 0.1% over greater than the expected ambient temperature conditions.

The detector bias is determined by the value of the R15 and the -12 volt supply. The fact that detector responsivity is almost a linear function of the bias is the reason for the care taken for the stability of the -12 volt power source. Resistor R15 is a stable resistor with a temperature coefficient of 2 ppm.

The input circuit for the IR preamplifier is a differential pair. Transistor Q2 provides a constant current source for Q3 and Q4. The detector is the only signal input at the base of Q3. Feedback from the output of amplifier AMP 1 which is a portion of the first amplifier stage, feedback from space look for DC stabilization from amplifier AMP 3, and input calibration signals are summed at R7 at the base of Q4. A DC bias through resistor R17 is also summed at this point. The value of R17 is chosen to allow amplifier AMP3 to operate at approximately 0 volt output to allow for maximum space look correction margin and to set operation at minimum output offset.

Amplifier AMP2 is a conventional inverting amplifier stage with a gain of approximately 5.

Capacitor C11 stores the output of the data amplifier prior to the 3 volt offset at the time the scan mirror views space. Amplifier AMP 4 is a unity gain non-inverting stage with high input impedance for buffering to the following stage. Amplifier AMP 3 is a low pass filter stage with a very low high frequency cut-off as determined by C9 and R27 and a DC gain of 220. R28 and C10 comprise a lead network for stability to prevent over-correction for scan to scan sample differences.

The individual amplifier stages provide essentially flat response to 50 KHz so that the frequency response is determined by the filter network in the Post Amplifier.

The input calibration signal at terminal E6 is attenuated by the network comprised of R20, R21, R22 and R23. These values are tailored after the amplifier gain is determined to provide the 1 Volt input calibration steps.

7.7.2 IR Post Amplifier

The schematic of the post amplifiers for the two IR channels is shown on drawing 8116446. The two amplifiers are identical in function and the designators for channel 1 will be used in the following discussion but apply equally to channel 2.

Amplifier AMP 1 is a conventional inverting amplifier with a gain of approximately 5. R5, L1, C4, L2, C5, and R6 comprise a linear phase filter for noise attenuation. Amplifier AMP 2 is a non-inverting stage with a gain of 5. The output of AMP 2 is the full value output of the channel prior to the insertion of the 3 volt offset and as such has a full scale output of +9 volts.

The output of this stage is sampled through R10 across CR1 and CR2 at the time the scan mirror is viewing space. CR1 and CR2 are used to limit the feedback signal at turn on before the amplivier chain stabilizes. Limiting the signal in this manner allows better response in the space look feedback loop during normal operation. U1 and U2 are dual FET switches assemblies with logic compatible drivers. One section of U2 (pins 12 and 13) gates the output to the preamplifier.

Amplifiers AMP3 and AMP are a driver stage with an inverting gain of unity and a non-inverting gain of two. Amp 3 is a voltage amplifier and Amp 4 is a unity gain current driver provided to drive the output line capacitance. One section of U1 gates the output of AMP 2 (Video) to the inverting input of AMP 3 (pins 12 and 13). A DC offset signal through R12 and R13 provide a signal to offset the video output by -3 volts. The offset voltage at pin 7 and the values of R12 and R13 are tailored to provide a current to the summing point equal to the current of a 3 volt signal through feedback resistor R17. Diode CR4 blocks all positive going signals. Diode CR3 provides a low impedance feedback path for positive signals to prevent amplifier input saturation. This clipping action with the current bias provides a 0 Volt to -6 Volt output for signals which correspond to the +3 volt to +9 volt signals at the output of AMP 2.

Output calibration signals are switched in through U2 (pins 10 and 9). Blackbody TM signals are switched in through U1 (pins 10 and 9). Each is attenuated by a factor of 2 due to the gain of 2 of the output stages operating in the non-inverting mode. The two sync pulses and the 10 KHz pre-cursor boost are 6 volt levels from the D to A on the Output Calibration line and are switched in at the appropriate times under logic control.

The flight model operates with a 7 ma bias on the channel 1 detector and a combined preamplifier and Post Amplifier gain of 20,700. Channel 2 has a 5 ma bias and a gain of 24,000.

7.7.3 Visible Amplifier

The schematic for the visible channel preamplifier is shown in Figure 7.7-1. The Visible Post Amplifier is shown on schematic 8116530. The silicon photodiode is operated with reverse bias as a current source to inverting input of the operational amplifier buffered by the FET input stage.

The Post Amplifier for the Visible Channel is identical in operation to the IR Post Amplifier. The zero reference feedback circuits utilizing a sample of amplifier output while viewing space are identical to the equivalent circuits in the IR Preamplifier.

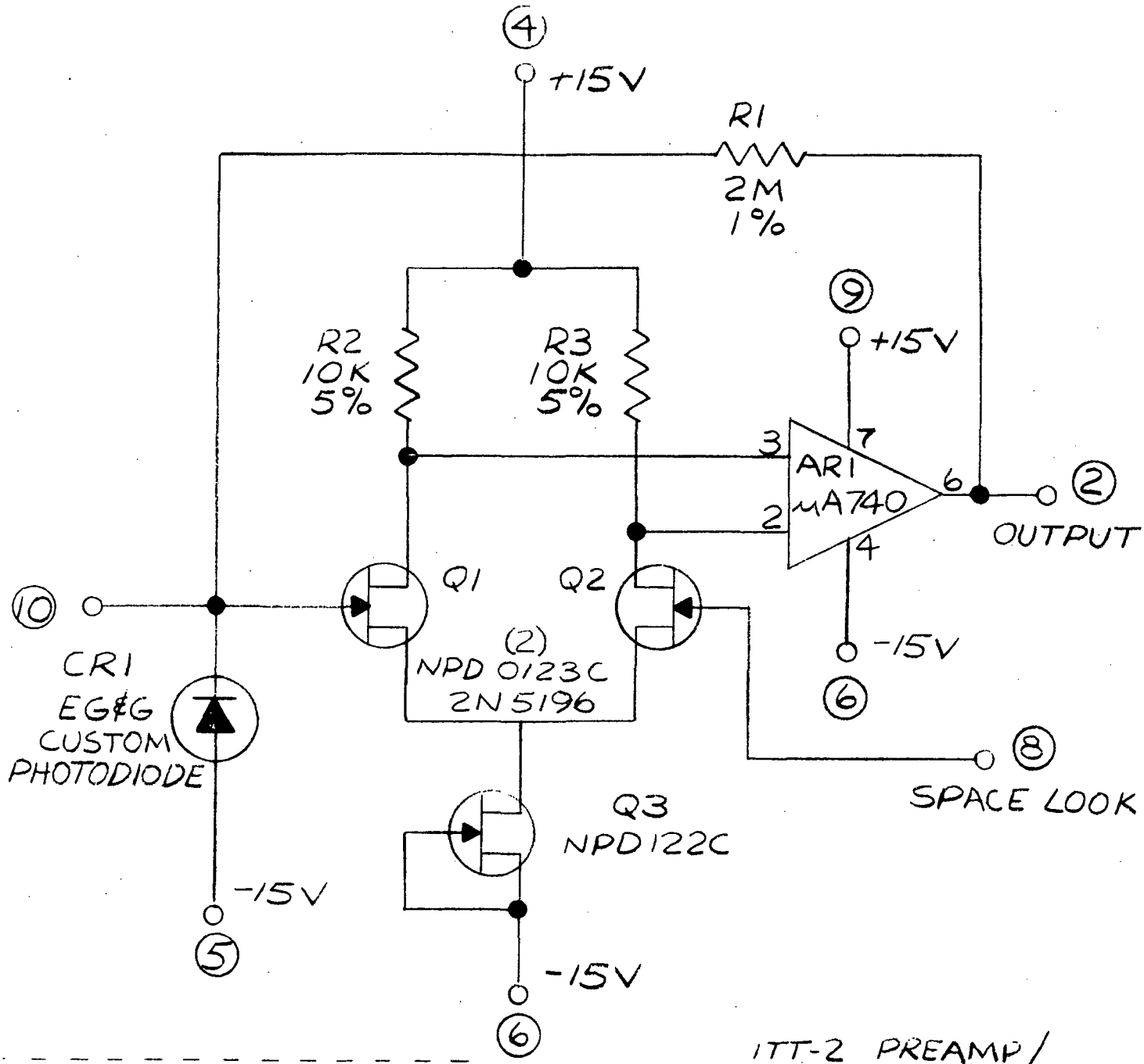

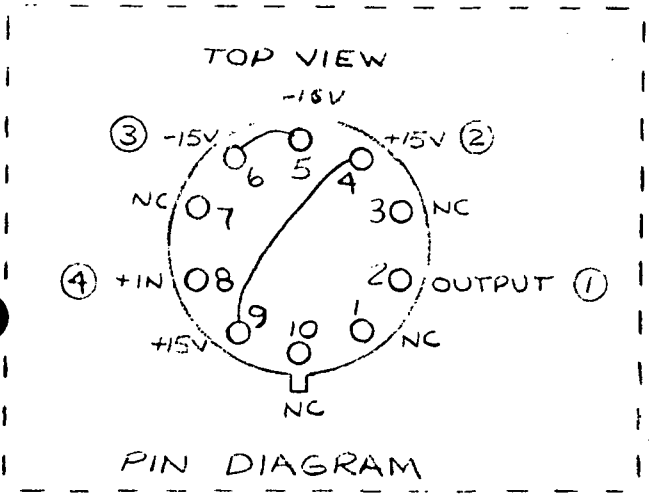

ITT-2 PREAMP/ PHOTODIODE SCHEMATIC DIAGRAM

Figure 7.7-1

7.7.4 Motor Power Supply

The Power Supply for the SCMR Scan and Momentum Compensator motors is a conventional bridge switching amplifier. The circuit for the Momentum Compensator is powered from the -24 Volt bus. The circuits for the scan motor can be powered directly from the bus or from the switching regulator which supplies -15 VDC. Base drive for the switching transistors is derived from the spacecraft 400 Hz 2 phase clock through an isolation transformer.

7.8 Analog Telemetry

The SCMR Analog Telemetry signals together with location of associated are:

Signal	Circuit Location
Electronics Temperature	Temp Tel and Control
Baseplate Temperature	Temp Tel and Control
Blackbody No. 1 Temperature	Temp Tel and Control
Blackbody No. 2 Temperature	Temp Tel and Control
Cone Wall Temperature	Temp Tel and Control
Patch Temperature	Temp Tel and Control
Patch Heat	Temp Tel and Control
Motor Current	Temp Tel and Control
Cone Cover Position	Temp Tel and Control
Electronics Current	Telemetry No. 2
Purge Pressure	Telemetry No. 2
Cone Wall Housing	Telemetry No. 2
Motor Housing Temperature	Telemetry No. 2
Momentum Compensator Speed	Motor Speed TM
Scan Motor Speed	Motor Speed TM
+15 Volt Electronics Supply	Voltage Regulator
-15 Volt Electronics Supply	Voltage Regulator
+5 Volt Electronics Supply	Voltage Regulator
-15 Volt TM Supply	Voltage Regulator
Detector Bias No. 1	Ch. 1 Preamplifier
Detector Bias No. 2	Ch. 2 Preamplifier
Offset Bias Voltage	Logic No. 2

Calibration curves for the Flight Model Analog TM signals are given in Volume 1 of the Flight Model Instruction Manual. Table 7.8-1 is a summary of the analog telemetry points.

7.9 Calibration Signals

The input and output calibration signals are generated by the Digital to Analog Converter V6 on the Logic No. 2 Board. This device is one-half of a basic 8 bit device with an accuracy of $\pm$ ½ LSB. The reference voltage for the D to A is supplied by negative voltage regulator REG 1. This device is temperature compensated to a stability of $\pm$ 0.1% in the same manner as those in the IR

Preamplifiers. This stabilized regulator is also used as the source voltage for the 3 volt offset in the data amplifiers. Separate amplifiers are provided for input and output calibration outputs. Tailoring resistors for output calibration for each channel are provided on the Logic No. 2 board.

TABLE 7.8-1

SCMR FLIGHT MODEL
ANALOG TELEMETRY SUMMARY

1. ELECTRONICS TEMPERATURE T/M

FUNCTION	MEASURES THE TEMPERATURE OF THE ELECTRONICS MODULE STRUCTURE
RANGE	-2 TO +60°C
RESOLUTION	103 MV/DEGREE CENTIGRADE

2. CONE TEMPERATURE T/M

FUNCTION	MEASURES THE TEMPERATURE OF THE CONE WALL STRUCTURE
RANGE	144 TO 297°K
RESOLUTION	42 MV/DEGREE KELVIN

3. BASEPLATE TEMPERATURE T/M

FUNCTION	MEASURES THE TEMPERATURE OF THE BASEPLATE AT ONE OF THE MOUNTING FEET IN THERMAL CONTACT WITH THE SPACECRAFT.
RANGE	-2 TO +60° CENTIGRADE
RESOLUTION	103MV/DEGREE CENTIGRADE

4. BLACKBODY #1 TEMPERATURE T/M

FUNCTION	MEASURES THE TEMPERATURE OF THE BACK-SCAN BLACKBODY TARGET FOR IN-FLIGHT CALIBRATION CHECK.
RANGE	-2 TO +60° CENTIGRADE
RESOLUTION	103MV/DEGREE CENTIGRADE

5. BLACKBODY #2 TEMPERATURE T/M

FUNCTION	MEASURES THE TEMPERATURE OF THE BACK-SCAN BLACKBODY TARGET FOR IN-FLIGHT CALIBRATION CHECK.
RANGE	-2 TO +60° CENTIGRADE
RESOLUTION	103 MV/DEGREE CENTIGRADE

6. PATCH TEMPERATURE T/M

FUNCTION MEASURES THE TEMPERATURE OF THE RADIANT COOLER DETECTOR MOUNTING STRUCTURE.

RANGE 85 TO 127^{O}K

RESOLUTION 152MV/DEGREE KELVIN

7. MOTOR DRIVE CURRENT T/M

FUNCTION MEASURES CURRENT TO THE MOTOR POWER SUPPLY FOR THE COMPENSATION AND MIRROR DRIVE MOTORS.

RANGE 0 TO 354 MA

RESOLUTION 18MV/MA

8. +15 VOLT T/M

FUNCTION MONITORS THE OUTPUT VOLTAGE OF THE ELECTRONICS +15V REGULATOR

RANGE +1.8 TO +30 V

RESOLUTION 1MV/4.2 MV

9. -15 VOLT T/M

FUNCTION MONITORS THE OUTPUT VOLTAGE OF THE ELECTRONICS -15V REGULATOR

RANGE 0 TO -19.1V

RESOLUTION 1 MV/3 MV

10. +5 VOLT T/M

FUNCTION MONITORS THE OUTPUT VOLTAGE OF THE ELECTRONICS +5V REGULATOR

RANGE 0 TO +15 V

RESOLUTION 1 MV/2.35 MV

11. DETECTOR #1 BIAS SUPPLY T/M

FUNCTION MONITORS THE OUTPUT VOLTAGE OF THE -12V REGULATOR ON THE PRE-AMPLIFIER #1 BOARD.

RANGE 0 TO -12.75V

RESOLUTION 0.5V/VOLT

12. DETECTOR #2 BIAS SUPPLY T/M

FUNCTION MONITORS THE OUTPUT VOLTAGE OF THE -12V REGULATOR ON THE PRE-AMPLIFIER #2 BOARD

RANGE 0 TO -12.75V

RESOLUTION 0.5V/VOLT

13. TELEMETRY POWER T/M

FUNCTION MONITORS THE OUTPUT VOLTAGE OF THE TELEMETRY -15V REGULATOR

RANGE 0 TO -19V

RESOLUTION 1 MV/3 MV

14. CONE COVER POSITION T/M

FUNCTION MONITORS POSITION OF THE RADIANT COOLER COVER

RANGE 0 TO 150 DEGREES

RESOLUTION 41.7 MV/DEGREE

15. PATCH POWER T/M

FUNCTION MONITORS THE OUTPUT VOLTAGE OF THE PATCH TEMPERATURE CONTROL CIRCUIT

RANGE 0 TO 6 MW

RESOLUTION > .57 V/MW

16. CONE WALL HOUSING TEMPERATURE T/M

FUNCTION MONITORS THE TEMPERATURE OF THE CONE WALL HOUSING STRUCTURE

RANGE +60 TO -25^{o}C

RESOLUTION >60MV/DEGREE CENTIGRADE

17. ELECTRONICS CURRENT

FUNCTION MEASURES CURRENT TO THE ELECTRONICS CIRCUITRY.

RANGE 0 TO 625 MA

RESOLUTION 10MV/MA

18. PURGE PRESSURE

FUNCTION MEASURES THE PRESSURE OF THE PATCH DECONTAMINATION PURGE SUPPLY

RANGE 0-100 PSIΔ

RESOLUTION 63MV/PSI

19. OFFSET BIAS VOLTAGE

FUNCTION MEASURES OFFSET BIAS REGULATOR SUPPLY VOLTAGE.

RANGE -0.25 TO -7.9V

RESOLUTION .833V/VOLT.

20. MOTOR HOUSING TEMPERATURE

FUNCTION MEASURES THE TEMP. OF THE SCANNER MOTOR HOUSING.

RANGE -5 TO +50^{o}C

RESOLUTION 116MV/DEGREE CENTIGRADE

21. SCAN MOTOR SPEED

FUNCTION MONITORS SPEED OF THE SCAN MOTOR

RANGE 0-640 RPM

RESOLUTION 10MV/RPM

22. MOMENTUM COMPENSATOR SPEED

FUNCTION MONITORS SPEED OF THE MOMENTUM COMPENSATOR MOTOR.

RANGE 1400 - 5000 RPM

RESOLUTION 1.77MV/RPM

8.0 INSTRUMENT TEST SUMMARY/FINAL CALIBRATION

Complete test procedures and data are available in the flight model, "Instruction Manual for the Surface Composition Mapping Radiometer Vol. II." Table 8.0-1 is a summary extracted from the manual.

8.1 Final calibration curves for the 3 data channels of the flight model are shown in Figures 8.1-1 thru 8.0-7.

8.2 Figure 8.2-1 is a thermal profile generated from telemetry readings taken during the final vacuum thermal cycle.

The data indicates that for a 40°C ΔT at the instrument baseplate[1]:

ELECTRONICS	ΔT	=	30°C
CONE HOUSING	ΔT	=	8.8°C
CONE WALL	ΔT	=	4.5°C
UNCONTROLLED PATCH [2]	ΔT	=	5.4°C

The Radiant cooler margin to maintain control at nominal instrument temperature (+15°C) = 4.0 milliwatts x 1.8° = 7.2 DEGREES KELVIN.

---

1. At the flight level of the thermal vacuum temperature cycle.
2. Patch margin = 1.8°K/Milliwatt

FIELD OF VIEW

	CH 1(SWL)	CH2(LWL)
NORMAL TO SCAN AXIS	.84 mr	.6 mr
PARALLEL TO SCAN AXIX	.74 mr	.69 mr

REGISTRATION

LWL/SWL NORMAL TO SCAN AXIS	.072 mr
LWL/VIS. NORMAL TO SCAN AXIS	.078 mr
LWL/SWL PARALLEL TO SCAN AXIS	.20 mr
LWL/VIS PARALLEL TO SCAN AXIS	.06 mr

DETECTOR OPERATING TEMP.	116° KELVIN	
	CH 1	CH2
DETECTOR RESPONSIVITY (110°K)	42×10^3 V/WATT(7MA)	63×10^3 V/WATT (5 MA)
DETECTOR D* (110°K)	3.38×10^{10} CM HZ½ W^{-1}	2.36×10^{10} CM HZ½ W^{-1}
NE ΔT	0.31°K	0.8°K
NOISE (RMS MV		
SLOPE (MV/°K) @ 280°K		
SINGLE ELEMENT RESOLUTION	47%	57%

VISIBLE DETECTOR

RESPONSIVITY	0.356AMPS/WATT(.9μ)
DARK CURRENT	0.430NA.

MOTOR JITTER

LOW POWER MODE LINE/LINE AVG.	5μSEC.(.3mr.)
HI POWER MODE LINE/LINE AVG.	2μSEC.(.12 mr)

TABLE 8.0-1
TEST SUMMARY

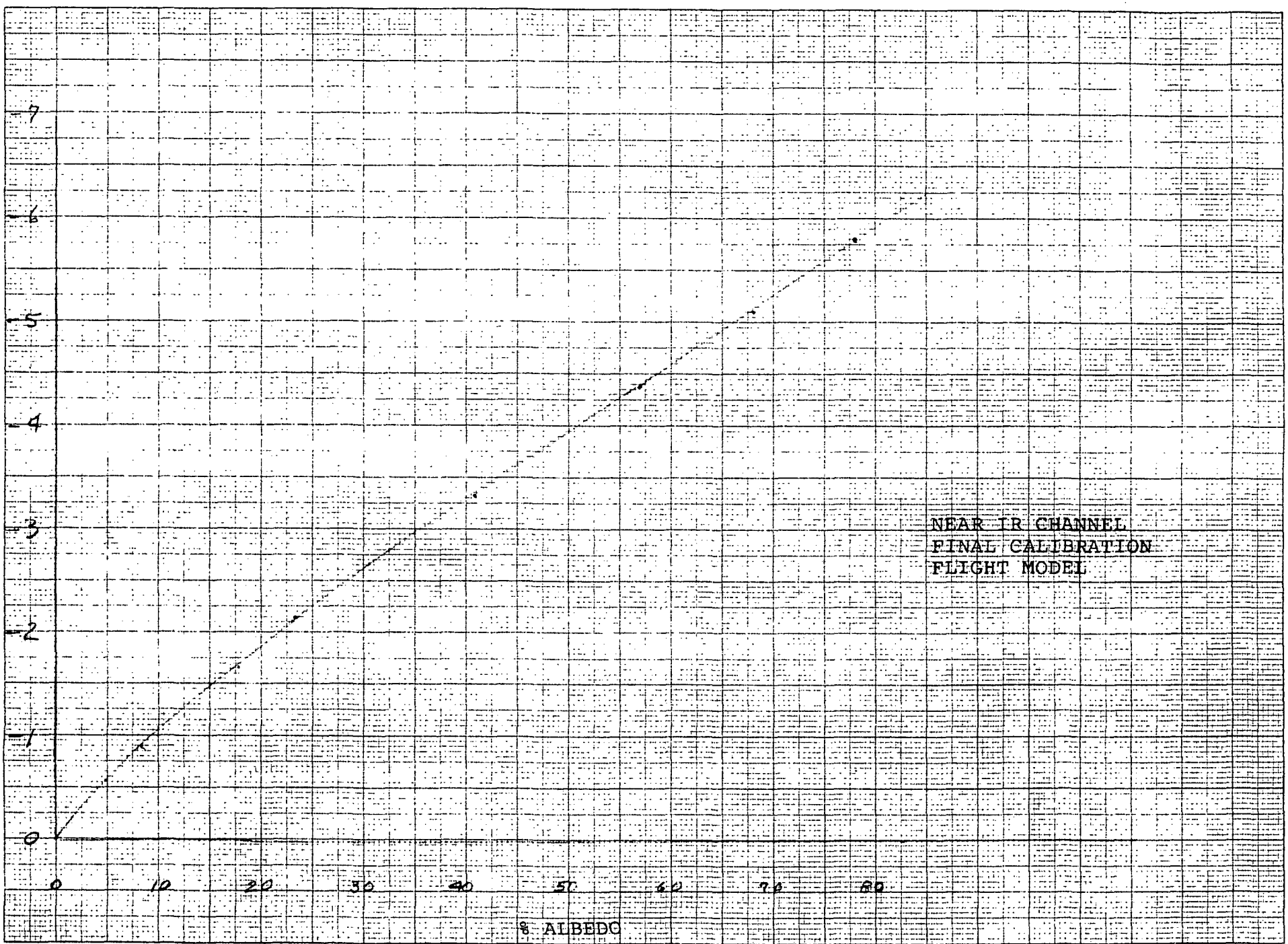
NEAR IR CHANNEL
FINAL CALIBRATION
FLIGHT MODEL
OUTPUT VOLTS
-7
-6
-5
-4
-3
-2
-1
0
0
10
20
30
40
50
60
70
80
% ALBEDO
AE
9-29-72

FIGURE 8.1-1

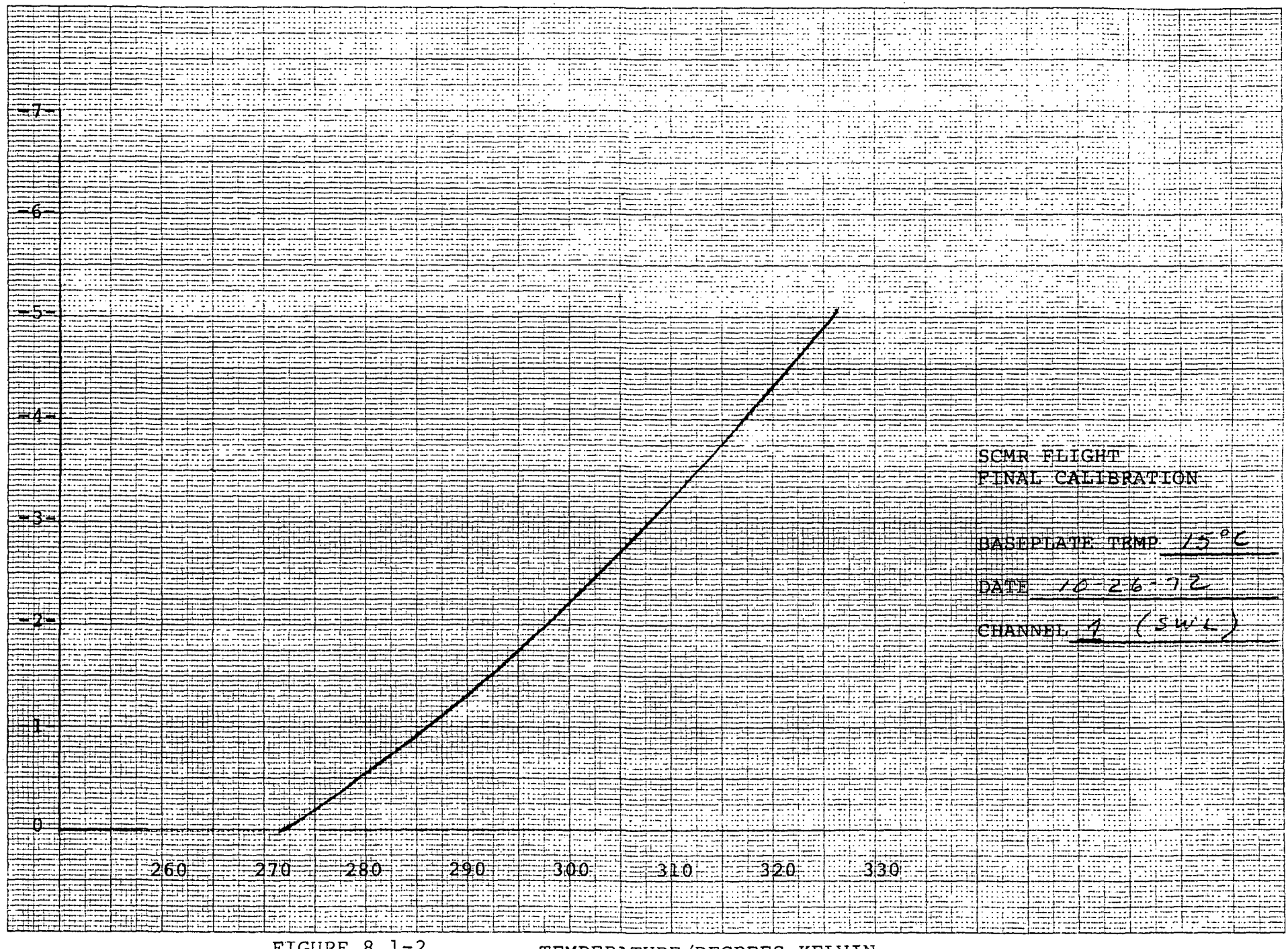

FIGURE 8.1-2

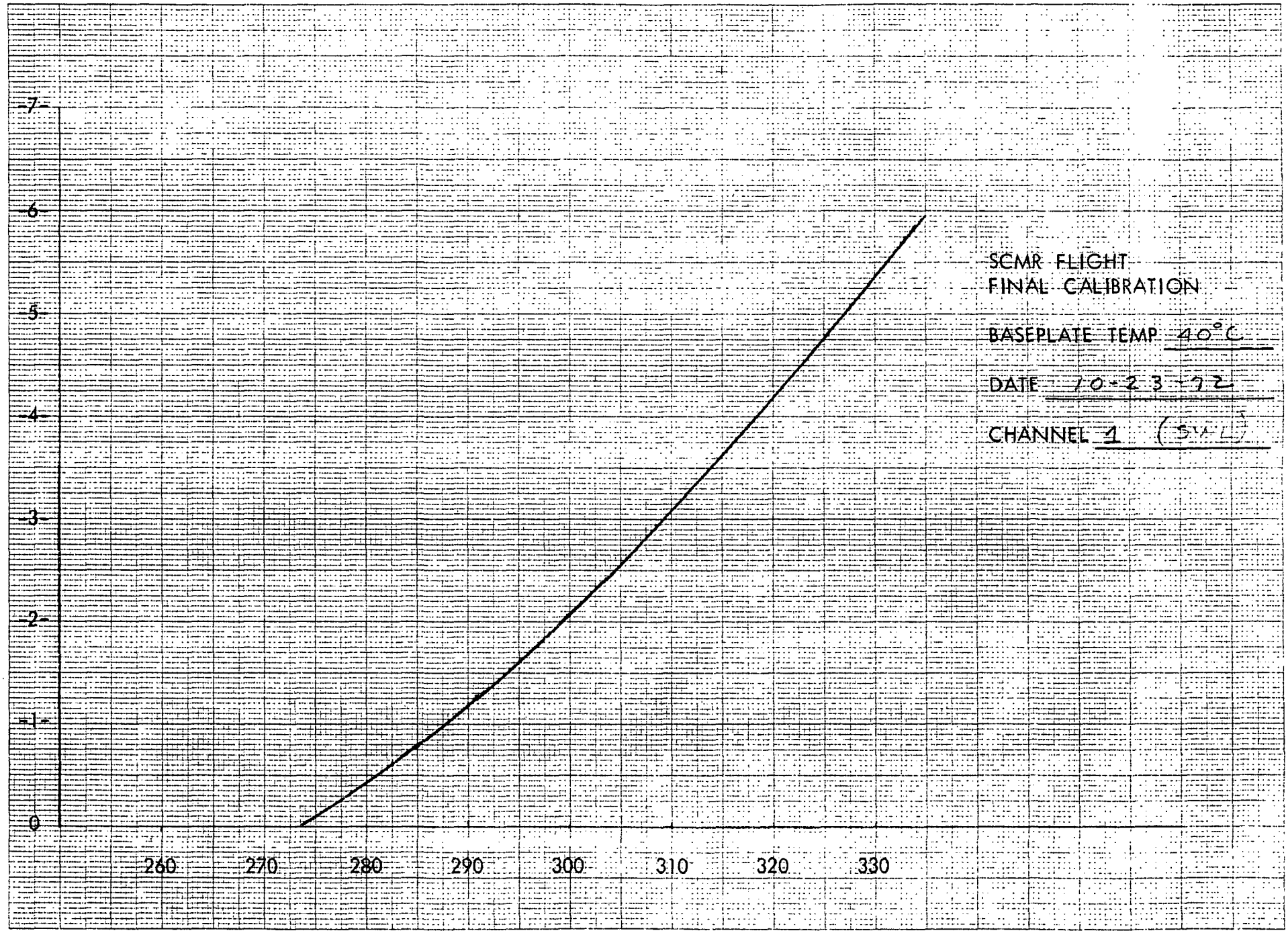

FIGURE 8.1-3 TEMPERATURE/DEGREES KELVIN

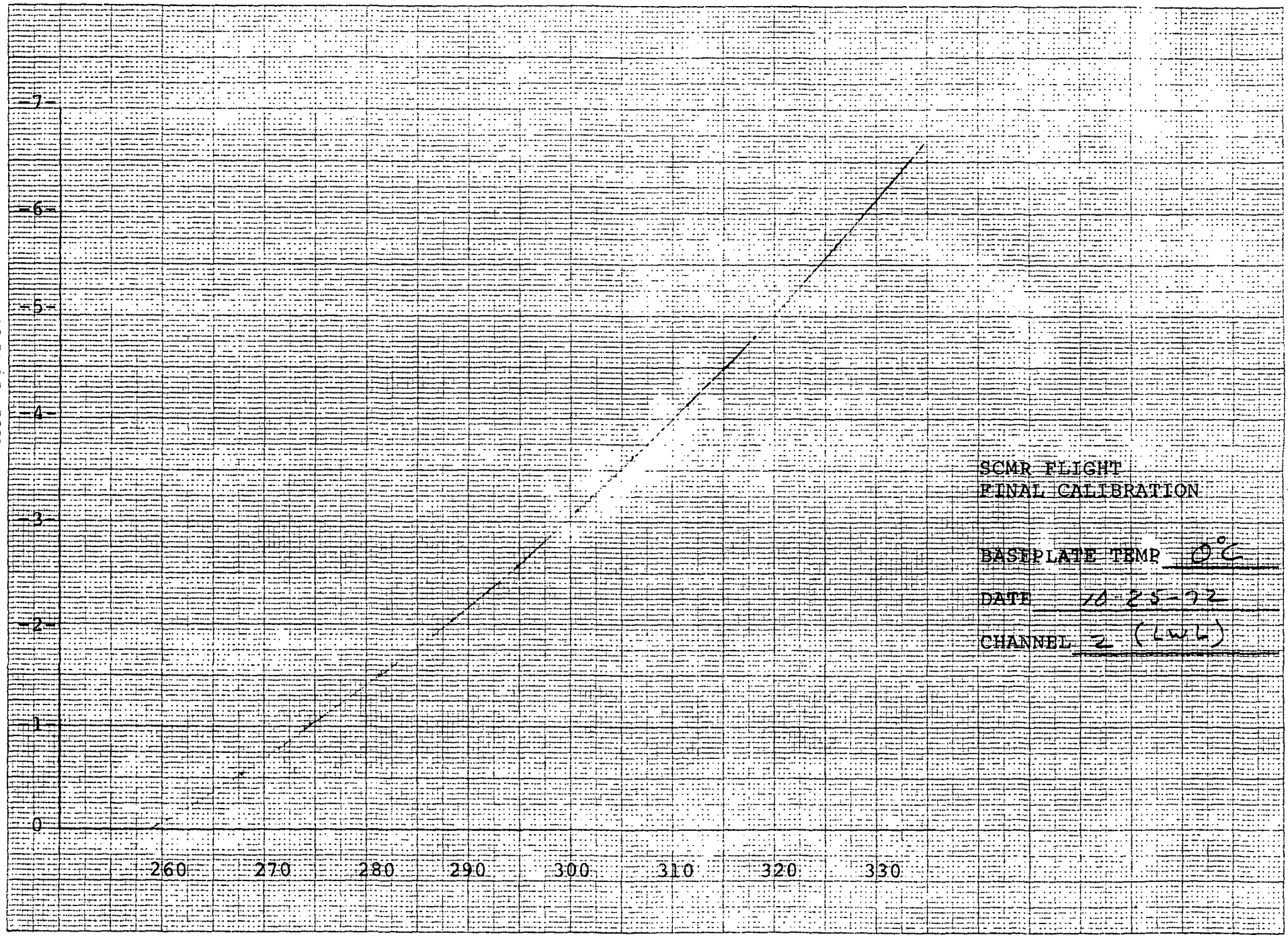

FIGURE 8.1-4 TEMPERATURE/DEGREES KELVIN

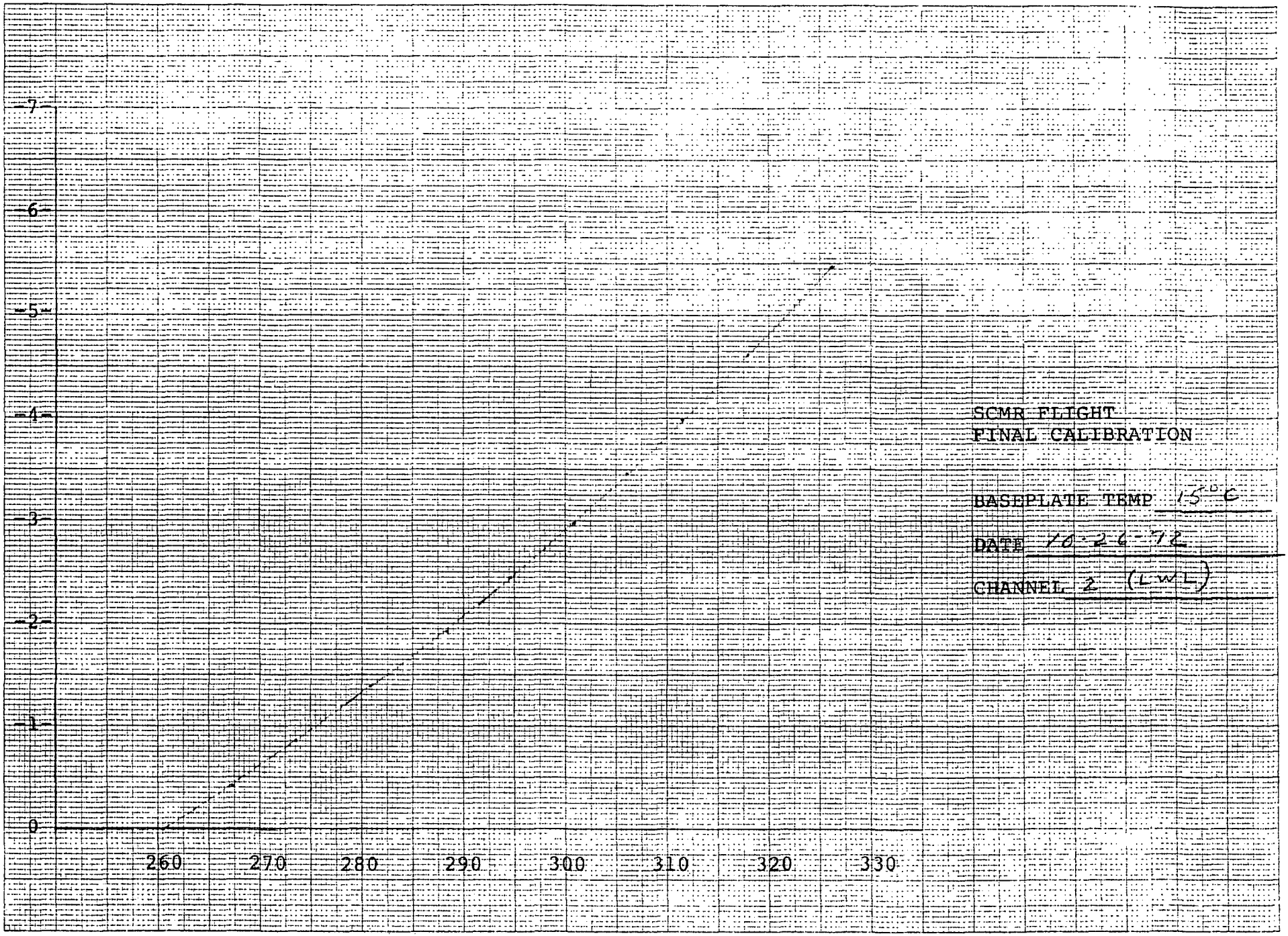

FIGURE 8.1-5 TEMPERATURE/DEGREES KELVIN

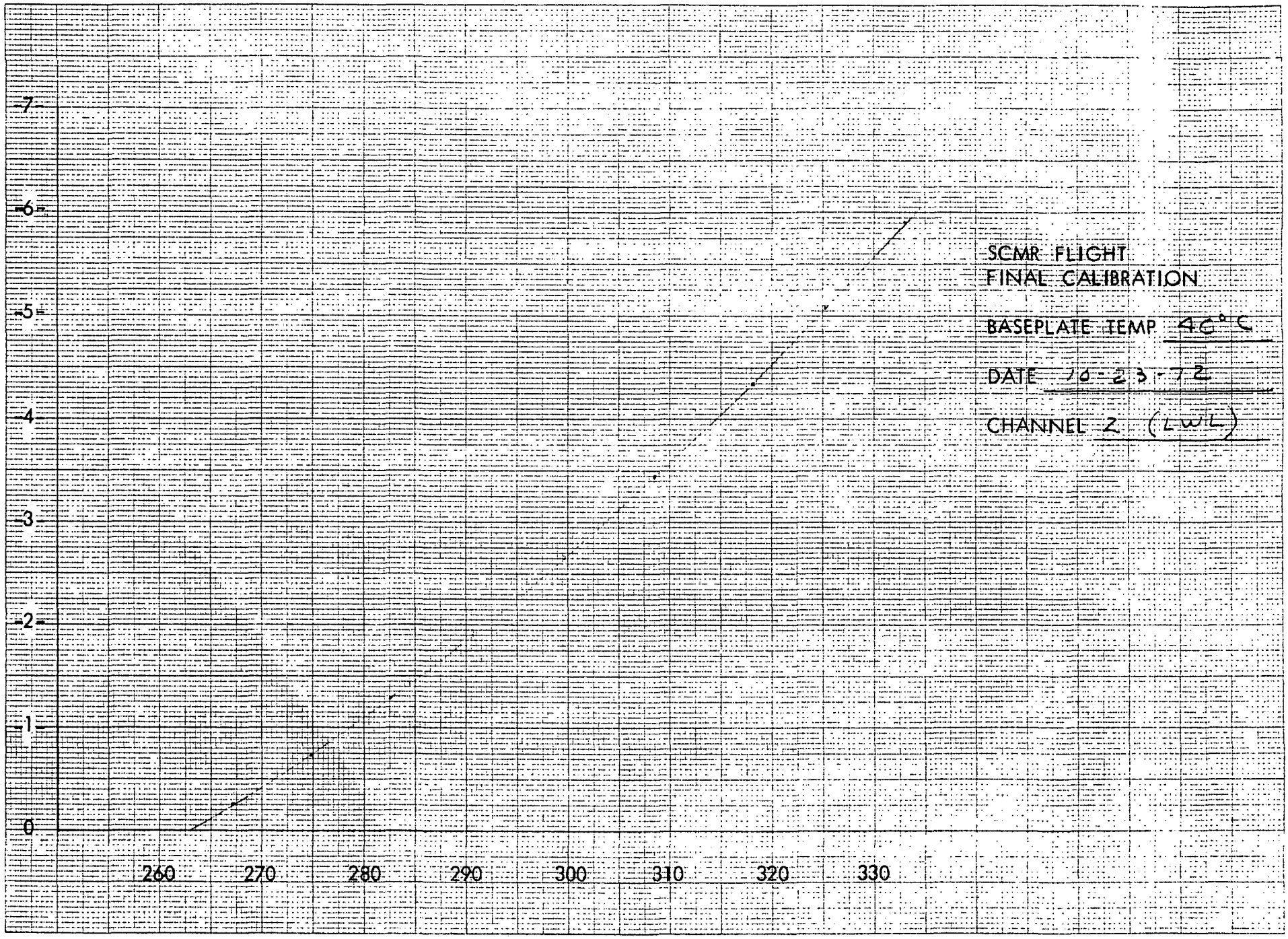
SCMR FLIGHT
FINAL CALIBRATION
BASEPLATE TEMP 46°C
DATE 10-23-72
CHANNEL 2 (LWL)
VOLTAGE OUTPUT
-7
-6
-5
-4
-3
-2
-1
0
260
270
280
290
300
310
320
330
TEMPERATURE/DEGREES KELVIN

FIGURE 8.1-6

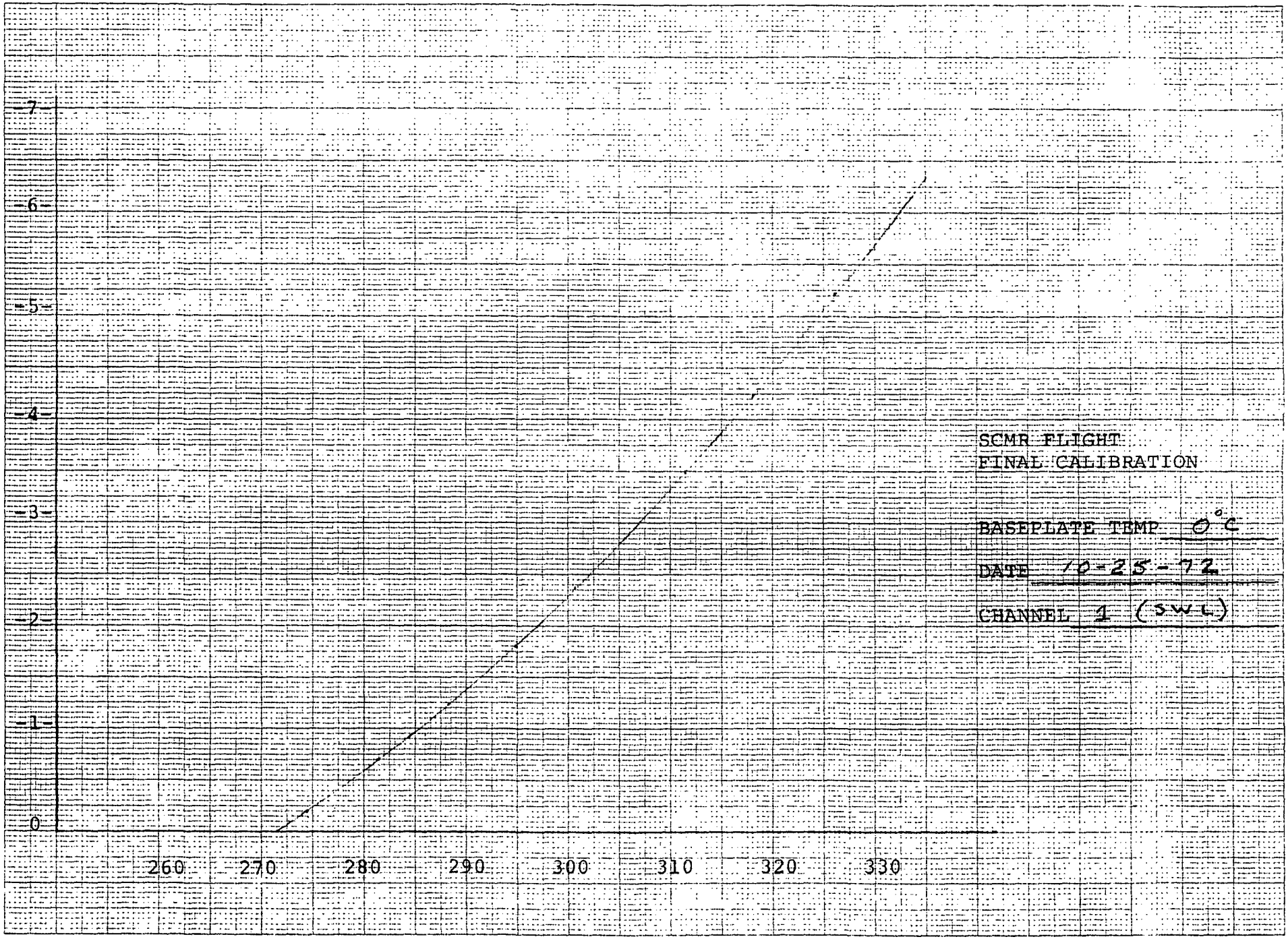

FIGURE 8.1-7 TEMPERATURE/DEGREES KELVIN

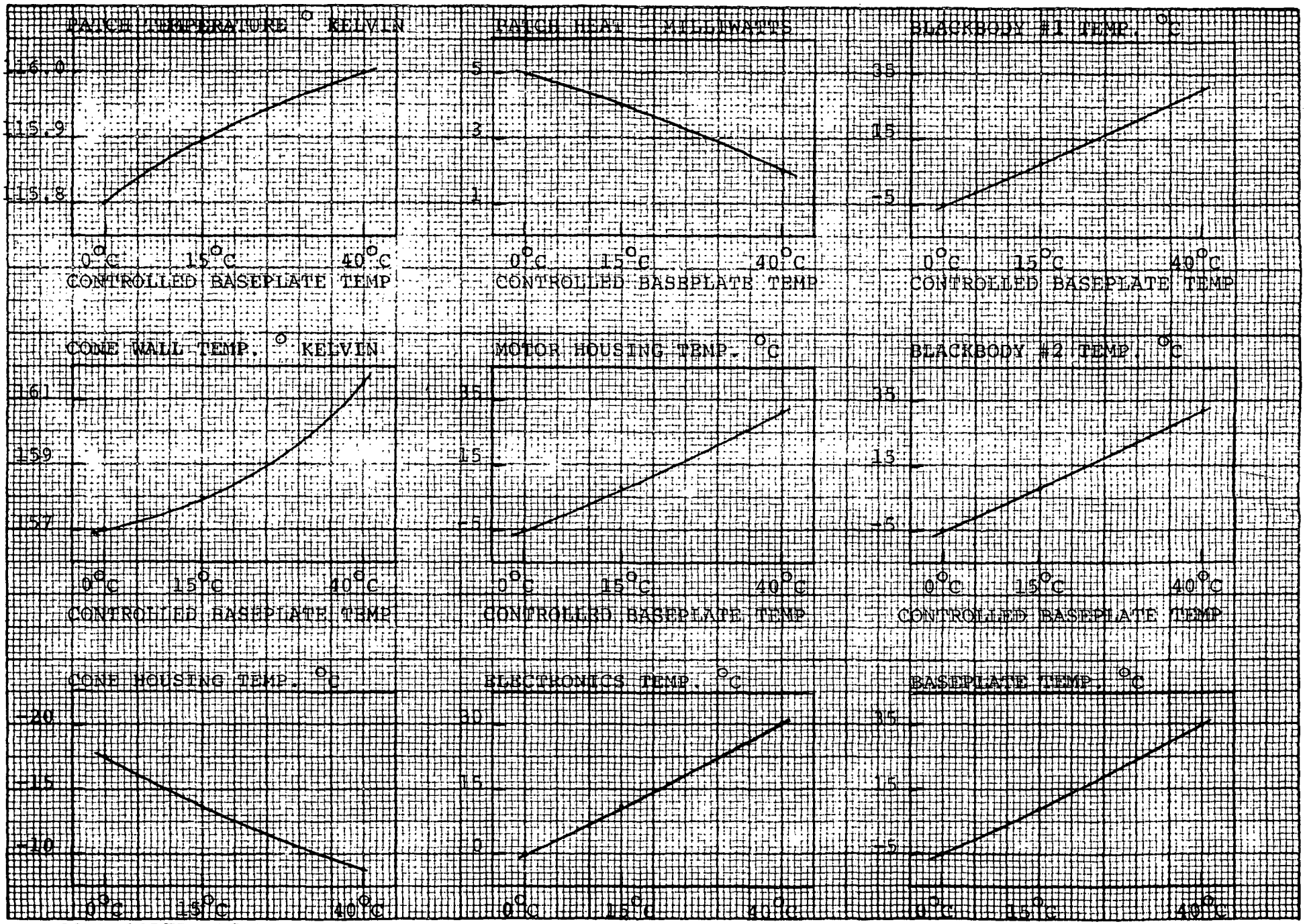

FIGURE 8.2-1 THERMAL PROFILE

APPENDIX

CONTENTS

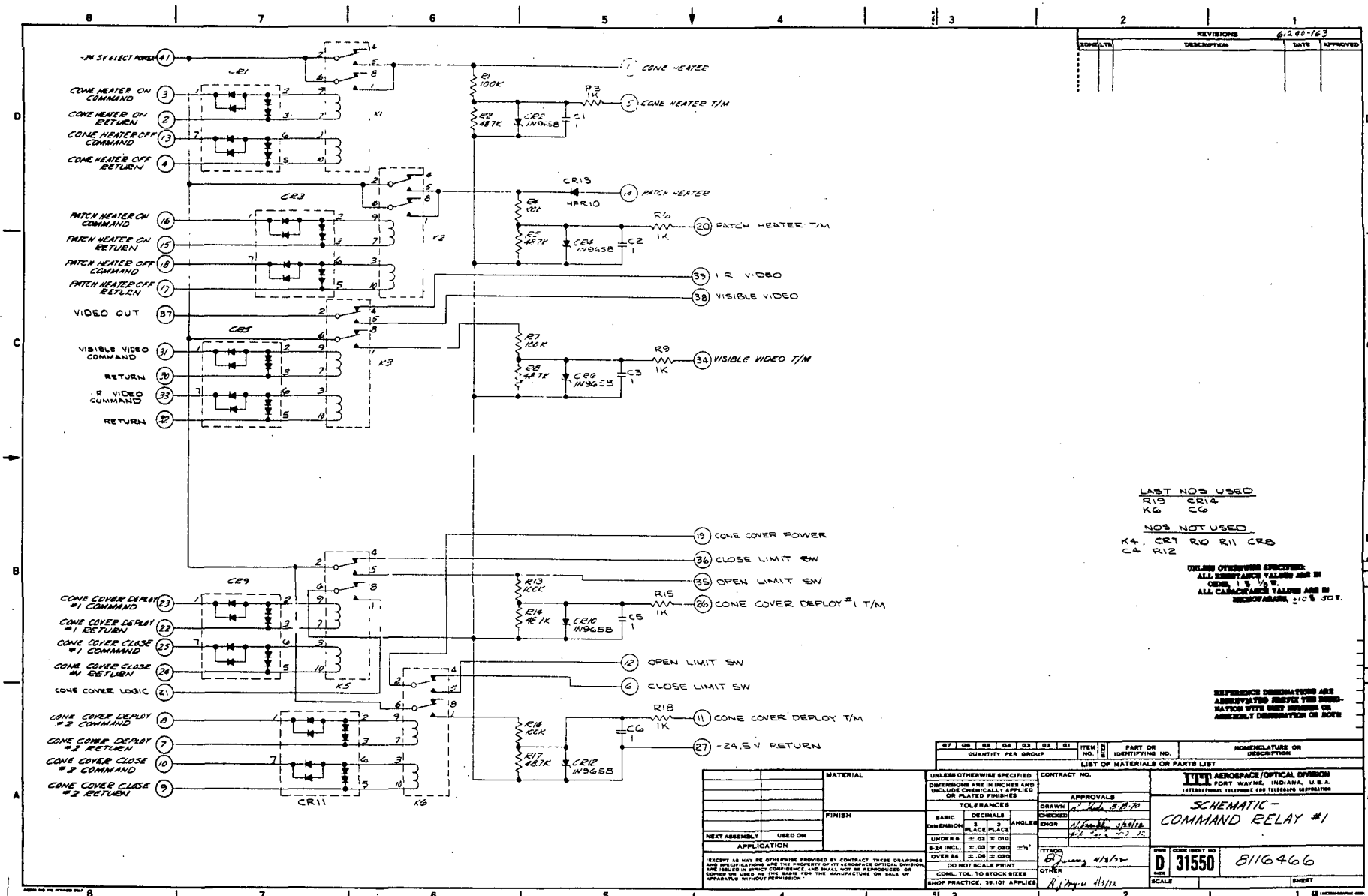

LAST NOS USED

R19	CR14
K6	C6

NOS NOT USED

K4, CR7 R10 R11 CR8
C4 R12

UNLESS OTHERWISE SPECIFIED:
ALL RESISTANCE VALUES ARE IN OHMS, 1 % 1/2 W.
ALL CAPACITANCE VALUES ARE IN MICROFARADS, ±10 % 50 V.

REFERENCE DESIGNATIONS ARE ABBREVIATED ABOVE PER DESIGNATIONS WITH THEIR NUMBERS ON ASSEMBLY DESIGNATION OR BOM'S

REVISIONS				6280-163
ZONE	LTR	DESCRIPTION	DATE	APPROVED

07	06	05	04	03	02	01	ITEM NO.	SIZE	PART OR IDENTIFYING NO.	NOMENCLATURE OR DESCRIPTION
QUANTITY PER GROUP									LIST OF MATERIALS OR PARTS LIST	

		MATERIAL
		FINISH
NEXT ASSEMBLY	USED ON	
APPLICATION		

UNLESS OTHERWISE SPECIFIED
DIMENSIONS ARE IN INCHES AND INCLUDE CHEMICALLY APPLIED OR PLATED FINISHES
TOLERANCES

BASIC DIMENSION	DECIMALS 2 PLACE	DECIMALS 3 PLACE	ANGLES
UNDER 6	± .03	± .010	±½°
6-24 INCL.	± .03	± .060	
OVER 24	± .06	± .090	

DO NOT SCALE PRINT
COMM. TOL. TO STOCK SIZES
SHOP PRACTICE, 39.101 APPLIES

CONTRACT NO.

APPROVALS

DRAWN		8.28.70
CHECKED		8/28/70
ENGR		8/28/70
ITTAOD		4/28/72
OTHER		4/11/72

ITT AEROSPACE/OPTICAL DIVISION
FORT WAYNE, INDIANA, U.S.A.
INTERNATIONAL TELEPHONE AND TELEGRAPH CORPORATION

SCHEMATIC – COMMAND RELAY #1

DWG SIZE	CODE IDENT NO	
D	31550	8116466
SCALE		SHEET

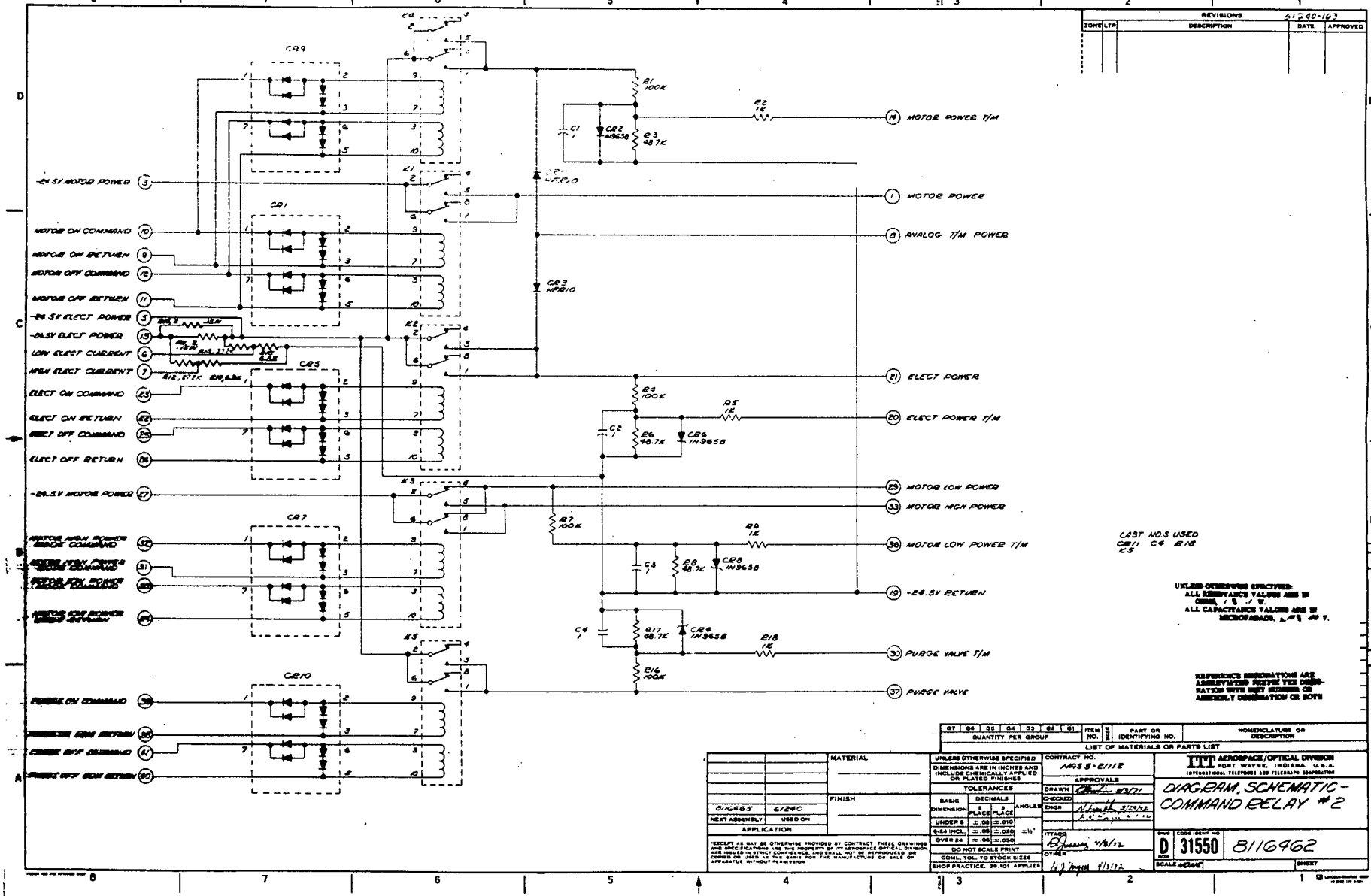
REVISIONS
ZONE LTR DESCRIPTION DATE APPROVED
61240-163
-24.5V MOTOR POWER
MOTOR ON COMMAND
MOTOR ON RETURN
MOTOR OFF COMMAND
MOTOR OFF RETURN
-24.5V ELECT POWER
-24.5V ELECT POWER
LOW ELECT CURRENT
HIGH ELECT CURRENT
ELECT ON COMMAND
ELECT ON RETURN
ELECT OFF COMMAND
ELECT OFF RETURN
-24.5V MOTOR POWER
PURGE ON COMMAND
PURGE ON RETURN
PURGE OFF COMMAND
PURGE OFF RETURN
CR9
CR1
CR5
CR7
CR10
K1
K2
K3
K4
K5
CR3 HP610
CR4 HP610
R1 100K
R2 1K
R3 100K
R4 100K
R5 1K
R6 98.7K
R7 100K
R8 98.7K
R9 1K
R10 100K
R17 98.7K
R18 1K
R16 100K
C1 1
C2 1
C3 1
C4 1
CR2 IN3638
CR6 IN3638
CR8 IN3638
CR9 IN3638
MOTOR POWER T/M
MOTOR POWER
ANALOG T/M POWER
ELECT POWER
ELECT POWER T/M
MOTOR LOW POWER
MOTOR HIGH POWER
MOTOR LOW POWER T/M
-24.5V RETURN
PURGE VALVE T/M
PURGE VALVE
LAST NO.S USED
CR11 C4 R18
K5
UNLESS OTHERWISE SPECIFIED:
ALL RESISTANCE VALUES ARE IN OHMS, 1/4 W.
ALL CAPACITANCE VALUES ARE IN MICROFARADS, 100 V.
REFERENCE DESIGNATIONS ARE ABBREVIATED PREFIX FOR DESIGNATION WITH SEQUENCE OR ASSEMBLY DESIGNATION OR BOTH
ITEM NO.
PART OR IDENTIFYING NO.
NOMENCLATURE OR DESCRIPTION
QUANTITY PER GROUP
LIST OF MATERIALS OR PARTS LIST
MATERIAL
FINISH
61240-163
61240
NEXT ASSEMBLY
USED ON
APPLICATION
UNLESS OTHERWISE SPECIFIED
DIMENSIONS ARE IN INCHES AND INCLUDE CHEMICALLY APPLIED OR PLATED FINISHES
TOLERANCES
BASIC DIMENSION
DECIMALS
1 PLACE
2 PLACE
ANGLES
UNDER 6 ± .03 ± .010
6-24 INCL. ± .05 ± .030
OVER 24 ± .06 ± .030
± 1°
DO NOT SCALE PRINT
COML. TOL. TO STOCK SIZES
SHOP PRACTICE, 38.101 APPLIES
CONTRACT NO. N00 5-2111E
APPROVALS
DRAWN
CHECKED
ENGR
ITT AERO
OTHER
ITT AEROSPACE/OPTICAL DIVISION
FORT WAYNE, INDIANA, U.S.A.
INTERNATIONAL TELEPHONE AND TELEGRAPH CORPORATION
DIAGRAM, SCHEMATIC - COMMAND RELAY #2
SIZE D
CODE IDENT NO. 31550
DWG NO. 8116462
SCALE NONE
SHEET
8116462
"EXCEPT AS MAY BE OTHERWISE PROVIDED BY CONTRACT, THESE DRAWINGS AND SPECIFICATIONS ARE THE PROPERTY OF ITT AEROSPACE OPTICAL DIVISION AND ISSUED IN STRICT CONFIDENCE, AND SHALL NOT BE REPRODUCED OR COPIED OR USED AS THE BASIS FOR THE MANUFACTURE OR SALE OF APPARATUS WITHOUT PERMISSION."

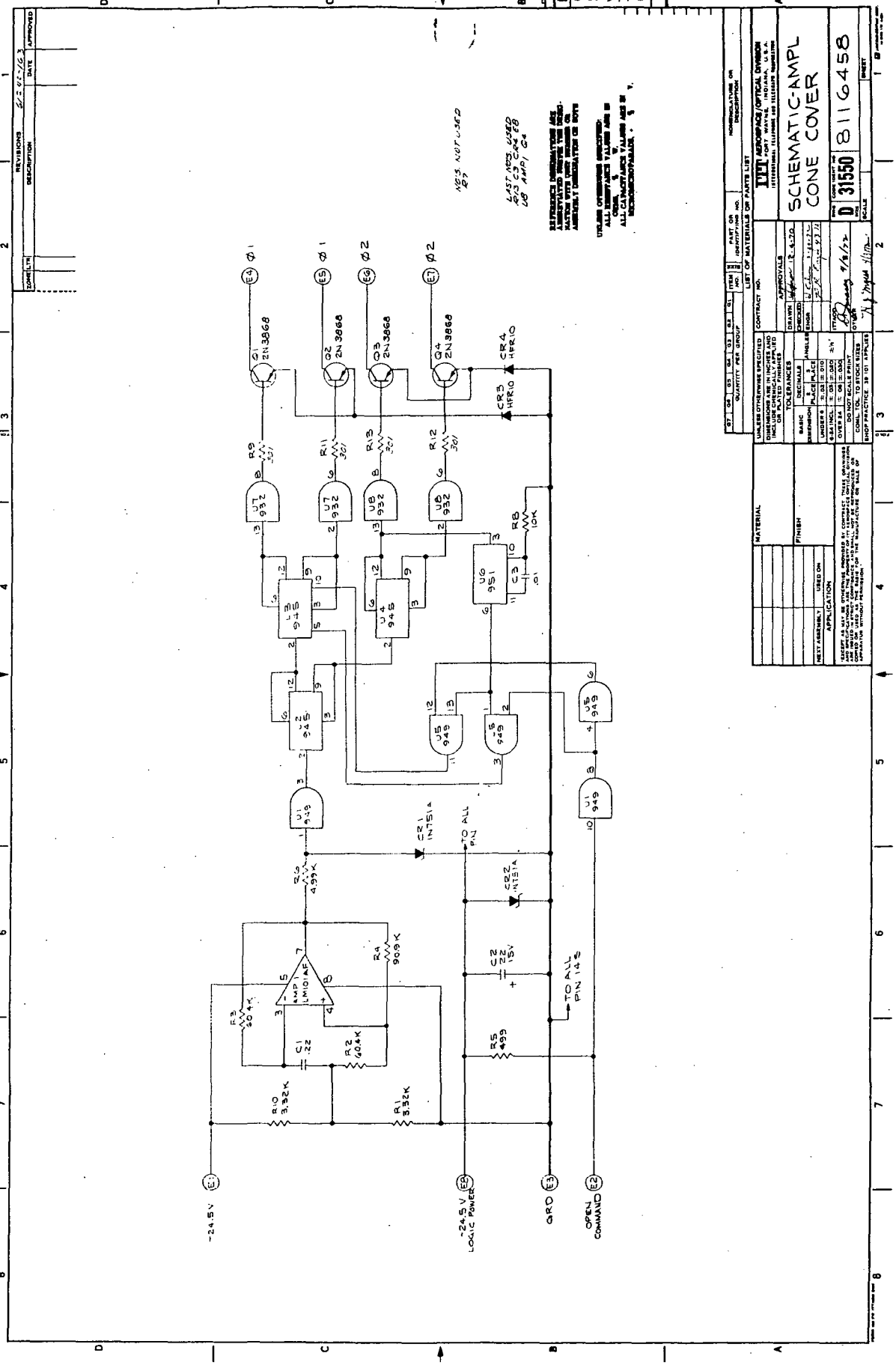
SCHEMATIC-AMPL
CONE COVER
D 31550
8116458
ITT AEROSPACE/OPTICAL DIVISION
FORT WAYNE, INDIANA, U.S.A.
-24.5 V
-24.5 V LOGIC POWER
GRD
OPEN COMMAND
TO ALL PIN 14
TO ALL PIN
AMPL LM101AF
Q1 2N3868
Q2 2N3868
Q3 2N3868
Q4 2N3868
CR1 IN5614
CR2 IN5614
CR3 HER10
CR4 HER10
U1 946
U2 946
U3 946
U4 946
U5 946
U6 951
U7 932
U8 932
U9 932
R1 3.32K
R2 604K
R3 20.4K
R4 909K
R5 499
R8 10K
R9 301
R10 3.32K
R11 301
R12 301
R13 301
C1 .22
C2 22 15V
C3 .01

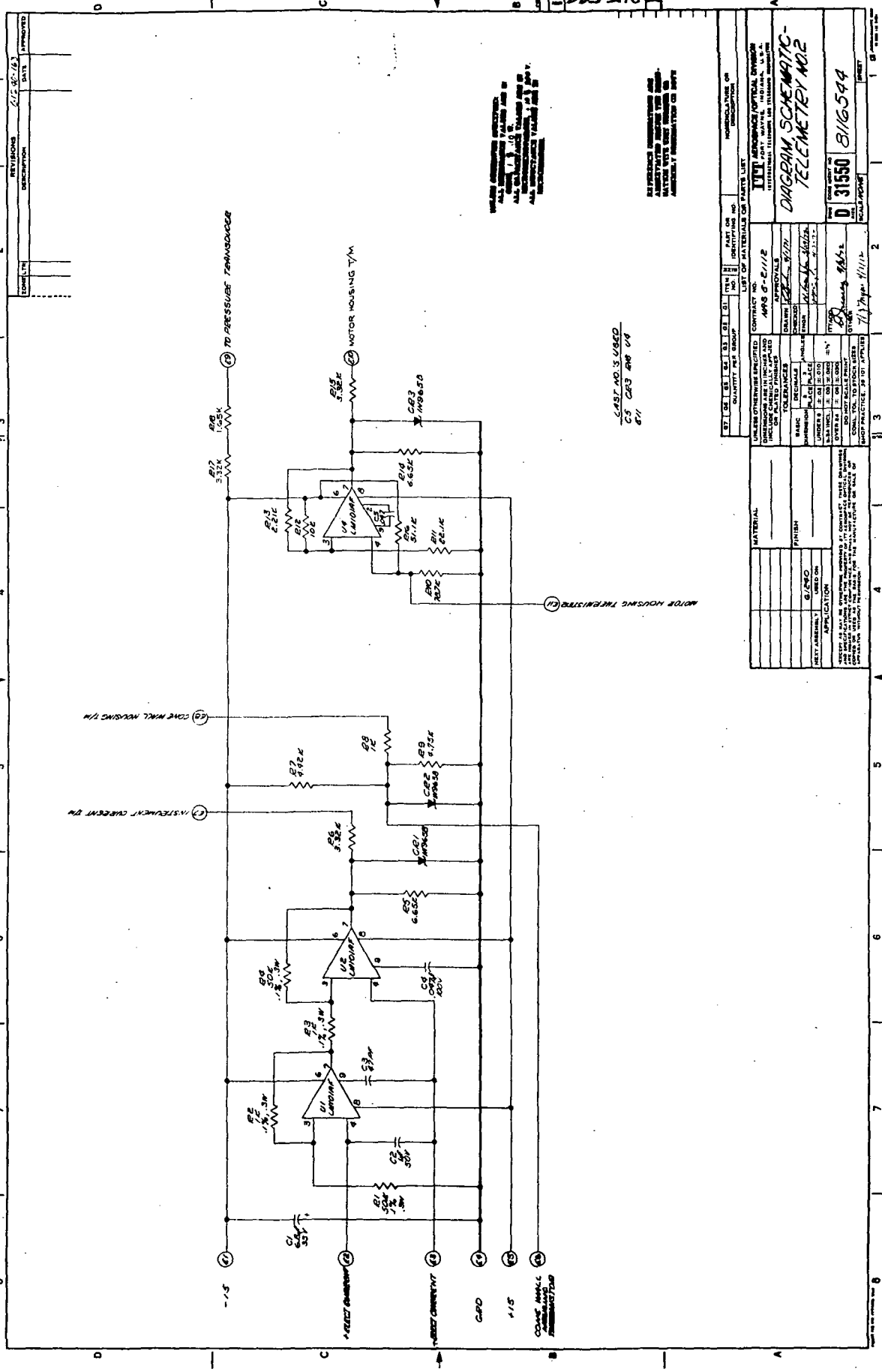
81G544
DIAGRAM, SCHEMATIC-TELEMETRY NO2
D 31550
81G544
ITT
REVISIONS
DESCRIPTION
DATE
APPROVED
TO PRESSURE TRANSDUCER
MOTOR HOUSING T/M
MOTOR HOUSING THERMISTOR
CASE NO IS USED
C5 C83 AND C4
6/1
CONE HALL HOUSING T/M
INSTRUMENT CURRENT T/M
+REACT CURRENT
GND
+15
-15
CONE HALL TRANSDUCER
U4 LM124AJ
U5 LM124AJ
U1 LM124AJ
R17 332K
R26 1.65K
R15 3.32K
R14 6.65K
R13 2.21K
R16 10Ω
R11 82.5K
R10 332K
R27 402K
R28 1Ω
R29 6.13K
R24 3.32K
R25 6.65K
R23 .1Ω 3W
R22 .1Ω 3W
R21 .1Ω 3W
C83 IN9638
C22 IN9638
C21 IN9638
C1 50V
C2 50V
C3 3W
C4 CAP 100V
MATERIAL
FINISH
APPLICATION
NEXT ASSEMBLY
USED ON
CONTRACT NO. NAS 6-2112
APPROVALS
DRAWN
CHECKED
ENGR
MGR
QUALITY
PROJ ENGR
DO NOT SCALE PRINT
SHEET
SIZE
CODE IDENT NO 31550
SCALE NONE

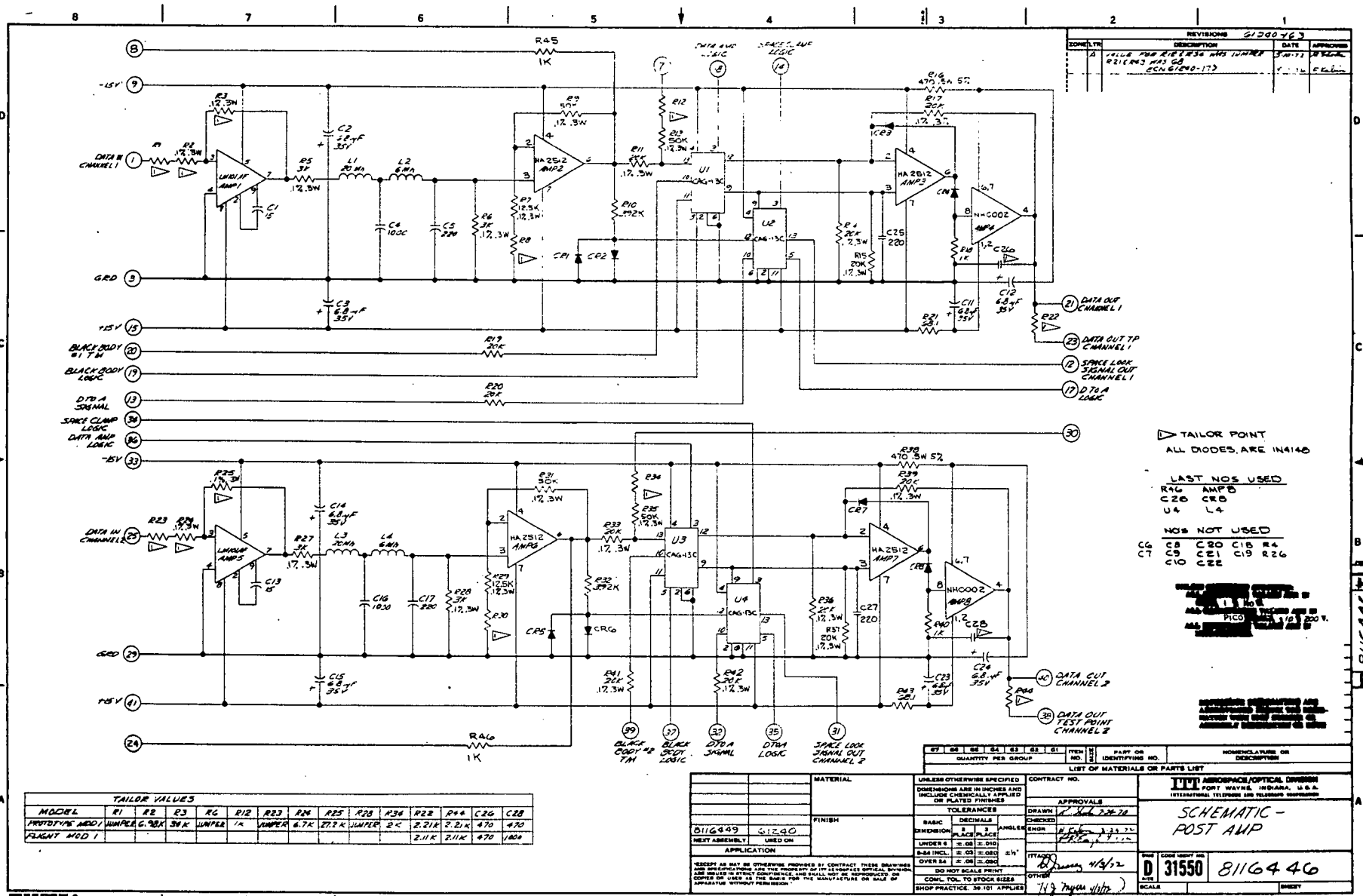

TAILOR POINT
ALL DIODES ARE IN4148

LAST NOS USED
R46 AMP8
C26 CR8
U4 L4

NOS NOT USED
C6 C8 C20 C18 R4
C7 C9 C21 C19 R26
C10 C22

PICO

8116446 P

TAILOR VALUES													
MODEL	R1	R2	R3	R6	R12	R23	R24	R25	R28	R34	R22	R44	C26	C28
PROTOTYPE MOD I	JUMPER	6.98K	39K	JUMPER	1K	JUMPER	6.7K	27.7K	JUMPER	2K	2.21K	2.21K	470	470
FLIGHT MOD I											2.11K	2.11K	470	180

REVISIONS 61200-463			
ZONE	LTR	DESCRIPTION	DATE	APPROVED
	A	VALUE FOR R1 & R34 WAS JUMPER R2 & R43 WAS 6Ω ECN 61240-173	3-10-72	4-11-72	

QUANTITY PER GROUP	ITEM NO.	REV	PART OR IDENTIFYING NO.	NOMENCLATURE OR DESCRIPTION
67 66 65 64 63 62 61				

LIST OF MATERIALS OR PARTS LIST

MATERIAL	UNLESS OTHERWISE SPECIFIED DIMENSIONS ARE IN INCHES AND INCLUDE CHEMICALLY APPLIED OR PLATED FINISHES	CONTRACT NO.	ITT AEROSPACE/OPTICAL DIVISION FORT WAYNE, INDIANA, U.S.A.
FINISH	TOLERANCES	APPROVALS	SCHEMATIC - POST AMP
8116449 / 61240	BASIC DIMENSION: DECIMALS 2 PLACE ±.05, 3 PLACE ±.010; ANGLES ±½°	DRAWN	
NEXT ASSEMBLY / USED ON	UNDER 6 ±.06 ±.010; 6-84 INCL. ±.03 ±.030; OVER 24 ±.05 ±.050	CHECKED	
APPLICATION	DO NOT SCALE PRINT	ENGR	
	COML. TOL. TO STOCK SIZES	ITT AGO	4/3/72
	SHOP PRACTICE, 30.101 APPLIES	OTHER	
SIZE D	CODE IDENT NO. 31550	8116446	
SCALE		SHEET	

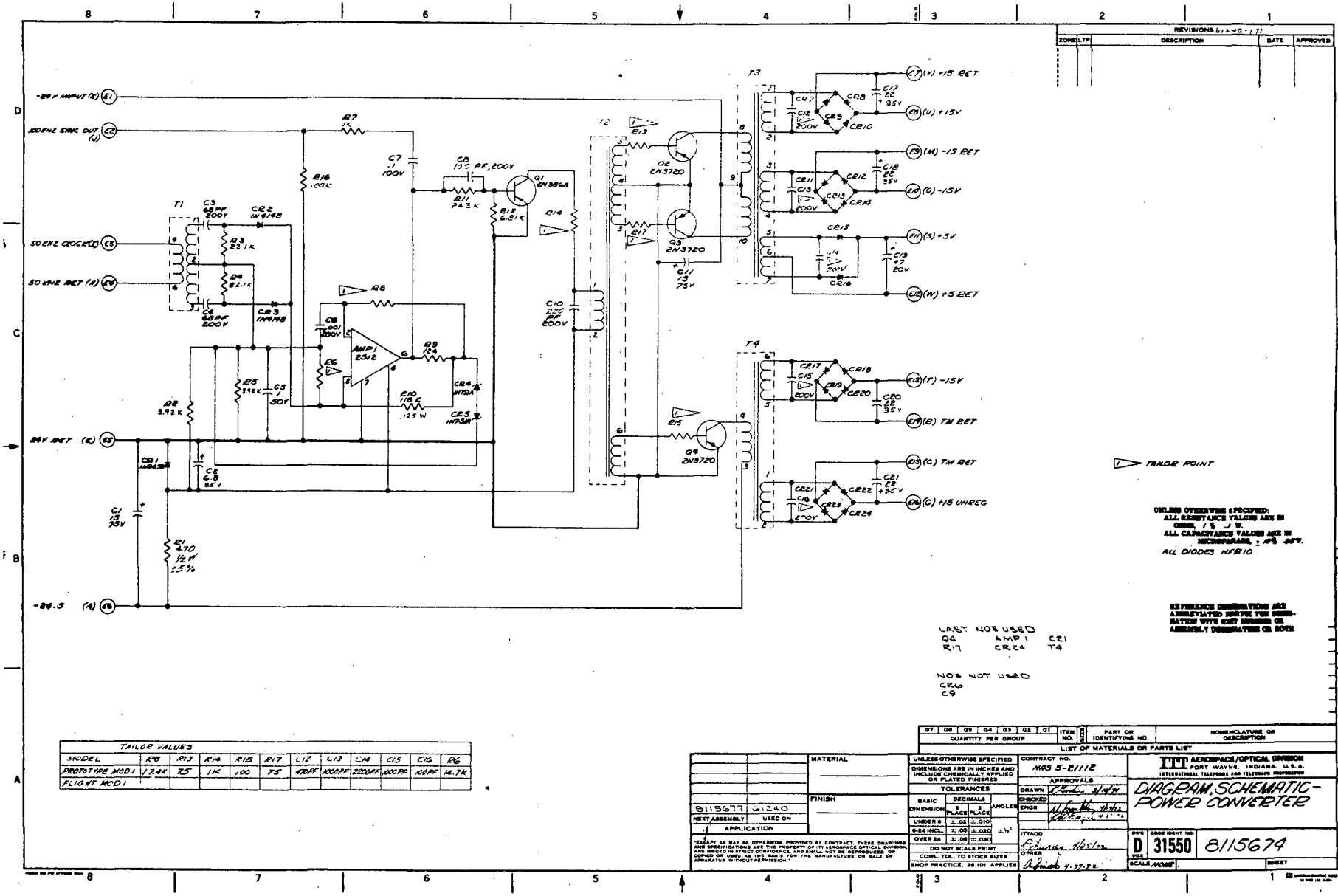

TAILOR VALUES											
MODEL	R8	R13	R14	R15	R17	C12	C13	C14	C15	C16	R6
PROTOTYPE MOD I	12.4K	75	1K	100	75	470PF	1000PF	2200PF	1000PF	100PF	14.7K
FLIGHT MOD I											

LAST NOS USED
Q4 AMP1 C21
R17 CR24 T4

NOS NOT USED
CR6
C9

UNLESS OTHERWISE SPECIFIED:
ALL RESISTANCE VALUES ARE IN OHMS, 1/8 W.
ALL CAPACITANCES VALUES ARE IN MICROFARADS, ±4% 50V.
ALL DIODES HER10

REFERENCE DESIGNATORS ARE ABBREVIATED FROM THE DESIGNATION WITH UNIT NUMBER OR ASSEMBLY DESIGNATING CH NOTE

ZONE	LTR	DESCRIPTION	DATE	APPROVED

REVISIONS (1 THRU 7)

QUANTITY PER GROUP	ITEM NO.	PART OR IDENTIFYING NO.	NOMENCLATURE OR DESCRIPTION
Q7 Q8 Q9 Q4 Q3 Q2 Q1			

LIST OF MATERIALS OR PARTS LIST

MATERIAL	UNLESS OTHERWISE SPECIFIED	CONTRACT NO.	ITT AEROSPACE/OPTICAL DIVISION, FORT WAYNE, INDIANA, U.S.A.
FINISH	DIMENSIONS ARE IN INCHES AND INCLUDE CHEMICALLY APPLIED OR PLATED FINISHES	NAS 5-21112	DIAGRAM, SCHEMATIC - POWER CONVERTER
8115677 61240	TOLERANCES	APPROVALS	
NEXT ASSEMBLY / USED ON	BASIC DIMENSION: DECIMALS 2 PLACE, 3 PLACE; ANGLES	DRAWN	
APPLICATION	UNDER 6: ±.02, ±.010; ±½°	CHECKED	
	6-24 INCL.: ±.03, ±.020	ENGR	
	OVER 24: ±.06, ±.030	ITTAOD	
	DO NOT SCALE PRINT	OTHER	
	COMM. TOL. TO STOCK SIZES	SIZE D	CODE IDENT NO. 31550
	SHOP PRACTICE, 30.101 APPLIES	SCALE NONE	SHEET

8115674

"EXCEPT AS MAY BE OTHERWISE PROVIDED BY CONTRACT, THESE DRAWINGS AND SPECIFICATIONS ARE THE PROPERTY OF ITT AEROSPACE OPTICAL DIVISION, ARE ISSUED IN STRICT CONFIDENCE AND SHALL NOT BE REPRODUCED OR COPIED OR USED AS THE BASIS FOR THE MANUFACTURE OR SALE OF APPARATUS WITHOUT PERMISSION."

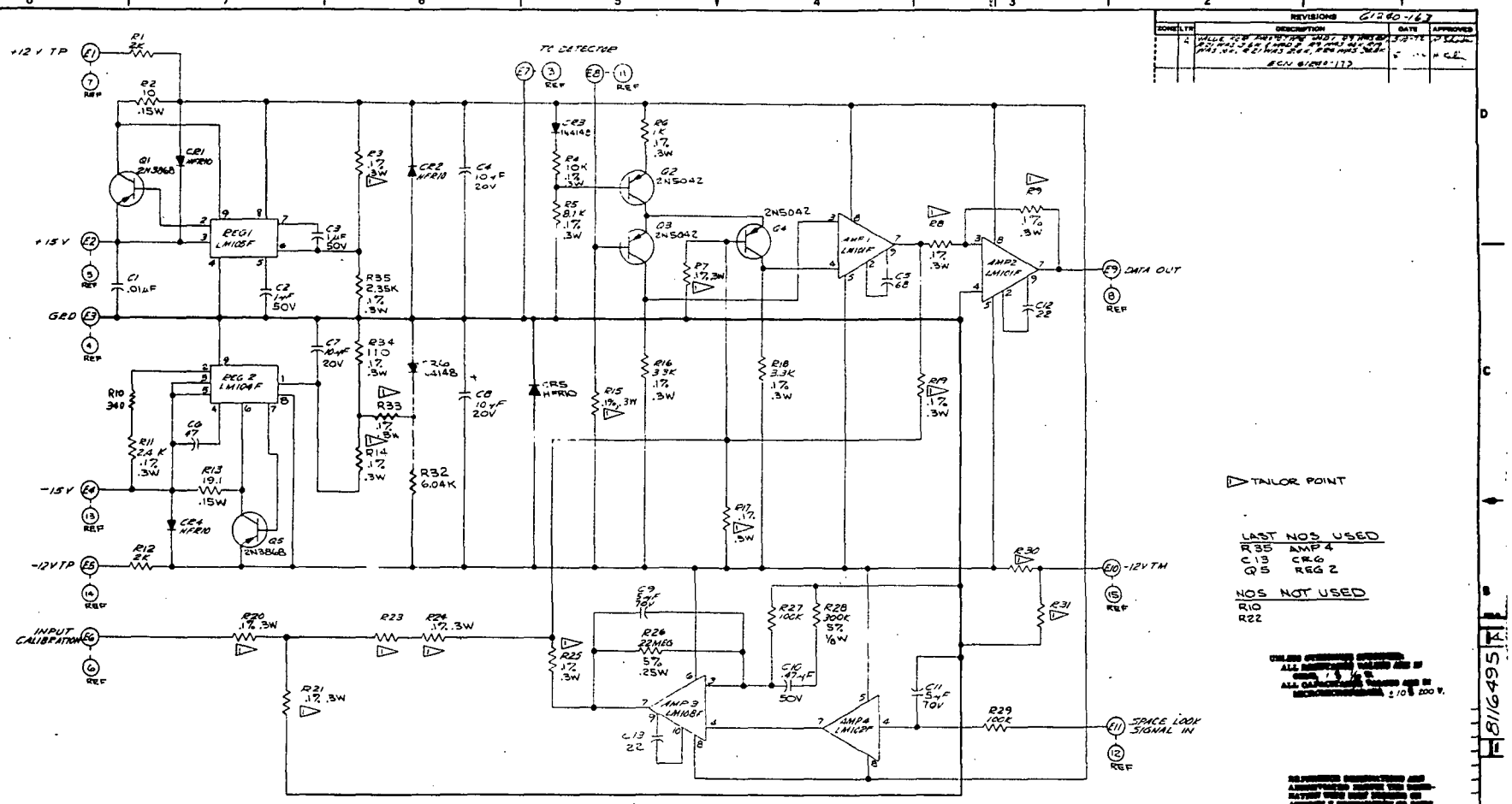

LAST NOS USED
R35 AMP 4
C13 CR6
Q5 REG 2

NOS NOT USED
R10
R22

TAILOR VALUES															
MODEL	R3	R7	R8	R9	R16	R15	R17	R19	R20	R21	R23	R24	R25	R33	R30	R31
PRECEPTYPE MOD 1	13.6K	30A	6.8K	412K	5.6K	2.4K	2K	10K	20.6K	3.3K	JUMPER	39.4K	500A	1K	3.32K	3.32K
PRECEPTYPE MOD 2	13.6K	30A	6.8K	294K	5.6K	1.72K	1.4K	8.8K	17K	6.8K	JUMPER	38.3K	500A	1K	3.32K	3.32K
FLIGHT MOD 1	13.9K				5.8K									1K	8.06K	8.06K
FLIGHT MOD 2	13.6K				5.8K									1.34K	8.06K	8.06K

REVISIONS 61240-167			
ZONE	LTR	DESCRIPTION	DATE	APPROVED
	4	WIRE TO R35 WAS CHGD. BY MFG TO R33 PER 3 SEC LABEL & PARTS LIST CHG. PER MFG. ECN 61240-167	3-31-72	

							ITEM NO.	PART OR IDENTIFYING NO.	NOMENCLATURE OR DESCRIPTION
Q7	Q6	Q5	Q4	Q3	Q2	Q1			
QUANTITY PER GROUP									

LIST OF MATERIALS OR PARTS LIST

MATERIAL		
FINISH		
8116498	61240	
NEXT ASSEMBLY	USED ON	
APPLICATION		

UNLESS OTHERWISE SPECIFIED
DIMENSIONS ARE IN INCHES AND INCLUDE CHEMICALLY APPLIED OR PLATED FINISHES
TOLERANCES

BASIC DIMENSION	DECIMALS 2 PLACE	DECIMALS 3 PLACE	ANGLES
UNDER 6	±.03	±.010	±1°
6-84 INCL.	±.03	±.020	
OVER 84	±.06	±.030	

DO NOT SCALE PRINT
CONFL. TOL. TO STOCK SIZES
SHOP PRACTICE, SP 101 APPLIES

CONTRACT NO.
APPROVALS
DRAWN
CHECKED
ENGR
ITT/AOD
OTHER

ITT AEROSPACE/OPTICAL DIVISION
FORT WAYNE, INDIANA, U.S.A.
INTERNATIONAL TELEPHONE AND TELEGRAPH CORPORATION

SCHEMATIC - PRE AMP

SIZE D | CODE IDENT. NO. 31550 | 8116495
SCALE | SHEET

8116495 REV L

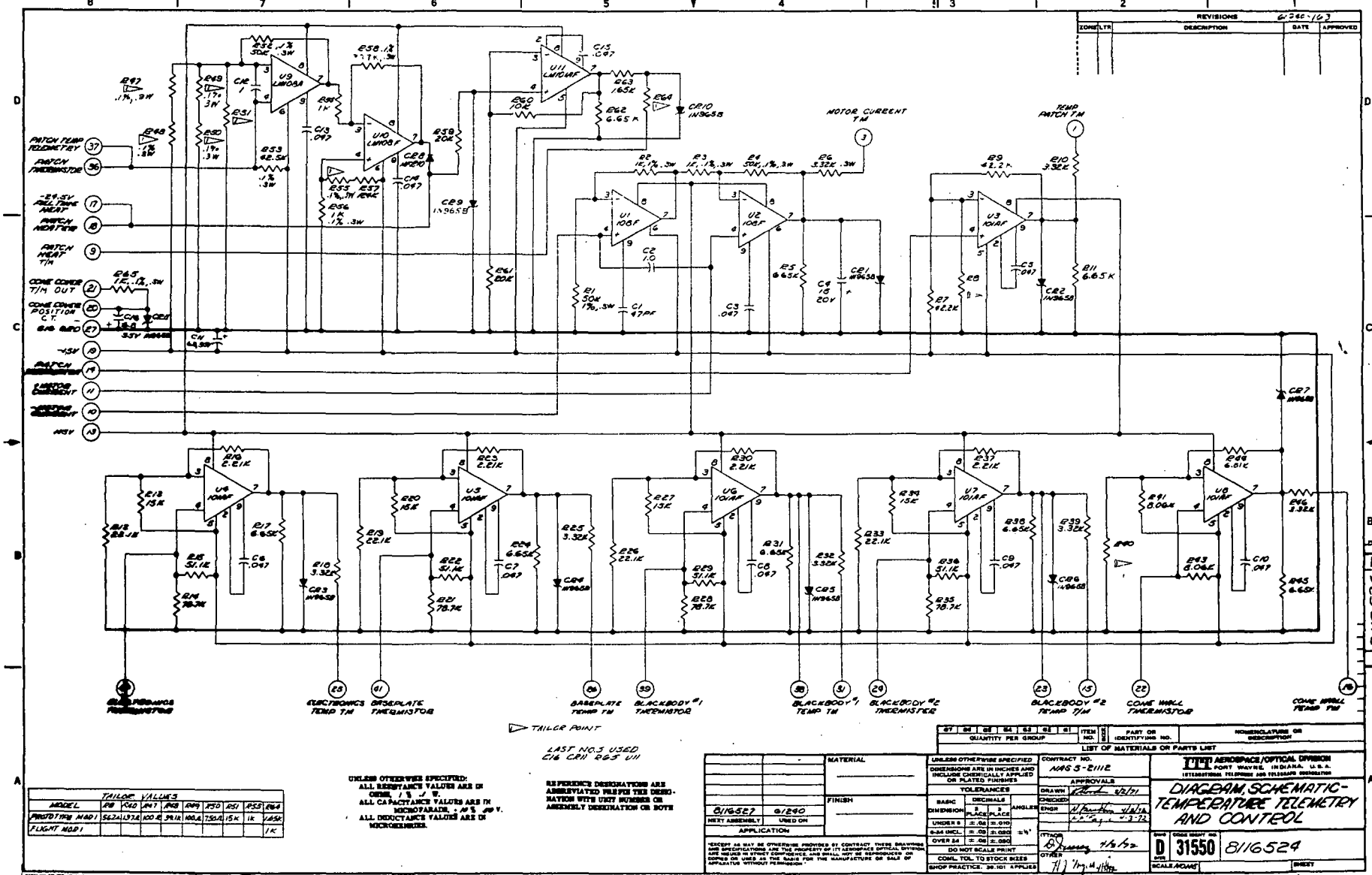
REVISIONS
ZONE/LTR | DESCRIPTION | DATE | APPROVED
PATCH TEMP TELEMETRY
PATCH THERMISTOR
PATCH HEATER
PATCH HEAT T/M
CONE CENTER T/M OUT
CONE CENTER POSITION C.T.
-15V
MOTOR CURRENT T/M
TEMP PATCH T/M
ELECTRONICS THERMISTOR
ELECTRONICS TEMP T/M
BASEPLATE TEMP T/M
BASEPLATE THERMISTOR
BLACKBODY #1 THERMISTOR
BLACKBODY #1 TEMP T/M
BLACKBODY #2 THERMISTER
BLACKBODY #2 TEMP T/M
CONE WALL THERMISTOR
CONE WALL TEMP T/M
TAILOR POINT
LAST NO.3 USED C16 CR11 R65 U11
UNLESS OTHERWISE SPECIFIED: ALL RESISTANCE VALUES ARE IN OHMS, 1 % ¼ W. ALL CAPACITANCE VALUES ARE IN MICROFARADS, ±10 % 200 V. ALL INDUCTANCE VALUES ARE IN MICROHENRIES.
REFERENCE DESIGNATIONS ARE ABBREVIATED PREFIX THE DESIGNATION WITH UNIT NUMBER OR ASSEMBLY DESIGNATION OR BOTH
TAILOR VALUES
MODEL | R8 | R40 | R47 | R48 | R49 | R50 | R51 | R55 | R64
PROTOTYPE MOD1 | 56.2A | 97.6 | 100 K | 39.1K | 100.A | 750.A | 15K | 1K | 1.45K
FLIGHT MOD1 | | | | | | | | | 1K
QUANTITY PER GROUP | ITEM NO. | PART OR IDENTIFYING NO. | NOMENCLATURE OR DESCRIPTION
LIST OF MATERIALS OR PARTS LIST
MATERIAL
FINISH
8116527 | 8/240
NEXT ASSEMBLY | USED ON
APPLICATION
UNLESS OTHERWISE SPECIFIED
DIMENSIONS ARE IN INCHES AND INCLUDE CHEMICALLY APPLIED OR PLATED FINISHES
TOLERANCES
DO NOT SCALE PRINT
COML. TOL. TO STOCK SIZES
SHOP PRACTICE, 30.101 APPLIES
CONTRACT NO. NAS 5-21112
APPROVALS
DRAWN
CHECKED
ENGR
ITT AEROSPACE/OPTICAL DIVISION
FORT WAYNE, INDIANA, U.S.A.
DIAGRAM, SCHEMATIC-TEMPERATURE TELEMETRY AND CONTROL
SIZE D | CODE IDENT NO. 31550 | 8116524
SCALE NONE | SHEET
8116524

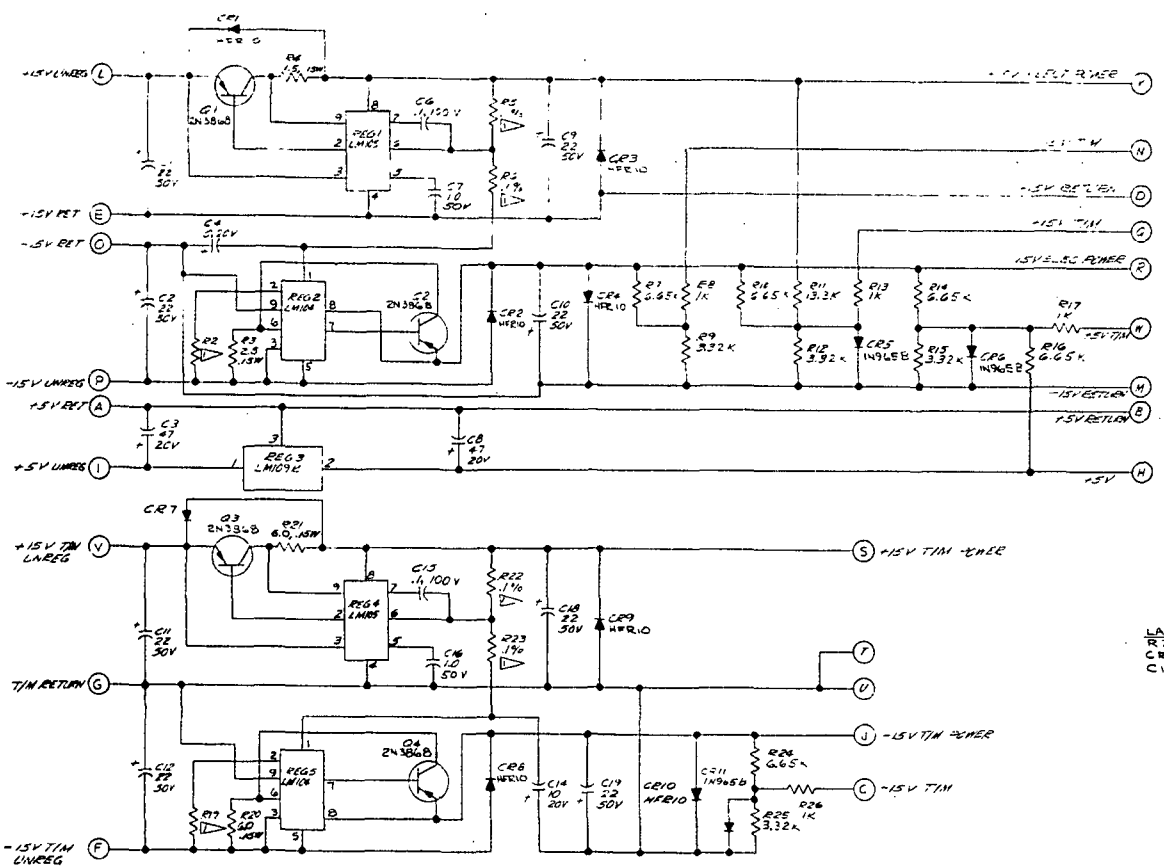

TAILOR POINT

LAST NOS USED		NUMBERS NOT USED
R26	REG5	R1
CR11	Q4	R18
C19		

TAILOR VALUES						
MODEL	R2	R5	R6	R9	R22	R23
PROTOTYPE MOD I	2.43K	13.2K	9.42K	2.43K	13.2K	9.31K
FLIGHT MOD I	2.43K	13.2K	9.20K	2.43K	13.2K	9.20K

REVISIONS				61280-163
ZONE	LTR	DESCRIPTION	DATE	APPROVED

ITEM NO.	PART OR IDENTIFYING NO.	NOMENCLATURE OR DESCRIPTION	QUANTITY PER GROUP
		LIST OF MATERIALS OR PARTS LIST	

MATERIAL	
FINISH	
NEXT ASSEMBLY	USED ON
APPLICATION	

UNLESS OTHERWISE SPECIFIED
DIMENSIONS ARE IN INCHES AND INCLUDE CHEMICALLY APPLIED OR PLATED FINISHES
TOLERANCES

	DECIMALS		ANGLES
BASIC DIMENSION	1 PLACE	2 PLACE	
UNDER 6	± .02	± .010	±4°
6 TO 24 INCL	± .03	± .030	
OVER 24	± .08	± .060	

DO NOT SCALE PRINT
CONFL. TOL. TO STOCK SIZES
SHOP PRACTICE 38 101 APPLIES

CONTRACT NO.

APPROVALS

DRAWN	[signature]	7-1-72
CHECKED		
ENGR	[signature]	7-1-72
	[signature]	7-1-72
ITT AGD	[signature]	7/5/72
OTHER	[signature]	7/8/72

ITT AEROSPACE/OPTICAL DIVISION
FORT WAYNE, INDIANA, U.S.A.
INTERNATIONAL TELEPHONE AND TELEGRAPH CORPORATION

SCHEMATIC - VOLTAGE REGULATORS

SIZE	CODE IDENT NO.	DRAWING NO.
D	31550	8116516
SCALE		SHEET

8116516

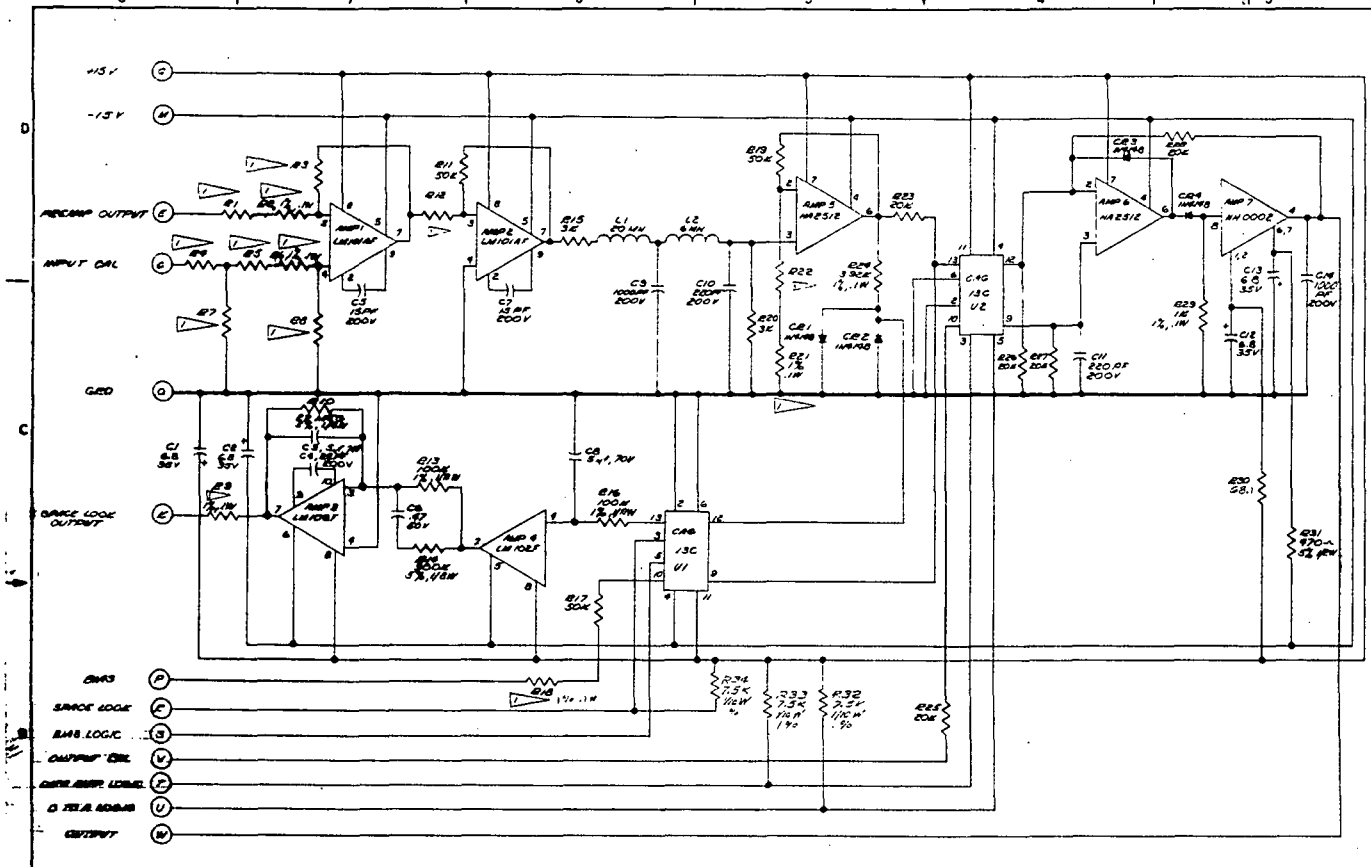

TAILOR VALUES													
MODEL	R1	R2	R3	R4	R5	R6	R7	R8	R12	R18	R21	R22	R29
PROTOTYPE MOD I	13.3K	4.53	822K	5.8K	37.3K	768	10K	7.5K	11K	866	JUMPER	20K	221
FLIGHT MOD I													

REVISIONS			
ZONE	LTR	DESCRIPTION	DATE	APPROVED

QUANTITY PER GROUP	ITEM NO.	SIZE	PART OR IDENTIFYING NO.	NOMENCLATURE OR DESCRIPTION

LIST OF MATERIALS OR PARTS LIST

MATERIAL	
FINISH	
NEXT ASSEMBLY	USED ON
APPLICATION	61290

UNLESS OTHERWISE SPECIFIED
DIMENSIONS ARE IN INCHES AND INCLUDE CHEMICALLY APPLIED OR PLATED FINISHES
TOLERANCES

BASIC DIMENSION	DECIMALS 2 PLACE	DECIMALS 3 PLACE	ANGLES
UNDER 6	± .03	± .010	±½°
6-24 INCL.	± .03	± .020	
OVER 24	± .06	± .030	

DO NOT SCALE PRINT
CONFL. TOL. TO STOCK SIZES
SHOP PRACTICE: SP 101 APPLIES

CONTRACT NO. NAS 5-21112
APPROVALS
DRAWN 3/5/71
CHECKED
ENGR
ITTAOD 4/6/72
OTHER

ITT AEROSPACE/OPTICAL DIVISION
FORT WAYNE, INDIANA, U.S.A.

DIAGRAM, SCHEMATIC — VISIBLE CHANNEL

SIZE D | CODE IDENT NO. 31550 | 8116530
SCALE NONE | SHEET

8116530 A

A-11

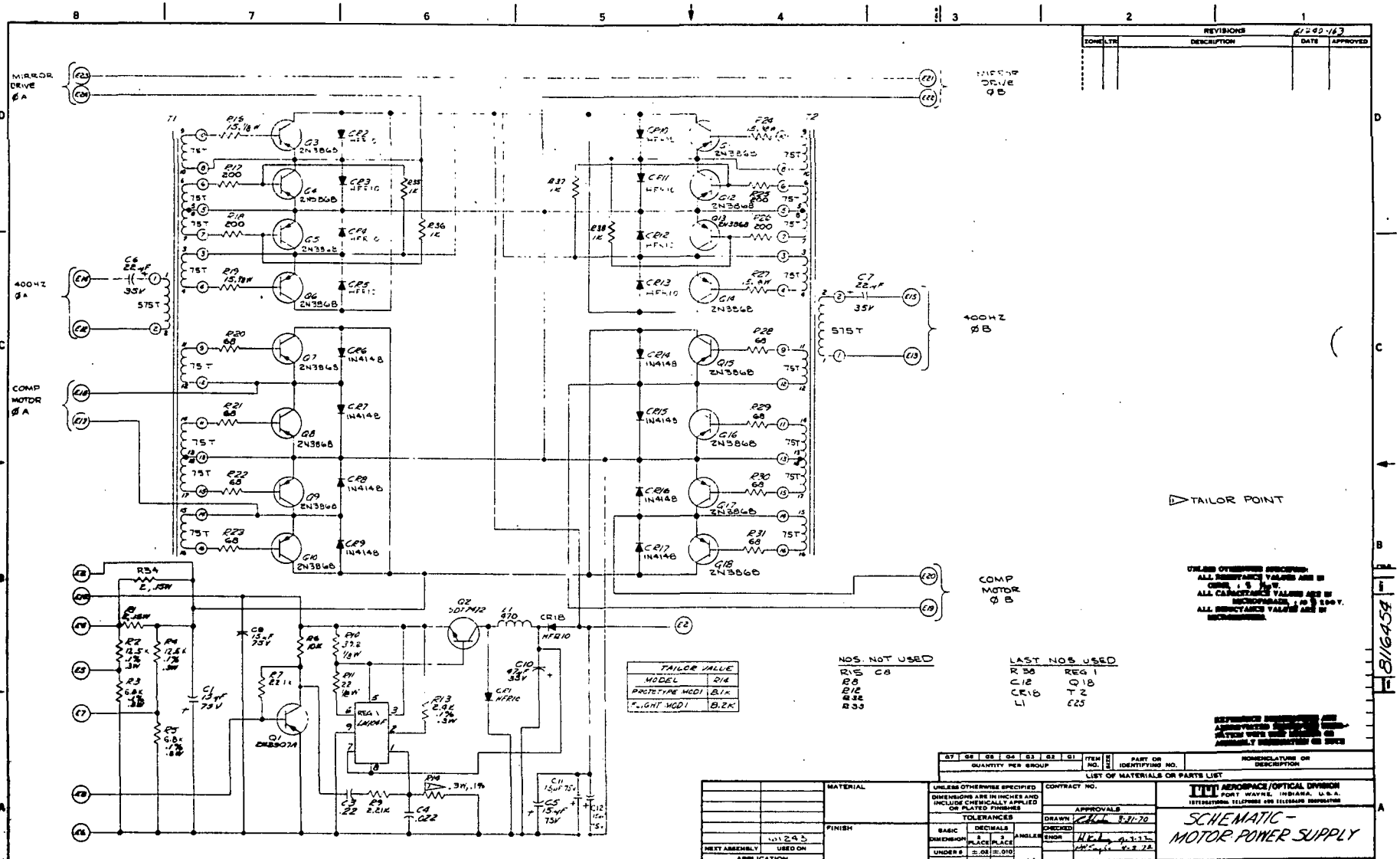
MIRROR DRIVE ØA
400HZ ØA
COMP MOTOR ØA
MIRROR DRIVE ØB
400HZ ØB
COMP MOTOR ØB
TAILOR POINT
T1
T2
Q1 2N3907A
Q2 2N3700
REG 1 LM109H
NOS. NOT USED
R15 C8
R28
D12
Q32
R33
LAST NOS USED
R38 REG 1
C12 Q18
CR16 T2
L1 E25
TAILOR VALUE
MODEL 21A
PROTOTYPE MOD1 8.1K
FLIGHT MOD1 8.2K
REVISIONS
ZONE LTR DESCRIPTION DATE APPROVED
61240-163
ITT AEROSPACE/OPTICAL DIVISION
FORT WAYNE, INDIANA, U.S.A.
SCHEMATIC - MOTOR POWER SUPPLY
SIZE D
CODE IDENT NO. 31550
8116454
SCALE
SHEET
8116454-1
A-12

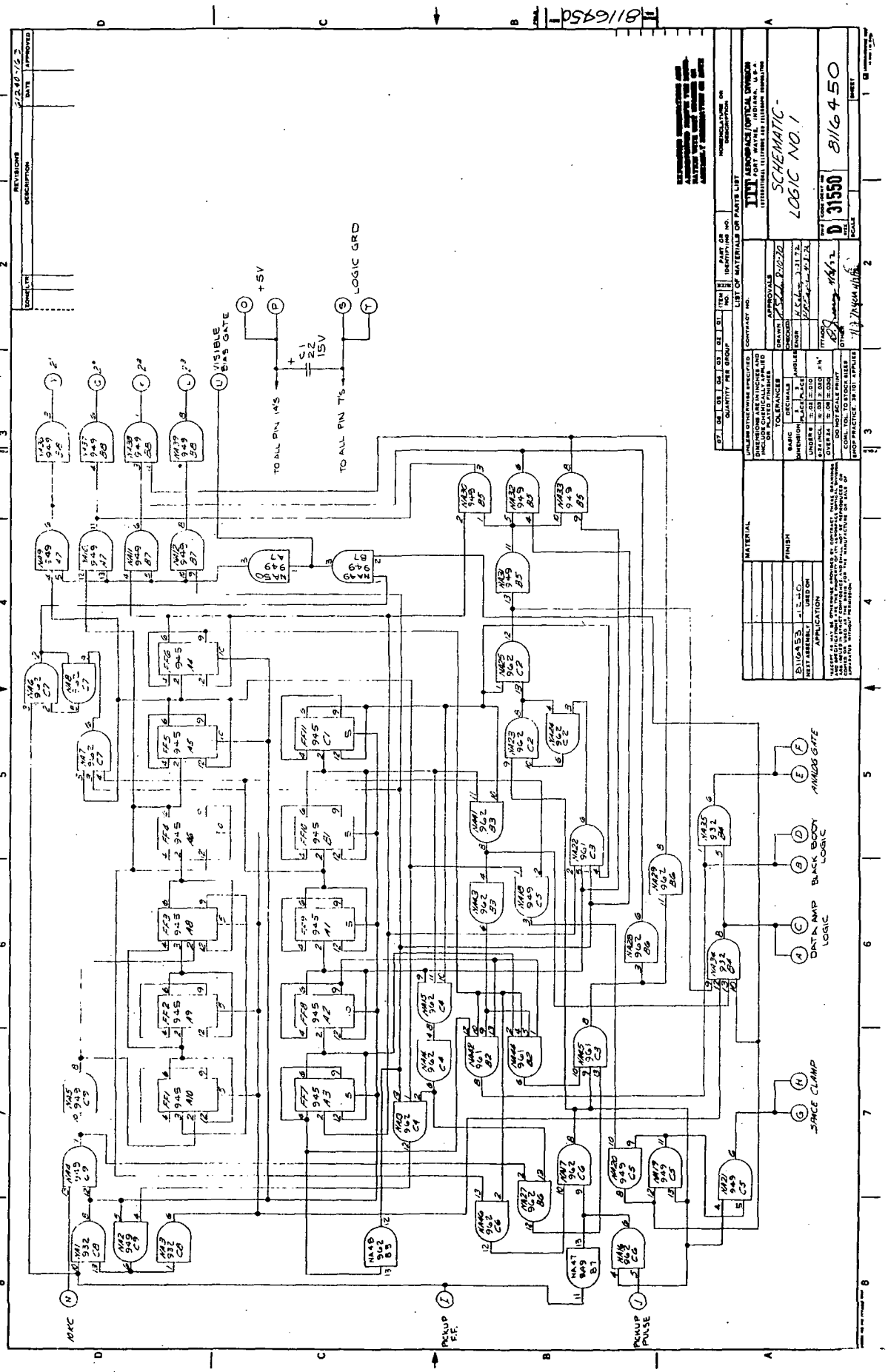
SCHEMATIC-
LOGIC NO. 1
8116450
D 31550
ITT AEROSPACE/OPTICAL DIVISION
FORT WAYNE, INDIANA
+5V
LOGIC GRD
VISIBLE
BIAS GATE
TO ALL PIN 14'S
TO ALL PIN 7'S
C1
22
15V
DATA AMP
LOGIC
BLACK BODY
LOGIC
ANALOG GATE
SPACE CLAMP
PICKUP
F.F.
PICKUP
PULSE
MXC

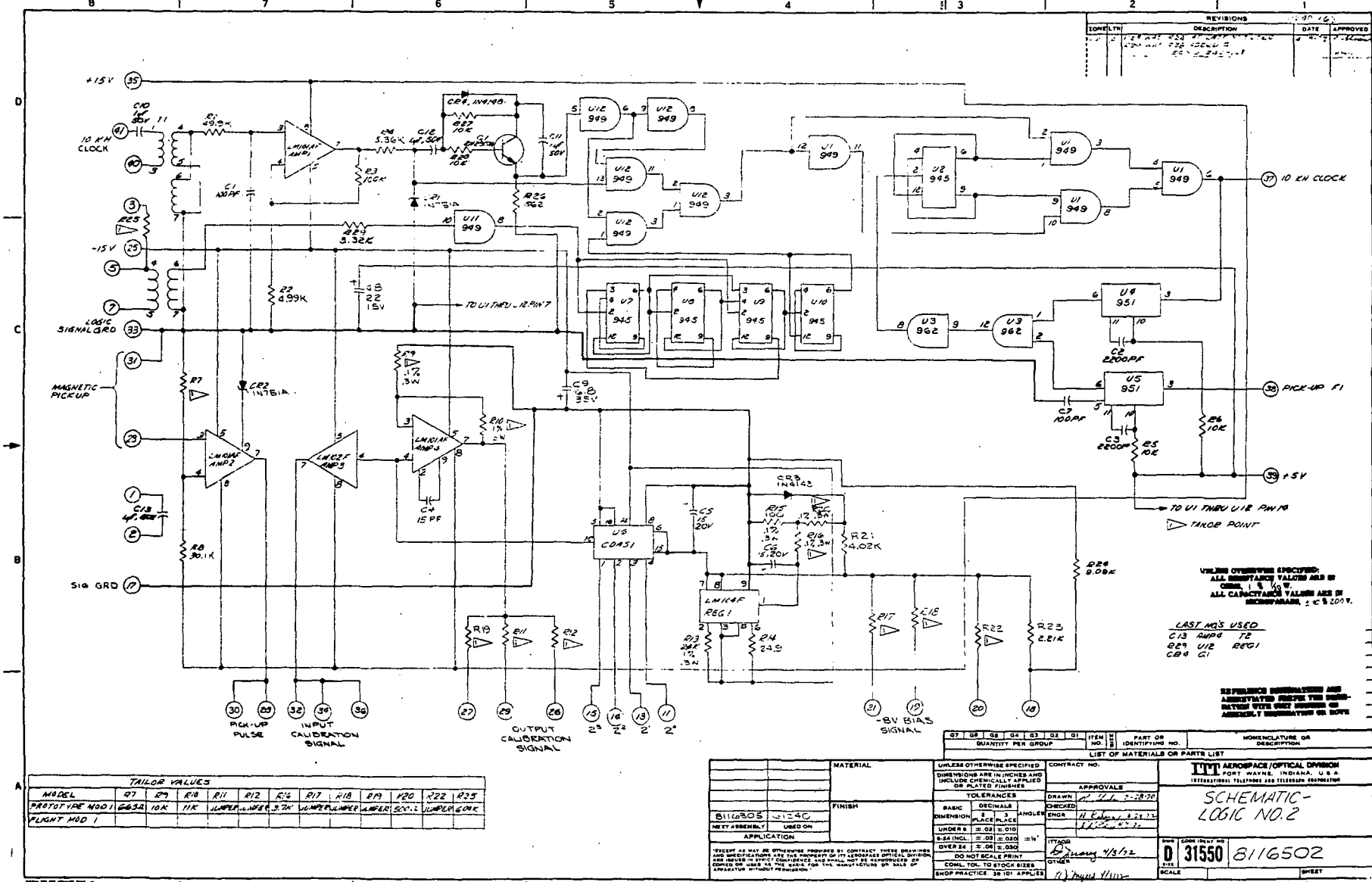

TAILOR VALUES												
MODEL	R7	R9	R10	R11	R12	R16	R17	R18	R19	R20	R22	R23
PROTOTYPE MOD 1	6652	10K	11K	JUMPER	JUMPER	3.7K	JUMPER	JUMPER	JUMPER	500Ω	JUMPER	6.8K
FLIGHT MOD 1												

REVISIONS				
ZONE	LTR	DESCRIPTION	DATE	APPROVED

QUANTITY PER GROUP								ITEM NO.	SYM	PART OR IDENTIFYING NO.	NOMENCLATURE OR DESCRIPTION
Q7	Q6	Q5	Q4	Q3	Q2	Q1					

LIST OF MATERIALS OR PARTS LIST

8116805	-1240	MATERIAL	FINISH	NEXT ASSEMBLY	USED ON
APPLICATION					

UNLESS OTHERWISE SPECIFIED: DIMENSIONS ARE IN INCHES AND INCLUDE CHEMICALLY APPLIED OR PLATED FINISHES. TOLERANCES: DECIMALS 2 PLACE ±.02, 3 PLACE ±.010; ANGLES ±½°; 0-24 INCL. ±.03 ±.030; OVER 24 ±.08 ±.030. DO NOT SCALE PRINT. COML. TOL. TO STOCK SIZES. SHOP PRACTICE 38101 APPLIES.

CONTRACT NO.

APPROVALS: DRAWN A. Wilson 2-28-70; CHECKED; ENGR H. Eckert 4-24-72; ITT/AOD D. Quarry 4/13/72; OTHER; M. Wood 4/13/72

ITT AEROSPACE/OPTICAL DIVISION, FORT WAYNE, INDIANA, U.S.A. INTERNATIONAL TELEPHONE AND TELEGRAPH CORPORATION

SCHEMATIC - LOGIC NO. 2

SIZE D | CODE IDENT NO 31550 | 8116502 | SCALE | SHEET

8116502-A